hysics Lib.

VOLUME 35 SECOND SERIES NUMBER 12

THE PHYSICAL REVIEW

A JOURNAL OF EXPERIMENTAL AND THEORETICAL PHYSICS

CONDUCTED BY

THE AMERICAN PHYSICAL SOCIETY

BOARD OF EDITORS

Managing Editor JOHN T. TATE, University of Minnesota, Minneapolis

I. S. BOWEN, R. S. MULLIKEN, H. D. SMYTH, E. U. CONDON, C. J. DAVISSON, F. K. RICHTMYER, K. F. HERZFELD, A. W. HULL, F. W. LOOMIS

JUNE 15, 1930

Possible Effects of Nuclear Spin on X-Ray Terms — G. BREIT 1447

On the Reflection of the $K\alpha$ Line of Carbon from a Glass Mirror — JEAN THIBAUD 1452

Molybdenum K Series Wave-Lengths by Ruled Gratings — J. M. CORK 1456

Independence of X-Ray Absorption on Temperature — J. A. BEARDEN 1463

Effect of an Electric Field on the X-Ray Diffraction Pattern of a Liquid — RONALD L. MCFARLAN 1469

Resolving Power of Calcite for X-Rays and the Natural Widths of the Mo $K\alpha$ Doublet — SAMUEL K. ALLISON AND JOHN H. WILLIAMS 1476

Vibrational Quantum Analysis of the Blue-Green Bands of Magnesium Oxide — P. N. GHOSH, P. C. MAHANTI AND B. C. MUKHERJEE 1491

Zeeman Effect in the OH Bands — GERALD M. ALMY 1495

Zeeman Effect in the Red CaH Bands — WILLIAM W. WATSON AND WILLIAM BENDER 1513

Infrared Absorption of some Organic Liquids Under High Resolution — R. BOWLING BARNES 1524

Quantum Kinetics and the Planck Equation — GILBERT N. LEWIS 1533

Contribution to the Quantum Mechanical Theory of Radioactivity and the Dissociation by Rotation of Diatomic Molecules — OSCAR KNEFLER RICE 1538

Perturbations in Molecules and the Theory of Predissociation and Diffuse Spectra, II — OSCAR KNEFLER RICE 1551

Concerning the Absorption Method of Investigating β-Particles of High Energy: The Maximum Energy of the Primary β-Particles of Mesothorium 2 — N. FEATHER 1559

Motion of Electrons in Carbon Monoxide — H. B. WAHLIN 1568

Magnetic Susceptibility of Gases. I. Pressure Dependence — FRANCIS BITTER 1572

Letters to the Editor — 1583

Book Reviews — 1588

Index to Volume 35 — 1589

PUBLISHED BY THE AMERICAN PHYSICAL SOCIETY

PUBLICATION OFFICES: 450–454 AHNAIP STREET, MENASHA, WIS.

EDITORIAL OFFICES: MINNEAPOLIS, MINN.

THE AMERICAN PHYSICAL SOCIETY

OFFICERS OF THE SOCIETY

President:	HENRY G. GALE	University of Chicago, Chicago, Ill.
Vice-President:	W. F. G. SWANN	Bartol Research Foundation, Philadelphia, Pa.
Secretary:	W. L. SEVERINGHAUS	Columbia University, New York City
Treasurer:	G. B. PEGRAM	Columbia University, New York City
Editor:	JOHN T. TATE	University of Minnesota, Minneapolis, Minn.
Local Secretary for the Pacific Coast:	L. B. LOEB	University of California, Berkeley, Calif.

THE PHYSICAL REVIEW

Published by the American Physical Society at 450 Ahnaip St., Menasha, Wis. Executive office: University of Minnesota, Minneapolis, Minn. Two volumes annually, twelve issues per volume.

First series. From July 1, 1893, to January 1, 1913, the REVIEW was conducted by Edward L. Nichols, Ernest Merritt and Frederick Bedell, with the financial support of Cornell University. The first four volumes were issued annually; subsequent volumes, semi-annually; thirty-five volumes in all.

Second series. On January 1, 1913, the REVIEW was transferred to the American Physical Society as announced on the first page of the new series which was then begun. Since then it has been conducted by a Board of Editors elected by the Society. Semi-annual volumes begin in January and July. Since July 1, 1929, the REVIEW has been issued twice a month.

Contributors are referred to page 2 of the advertisements for further information.

Annual Subscription, throughout the Postal Union, $10.00 in advance.

Single copies of current volume, $.60.

General index, 1893-1920, $4.00, in advance.

Back Volumes, $6.00 per volume; Back Numbers, $1.00 per copy for issues prior to July 1, 1929 (Vols. 1-33), $.60 per copy for issues subsequent thereto. Postage is free if remittance accompanies order; otherwise postage is extra. No bound volumes can be supplied. The REVIEW offers to purchase a limited number of First Series, Vol. 1, No. 1 (at $2.00 each); Second Series, Vol. 7, No. 1, January 1916; Vol. 7, No. 2, February 1916; Vol. 7, No. 4, April 1916; and Vol. 7, No. 5, May 1916 (at $2.00 each).

Advertisements. Rates will be supplied by the Editor on request. Copy for each number must be received at Minneapolis two weeks prior to the dates of issue; old copy is used until new copy is received. Send electrotypes direct to the printers, George Banta Publishing Co., Menasha, Wis.

Discount of ten percent is allowed subscription agencies and members of the American Physical Society.

Changes of address and Complaints of failure to receive the REVIEW, in the case of members of the Physical Society, should be addressed to the Treasurer; in the case of other subscribers to 450 Ahnaip St., Menasha, Wis.; or to the Editor. New copies can be sent free in response to complaint of non-delivery only if notice of non-delivery is received within three months of date of issue.

Editorial Correspondence should be addressed to the PHYSICAL REVIEW, University of Minnesota, Minneapolis, Minn.

Entered at the postoffice at Menasha, Wis., as second class matter.
Acceptance for mailing at special rate of postage provided for in section 1103, Act of October 3, 1917, authorized September 6, 1926.

Second Series *June 15, 1930* *Vol. 35, No. 12*

THE

PHYSICAL REVIEW

POSSIBLE EFFECTS OF NUCLEAR SPIN ON X-RAY TERMS

By G. Breit

Department of Physics, New York University

(Received May 5, 1930)

Abstract

It is shown that magnetic moments of nuclei are likely to cause small but presumably measurable separations of x-ray terms. A nucleus having a spin of 9/2 (in units of $h/2\pi$) and a magnetic moment 9/2 in protonic units should cause the K terms of the heaviest elements to split into two components separated by about 22 volts. Such separations require for their detection a resolving power of 4200. For lighter elements the effect is relatively smaller. The same nuclear spin and magnetic moment would cause a separation of only 0.9 volts in Mo which would require for its detection a resolving power of 1.9×10^4

The calculations are made using Dirac's equation for a single electron without approximations. The effect of electrons in another shell, however, is neglected. It is estimated to be very small for a single K electron. If the observation of hyperfine structures in the K series of the heavier elements proves feasible, it should offer a simple means of determining magnetic moments of nuclei having a known spin.

THE hyperfine structure of spectral lines is at present attributed to the nuclear spin. The quantitative theory of the effect has been worked out by Hargreaves, Fermi, Goudsmit and Bacher and by Casimir.[1] A quantitative application of the theory is simple in a few cases such as e.g. the Li^+ hyperfine structure. For most spectra it is necessary to use approximate solutions for the electronic eigenfunctions which are at present usually carried out by the Hartree method. Quantitative determinations of the nuclear magnetic moment become, therefore, difficult. An examination of Fermi's result shows however that the order of magnitude of the effect can be expected to be much larger for the spectral terms in the x-ray region than for visible spectra. The absolute value of the splitting of an s term due to a single electron is according to Fermi

$$(F) \qquad (8\pi/3)[(2k+1)/k]\mu\mu_0\psi^2(0)$$

where k is the angular momentum of the nucleus, μ its magnetic moment, μ_0 the Bohr Magneton, and $\psi(0)$ is the value of the Schroedinger function

[1] J. Hargreaves, Proc. Roy. Soc. **A124,** 568 (1929). E. Fermi, Zeits. f. Physik **60,** 320 (1930). S. Goudsmit and R. F. Bacher, Phys. Rev. **34,** 1501, (1929). S. Goudsmit and L. A. Young, Nature, March 22, (1930).

at $r=0$. For large atomic numbers the value of $\psi(0)$ for a $(1s)K$ electron is large. In fact it is seen that $\psi^2(0)$ must increase as the cube of the reciprocal of the radius of the K orbit i.e., as Z^3 where Z is the atomic number. The energy of the K level increases only as Z^2 so that the splitting $\Delta\nu$ increases more rapidly than the term value ν. The values of the magnetic moments of the nuclei are not known at present and so it is necessary to be content with approximate estimates using the known orders of magnitude derived from hyperfine structure observations in the visible region. Making such estimates it is found that for heavy elements the separation $\Delta\nu$ may be expected to be of the order of 1/5000 of the frequency of the K line. The double crystal spectrometer developed by Bergen Davis appears to offer at least a possibility of observing such separations. The main purpose of this note is to call attention to the possibility of determining the magnetic moments of the nuclei by means of observations of the hyperfine structure of the lines in the K series. Corresponding effects in the L and M series are estimated to be smaller, though not necessarily beyond the range of experimental accuracy.

In order to form proper estimates for the case of x-rays it is necessary to perform somewhat more precise calculations than those of Fermi. The inaccuracy of his method lies in the fact that $E+(Ze^2/r)+mc^2$ is replaced by $2mc^2$. This is a good approximation as long as the region of large values of Ze^2/r is relatively small and as long as $E\sim mc^2$. Both of these conditions are satisfied for the lighter elements. The approximate dimensions of the regions in which the eigenfunction is appreciable are then of the order of 10^{-8} cm while $e^2/r>mc^2$ only if $r<2.5\times10^{-13}$ cm. For the heavier elements this is not so because the charge density is more concentrated and Ze^2/r is greater for the same r. It thus becomes necessary to use exact solutions of Dirac's equation as a starting point in the calculation of the perturbation due to the magnetic moment of the nucleus.

Using Gordon's form of the solution of the Dirac equation for a Coulomb field of force[2] it is seen that for s terms of a single electron any set of four ψ's can be expressed as a linear combination of the following two sets

$$(I)\qquad \begin{aligned}\Psi_1 &= ((i/r)\cos\theta\phi_1, (i/r)\sin\theta e^{i\varphi}\phi_1, \phi_2/r, 0)\\ \Psi_2 &= ((i/r)\sin\theta e^{-i\varphi}\phi_1, -(i/r)\cos\theta\,\phi_1, 0, \phi_2/r)\end{aligned}$$

where ϕ_1, ϕ_2 are two functions (denoted by Gordon as ψ_1, ψ_2) given by

$$(G)\qquad \phi_1 = (1-E/mc^2)^{1/2}(\sigma_1-\sigma_2);\ \phi_2 = (1+E/mc^2)^{1/2}(\sigma_1+\sigma_2)$$

where
$$\sigma_1 = c_0^{(1)}e^{-k_0 r}r^\rho F(-n'+1, 2\rho+1; 2k_0 r);\quad \rho = (1-\alpha^2)^{1/2}$$
$$\sigma_2 = c_0^{(2)}e^{-k_0 r}r^\rho F(-n', 2\rho+1; 2k_0 r);\qquad \alpha = 2\pi Ze^2/hc$$

$$F(\alpha,\beta;x) = 1+\frac{\alpha x}{1!\beta}+\frac{\alpha(\alpha+1)x^2}{2!\beta(\beta+1)}+\cdots;\ k_0 = (2\pi mc/h)\left[1-(E/mc^2)^2\right]^{1/2}$$

$$c_0^{(1)}/c_0^{(2)} = -n'/\left[1+\alpha(1-(E/mc^2)^2)^{-1/2}\right];\ E/mc^2 = \left[1+\alpha^2/(n'+\rho)^2\right]^{-1/2}$$

Here $n'=0, 1, 2, \cdots$ for $(1s)$, $(2s)$, $\cdots$ terms.

[2] W. Gordon, Zeits. f. Physik **48**, 22 (1928).

In particular for (1s) terms $c_0^{(1)}/c_0^{(2)}=0$ and σ_2 contains only one term.

The perturbation function due to the magnetic moment of the nucleus we take to be the same as Fermi's

$$w = (e/r^3)\vec{\mathfrak{a}}[\vec{\mu}\times\vec{r}].$$

The unperturbed orthogonal Eigenfunctions can be taken to be

$$\begin{matrix} u_k^{(1)}, u_{k-1}, \cdots, u_{-k}^{(1)} \\ u_k^{(2)}, \cdots, u_{-k+1}^{(2)}, u_{-k}^{(2)} \end{matrix} \tag{1}$$

corresponding to angular momenta

$$(k+\tfrac{1}{2}, k-\tfrac{1}{2}, \cdots, -k-\tfrac{1}{2})(h/2\pi)$$

To every angular momentum in the direction of the Z axis there correspond in general two unperturbed functions. Each of these is a rectangular matrix. The superscripts (1), (2) indicate wherther Ψ_1 or Ψ_2 of I are used. Thus the function $u^{(1)}{}_{k-l}$ has for elements zeros in the first l rows; Ψ_1 stands with its four elements in the lth row, and the remaining elements are zero. This is exactly as in Fermi's article. We remark that in the secular determinant we can have matrix elements only between such functions which are in the same vertical column of (1).

There are two multiple roots of the secular determinant one of which occurs $2k+2$ and the other $2k$ times. The functions at the extreme right and left correspond to the first of these two roots. This can be calculated first and the remaining root can be ascertained by obtaining the diagonal elements of the subdeterminant formed by the combinations of any other vertical pair in (1). The first root is therefore $\int u_k^{*(1)} w\, u_k^{(1)}\, d\tau$. This integral sign is of course understood to include in it a summation over the indices of the matrix eigenfunctions. The operations μ are on the columns and the operations α are on the rows. We are therefore only interested in that part of $wu_k^{(1)}$ which on performing the operations μ involves the index k. This part is due to μ_z and is $(e\mu/r^3)\ (x\alpha_y - y\alpha_x)u_k^{(1)}$. The remaining operation is entirely on Ψ_1. Performing it and substituting in the intergral it is found that

$$w_1 = \int u_k^{(1)*} w u_k^{(1)} d\tau = (16\pi/3)c\mu \int_0^\infty (\phi_1\phi_2/r^2)dr \tag{2}$$

This is therefore one of the roots. The sum of the two roots is $\int[u_{k-1}^{(1)*}\ w\ u_{k-1}^{(1)} + u_k^{(2)*}\ w\ u_k^{(2)}]\ d\tau$, with the same understanding about the integral as before. The calculation of the first term in brackets is the same as before with the difference that a factor $(k-1)/k$ is introduced. In the second term the result (2) is obviously obtained but with opposite sign due to the occurrence of Ψ_2 instead of Ψ_1. The sum of the two roots is therefore

$$w_1 + w_2 = -w_1/k. \tag{3}$$

Hence

$$\Delta\nu = w_1 - w_2 = ((2k+1)/k)w_1. \tag{4}$$

The difference between this result and Fermi's can be expressed by saying that Fermi's

$$\psi^2(0) \rightarrow (2e/\mu_0)\int_0^\infty (\phi_1\phi_2/r^2)dr = -(8\pi mc/h)\int_0^\infty (\phi_1\phi_2/r^2)dr.$$

Equation (4) is practically exact for any s term; in a Coulomb field the only approximation made being that of supposing the effect of the nuclear magnetic moment to be small.

In applying (4) it must be remembered that ϕ_1, ϕ_2 are supposed to be normalized in such a way that

$$4\pi\int(\phi_1^2+\phi_2^2)dr = 1 \tag{5}$$

as is obvious from (I). For $(1s)$ terms

$$\phi_1 = -C[1-(E/mc^2)]^{1/2}e^{-k_0 r}r^\rho;\ \phi_2 = C[1+(E/mc^2)]^{1/2}e^{-k_0 r}r^\rho. \tag{6}$$

These expressions are substituted into (4), the normalization constant C being determined by (5). The integrals are expressible by means of the Γ function. Using $\Gamma(x+1)=x\Gamma(x)$ and the relations G it is found that the exact quantity which replaces Fermi's $\psi^2(0)$ is (see (4′))

$$(4\pi mc/h)^3(\alpha^3/8\pi)[2\rho^2-\rho]^{-1}. \tag{7}$$

Here the first two factors are Fermi's $\psi^2(0)$. and the factor in brackets is a correction due to relativity effects brought in by this calculation.* Substituting (7) into (F)

$$\begin{aligned}\Delta\nu &= 0.0169Z^3(k+\tfrac{1}{2})(1840\mu/2k\mu_0)[2\rho^2-\rho]^{-1}\,\text{cm}^{-1}\\ &= 2.08(Z/100)^3(k+\tfrac{1}{2})(1840\mu/2k\mu_0)[2\rho^2-\rho]^{-1}\,\text{volts}.\end{aligned} \tag{8}$$

In order to estimate the order of magnitude of the effect we suppose that $k=9/2$ and that $1840\mu=2k\mu_0$. We find for

	U	Bi	W	Mo
$Z=$	92	83	74	42
$\Delta\nu=$	22.5	12.6	7.31	0.896 volts
$\nu_{Ka}=$	(9.395	7.436	5.912	$1.734)\times10^4$ volts
$\nu_{Ka}/\Delta\nu=$	4175	5911	8092	19361

Of these elements Bi is known[3] to have a nuclear spin 9/2. It is clear from the above table that for the heavier elements the separation is sufficiently large not to be confused with chemical effects and that the resolving power tabulated in the last row is sufficiently small to make the possibility of experimental detection of $\Delta\nu$ at least hopeful.

In a similar way the separation of $2s$ terms has been worked out. In this case the correction factor to Fermi's formula is

$$[2/(1+\rho)]^{3/2}[1+(2\rho+2)^{1/2}]\cdot[\rho(4\rho^2-1)]^{-1}.$$

* In fact it is readily found that $\psi^2(0)=1/\pi a_0^3n^3$ where $a_0=h^2/(4\pi^2mZe^2)$ and n is the total quantum number.

[3] E. Back and S. Goudsmit, Zeits. f. Physik **43**, 321 (1927); **47**, 174 (1928).

This correction factor is even larger than that derived for 1*s* electrons. For U it is 3.94. Neglecting screening the splitting of the L_{11} level of U can be expected to be $3.94/2.78\times(1/8)=1/5.64$ of the K level splitting. For the lighter elements this fraction approaches 1/8. It is presumably much less accurate however to apply the present method of calculation to the L electrons because screening effects must be more important here. Their importance may be expected to be least for the heaviest elements. The order of magnitude of the splitting of the L_{11} level of U supposing its nucleus to have a spin 9/2 and a magnetic moment 9/2 proton units is 4.0 volts. The frequency of the L_{11}—M_{21} line of the L series is 1221×13.55 volts. For the L series $\nu/\Delta\nu$ is therefore also of the order 4150. This estimate is, however, not as accurate as the one for the K series on account of the screening effects. It is mentioned here only because it is of interest to see that the same order of magnitude of the splitting can be expected for both series and because the L series is more accessible experimentally.[4]

The writer is very grateful to Dr. E. Wigner for an interesting discussion.

[4] A single observation of the fine structure separation of the K levels gives only $(2k+1)\mu/k$. In order to obtain μ it will be necessary to determine k either by optical means (band spectra, hyperfine structure) or else by observing multiplicities of other X terms, or perhaps by intensity measurements of the hyperfine structure components in the K series.

ON THE REFLECTION OF THE $K\alpha$ LINE OF CARBON FROM A GLASS MIRROR

By Jean Thibaud
Laboratoire de Physique des Rayons X, Paris

(Received January 14, 1930)

Abstract

The author recalls previous experiments which he tried in order to determine the limiting angle of total reflection from a glass grating, for a set of radiations between 20 and 65A, making a slight correction to a recent work of E. Dershem on the reflection of the $K\alpha$ line of carbon. In the case of glass, with $\lambda = 44.9$A, if we take into account the discontinuities of absorption in the dispersive medium, the Kallman-Mark dispersion formula leads us to a result ($\delta = 1 - n = 5.73 \times 10^{-3}$) of the same order as the Drude-Lorentz simplified formula. The reflected intensity from the mirror is calculated from the angle of incidence, account being taken of the absorption. The result is then compared with the experimental curve given by Dershem for the $K\alpha$ line of carbon, and shows that it is possible to determine the critical angle of total reflection from glass ($\theta_m = 6°12'$) and the refractive index ($\delta = 1 - n = 5.84 \times 10^{-3}$).

IN a previous work,[1] I have endeavored to determine the critical angle θ_m of total reflection for a beam of soft x-rays (wave-length between 20 and 65A) by varying the glancing angle of incidence of the beam upon a glass grating and measuring the angles $\theta_{1/2}$ at which the intensity of each line of the spectrum had decreased to one-half value. The conclusions were then: *a*. The reflected intensity does not *suddenly* decrease for a certain angle θ_m: instead of this limit in total reflection, we find for the reflected intensity a somewhat *flattened* curve, the shape of which may be computed by using the Fresnel formulae and taking into account the intense absorption of soft x-rays in the medium.[2] *b*. An increase in the flattening of the reflection curve is observed, with increase of the wave-length (from $\lambda = 45$A to $\lambda = 65$A). *c*. The $\theta_{1/2}$ angles of half-decreased intensities increase in proportion to the wave-length λ. They are equal to several degrees. $\delta = 1 - n$ (n = index of refraction) therefore varies as the square of λ.

The simplified form of the Drude-Lorentz dispersion formula seems to be verified:

$$\delta = \frac{e^2}{2\pi m} \frac{N}{c^2} \lambda^2, \tag{1}$$

if we add a numerical coefficient 0.5 in the calculation of $\theta_{1/2}$.

Recently E. Dershem[3] has determined the curve connecting the reflected intensity with the glancing angle of incidence for the $K\alpha$ line of carbon and a glass mirror. He concludes that his measures do not confirm my previous

[1] Thibaud, Comptes rendus, **187**, 219 (1928).
[2] Cf: especially: J. Thibaud, Annales Soc. Scientifique Bruxelles, Series B, **48**, 167 (1928).
[3] E. Dershem, Phys. Rev. **34**, 1015 (1929).

results. A mistake has crept in Dershem's paper regarding his interpretation of my results. The θ_m angles in my numerical table are not connected with the complete disappearance of the reflected line (I have assumed for θ_m almost the same number as for the measured angle $\theta_{1/2}$). I insisted rather (see for instance reference 2) upon the gradual decrease of the intensity with increase of angle, and upon the great difficulty of locating with some definiteness the critical angle of total reflection.

The only difference between Dershem's results and mine is that the decrease as a function of the angle in the intensity diffracted by a grating seems more rapid than when determined from an ordinary glass mirror. Prins[4] has made a remark on this subject. A grating seems thus less fit for an accurate determination of θ_m. At another place[5] Dershem says that the shape of the curve makes it difficult to determine the limiting angle θ_m and that, on the other hand, it seems doubtful to him whether the index of refraction may be computed from the simplified Drude-Lorentz formula. I wish to discuss further these two points.

1. Kallman and Mark have changed, for the case of x-rays, the dispersion formula as quoted in Eq. (1) into another expression, which takes into account the presence of critical frequencies in the dispersive medium:

$$\delta = \frac{e^2}{2\pi m}\sum\frac{Ni}{\nu^2} = 1 + \frac{\nu_i^2}{\nu^2}\ln\left(1 - \frac{\nu^2}{\nu_i^2}\right) \qquad (2)$$

and which seems to be correctly verified with ordinary x-rays.[6]

I have already pointed out[7] that the results as computed from Eq. (2) in the case of about 50A x-rays, the absorption discontinuities being taken into account, show but little difference from the numbers given by the simplified formula (1): the atomic "resonators" for the wave-length considered effect no important disturbance of index.

Let us consider with especial care the case of the reflection of the $K\alpha$ carbon line ($\lambda = 44.9$A) from an ordinary glass mirror.

If we take into account[8] the K and L discontinuities of the different constituents of glass (Si, O, Na, Ca, etc.), we find by using formula (2):

$$\delta = 5.73 \times 10^{-3},$$

whereas formula (1) would give:

$$\delta = 7.08 \times 10^{-3}$$

which is quite of the same order.

The discrepancy between the results of the two formulae becomes appreciable only for wave-lengths very near (1 or 2A) to an L, or especially an

[4] Prins, Nature, Sept. 7, 1929.

[5] Reference 3, p. 1020.

[6] A. Larsson, Dissertation. Uppsala (1929).

[7] Thibaud et Soltan. Journ. de Physique **8,** 494 (1927) and: Thibaud, Phys. Zeits. **29,** 259 (1928).

[8] The calculation will appear very soon in the Journ. de Physique.

M or N discontinuity of one of the constituent elements of the reflecting mirror. But for glass and ordinary metals, the latter case is reached only for radiations of more than 100A.

2. Reflected intensities may be computed from angles, in the case of a medium strongly absorbing for the radiation, by using the Fresnal equations relative to the components of incident and reflected radiations, which are parallel to the mirror plane. In the case of a complex index[9]

$$n' = (1 - \quad) - i\kappa$$

(κ = extinction coefficient; $\kappa = \mu\lambda/4\pi$; μ = absorption coefficient for λ in the medium). We thus arrive at an expression of the ratio A of reflected and incident intensities as a function of the angle θ,

$$A = \frac{(1+m)^2 + 2(m^2+a^2)^{1/2} + 2(1+m)\left[2(m^2)^{1/2}\right]^{1/2} + a^2\cos\phi/2}{(1+m)^2 + 2(m^2+a^2)^{1/2} - 2(1+m)\left[2(m^2+a^2)^{1/2}\right]^{1/2}\cos\phi/2} \qquad (3)$$

in which: $\theta = (1+m)\theta_m$; $a = \kappa/2\delta = \mu\lambda/4\pi\theta_m{}^2$; $\tan\phi = -a(1-\delta)/m$; $\pi < \phi < 2\pi$. The graphic representation of (3) is given on Fig. 1 for different values of the coefficient a between 0.01 and 1.

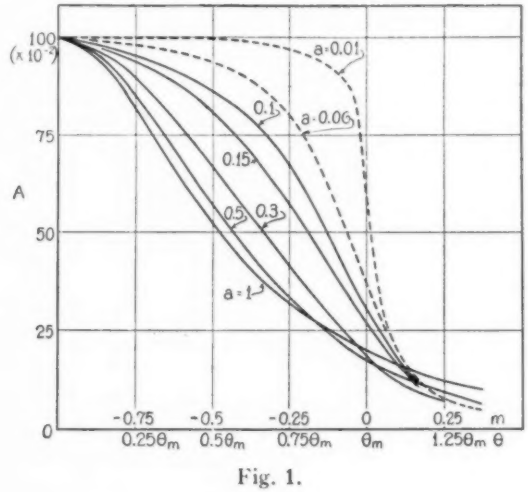

Fig. 1.

It is easy to see, with formula (3), that the reflecting power A_0 connected with the angle $\theta = \theta_m$, goes thrugh a minimum ($A_0 = 0.17$) for $a = 0.5$. Thus, for wave-lengths much longer than 45A and very strong absorptions μ, one would notice an *increase* in the reflected intensity for angles $\theta > \theta_m$.

The curves show that, in the neighborhood of $a = 0.5$, the reflecting power A_0 suffers only small variations, around 20 percent, and that for $\theta_{1/2} = 0.5\theta_m$, the reflected intensity is about one-half of incident intensity.

In the case of the reflection of the $K\alpha$ line of carbon, from a glass mirror, we have no accurate measurements of the absorption coefficient μ of glass.

[9] See also: R. Forsler, Helv. Phys. Acta **1**, 18 (1927). and J. Prins, Zeits. f. Physik **47**, 479 (1928).

The most probable value, as concluded particularly from unpublished measurements of Holweck, is $\mu = 10^5$. If we adopt the above computed value $\delta = 5.73 \times 10^{-3}$, we find: $a = 0.31$.

One may notice a close similarity between the curve $a = 0.3$ (Fig. 1) as computed from (3), with the experimental curve of reflection given by Dershem. For $a = 0.3$ we find $A_0 = 0.19$. The angle θ for which the reflected intensity is reduced to 19 percent of initial intensity is equal, on Dershem's curve to 6°12′. It is the critical angle θ_m of total reflection of the $K\alpha$ carbon line from glass. The corresponding value of the index is:

$$\delta = \frac{\theta_m^2}{2} = 5.84 \times 10^{-3}.$$

It is therefore possible to determine, from the experimental curves of reflection, the limiting angle and the refractive index $n = 1 - \delta$. The result is in good accord with the value as deduced from the Kallman and Mark formula (2) ($\delta = 5.73 \times 10^{-3}$). It follows moreover that the extinction coefficient, in the case of the $K\alpha$ line of carbon and glass, is approximately: $\kappa = \alpha \times 2\delta = 3.5 \times 10^{-3}$.

Lastly the curves show that the desired limiting angle θ_m is almost double the angle $\theta_{1/2}$, and thus we find the reason a 0.5 coefficient was to be introduced in my previous researches when θ_m was (arbitrarily) taken equal to $\theta_{1/2}$.

MOLYBDENUM *L*-SERIES WAVE-LENGTHS BY RULED GRATINGS

By J. M. Cork
Department of Physics, University of Michigan

(Received May 12, 1930)

Abstract

With plane ruled gratings having 30,000 lines per inch and 14,400 lines per inch and grating to photographic plate distances up to a meter in length in vacuo, about 160 plates were taken of the Mo *L*-series lines. The wave-lengths for $L\alpha_1$, and $L\beta_1$, as given by Siegbahn using a gypsum crystal are 5.3943A and 5.1658A. If a calcite crystal were employed and approximate correction made for refraction, wave-lengths 5.3960A and 5.1674A should be expected, whereas the average of the ruled grating measurements gave 5.4116A and 5.1832A. A comparison of the two values leads to an apparent value of the electronic charge 4.8162×10^{-10} e.s.u., being slightly higher than Bearden's value using Cu *K* lines. The possibility of the variation being due to anomalous variation in the refractive index of the crystal is discussed.

THE possibility of the absolute determination of x-ray wave-lengths by means of ruled diffraction gratings, has now been demonstrated.[1] The most precise results so far obtained[2] indicate that x-ray wave-lengths determined by the ruled grating method are somewhat longer than when determined by the crystal reflection method. Unfortunately, however, agreement regarding the magnitude of this discrepancy is still lacking. Since this wave-length difference may be given the interpretation that the Avogadro number, used in calculating the dimensions of the unit cell in the fundamental crystal lattice, was in error and hence also the value of the electronic charge, its importance is evident. In comparing wave-length values obtained by the two methods, the results from the crystal method should first be corrected for the index of refraction of the crystal. For long wave-lengths, that is, crystals of large lattice constant, this correction is appreciable and it may be further complicated at certain wave-lengths by anomalous effects.

It was the original intention in this investigation to report on the *L* series wave-lengths for the metallic elements from Mo 42 to Ba 56 and several plates were taken for each of these elements, but in view of the significance of the results it was considered more important at this time to carry out an exhaustive study with one of the elements. For various reasons molybdenum was chosen for the target material.

Granting a certain error in setting upon a spectral line in the measurement of the photographic plates, the overall accuracy is increased by having the final result depend upon large distances upon the photographic plate. For a

[1] Compton and Doan, Proc. Nat. Acad. Sci. **11**, 598. 1925; Thibaud, Comptes rendus, **182**, 55, (1926).

[2] Wadlund, Phys. Rev. **32**, 841, (1928); Bäcklin, Dissertation, Upsala, 1928, Bearden, Proc. Nat. Acad. Sci. **15**, 528, (1928).

given wave-length, two main factors contribute to the distance between lines on the photographic plate, namely, the grating constant (i.e. distance between adjacent ruled lines) and the distance between grating and photographic plate. For large displacements the grating constant should be small and the distance between grating and photographic plate large. The dispersion also depends to a slight extent upon the value of the incident grazing angle employed, being greatest when this angle is least. The use of inside spectral orders, that is, those lying between the regularly reflected beam and the diffracted beam parallel to the grating, has been proposed,[3] since it leads to very large dispersion when the diffracted beam becomes parallel to the grating. Although this method is eminently satisfactory to show fine structure in this narrow region, its value in the absolute determination of wave-length must not be overestimated. The use of sufficiently large incident angles to give linear displacements on the plate comparable with those of high outside orders is prohibited due to the critical grazing angle for the grating material.

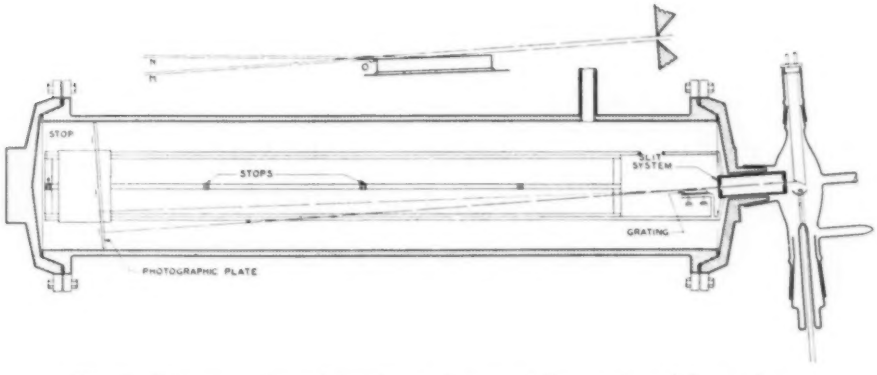

Fig. 1. Diagram of spectrometer and x-ray tube as viewed from above.

Apparatus

For this wave-length region the complete spectrometer must be in a vacuum with no absorbing layer between the x-ray tube and diffraction chamber. Fig. 1 is a schematic drawing of spectrometer and x-ray tube as viewed from above. The x-ray tube was made of glass and provided with a water-cooled target. The cathode was an activated platinum spiral. Both cathode and anode were removable by ground glass joints. The tube as a whole was mounted on the end of the brass spectrometer tube by a ground glass to metal joint.

Radiation from the target was collimated by parallel slits so as to be incident upon the grating at grazing angles from ten to forty minutes of arc. The slits were approximately 0.05 mm in width and were adjustable in distance from 12 cm to 24 cm. In the adjustment of the grating, part of the collimated beam was allowed to miss the grating surface, giving a

[3] Howe, Phys. Rev. **35**, 717 (1929).

beam direct to the photographic plate one edge of which was sharply defined by the shadow of the grating edge.

The photographic plate is carried by a plate holder in such a position that the direct beam is incident upon it normally. The plate holder travels upon a heavy grooved track carefully adjusted for parallelism. Four definite positions for stopping are provided by allowing the carriage to make contact with stops, the distances between which were accurately measured upon the same comparator used for the photographic plates. Two positions would have sufficed to determine the distance between plate and grating by triangulation. The photographic plates were changed by removing a metal cap from the end of the spectrometer tube, fitted by ground metal joint.

The slit system, grating and plate holder bed were all a single rigidly connected unit which could be removed completely from the tube without disturbing the adjustment. The containing brass tube had a diameter of 21 cm and a length of 110 cm. The x-ray tube and spectrometer chamber were evacuated by separate mercury vapor pumps with liquid air traps, although gas could pass freely between them through the slit system. The spectrometer tube and the end brass castings were tinned inside and out by immersion for a short time in a bath of molten tin.

The mounting for the grating was provided with adjusting screws so that the grating could be tilted in any direction. In the present investigation four different glass gratings were employed. Three of these were nominally ruled 30,000 lines per inch by Professor R. W. Wood at Johns Hopkins University, while the fourth was a 14,400 line per inch grating ruled at this University by Professor E. F. Barker and Mr. Weyrich.

Calculation

The fundamental grating relationship for constructive interference is

$$n\lambda = \pm d[\cos\theta - \cos\phi]$$

where θ is the small grazing incident angle and ϕ is the angle between the diffracted beam and the grating surface. The distance in Angstroms between adjacent ruled lines on the grating is represented by d, and n represents the spectral order. For the regularly reflected beam θ and ϕ are equal, while for outside orders, ϕ exceeds θ and the plus sign is used, whereas for inside orders ϕ is less than θ and the sign is negative.

The dispersion for a given setting of θ then (for outside orders) becomes:

$$\frac{\partial\phi}{\partial\lambda} = \frac{n}{d\sin\phi}.$$

This is not independent of θ since for smaller values of θ the value of ϕ and hence $\sin\phi$ for any particular wave-length becomes smaller.

In the upper part of Fig. 1 is shown an enlarged sketch of the grating with the direct and reflected beam. It is evident that the ray m in the direct beam and the ray n in the reflected beam have a common origin in the edge of the

grating at 0. Thus by measuring on the photographic plate the distance between outside edges of direct and reflected lines and dividing by the distance between the grating edge and photographic plate the tan 2θ and hence θ is at once determined.

The origin of the spectral lines is not the edge of the grating but an effective diffracting center which may be as much as a millimeter farther from the plate if a 2 mm width of the ruled surface is employed. To determine the distance between the photographic plate and the effective grating centre, the following procedure is carried out. With some particular x-ray source, spectrograms are obtained for the photographic plate in each of the four positions. By measuring the distance between any pair of these lines sufficiently far apart on any two of the plates and solving by similar triangles the origin or effective center may be located. While two positions would be sufficient, in most cases all four positions were used for confirmation of results. Such spectra for three positions for a molybdenum target are shown in Fig. 2.

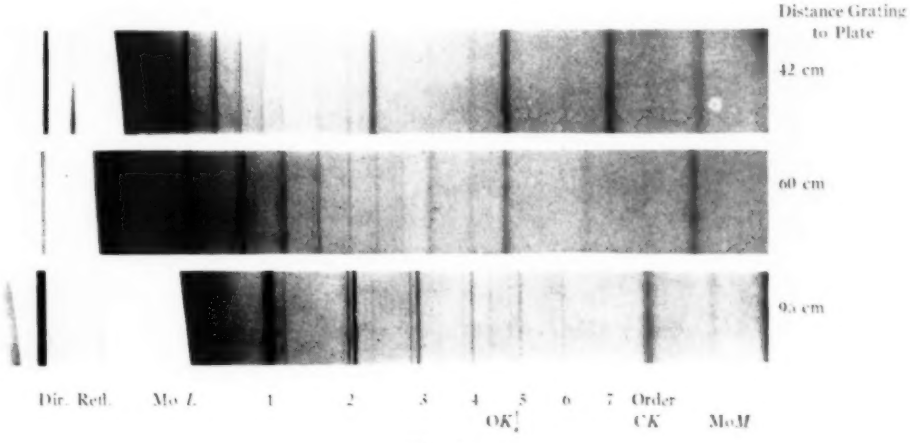

Fig. 2.

Now to calculate wave-lengths, the distance between the outside edge of the direct beam and each spectral line is measured on the comparator. This distance in each case divided by the respective normal plate to grating distance gives tan $(\theta+\phi)$ and hence the ϕ for any spectral line. Since θ is already calculated for all of the lines the approximate value of λ is at once determined. The term approximate is used, since the edge of a line may be somewhat altered in position by growth of blackening due to over exposure. This does not, however, lead to any error in the final result because the spectral line is observed in many orders, thus on the molybdenum plates shown in Fig. 2 seven orders are available for calculation. Now if the wave-lengths as calculated from the various orders show a systematic variation, the results may be made concordant by the addition or subtraction of a small amount from all observed distances of the spectral lines from the edge of the direct beam. Experience shows that errors in the value of θ by as much as 15″ of arc,

would automatically be corrected by this same operation, leading always to the same final values of λ when agreement between the various orders is obtained. Thus a real error in the exact location of the edge of the direct beam or of the incident angle θ need, if not too large, produce no appreciable error in final results, if several orders of some spectral line are available on the plate. In making the wave-length calculations, particularly in obtaining the cosines of the small angles, the fifteen place 'Andoyer—Tables Trigonometriques' is invaluable.

Results

The grating constant for the 30,000 line gratings was determined by an optical spectrometer using the strong lines in the mercury arc spectrum as known wave-lengths. The result of this experiment gave the number of lines per inch as 30,011 or d equal to 8, 463.3 Angstrom units. This is somewhat at variance with the result obtained by Thibaud[4] for gratings from the same source, namely 29,972 lines per inch or d equal to 8, 477 Angstrom units. This latter value would lead to even longer wave-lengths than those recorded in this paper.

Since the ruling machine was available on which the 14,400 line grating was ruled, it became possible to determine the constant for this grating in another way. This machine employed a wheel having 720 teeth mounted on the head of a screw whose pitch was nominally 1/20 of an inch. If the pitch of the screw therefore were accurately determined this would give the width of 720 lines. A special steel bar was prepared and ruled with light lines, one for every ten revolutions of the screw. This scale was then calibrated in terms of the International meter. The result showed the pitch of the ruling machine screw in the part used to be very uniform and to be 0.050008 inch, such that there were 14,397.6 lines per inch or a value of d equal to 17,641.8 Angstrom units. In all, about 160 plates were taken on molybdenum using the different gratings with different adjustments on each, as well as various plate to grating distances. The average of all calculations are given in Column 1 in the following Table I in Angstrom units.

Table I.

Grating Measurement	Gypsum crystal	Calcite crystal (Calc.)	Corrected for crystal refraction
$\lambda MoL\alpha_1$ 5.4116	5.3943	5.3967	5.3960
$\lambda MoL\beta_1$ 5.1832	5.1658	5.1681	5.1674

The values obtained by the crystal method using a gypsum crystal are given in column 2.* Siegbahn and Hjalmar[5] have shown that if the ratio

[4] Thibaud, J.O.S.A. and R.S.I. *17* 145 (1928).

* The values of λ published in the abstract of a paper presented at the Chicago meeting of the American Physical Society, Nov., 1930, were, by error, these values from Siegbahn with which the experimental values were compared to obtain the value of e therein given.

[5] Siegbahn and Hjalmar, Nature **115,** 85, (1925).

$d_{\text{calcite}}/d_{\text{gypsum}}$ be obtained with different wave-lengths, a variation in this quantity from 0.39976 at 1A to 0.39959 at 5.5A is observed, with anomalous peaks at 3.06A and 5.01A corresponding to the K absorption edges of calcium and sulphur respectively. This relationship may then be employed to calculate what the wave-lengths of the Mo L lines would be if measured by a calcite crystal since for gypsum, $d = 7.578$A, was used at all wave-lengths. Such results are given in column 3. These values may now be corrected for the deviation to the Bragg law due to ordinary refraction in the crystal, by the approximate formula, as follows:

$$\lambda = \lambda' \left[1 - 5.4 \frac{\rho d^2}{n^2} \cdot 10^{-6} \right]$$

where λ' denotes the apparent wave-length, n the spectral order, ρ and d the density and lattice constant of the crystal respectively. For calcite this gives a correction factor of 0.014 percent for the first order spectra. Such results are recorded in column 4, and are the values to be compared with those of column 1.

It should be noted that the ratio $d_{\text{calcite}}/d_{\text{gypsum}}$ changes by as much as one half of a tenth of a percent for wave-lengths from 1A to 5A. This variation is of the nature of a difference effect and it may well be possible that the variation in calcite alone may be much greater than this.

The dispersion formula showing the effect of wave-length change upon the index of refraction as developed from polarization theory is as follows:

$$\delta = \mu - 1 = \frac{e^2}{2\pi m} \sum^{N} \frac{N_e}{\nu_e^2 - \nu_x^2}$$

where μ represents the index of refraction, N the total number of mobile electrons per cm^3, N_e the number of electrons per cm^3 having the natural frequency ν_e and ν_x represents the x-ray frequency. For x-rays in which ν_x is large compared with ν_e, the quantity δ is negative leading to a correction to the Bragg law as shown above, i.e. true wave-length less than apparent. Now as the x-ray wave-length increases or as the frequency decreases, the value of δ becomes more negative but upon passing through the K absorption limit of calcium the contribution of the calcium K electrons changes from negative to positive and at longer wave-lengths δ may actually become positive, in which case the true wave-length will be greater than the apparent.

If possibilities of error due to this variable refractive index be over looked, the values of column 1 may be compared with column 4 to determine what would be implied regarding the value of the electronic charge. The value of the electronic charge as determined by the oil drop method as corrected by Birge[6] for best values of the viscosity of air, velocity of light and transformation factors to change from International to absolute electrostatic units is $4.768 \pm 0.005 \times 10^{-10}$ abs. e.s.u. Tempering this value by the consideration of Wadlund's result from x-rays, the most probable value was

[6] Birge, Phys. Rev. Sup. **1**, 40, (1929).

given as $(4.770 \pm 0.008) \times 10^{-10}$ e.s.u. However, in the most accurate determination by calculation, of a fundamental crystal lattice, namely that of calcite by Compton, Beets and DeFoe,[7] the Avogadro number was assumed to be $(6.0594) \times 10^{23}$ which combined with Birge's most probable value of the Faraday, $(2.89270 \pm 0.00021) \times 10^{14}$ e.s.u. means that e was assumed to be 4.7739×10^{-10} e.s.u. The calcite lattice constant as so computed agreed exactly with the value as used by Siegbahn in his wave-length determinations, namely 3.02904A at 18°C.

For the α_1 line the wave-length by ruled grating is 0.288 percent greater than the corrected crystal measurement, while for the β_1 line a difference of 0.304 percent is observed. The average of these values gives for the electronic charge the apparent value of 4.8162×10^{-10} e.s.u. and for the Avogadro number $(6.0062) \times 10^{23}$. This value of the electronic charge is thus even larger than Bearden's value of 4.804×10^{-10} e.s.u. obtained by CuK wave-lengths.

The explanation of this effect as due to a surface contraction as discussed by Zwicky[8] is unlikely. Such contractions are supposed to be only a few atomic layers deep and certainly many hundred atomic planes must cooperate in the x-ray reflection even up to 5 Angstroms. Also there is good agreement between crystal measurements by the transmission and reflection methods. Furthermore, a surface contraction would have to be interpreted as increasing the discrepancy rather than decreasing it, since instead of multiplying the observed sin θ by an average d one should use the smaller surface d.

Attempts to explain the effect by altering the general grating formula for the case of grazing incidence, narrow grating width and ruling defects seem to prove inadequate for differences as large as observed.

[7] Compton, Beets and DeFoe, Phys. Rev. **25,** 625 (1925)
[8] Zwicky, Proc. Nat. Acad. Sci. **15,** 253 (1929).

THE INDEPENDENCE OF X-RAY ABSORPTION ON TEMPERATURE

By J. A. Bearden
Johns Hopkins University, Baltimore

(Received May 12, 1930)

Abstract

If the absorption coefficient of x-rays is dependent upon the temperature of the absorber it is pointed out that the effect can be made easily measurable by increasing the thickness of the absorber. Using this method in which the thickness was made very great, measurements have been made on Al, Cu, Fe, Ni, Ag, and Pb. Heterogeneous x-rays were used with voltages from 30 to 80 k.v., also the monochromatic x-ray lines $K\alpha_{1,2}$ of silver and copper were used. All measurements showed no effect of temperature on the absorption coefficients within the probable error involved in the thermal expansion coefficients.

It is also pointed out that the effect of temperature on the absorption of x-rays and γ-rays, as found by previous investigators, was probably due to an error in the determinations of the linear absorption coefficient. When their results are corrected, using the absorption coefficient of the beam transmitted by the absorber, the results are in agreement with the present experiments.

MEASUREMENTS have been reported[1,2] which indicated a change in the atomic absorption coefficient of x-rays with a change in the temperature of the absorbing screen. In the first[1] series of these measurements using the direct x-rays from a Coolidge tungsten x-ray tube and absorbing screens of Al, Cu, Fe, Ni, Ag, and Pb an increase in the atomic absorption coefficient was observed as the temperature of the absorber was increased. The increase was about 0.2 percent per 100°C up to temperatures near the melting point of the absorber. The second[2] series of measurements were made using narrow bands of x-rays of various wave-lengths absorbed in Ag and Ni. For some wave-lengths the absorption was greater than the normal absorption and for others it was less. Similar observations[3] have been made using -γ rays and absorbers of Pb, Fe, Sn, and Al. In each case it was found that the absorption coefficient increased with an increase in the temperature of the absorber. For both γ-rays and x-rays, if the change in absorption is expressed as a linear function of the temperature as $\mu' = \mu(1+\beta T)$ where μ' and μ are the linear absorption coefficients of the absorber when hot and cold respectively it is found that β is proportional to the thermal expansion coefficient of the absorber.

Existing theories of absorption of x-rays and γ-rays offer no explanation of such an effect. Thus the effect offers a critical experimental check on the theoretical correctness of absorption theories. The present experiments were

[1] Read, Phys. Rev. **27,** 373 (1926).
[2] Read, Phys. Rev. **28,** 898 (1926).
[3] Bastings, Nature CXIX, **51** (1927), Phil. Mag. **7,** 337 (1929).

undertaken with the purpose of making more accurate observations of the change in absorption of x-rays with various wave-lengths and absorbing screens.

Method

The expected change in the intensity transmitted by the absorber when cold and hot due to the thermal expansion of the absorber may be calculated as follows:

Let I_0, I_c and I_h be the intensities of the direct x-ray beam, the beam transmitted by the absorber when cold, and when hot respectively.

Then $I_c/I_0 = e^{-\mu_c x}$

and

$$\frac{I_h}{I_0} = e^{-\mu_h x/(1+\alpha T)^2} \tag{1}$$

where μ_c and μ_h are the linear absorption coefficients of the absorber when cold and hot respectively, x the thickness, and αT the linear expansion of the absorber. The ratio of intensity transmitted by the absorber when cold and hot is then

$$\frac{I_h}{I_c} = e^{(\mu_c-\mu_h)x+2\mu_h x\alpha T}. \tag{2}$$

For a heterogeneous beam μ_c and μ_h refer to the effective linear absorption coefficient of the beam transmitted by the absorber when cold and hot respectively. This of course would have to be measured by using absorbers of the same material and extrapolating to a thickness equal to the thickness x of the absorber used in Eq. (2). The percentage change in transmitted x-ray intensity is

$$\frac{I_h - I_c}{I_c} = (\mu_c - \mu_h)x + 2\mu x\alpha T \tag{3}$$

in this equation μ is really μ_h but since μ and μ_h cannot differ by more than 0.1 percent, the use of the normal absorption coefficient introduces practically no error in the value of $(I_h - I_c)/I_c$

From Eq. (3) it will be seen that the greatest change in x-ray intensity will be for an absorber of maximum thickness x. Experimentally one must make x such that I_c and I_h are easily measured. For direct radiation from an x-ray tube the area of the collimating slits can be made very great and correspondingly x made larger. In the case of x-rays reflected from a crystal the area is very limited but with water cooled x-ray tubes where the x-ray intensity is very great x can still be made large. It will be noticed in Eq. 3 that a measurement of the intensity I_0 which may be 1000 times I_c or I_h is not needed. In the present experiments I_c and I_h were measured using two exactly similar pieces of metal for the absorbing screen so placed on an eccentric that either could be inserted in the path of the x-ray beam. One piece was placed in a furnace and the other kept at room temperature. After a series of measurements of I_c and I_h had been made the two absorbers

were interchanged and a new set of readings taken. This procedure was adopted to make it possible to obtain I_c and I_h without a time lag and without a change in temperature of slits, sensitivity of electrometer, etc. Previous experiments[1,2,3] have indicated that

$$(\mu_c - \mu_h)x = \mu x \alpha T$$

so if one makes x large enough to make $(I_h - I_c)/I_c = 0.1$ or larger the effect of such a change in absorption would change the x-ray intensity by 5 percent or more. Such a change in intensity can be easily measured.

Apparatus

The high voltage outfit consisted of a regular high voltage transformer (165 k.v. 500 m.a.) connected to a four kenetron full wave rectifier. The kenetrons and all filament transformers were immersed in oil in order to reduce the corona discharge. The source of a.c. was a motor generator set (15 k.w.) with the field of the generator connected to a large capacity storage battery. With this arrangement it was possible to hold the primary a.c. constant to 0.2 percent over a long period of time. Two x-ray tubes were used, one was a water-cooled copper target Coolidge tube, the other a water-cooled silver target Coolidge tube. A thin window (0.01 mm al.) was provided

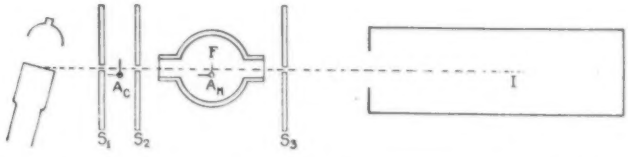

Fig. 1. Diagram of apparatus as used with heterogeneous x-rays. For the $K\alpha_{1,2}$ lines of Ag and Cu a calcite crystal was inserted between S_3 and the ionization chamber.

for the copper target tube to reduce the absorption of the characteristic copper x-rays. The x-ray tubes were operated at 20 to 40 m.a. and 25 to 80 k.v.

The ionization chamber was 7.5 cm in diameter and 30 cm long filled with argon. The electrometer (Compton type) was mounted directly above the chamber in order to reduce the electrical capacity. The sensitivity of the electrometer was about 10,000 division per volt.

The furnace was made up from a heavy wall copper tube 7 cm long with copper top and bottom (Fig. 1). The tube was insulated with asbestos on the top and sides and was heated with a gas flame from the bottom. The openings for the x-rays to pass through were made by inserting brass tubes into the side of the furnace and covering the ends of the tubes with aluminum (0.01 mm thick). The furnace was filled with hydrogen to prevent oxidation of the absorbing screens. The temperature was measured with a 600°C mercury in glass thermometer, placed so the bulb of the thermometer was very near the absorbing screen. The absorbing screen was mounted on a rod (Fig. 1) so it could be placed in or out of the path of the x-rays by rotating the supporting rod from outside the furnace. A long arm was attached to the supporting rod outside the furnace and a stop arranged so the absorber could be rotated

back into exactly the same position for each measurement. A similar method was used for moving the cold absorber in and out of the x-ray beam. In the case of the thin foils it was found necessary to use a frame (made of the same material as the absorber) to hold the absorbers so they would not bend or warp when heated. This was accomplished by making two frames and placing the foil between the frames and then fastening the frames to the rotating support.

Methods of Making Measurements

Three types of radiation were used. First, the copper $K\alpha_{1,2}$ line and the silver $K\alpha_{1,2}$ line reflected from calcite; secondly, the direct rays from the copper and silver targets operated at voltages from 20 to 80 k.v. and third, the direct ray from these tubes filtered through copper and aluminum. The dispositon of the apparatus is shown in Fig. 1. The slits were made of lead in the usual manner and were protected by sheets of asbestos from the heat given off by the furnace so that no appreciable expansion took place. When the heterogeneous rays from the tube were used, the slits were 4 mm wide and 2 cm high. In the case of the x-rays reflected from calcite the slits were 1 mm wide and 2 cm high. It will also be noticed that an expansion or shift of slits cannot effect the results taken by this method of comparison. The cold absorber A was placed perpendicular to the x-ray beam. With the furnace cold the angular position of the absorber B in the furnace was adjusted until it absorbed the same amount (to within 1 percent) of x-rays as the absorber A outside the furnace. The furnace was then heated to 600°C and allowed to cool to room temperature again. A series of measurements (usually 10) were then made, alternately placing the absorber A and B in the path of the rays. The furnace was then raised to a temperature 90 to 100°C above room temperature. A series of measurements similar to those made above were then made. This process was repeated advancing the temperature in steps of 90 to 100°C for each series until a temperature of 600°C (except in the case of Pb) had been reached. The process was then reversed and the temperature lowered in similar steps and similar measurements taken until the furnace was brought back to its original temperature (room temperature).

The intensity transmitted by each absorber was never exactly the same so a small correction factor (less than 1 percent) had to be applied in order to obtain the true values of I_c and I_h. The absorption coefficient μ in Eq. (3) was measured by placing A or B in the path of the x-ray beam and then adding thin layers of the same material in the path of the x-ray beam and measuring μ for each layer. By extrapolation the value of μ was obtained for 0 thickness of added absorbers which was the value used in Eq. (3).

The values for the thermal expansion coefficients used were taken from the tables of Landolt and Börnstein, 5th edition.

Results

The results for the heterogeneous x-rays are plotted in the graphs of Fig. 2, in which the values of $I_h - I_c/I_c$ are plotted against the temperature of the

absorber. The solid line is calculated from Eq. (3) in which the term $(\mu_c - \mu_h)x$ has been neglected. The dotted line was calculated assuming that

$$(\mu_c - \mu_h)x = \mu x \alpha T$$

which seemed to fit with the experimental measurments of previous experiments.[1,2,3] The circle represents the experimental values obtained in the

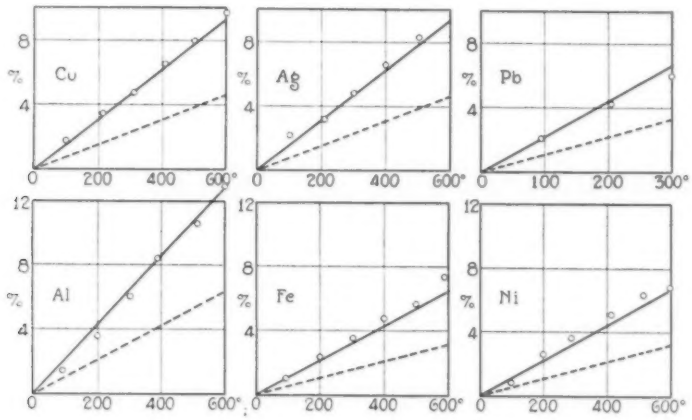

Fig. 2. The experimental points (small circles) were determined with heterogeneous x-rays from a Cu target operated at 50 kv. The solid line is drawn assuming no temperature effect on absorption of x-rays.

present work. It will be seen that the experimental points lie on the solid line within the error of the measurements and the error which must be present in

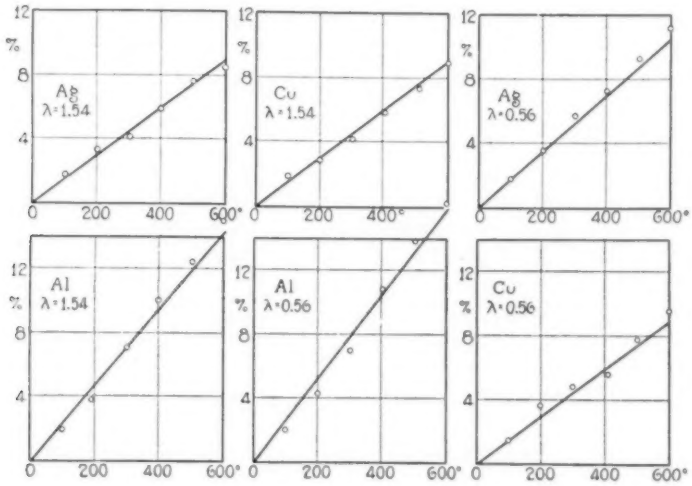

Fig. 3. Same as Fig. 2 except the monochromatic $K\alpha_{1,2}$ lines of Ag and Cu were used.

the thermal expansion coefficients. In the case of aluminum and copper the experimental points seem to be a little higher than the solid line but there

are differences in the thermal expansion coefficients given by various experimenters which would account for the difference observed here. The results using the monochromatic wave-length $K\alpha_{1,2}$ of copper and silver absorbed in silver, aluminum and copper are shown in Fig. 3. In each case the experimental points, as above, agree with the theoretical curve within the error of the measurements and the error involved in the thermal expansion coefficient.

Similar results were obtained using x-rays filtered through copper and aluminum. The x-ray measurements are believed to be more accurate than the thermal expansion coefficients are known. Thus the method may be conveniently used to measure the change in the thermal expansion coefficients with change in temperatures.

Discussion and Conclusion

The change in absorption found by Read in his first experiments[1] using a heterogeneous x-ray beam is undoubtedly due to the use of the wrong absorption coefficient μ in Eq. (3). He measured μ by removing the absorber and measuring I_0 of the direct beam. This gives a value of μ which is entirely too high. It is clear from the way in which Eq. (3) is derived that the correct μ is the μ of the transmitted beam and not that obtained by using the I_0 of Eq. (1). If this were not the case, the change in absorption with temperature would be a function of the thickness of the absorbing screen which obviously cannot be true.

The error in the second series of measurements[2] is not so apparent. In these measurements, narrow bands of wave-lengths were used so the above effect would be greatly reduced. These measurements seemed to be somewhat erratic and some undetected experimental error must have been present. Precision absorption measurements are extremely difficult to make so that an error of a fraction of 1 percent is easily made. In the measurements of Bastings[3] on the temperature coefficient of γ-ray absorption he derives an equation

$$\beta = \frac{n'\mu'd'(1 + 2\alpha T) - n\mu d}{n\mu d T} \tag{4}$$

in which n is the number of atoms per cc, μ is the linear absorption coefficient, d the thickness of the absorber, α the thermal expansion coefficient, T the temperature of the absorber, and the prime letters refer to the absorber when hot. This equation also neglects the change in effective wave-length of the heterogeneous γ-rays in passing through an absorber. Even though there were no change in absorption with temperature it can be shown that Eq. (4) would give $\beta \propto \alpha$ which is what Bastings observes. Substituting the results of Bastings in Eq. (3) using an estimated value of μ from other sources gives no temperature effect within the error of the calculation.

Thus one is lead to the conclusion that there is no effect of temperature on the absorption of x-rays or γ-rays within the error of the present determinations of the thermal expansion coefficient.

THE EFFECT OF AN ELECTRIC FIELD ON THE X-RAY DIFFRACTION PATTERN OF A LIQUID

By Ronald L. McFarlan
Ryerson Physical Laboratory, University of Chicago

(Received April 28, 1930)

Abstract

An investigation is made of the effect produced on the x-ray liquid diffraction pattern by an electric field so designed as to give the Kerr effect for the liquid under examination. The liquid diffraction pattern is obtained by replacing the crystal of a Bragg spectrometer with a cell containing the liquid. The electric field is approximately normal to the x-ray beam. Nitrobenzene is found to show an increase in peak intensity, on applying the field, ranging from four to seven times the probable error of observation, while benzene shows no observable effect. For the type of field used nitrobenzene shows a large Kerr effect, while benzene shows only a slight effect. Theoretical considerations indicate that this effect cannot be due to molecular orientation alone, but that an increase in the regularity of the spatial distribution of molecular scattering centers must occur.

Introduction

THE form of the x-ray liquid diffraction pattern is usually interpreted as being primarily due to the arrangement of the molecules in the liquid, the arrangement of the atoms in the molecule and the electrons in the atom producing secondary effects. To the space array of molecules producing this pattern one worker has given the name cybotaxis.[1] In attempting to derive a theoretical expression for the observed distribution of intensity in the liquid diffraction pattern Prins[2] assumes that;

1. The electricity (average electron density) is distributed continuously in each molecule.
2. This electricity vibrates in the plane of incidence of the x-ray wave.
3. The phases of the emitted partial waves from all the elementary volumes must be added in order to calculate the intensity of the diffracted ray for any particular angle of diffraction.

Starting with these assumptions Prins arrives at the following formula for the intensity of the scattered rays as a function of the angle of diffraction.

$$I(s) = N\overline{A}^2 + N\overline{A^2}\int_0^\infty dr 4\pi r^2 g(r)\frac{\sin sr}{sr} \qquad (1)$$

where $s = 4\pi/\lambda \sin \phi/2$, ϕ is the angle of diffraction, r represents the distance from a fixed but arbitrary center, and N is the number of molecules which scatter the x-rays. The scattering power A of a rigid molecule is thought of as localized at this center. The average of the scattering power over all possible

[1] Stewart and Morrow, Phys. Rev. **30,** 232 (1927).
[2] J. A. Prins, Zeits. f. Physik **56,** 617 (1929).

orientations of the molecule is indicated by the horizontal line above A. The function $g(r)$, first introduced by Zernicke and Prins,[3] describes the distribution of molecular scattering centers throughout the liquid, and is defined in such a way as to make $4\pi r^2 dr\, g(r)$ represent the probability that a molecular center will lie between a distance r and $r+dr$ from a fixed but arbitrary center. The first term on the right-hand side of Eq. (1) gives the intensity due to N molecules scattering independently. The second term takes account of the interference between the rays scattered by the different molecules, and may have a negative sign.

It is a well-known phenomenon of optics that if certain liquids are placed in a strong electric field they become slightly double-refracting, behaving somewhat like a uniaxial crystal. This experiment was originally performed by J. Kerr,[4] and is known as the Kerr effect. It has, perhaps, been most successfully explained by the orientation hypothesis as developed, by Langevin Born, and others.[5] According to this hypothesis when an electric field is applied across a liquid an asymmetry is produced in it as a result of a tendency of the molecules to orient themselves in a definite direction with respect to the field because of the electric moment associated with each molecule. Two factors may contribute to the presence of this moment. In the first place the molecule may not be equally polarizable in all directions, and consequently will endeavor to set itself so that its axis of maximum polarizability is turned parallel to the field. Secondly, there may be a permanent moment associated with the molecule. Both factors are usually present.

Now, if an electric field applied across a liquid produces in the molecules a tendency to orient themselves in a particular direction with respect to the field, and consequently produces an asymmetry in the liquid it might be expected that the angular distribution of the intensity of the scattered x-rays would be altered. Since the liquid diffraction pattern is primarily molecular in origin there are two possibilities to be considered. The first is the effect which the electric field would have on the scattering of the molecules considered separately, while the second is the effect on the distribution of molecular scattering centers throughout the liquid.

Calculation of the Anticipated Effect

The effect of the field on the molecules scattering separately can be considered in the following manner. Assume that the molecules are diatomic, that they have a permanent moment m, and that the scattering power of each atom is located at its center. Then, referring to Fig. 1, the scattered intensity due to the electric vector of the incident beam which is parallel to the plane XOP will be[6]

$$I_{11} = 4\beta A_\phi^2 \cos^2\left(\frac{4\pi a}{\lambda} \sin\frac{\phi}{2} \cos\alpha\right) = 4\beta A_\phi^2 \cos^2(x \sin\alpha)$$

[3] Zernicke and Prins, Zeits. f. Physik **41,** 184 (1927).
[4] J. Kerr, Phil. Mag. **50,** 337 (1875).
[5] Cf. P. Debye, Marx Handbuch der Radiologie, Vol. VI, p. 754
[6] A. H. Compton, X-rays and Electrons, Appendix IV, p. 384.

where $2a$ represents the distance between the atomic centers, $A_\phi = zAe^2\cos\phi/rmc^2$, z represents the number of scattering electrons in each atom, ϕ is the angle of diffraction, β is a constant defined by $I = \beta A^2$ and $x = 4\pi a/\lambda \sin \phi/2$.

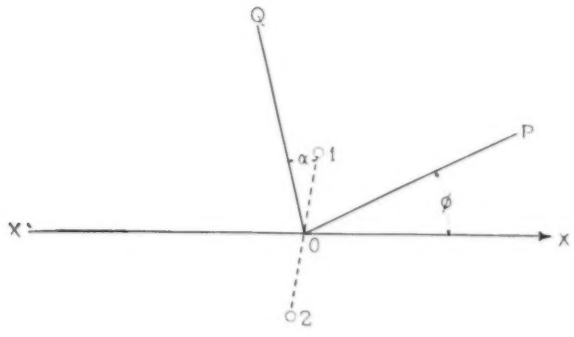

Fig. 1.

If an electric field of strength E is applied in the direction OQ the probability that the moment m will lie in a solid angle $d\Omega = \sin \alpha d\alpha d\psi$ is, according to the Boltzmann-Maxwell law

$$\frac{1}{4\pi} e^{mE\cos\alpha/kT} \sin \alpha d\alpha d\psi .$$

The average intensity of I_{11} that is scattered in the direction ϕ on applying the field E is then

$$I_{11} = \frac{4\beta . 1_\phi^2}{4\pi} \int_{\psi=0}^{\psi=2\pi} \int_{\alpha=0}^{\alpha=\pi} \cos^2 (x \cos \alpha) e^{mE\cos\alpha/kT} \sin \alpha d\alpha d\psi$$

$$= 2\beta . 1_\phi^2 \left[P(x) + \frac{m^2E^2}{2k^2T^2} Q(x) \right]$$

where

$$P(x) = 1 + \frac{\sin 2x}{2x}, \quad Q(x) = \frac{1}{6} + \frac{\sin 2x}{2x}\left[1 + \frac{1}{4x^2}\right] - \frac{\cos 2x}{2x^2},$$

and powers of mE/kT greater than the second are neglected. Following the usual method the total intensity of the scattering at an angle ϕ is found to be

$$I_\phi = 2ZI_e \left[P(x) + \frac{m^2E^2}{2k^2T^2} Q(k) \right] \tag{2}$$

where I_e is the scattering at an angle ϕ due to a single electron. It will be seen that the effect should be proportional to the square of the field applied. A similar calculation was carried out for a model of the nitrobenzene molecule in which five CH groups and one NO_2 group were evenly spaced on the circumference of a ring. It was assumed that these groups scattered as units, and that the ring possessed á permanent moment due to the asymmetry produced by the NO_2 group. An intensity formula analogous to Eq. (2) was obtained and as in Eq. (2) $P(x)$ and $Q(x)$ were found to be of approximately

the same order of magnitude. In order to estimate the relative importance of the additional term introduced because of the presence of the electric field let E be taken as 5 k.v. per cm, one of the values used in this experiment, let m be given the value 3.9×10^{-18} e.s.u. as determined by polarization measurements,[7] let T be taken as 300°K, and k given its usual value 1.39×10^{-16}. The value of $m^2E^2/2kT^2$ then becomes of the order of 10^{-6}. It would thus seem that the effect of the field on the scattering of the molecules considered independently would be very small, probably too small to be detected by the usual methods of measuring intensity.

On the other hand the optical effect of the electric field on the liquid is to make it act as if it were a uniaxial crystal. If the electric field tends to arrange the molecules into something approximating crystalline structure the second term on the right-hand side of Eq. (2) would be affected, in that the distribution function would correspond to an increased regularity in the spatial arrangement of the scattering centers. The effect on the diffraction pattern would be an increase in the intensity of the peak, and also a sharper peak. Thus in looking for an effect of the electric field on the liquid diffraction pattern it would appear best to investigate the peak intensity with and without the field. This has been done in the following experiment.

Experimental Procedure

The cell in which the liquids were put for investigation is shown in Fig. 2. The window was made of cellophane 0.025 mm thick, on the inner side of

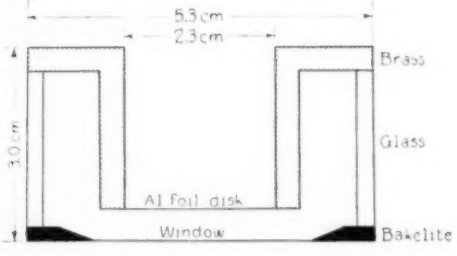

Fig. 2. Diagram of cell.

which aluminum leaf 0.00065 mm thick was fastened. The high potential was applied to the aluminum leaf by means of the electrode E, Fig. 3, and a strip of aluminum foil leading from the electrode to the inner side of the window. Separated from the window by a distance of 3.5 mm was a heavy aluminum foil disk which was grounded by means of the earthed brass back of the cell. The x-rays entering through the window were scattered by the liquid lying between the window and the aluminum foil disk. In this way the field was given the direction OQ of Fig. 1 with respect to the x-ray beam. Fig. 3 illustrates the arrangement of the apparatus used.

In order to apply the field as nearly at right angles to the x-ray beam as possible, since the Kerr effect is observed when the light beam is traveling

[7] P. Debye, Polar Molecules, p. 54.

normal to the field, the ordinary Bragg crystal reflection method was used to obtain the x-ray diffraction pattern. The incident x-ray beam was collimated by a Soller slit set each slit of which was 9 cm long, 1.5 cm high, and 0.045 cm wide. Attached to the front of the ionization chamber and rotating with it was another slit set with slits 6 cm long, 1.5 cm high, and 0.022 cm wide. An adjustable slit, kept at a width of about one mm, was placed between the second slit set and the celluloid window of the ionization chamber. This slit system served to prevent the rays scattered either by the cellophane-aluminum window, or the aluminum disk at the back of the cell from entering the ionization chamber. The chamber was filled with methyl bromide at atmospheric pressure, and the ionization currents were measured by a Compton electrometer adjusted to a sensitivity of 10,000 mm divisions per volt at a scale distance of 3 meters. Unfiltered x-rays obtained from a molybdenum-target tube operated at 35 k.v. and 32 milliamperes were used. The current supplied to the x-ray tube was rectified by means of a full-wave balanced-circuit kenotron rectifier.

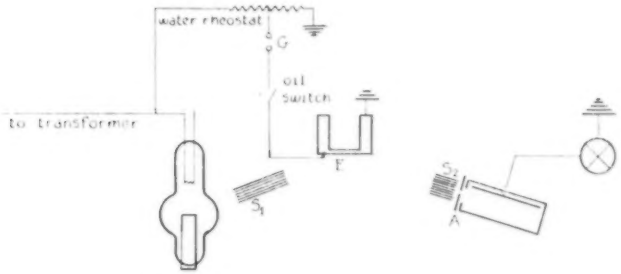

Fig. 3. Arrangement of apparatus.

Since the Kerr effect is most prominent when the electric field consists of a rapid succession of short, sharp peaks it was thought best to look for the effect with the same type of field. In order to synchronize the peaks of the applied field with the peaks of the voltage across the x-ray tube the same high voltage source was used for both. The voltage applied to the cell was stepped down by means of a water rheostat. The peaks of the electric impulses across the cell were sharpened by means of a spark gap, across which a jet of air was blown, inserted between the rheostat and the cell. This device permitted the use of higher fields, and also gave a field more nearly like that used in observing the Kerr effect for nitrobenzene.

With this arrangement the liquid diffraction curves shown in Fig. 4 and Fig. 5 were obtained. These curves do not differ appreciably from the diffraction curves obtained by other methods. They show the same approach toward zero scattering at small angles of diffraction, and the same principal maximum of intensity. The nitrobenzene curve appears to be somewhat broader than the benzene curve.

To observe the effect of the electric field on the diffraction pattern the cell and ionization chamber were set at angles corresponding to the diffraction

peak. The following procedure was observed in taking all readings. The field was applied across the cell, and 45 sec. later an observation of the intensity was made. The field was then removed, and 45 sec. were allowed to

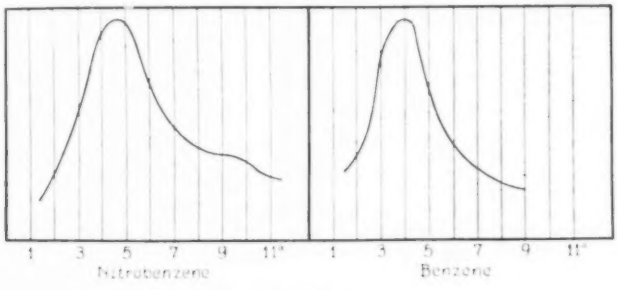

Figs. 4 and 5. Diffraction curves.

elapse before the reading without the field was taken. Alternate readings, with and without the field, were taken in this way for nitrobenzene and benzene.

Results

The results obtained are shown in Table I. The + sign is used to indicate an increase in peak intensity on applying the field, the − sign a decrease. The probable error listed in each case is the probable error of the arithmetic mean as computed in the ordinary way from least squares theory. The values given for nitrobenzene under fields of 5 k.v. per cm and 9 k.v. per cm, and for benzene represent the average of 100 pairs of readings taken as described above. The change in intensity listed for nitrobenzene under a field of 14 k.v. per cm is the average of 37 pairs of readings, the breaking down of the cell preventing further observations at this voltage. With so strong a field it was difficult to obtain steady conditions, and the results are not as reliable as the others listed.

Table I.

Liquid	Field Applied	Intensity Change	Probable Error
Nitrobenzene	5 kv per cm	+0.8 percent	0.2 percent
Nitrobenzene	9 kv per cm	+2.3 percent	0.3 percent
Nitrobenzene	14 kv per cm	+2.0 percent	0.8 percent
Benzene	9 kv per cm	−0.3 percent	0.3 percent

The same type of field was used for all observations. With this type of field benzene shows only a slight Kerr effect. As is seen the change in peak intensity for benzene is not significant, and is in the direction of lesser instead of greater intensity. This lack of any definite shift for benzene rules out the possibility that the effect observed for nitrobenzene might be due to mechanical causes such as the bending of the cellophane window as a result of electrostatic forces of attraction.

The increase in peak intensity for nitrobenzene appears to be a function of the potential drop across the cell. On the basis of the observations made for the two lower voltages it might appear as if the effect varied approximately as the square of the potential applied. Further experiment is necessary, however, to decide this point definitely. But it is reasonably certain that over a range of field strengths less than 9 k.v. per cm the effect increases with increasing field strength. The observations made at 14 k.v. per cm are not sufficiently accurate to permit any definite conclusions to be drawn from them.

Conclusions

Since the observed changes in intensity range from four to seven times the probable error, and as mechanical effects do not produce them it seems reasonably certain that the type of electric field described above produces an increase in the peak intensity of the nitrobenzene diffraction pattern. This change is a function of the strength of the field applied, and from the data now available appears to vary as the square of the field strength over a range of potential gradients less than 9 k.v. per cm.

The effect is far larger than would be expected from the orientation of the molecules considered as scattering separately. It would thus appear that molecular orientation alone is not capable of producing the observed change. If, however, the effect of the field is to bring about a more orderly arrangement of the molecular scattering centers with an increased regularity in the spatial distribution of these centers then such an effect as that observed might be expected. Such a tendency toward a crystalline arrangement was the explanation originally advanced by Kerr to account for the effect he observed.

It is possible that the effect just described is not associated with the Kerr effect, and that the correlation obtained for nitrobenzene and benzene is due to the large difference in their permanent moments. Liquids are known with permanent moments of the same order of magnitude as nitrobenzene but which do not show a Kerr effect of the same order of magnitude. Experiments with some of these liquids are desirable in order to gain further information regarding this point.

In conclusion the author wishes to express his appreciation to Professor A. H. Compton for his very helpful advice and his constant interest in the problem.

THE RESOLVING POWER OF CALCITE FOR X-RAYS AND THE NATURAL WIDTHS OF THE MOLYBDENUM $K\alpha$ DOUBLET

By Samuel K. Allison and John H. Williams
University of California, Berkeley

(Received May 14, 1930)

Abstract

The half widths at half maximum of the rocking curves in parallel positions of the double x-ray spectrometer have been observed for the first five orders of reflection of Mo$K\alpha_1$ from calcite. The calculated half widths for a single crystal have been compared with the theoretical results of Darwin and Ewald. The observed values are of the same order of magnitude as the theoretical, but slightly larger (1.4 times as large in the first order).

The rocking curve widths in 8 anti-parallel positions for Mo$K\alpha_1$ at 50 k.v. have been observed. Geometric corrections arising from the vertical spread of the beam have been applied. The half width at half maximum of Mo$K\alpha_1$ has been found to be 0.147 X.U. corresponding to an energy width of 3.6 volts. The variation of this width with voltage from 25 to 50 k.v. has been studied, and no significant variation found. The half width at half maximum of Mo$K\alpha_2$ at 50 k.v. was observed in 2 positions and found to be 0.161 X.U., the corresponding energy width being 3.9 volts. The observed difference between α_1 and α_2 is close to the experimental error and may not be real. The observed values are 2.5 times as great as the width to be expected from a classical electronic oscillator damped by its electromagnetic radiation.

The computed life of the excited K state of molybdenum is 1.8×10^{-16} seconds. No evidence of fine structure of Mo$K\alpha_1$ or α_2 was obtained.

THIS paper is a report of experiments performed with the double x-ray spectrometer recently constructed in this laboratory. Experiments analogous to those described here have been carried out by Davis and Stempel,[1] Wagner and Kuhlenkampff,[2] Ehrenberg and Mark,[3] Ehrenberg and von Susich,[4] Davis and Purks,[5] and Allison.[6] These experiments will be discussed later in connection with various topics in this report.

Apparatus

The double spectrometer with which these results were obtained has been described elsewhere.[7] Constants of the spectrometer, some of which were

[1] Davis and Stempel, Phys. Rev. **17,** 608 (1921), **19,** 504 (1922).

[2] Wagner and Kuhlenkampff, Ann. d. Physik **68,** 369 (1922).

[3] Ehrenberg and Mark, Zeits. f. Physik **42,** 807 (1927).

[4] Ehrenberg and von Susich, Zeits. f. Physik **42,** 823 (1927).

[5] Davis and Purks, Proc. Nat. Acad. Sci. **13,** 419 (1927), **14,** 172 (1928), Phys. Rev. **34,** 181 (1929).

[6] S. K. Allison, Phys. Rev. **34,** 176 (1929).

[7] Williams and Allison J.O.S.A. and R.S.I. **18,** 473 (1929). Opportunity is taken here to point out some errors in this paper. The equation on page 474 is only approximately true, the correct expression being Eq. (1) of the present paper. On page 475 the tube holding the slits is stated to be 35 cm long whereas it actually is 30 cm. It is also stated that "the horizontal width of the slits can be adjusted to give the maximum resolving power" whereas the resolving power of the double spectrometer is independent of the slits mentioned.

not previously given, are as follows: distance from the focal spot of the x-ray tube to the first crystal (crystal *A*), 53 cm; distance between the axes of crystals *A* and *B*, 19 cm; distance from the axis of crystal *B* to the ionization chamber window, 4.5 cm; length of the ionization chamber, 40 cm; diameter of the chamber, 4.3 cm. The ionization chamber was filled with a mixture of ethyl bromide and argon at partial pressures of 17 cm and 59 cm respectively. The slit for admitting x-rays into the ionization chamber was 3 mm wide.

Two slit systems were used simultaneously which will be referred to as the horizontal and vertical slits respectively. The vertical slits limited the spread of the beam in a horizontal plane (more generally, a plane perpendicular to the axes of rotation of crystals *A* and *B*). The horizontal slits limited the spread of the beam in a vertical plane (one including the axes of rotation). The vertical slits were 30 cm apart and each 1.5 mm in width. The horizontal slits were 30.95 cm apart. The widths used for them will be given later.

Molybdenum target tubes supplied by the General Electric Company for crystal analysis work were used. In these tubes the face of the target is normal to the impinging electron beam which lies in the long axis of the tube. The radiation used in the spectrometer was taken at a glancing angle of 8° from the target face. It will be shown later that this is not the most desirable arrangement for the double spectrometer. The tubes were cooled by pumping kerosene through the targets.

The high potential for operating the tubes was supplied by a 550 cycle transformer-kenetron-capacity set in which the calculated voltage fluctuations at 50 k.v. and 20 milliamperes tube current were 1.8 percent. The voltages were read on a high voltage electrostatic voltmeter which had been calibrated by measuring the short wave-length limit of the continuous spectrum.

The electrometer has been described in a previous paper.[7]

The calcite crystals used were freshly cleaved from an optically clear parallelopiped whose surfaces were cleavage planes, by placing a razor blade as accurately as possible parallel to the cleavage direction and tapping it sharply with a light hammer. The faces from which the x-rays were reflected were the fresh faces from a single fracture and were rhombs whose sides were 1.9 cm long. These faces were not by any means optically flat. Close inspection showed that the fracture had not been all in one plane but that there were very thin "steps" on the crystal face. The holders for the crystals could be slipped out of the dove-tailed guides[8] and replaced in them without changing the orientation of the crystals more than about 10 seconds of arc about a vertical axis. The crystals were removed in this manner after each set of readings and placed in a dessicator over dehydrated calcium chloride and a few sticks of sodium hydroxide. This was done to safeguard the fresh surfaces from attack by acid fumes which might be in the

[8] See reference 7, Fig. 2 p. 476. The springs *K* were unhooked, and *E* and its superstructure slid out of *F*.

air. There was no evidence of deterioration of the surfaces during the period of observation.

A thermometer which could be read to a few hundredths of a degree centrigrade was placed over the spectrometer and read at frequent intervals while working in anti-parallel positions.

Adjustments

It is convenient to speak of a "central ray" which may be defined as a ray passing through the geometric centers of the slit apertures. The adjustment of the instrument must insure the following conditions.

(1) The central ray must pass through the center of the focal spot of the x-ray tube.

(2) The central ray must intersect the reflecting surface of crystal A near its geometric center.

(3) The axis of rotation of crystal A must intersect the central ray at the point where the ray intersects A's surface.

(4) The axis of rotation of crystal A must lie in its reflecting surface.

(5) The central ray, after reflection from crystal A, must intersect the reflecting face of crystal B near its geometric center.

(6) The axis of rotation of crystal B must intersect the central ray at the point where the ray intersects B's surface.

(7) The axis of rotation of crystal B must be parallel to that of A.

(8) The axis of rotation of crystal B must lie in its reflecting surface.

(9) The central ray after reflection from crystal B, must enter the ionization chamber through the center of its slit and pass down the long axis of the chamber.

A necessary condition for the fulfillment of these requirements is that the central ray, the focal spot of the tube, the geometrical centers of the reflecting faces of the crystals and the axis of the ionization chamber lie in the same (horizontal) plane. This is accomplished partly in the original construction of the instrument and partly in the judicious placing of the crystals on their holders.

The spectrometer was levelled by means of levelling screws. The reflecting face of A was made vertical as follows. A cathetometer carrying a horizontal slit system was set up about 150 cm from the axis of A. The cathetometer was used merely as a rigid support for the slit system. The horizontal slit system of the cathetometer could be rotated about a horizontal axis until its central ray was horizontal to within 30 seconds of arc. This was accomplished by means of a sensitive spirit level. A parallel beam of light from an arc-lens combination was sent through the slits carried by the cathetometer and reflected from crystal A. The cathetometer was set in such a position that the reflected beam from the surface of A almost coincided with the incident beam. By means of a set screw in the crystal holder,[9] A was tilted about a horizontal axis until the beam reflected from it was in the same horizontal plane as the

[9] See reference 7, Fig. 2 476. R is the set screw referred to here.

incident beam. Due partially to the step-like structure of the cleavage surfaces previously mentioned, the reflected beam was not perfectly defined and this allowed an error of perhaps 2 minutes of arc to remain in the verticality of A.

The vertical slit system of the spectrometer was then made vertical by a plumb line or by setting an accurate right angle on the upper flat surface of the spectrometer and sighting past its vertical arm through the slits. The mechanism for closing the jaws of the vertical slits was such that they necessarily opened symmetrically about the central ray. The slits were then made about 0.05 cm wide and a beam of light from an arc sent into the spectrometer. This beam was observed on a ground glass or other translucent material after it had passed the axis of crystal A. Crystal A was then translated horizontally and rotated about its vertical axis until the ground glass showed that its face, when parallel to the light beam, extended just halfway into it. The crystal was then rotated through 180°. In this new position it did not, in general, again bisect the beam. Half of the adjustment necessary was taken up by rotation of the slit system about a vertical axis and half by translation of A horizontally and rotation about its vertical axis. A was then rotated through 180° again and the process repeated. By this method requirements (2), (3), and (4) of the preceding list could be satisfied.

In the adjustment of crystal B it was assumed that in the construction of the instrument requirement (7) has been met. It will be seen that this uncertainty may be a cause of error in the curves obtained in parallel positions. Crystal A was removed from the spectrometer. Crystal B was made vertical by the cathetometer method, and the arm carrying B's axis of rotation (this arm revolved about the axis of A) was set so that the beam of light from the spectrometer slits passed approximately over B's axis. The accurate adjustment was made similarly to that of A by repeated rotations of B through 180°. In this case the arm carrying the axis of B and the horizontal translation of B were adjusted until the surface of B was half-way across the beam at positions 180° apart. In this way requirements (5), (6), (7), and (8) were satisfied. In subsequent settings of the instrument the arm carrying the axis of B was rotated through twice the angle that the crystal A was turned around its axis.

The ionization chamber was set by noting where the beam of light entered its window. Later the position corresponding to requirement (9) was more accurately found by moving the ionization chamber across the reflected beam of x-rays from crystal B and setting it at the center of the angular range through which radiation entered its window.

When the adjustments of crystals A and B and the preliminary adjustment of the ionization chamber had been made the x-ray tube and horizontal slits were put in place. By means of a fluorescence screen it was ascertained that the x-ray beam (which in the actual experiments had a rectangular cross section about 0.15×0.1 cm at crystal A) was horizontal. The vertical slits were then further narrowed and the instrument used as a single crystal spectrometer with only crystal A in use. An emission line of the target was

found and the x-ray tube shifted horizontally until the maximum intensity was obtained. This made certain that the central ray passed through the most intense part of the focal spot of the tube.

Purpose of the Experiments

The purpose of the experiments can best be understood by a brief outline of the theory of the instrument. A notation for the double spectrometer has been suggested by the authors in a previous paper.[10] This notation has been of the greatest service in guiding the course of the experiments and will be retained. A fundmental expression for the instrument is that the dispersion D may be written as follows:

$$D \equiv \frac{d\theta_B}{d\lambda} = \frac{n_A}{2d \cos \theta_A} + \frac{n_B}{2d \cos \theta_B} \tag{1}$$

in which the meaning of the symbols and the convention as to sign of n_B have been previously given.[10] n_A is to be considered always positive. n_B is negative when the first incident and last reflected rays are on opposite sides of the first reflected ray,[11] otherwise it is also positive. A setting of the instrument is described by giving the values of n_A and n_B in the form (n_A, n_B) and of the wave-length reflected. Eq. (1) is derived by differentiation of the Bragg law and addition of the dispersions of the cystals.

The second equation for the double spectrometer that we shall consider here gives the observed width of the rocking curve for any line in the spectrum at any setting of the instrument. We will temporarily assume that geometric widths due to slit heights and deviations of the crystals from verticality have been made negligibly small. We then have[12]

$$W = (W_A^2 + W_B^2 + D^2 W_\lambda^2)^{1/2}. \tag{2}$$

In this equation, W represents the half width at half maximum in angular measure of the observed rocking curve, W_A the half width at half maximum in angular measure of the curve (assumed Gaussian error curve) representing the intensity of reflection from crystal A as a function of the deviations from the Bragg angle, W_B is the analogous quantity for crystal B, D is defined in (1) and W_λ is the half width at half maximum of the line in question in linear measure. In the derivation of (2) it is assumed that the line has a Gaussian error curve distribution of intensity.

From Eqs. (1) and (2) it is seen that the positions of the double spectrometer naturally fall into two classes, so-called parallel and anti-parallel positions. Parallel positions are distinguished by having $D = 0$, or $n_B = -n_A$. If $D = 0$ in Eq. (2) we see that the observed width is due to the angular range through which a crystal may be turned and reflect a single wave-length, in

[10] Allison and Williams, Phys. Rev. **35,** 149 (1930). The interpretation of negative values of D from Eq. (1) is also found here.

[11] Schwarzschild, Phys. Rev. **32,** 162 (1928).

[12] Schwarzschild, reference 11. This equation may be obtained by combining Eqs. (43) and (45) of his paper. Important special cases of this equation had been previously developed by Ehrenberg and Mark, reference 3.

other words, the widths in such positions are closely related to the limit of resolution of the instrument. Anti-parallel positions have $D \neq 0$ and are all positions for which $n_A \neq -n_B$. From Eq. (2) it is seen that the rocking curves in such positions include, in addition to the factors giving the widths in parallel positions, contributions from the widths of the spectrum lines themselves.

Results in Parallel Positions

If $D = 0$ in Eq. (2), it becomes

$$W = (W_A^2 + W_B^2)^{1/2}. \tag{3}$$

If we now assume that $W_A = W_B = W_c$ we may write this

$$W = 2^{1/2} W_c \tag{4}$$

where W is the observed width and W_c the interference pattern width from a single crystal.

We have investigated the values of W for the reflection of Mo$K\alpha_1$ in the first five orders from the cleavage face of calcite. If the adjustments previously described were not perfect, there would be an appreciable width to the rocking curve in these positions due to geometric causes, that is, there would be a width even if the width of the interference pattern of the crystals were zero. It has been shown by Schwarzschild[13] that this width would be

$$\delta\theta_B' = \frac{2\phi(\delta_A + \delta_B)}{\cos\theta} \tag{5}$$

where $\delta\theta'_B$ is the angular range in parallel positions through which crystal B may be turned and yet reflect some of the radiation sent to it by A. δ_A and δ_B are the angular deviations of the reflecting faces of crystals A and B from verticality, θ is the glancing angle, (the same for both crystals) and ϕ is one half of the maximum angle between any two rays in a plane parallel to the axes of rotation of the crystals. Eq. (5) is derived on the assumption that the axes of rotation of crystals A and B are parallel.

In our experiments it was found that the widths of the rocking curves in parallel positions were very sensitive to deviations from verticality of the crystals. The method of setting for verticality previously described was not sufficiently accurate in general to produce the narrowest curves. The following procedure was adopted. The face of crystal A was set vertical within the limits of accuracy of the cathetometer method. (The reflected light beam was somewhat sharper from A than from B). Crystal B was then set vertical within the limits of error and a rocking curve taken. B was then rotated in small steps[14] around a horizontal axis (a minute of arc at a time) and rocking curves taken for each position until a minimum width was found. If at this position δ_A and δ_B are zero, then from Eq. (4) the width observed should be

[13] Schwarzschild, reference 11. see Eq. (24) of his paper in which $R = 2(\delta_\alpha + \delta_\beta)/\cos\theta$ and $\phi = s/L$

[14] See the figure mentioned in reference 9. The screw R is used.

independent of ϕ. Several experiments were made to test this by changing the value of ϕ after the position of minimum width had been found. ϕ was varied by varying the width of the horizontal slits. The maximum value of ϕ was limited by the height of crystal B and was about 0.015.

TABLE I. *Minimum half width at half maximum in parallel positions as a function of* ϕ. *MoK*α_1.

Position	ϕ	Observed W seconds
(1, −1)	.015	3.0
(1, −1)	.012	3.0
(2, −2)	.015	1.0
(2, −2)	.0072	1.1
(2, −2)	.0054	.90

Table I shows that from a value of ϕ of 0.0054 to a value of 0.015 the changes in the width of the rocking curve observed were within the limit of error to which a given experiment could be duplicated. The low intensity of reflections such as (4, −4) and (5, −5) made the use of the larger value of ϕ very desirable and Table I seems to justify this procedure.

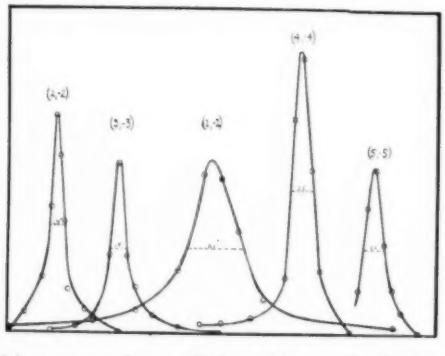

Fig. 1. Observed rocking curves in parallel positions. Ordinates are proportional to ionization currents, abscissae to angular settings of crystal B. The vertical scale is not the same for all the curves.

Fig. 1 shows some of the rocking curves obtained, and in Table II the half widths at half maximum, together with the values of W_c calculated from Eq. (4) are listed.

TABLE II. *Minimum half widths at half maximum in parallel positions. MoK*α_1

Position	W(seconds)	W_c(seconds)
(1, −1)	3.0	2.1
(2, −2)	.90	.64
(3, −3)	.95	.67
(4, −4)	1.1	.78
(5, −5)	1.2	.88

Discussion of Results in Parallel Positions

Sources of error. Probably the most important source of error in the values of Table II arises from a possible lack of parallelism of the vertical axes around which A and B were rotated. Unfortunately the apparatus was designed in such a manner that these axes were rigid with respect to each other and no adjustment could be made. Other sources of error are (1) irregularities in the slow motion screw moving B; (2), temperature differences between crystals A and B. No evidence of irregular motion of B was obtained; rotation in regular steps of one-half second of arc seemed possible. Although variations in the temperature of the room of a few tenths of a degree centigrade sometimes occurred while a curve was being taken, the possibility of significant temperature difference between the two crystals (19 cm apart) seems excluded.

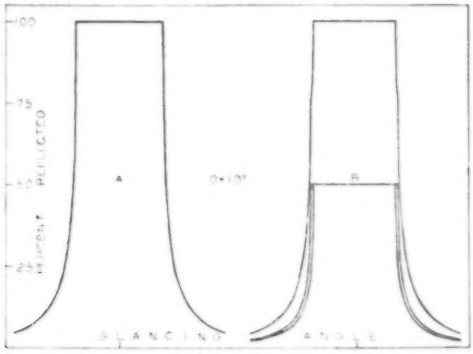

Fig. 2. A. Theoretical reflection curve from a perfect crystal for polarized x-rays (Eq. (6) and (7) and (8), or Eq. (9) and (7) and (8)). B. Theoretical reflection curve for unpolarized rays. The innermost curve represents the reflection of the component whose electric vector lies in the plane of incidence. The intermediate curve represents reflection of radiation polarized so that its electric vector lies perpendicular to the plane of incidence. The outermost curve is the sum of these components.

Comparison with theory of a perfect crystal. The reflection of plane waves from a so-called perfect or ideal crystal in which there is no warping or mosaic structure has been theoretically studied by Darwin[15] and Ewald.[16]

Plane, monochromatic waves fall on an idealised crystal made up of electrons lying on planes separated by a constant distance. The radiation is polarized in such a plane that the electric vector lies perpendicular to the plane of incidence. Fig. 2a shows the intensity of reflection to be expected as a function of glancing angle. The curve is symmetrical about a glancing angle which may be obtained from that calculated by Bragg's law by correcting for the index of refraction. The extent of the region of 100 percent reflection is given by

$$\Delta\theta = 4\delta \operatorname{cosec} 2\theta \tag{6}$$

[15] Darwin, Phil. Mag. **27,** 325 and 675, (1914).
[16] Ewald Phys. Zeits. **26,** 29 (1925).

where $\Delta\theta$ is the range of glancing angle θ; δ is the deviation of the index of refraction from unity. Outside the region of perfect reflection, the intensity falls off rapidly. The equation of the curve in these regions is given by

$$I_{\theta'-\theta} = I_0\left(\frac{\Delta\theta}{2(\theta'-\theta)+(4(\theta'-\theta)^2-\overline{\Delta\theta^2})^{1/2}}\right)^2, \quad \theta'-\theta > \frac{1}{2}\Delta\theta \tag{7}$$

$$I_{\theta'-\theta} = I_0\left(\frac{\Delta\theta}{2(\theta'-\theta)-(4(\theta'-\theta)^2-\overline{\Delta\theta^2})^{1/2}}\right)^2, \quad \theta'-\theta < -\frac{1}{2}\Delta\theta \tag{8}$$

where $I_{\theta'-\theta}$ is the intensity at a glancing angle θ', I_0 is the incident intensity, and $\Delta\theta$ is defined by Eq. (6). If $I_{\theta'-\theta}/I_0$ is set equal to $\frac{1}{2}$ in Eq. (7), and the half width at half maximum calculated it is found to lie at a value of $\theta'-\theta$ equal to $1.06\,\Delta\theta/2$.

If the incident radiation is plane polarized in such a manner that the electric vector lies in the plane of incidence, the analogous equation to Eq. (6) is

$$\Delta\theta = 4\delta \cot 2\theta. \tag{9}$$

The radiation used in these experiments was a characteristic emission line of the target, known to be unpolarised. We may consider the unpolarised incident light resolved into two components, with electric vectors parallel and perpendicular to the plane of incidence. The intensity of each one of these components will be half the incident intensity. The reflection curve for unpolarised incident rays will then be the sum of two curves given by Eqs. (6) and (9) and the Eqs. (7) and (8) appropriate to each. Such a curve is shown in Fig. 2b.

The half width at half maximum for the unpolarised curve will be slightly greater than 2δ cosec 2θ by a factor which approaches 1.06 as the glancing angle is decreased and falls off to unity at larger glancing angles. As will be seen later this correction is less than the uncertainty in the structure factors involved and will therefore be disregarded.

For a real crystal, the electrons are of course not situated on equidistant planes but are distributed throughout the structure. In this case the formula for the half width at half maximum for unpolarised radiation becomes

$$2F\delta \text{ cosec } 2\theta/Z \tag{10}$$

where

$$F = \sum_i F_i e^{2\pi n i(hx_i+ky_i+lz_i)}. \tag{11}$$

In the preceding equations, F is the structure factor, or equivalent reflecting power of the Z electrons in the unit cell of the crystal, F_i is the ionic structure factor, n is the order of reflection, h, k, l are the Miller indices of the plane, and x_i, y_i, z_i are the coordinates of the atom i in the unit cell.[17] The unit cell of

[17] Our thanks are due Professor Linus Pauling for his aid in calculating the structure factors given here.

calcite contains two molecules of $CaCO_3$. Its sides are not parallel to those of a natural cleavage parallelopiped, so that the Miller indices of a plane in the true unit and the cleavage unit are not the same. The cleavage plane, which has indices (100) in the cleavage unit, has indices (211) in the true unit,[18] and these are the values to use in Eq. (11) for *hkl*. The ionic structure factors for calcium and oxygen were taken from Bragg and West.[19] The ionic structure factor for carbon was assumed to be one-fourth of that for oxygen. The calculation of the structure factors used is indicated in Table III.

TABLE III. *Structure factors for* (100) *planes of calcite for* $MoK\alpha_1$.

Order	$(\sin\theta)/\lambda$	F_{Ca}	F_C	F_O	F
1	0.165	15.1	1.8	6.6	$2(F_{Ca}+F_C+F_O)=47.0$
2	.330	10.5	.9	3.3	$2(F_{Ca}+F_C)-2F_O=16.2$
3	.495	7.6	.4	1.7	$2(F_{Ca}+F_C+F_O)=19.4$
4	.660	5.9	.2	.9	$2(F_{Ca}+F_C)+6F_O=17.6$
5	.825	4.5	.1	.5	$2(F_{Ca}+F_C+F_O)=10.2$

The theoretical half widths at half maximum for the unpolarised $MoK\alpha_1$ radiation from calcite may now be found by inserting the values of F from Table III in Eq. (10), using $Z=100$. The value of δ taken from A. H. Compton[20] is 1.84×10^{-6}. In this way the theoretical values of Table IV were obtained, in which experimental values due to Davis and Purks[21] are included.

TABLE IV. *Comparison of theoretical and observed values of* W_c (*Eqs.* (10) *and* (4). $MoK\alpha_1$

Order	W_c Theory Eq. (10)	W_c Exp. Eq. (4)	W_c Davis and Purks
1	1.5 sec.	2.1 sec.	1.6 sec.
2	.28	.64	.45
3	.22	.67	
4	.16	.78	
5	.08	.88	

The values of Table IV are shown graphically in Fig. 3. It is seen that the crystal reported by Davis and Purks has very nearly the predicted half width for a perfect calcite crystal, while those used in this investigation were less perfect on this criterion. It is interesting to note that the theory gives results which agree well with experiment for the widths of the curves, although it is known that the intensity predictions are not verified.

[18] Strukturbericht of the Zeits. für Krystallographie, pp. 292–295.

[19] Bragg and West, Zeits. f. Krystallographie **69,** 118 (1928).

[20] A. H. Compton, X-rays and Electrons, p. 218 Table VII–2.

[21] Davis and Purks Phys. Rev. **34,** 181 (1929). These investigators state that their observed widths are less than those predicted for a perfect crystal. They used a theoretical formula, however, in which an effective width had been calcualted for the purpose of expressing the reflected energy as the product of the incident intensity by this effective region of 100% reflection.

Results in Anti-Parallel Positions

In the nomenclature which we have adopted for the instrument, D is finite in anti-parallel positions. The total geometrical width in anti-parallel positions is given by the formula

$$\delta\theta_B = \tfrac{1}{2}D\lambda\phi^2 \tag{12}$$

in which $\delta\theta_B$ is the *total* angular range through which crystal B can be turned while reflecting the wave-length λ.[22] Since what we have measured is the half width at half maximum, the correction for geometric width should not be the entire amount of Eq. (12). The purely geometric rocking curve corresponding to Eq. (12) is not symmetrical about its maximum.[23] Its shape depends on the

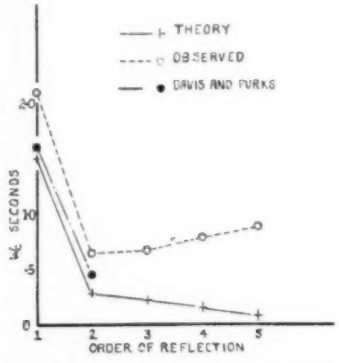

Fig. 3. Comparison of observed and calculated values of the half width at half maximum of the reflection curve from calcite.

intensity of the bundle of parallel rays passing through the slits and making an angle α with the central ray in a vertical plane relative to that of the bundle of rays proceeding parallel to the central ray. This will be referred to as the variation of intensity with vertical divergence of the beam. If the widths of the horizontal slits are h_1 and h_2, $(h_2 \geqq h_1)$, and the distance between them is L,

$$\phi = (h_1 + h_2)/2L. \tag{13}$$

ϕ calculated from Eq. (13) gives the upper limit of α. If we neglect variations of intensity in the focal spot itself, we may assume that the intensity of a parallel bundle of rays is proportional to its cross-section area. This gives

$$I_\alpha = I_0 \text{ for } 0 < \alpha < (h_2 - h_1)/2L \tag{14}$$

$$I_\alpha = I_0(h_1 + h_2)(1 - \alpha/\phi)/2h_1 \text{ for } h_2 - h_1/2L < \alpha < \phi. \tag{15}$$

[22] Eq. (12) occurs in Schwarzschild's paper as $\frac{1}{2}(\tan\theta_1 \pm \tan\theta_2)\phi^2$. It does not, of course, express the entire geometric width if the crystal faces and axes are not vertical. The percentage contribution to the geometric width from lack of verticality is much less in anti-parallel than in parallel positions due to the preponderating influence of the natural line breadths. In our experiments it was found by trial that using the cathetometer and horizontal slits we could set the crystals so nearly vertical that the minimum width was obtained at once in anti-parallel positions, although, as has been previously stated, this was not true in parallel positions. For this reason we do not include a term involving verticality corrections in Eq. (12)

[23] See Schwarzschild, reference 11, p. 166, Fig. 3b curve D. This curve corresponds to a function $I_\alpha = I_0(\phi - \alpha)$, or to horizontal slits of equal width.

In the preceding equations, I_α is the intensity of a bundle of parallel rays having a vertical angular divergence α; I_0 is the intensity of the bundle of rays parallel to the central ray. Due to geometric causes alone, as crystal B is rotated from the position in which the central ray makes the angle of best reflection for a certain wave-length, other vertically divergent rays also can make this glancing angle and be reflected. If ξ is the angular deviation of crystal B from the position of reflection for the central ray, and α the vertical divergence of the bundle of rays making the correct angle for reflection at ξ,

$$\xi = \tfrac{1}{2}D\lambda\alpha^2 \tag{16}$$

We wish to find the value of ξ at which this geometric rocking curve comes to half maximum. If we set $I\alpha/I_0 = \frac{1}{2}$ in Eq. (16) and solve for $\alpha_{\frac{1}{2}}$ we find

$$\alpha_{1/2} = h_2\phi/(h_1 + h_2) \tag{17}$$

and substitution in Eq. (16) gives

$$\xi_{1/2} = \frac{1}{2}D\lambda\phi^2\left\{\frac{h_2}{h_2 + h_1}\right\}^2. \tag{18}$$

In correcting our results for geometric width in anti-parallel positions we have substracted the values of $\xi_{\frac{1}{2}}$ calculated from Eq. (18) from our observed full widths at half maximum.

The temperature correction. In their paper on the natural widths of x-ray lines Ehrenberg and von Susich noted effects on the widths of the rocking curves in anti-parallel positions which they ascribed to a change in temperature of the crystals while the readings were being taken. It is easily shown that

$$d\theta_B/dT = -a\lambda D \tag{19}$$

where $d\theta_B$ is the angular range on crystal B corresponding to a temperature change dT. The negative sign has the same interpretation as that previously given.[10] a is the linear expansion coefficient of calcite in a direction perpendicular to the cleavage planes,[24] which is 1.04×10^{-5}. For the reflection of Mo$K\alpha_1$ in the (1, 1) position Eq. (19) gives $d\theta_B/dT = -0.51$ seconds of arc

TABLE V. *Half widths at half maximum for Mo$K\alpha_1$ at 50 kv.*

	$\lambda = 707.768$ X.U.					$d = 3.02904$ Å.			
Position (n_A, n_B)	$\lvert D\rvert$ "/X.U.	h_1 cm	h_2 cm	$\xi_{\frac{1}{2}}$	W	W_A	W_B	no. averaged	W_λ
(1, −2)	35.748	.23	.43	.63"	6.4"	2.1"	.64"	1	.154 X.U.
(1, −2)	35.748	.10	.23	.17	6.0	2.1	.64	3	
(2, −1)	35.748	.10	.23	.17	6.5	.64	2.1	1	.168
(1,1)	68.572	.10	.23	.34	11.2	2.1	2.1	4	.155
(1, −3)	74.777	.10	.23	.36	11.4	2.1	.67	2	.148
(1,2)	104.32	.10	.23	.51	15.0	2.1	.64	5	.139
(2,1)	104.32	.10	.23	.51	14.8	.64	2.1	1	.138
(2,2)	140.07	.23	.30	1.2	19.7	.64	.64	3	.136
(1,3)	143.34	.10	.23	.70	19.8	2.1	.67	2	.135
	Weighted average of $W\lambda = 0.147$ X.U.								
	Corresponding energy width 3.63 volts.								

[24] Siegbahn, Phil. Mag. **37**, 601, (1919).

per degree centigrade. During the readings in the anti-parallel positions, the thermometer was frequently read. The change of temperature during the observations was never over 0.5°C. Accordingly we have made no temperature corrections to our results.

We have investigated the half widths at half maximum of the rocking curves for Mo$K\alpha_1$ for as many positions of the instrument as were conveniently possible with the intensity available. The results are shown in Table V.

The values of W_λ in column 10 of Table V are in general averages of several trials, the number of trials being given in column 9. In taking the averages we have weighted our results according to our estimate of their reliability. Some of the curves taken are shown in Fig. 4.

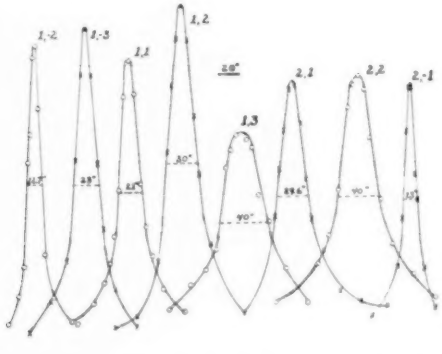

Fig. 4. Observed rocking curves in anti-parallel positions for Mo$K\alpha_1$ at 50 k.v. Ordinates are proportional to ionization currents, abscissae to angular settings of crystal *B*. The vertical scale is not the same for all the curves.

We have investigated the half width at half maximum of Mo$K\alpha_1$ as a function of voltage from the excitation voltage up to 50 k.v. If part of the observed width is due to satellites arising from multiply ionized states of the atom the width should depend on the voltage. The results are given in Table VI. The details given in Table V are omitted, although all corrections were made.

TABLE VI. *Variation of width of Mo$K\alpha_1$ with voltage. All observations in* (1,1) *position.*

Voltage	W_λ
25.0 kv	0.143 *X.U.*
37.0	.162
46.2	.150
50.0	.155

We have also investigated the width of the line Mo$K\alpha_2$ in the (1, 1 and (1, 2) positions as shown in Table VII. It was assumed that the crystal widths W_a and W_b were the same as had been measured for Mo$K\alpha_1$.

TABLE VII. *Half widths at half maximum for MoKα_2 at 50 k. v.*

Position (n_A,n_B)	λ=712.078 X. U. D ″/X.U.	h_1 cm	h_2 cm	$\xi_{\frac{1}{2}}$	W	W_A	d=3.02904 Å. W_B	no. of observations	W_λ
(1,1)	68.572	0.10	0.23	0.34″	12.2″	2.1″	2.1″	5	0.169X.U.
(1,2)	104.36	.10	.23	.52	16.2	2.1	.64	5	.151

Weighted average of W_λ=0.161 *X.U.*
Corresponding energy width 3.92 volts.

DISCUSSION OF RESULTS IN ANTI-PARALLEL POSITIONS

We shall first discuss the results given in Table V. It is seen that in positions in which D varies from 35.748 to 143.34 seconds per X. U. the half width at half maximum W_λ varies from 0.155 X. U. (if we disregard the single observation at (2, -1)) to 0.135 X. U. or a variation of about 13 percent. This variation is not random, however; there is a distinct trend toward lower values of W_λ with higher values of D. A systematic error is therefore indicated. We are not certain where this systematic error lies, but offer the following hypotheses (1). The actual shape of the lines differs from the Gaussian error curve shape sufficiently to make Eq. (2) inapplicable; (2) The effect is due to the finite size of the focal spot.

It is possible to calculate the size of focal spot which would explain the effect. Due to the fact that during the measurement of a line, crystal A is left stationary, the radiation reflected by B at various values of ζ must come from different parts of the target. This effect is increased for higher values of D (broader curves) and by the fact that the radiation was taken at a glancing angle of 8° from the target face. Let us assume that the adjustments have been correctly made and that therefore when crystal B is reflecting the tip of the peak for a line, the radiation reflected comes from the most intense part of the focal spot. As B is rocked to either side of this position, the radiation reflected will have a different initial intensity if the focal spot is finite in extent. We have calculated that if the distribution of intensity in the focal spot in the particular tube used is such that at a distance of 0.43 mm from the center of the spot the intensity has fallen to $\frac{1}{2}$ that at the center, a 10 percent decrease in rocking curve width in the (2, 2) position can be explained. This corresponds to a diameter of 0.86 mm for the most intense part of the focal spot. The region of discoloration of the target appeared to be about 2.5 mm in diameter so that this explanation does not seem obviously impossible. If in later work it is found that this decrease of wave-length width with increasing D persists when a broad focus tube is used and rays taken at a large glancing angle from the target this explanation must be abandoned.

From Table VI we conclude that there is no significant variation of the width of Mo$K\alpha_1$ from 25 kv to 50 kv. The excitation voltage is 19.945 kv, but from intensity considerations it was not possible to take measurements below 25 kv. This indicates that the observed width is not due to satellites.

We obtained no evidence of satellites of Mo$K\alpha_1$ or α_2 from our experiments.[25]

Table VII indicates that the width of Mo$K\alpha_2$ is slightly greater than Mo$K\alpha_1$. The observed difference between the widths of the two lines is however close to the experimental error and we cannot positively assert that there is a difference in width.

The half width at half maximum to be expected from the classical theory of an oscillating electron damped by the electromagnetic radiation emitted is[26]

$$\Delta\lambda = \frac{2\pi e^2}{3mc^2} \tag{20}$$

where e is the electronic charge in e.s.u., m the electronic mass and c the velocity of light. Eq. (20) gives $\Delta\lambda = 5.9\times10^{-13}$ cm. Our measured value of W_λ for Mo$K\alpha_1$ is 1.47×10^{-12} or 2.5 times as large. If we call τ the time required for the vibrations of the electron to decrease to $1/e$ of their initial amplitude,

$$\tau = \frac{3mc\lambda^2}{4\pi^2c^2} = \frac{\lambda^2}{2\pi c}\,\frac{1}{\Delta\lambda}. \tag{21}$$

Using $\Delta\lambda = 1.47\times10^{-12}$ we find $\tau = 1.8\times10^{-16}$ seconds, which gives the order of magnitude of the life of a molybdenum atom excited to the K state.

Ehrenberg and Mark,[3] using diamond crystals, found $W_\lambda = 0.204$ X. U. for Mo$K\alpha_1$ and 0.199 for Mo$K\alpha_2$. Ehrenberg and von Susich[4] found, using calcite, $W_\lambda = 0.19$ X. U. for Mo$K\alpha_1$. These observations were made using only the (1, 1) and (1, -1) positions.

Davis and Purks[25] observed the rocking curves in the (2, 2) and (3, 3) positions but did not give a definite value to the line width as they interpreted their curves as being composed of satellites. The present results may be considered as an extension of the work of Ehrenberg and Mark and Ehrenberg and von Susich. Their results are confirmed in the sense that a line width in excess of the classically predicted value was found. The lower value found here may be partially due to the limitation of the vertical divergence of the x-ray beam.

[25] Davis and Purks, Proc. Nat. Acad. Sci. **14,** 172 (1928). Allison and Williams, Phys. Rev. **35,** 149 (1930).

[26] W. C. Mandersloot, Jahrb. der Radioakt. und Elektron. **13,** 16 (1916), A. H. Compton, X-rays and Electrons, p. 56. The expression given here corresponds to full width at half maximum.

THE VIBRATIONAL QUANTUM ANALYSIS OF THE BLUE-GREEN BANDS OF MAGNESIUM OXIDE

By P. N. Ghosh, P. C. Mahanti and B. C. Mukkerjee
University College of Science and Technology, Calcutta

(Received March 14, 1930)

Abstract

The paper deals with the assignment of the vibration quantum numbers of the violet degrading system of the magnesium oxide bands. The frequencies of vibration for infinitesimal amplitude are found to be 716 cm^{-1} and 751 cm^{-1} for the upper (initial) and lower (final) states respectively. The heat of dissociation as calculated from the extrapolation of the ω^n:n curve is nearly 5.8 volts.

Introduction

A REVIEW of the studies of the band spectrum of magnesium oxide has been given by Kayser[1] till the year 1910. Since then there has been no further investigation of the bands which are found to lie in the red, green and ultraviolet regions.

Lecoq[2] was the first to observe the bands of MgO in the green region. The bands lying in this as well as in the two other regions have been measured by Eder,[3] Brooks,[4] Olmstedt[5] and others. They excited these bands either by sparking through a solution of magnesium chloride, or by burning magnesium ribbon in air, or by burning the salts in an oxy-hydrogen flame or by arcing or sparking between magnesium electrodes in oxygen at reduced pressure.

The necessity of the presence of oxygen in the production of these bands has been shown by Dewar[6] and also by Brooks.[4] These bands were found to come out in the presence of air and CO_2 but would completely disappear when nitrogen or hydrogen was substituted. Even when the sparking between the magnesium electrodes was continued for a long time in the atmosphere of CO_2, these bands would gradually become fainter and finally disappear.

By using a new method of excitation, we have obtained the bands lying in the blue and green regions but the bands in the ultraviolet region observed by Olmstedt did not come out.

So far no relations, either empirical or theoretical, have been found among the various heads of the magnesium oxide bands. The object of the present paper is to obtain the vibrational quantum analysis of the bands com-

[1] Kayser, Handbuch der Spectroscopie, **5,** 717 (1920).
[2] Lecoq, Spectres Lumineu, Paris, 1874.
[3] Eder, Beitrage zur Photochemie und Spectral Analysis, 1904, pp. 410.
[4] Brooks, Proc. Roy. Soc. **A80,** 218 (1908); Nat. Acad. **78,** 198 (1908).
[5] Olmstedt, Zeits. f. Wiss. Photogr. **4,** 255 (1906).
[6] Dewar, Proc. Roy. Inst. **9,** 204 (1882).

posing the blue-green system. The rotational structure of these bands shall be treated in a later communication.

Experimental

A quartz spectrograph (Model E 1 of Adam Hilger) of the Littrow type has been used in the investigation. The burning of magnesium ribbon in air or in an atmosphere of oxygen is certainly the most natural way of exciting the oxide bands for they come out only during the combination of magnesium with oxygen. But the magnesium ribbon while so burning forms a flocculent white oxide which glows in the light and becomes a source of continuous radiation. To avoid this, a mixture of powdered magnesium metal and nitrate of magnesium in suitable proportions was used. This mixture, on being ignited, produces an explosive flash and quickly disperses away the flocculent oxide. In this case it was found that the spectrum showed a larger number of bands than when magnesium ribbon was simply burned in air or in the atmosphere of oxygen. The heat generated during the flash was enough to melt a platinum wire (about a millimeter in thickness) which was used as the sparking arrangement. The flash so produced was focussed by a quartz lens on the slit of the spectrograph and the number of flashes required for

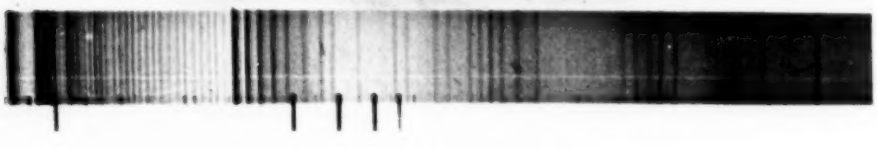

Fig. 1.

an exposure depended on the sensitiveness of the photographic plate in the region in which the bands were photographed. From a preliminary observation, these bands were found to lie between the regions λ5210 and λ4700. Ilford Special Process Panchromatic Plates were used which gave the best results in these regions.

The comparison lines for calculating the wave-lengths were obtained from a Pfund iron arc. They were photographed on either side of the bands. The standard wave-lengths used were those of Meggers, Kiess and Burns. Actual measurements of the band-heads were done on a Hilger comparator. On account of a general diffuse character of some of the bands and high magnifying power of the comparator used, difficulties were encountered in the correct location and measurement of the weak bands. It is, however, very well known that it is the identification and location of the "null" or "zero" line in an individual band, which is of more importance than that of its head or edge, in arranging the bands into various n' and n'' progressions. Unless the line structure of a band be studied under sufficient dispersion, the "null" line can hardly be located. Thus the frequency of the head may be taken to fit the various progressions. This, however, will produce some error. R. S. Mulliken[7] is in favour of setting the cross-wire of the comparator on the point

[7] R. S. Mulliken, Phys. Rev. **26,** 2 (1925).

of maximum blackening for each band as it reduces the uncertainty in locating a band-head. This procedure has been adopted by us in the measurements of the bands where possible. No where within the range of our measurements could we find a band in which the head could be distinguished from the "null" line either by a gap in the shading or even by a mere lightening—so the method of indirectly calculating the null lines from the observed bands could not be applied.

Analysis of MgO Bands

A visual inspection of the plate indicates that the bands near about λ 5211 have been resolved inspite of the low dispersion of the quartz spectrograph in this region. They have, however, been identified to be the hydride bands of magnesium. Considerable difficulty was, therefore, met with in locating the oxide bands lying in this region. It is, however, found that the bands at λ 5007 come out very easily, even when magnesium ribbon is simply burned in air. This fact seems to be in agreement with the intensity measurements and with the excellent reproduction of Eder and Valenta ("Atlas typischer Spektren," Wien, 1928). Hence they were taken as the O-sequence.

Wave-length Data

The results of the present measurements together with the data of the previous investigators are given in the following table.

Table I.

Authors					Previous investigators		
n'	n''	λ_{air}(I.A.)	ν (Vac)	O−C	Eder λ (R.S.)	Brooks λ (R.S.)	Morse λ (R.S.)
0	1	5190.91	19,259	−1.00	5190.60 (1)	5191.00	
1	2	5177.18	19,310	2.00	5177.23 (1)		
2	3	5162.99	19,363	1.00	5162.81 (½)	5162.00	
3	4	5148.50	19,418	−4.00	5145.87 (½)	5145.00	
4	5	5130.34	19,486	0.00	5130.34 (½)		
5	6	5113.47	19,551	3.00			
6	7	5097.95	19,610	1.00	5096.02 (1)		
7	8	5085.42	19,659	−4.00			5086.50
8	9	5072.64	19,708	1.00			5072.00
0	0	5007.13	19,966	−1.00	5007.44 (10)		
1	1	4996.84	20,007	4.00	4996.85 (8)		
2	2	4986.32	20,049	2.00	4986.23 (6)		
3	3	4975.51	20,093	−3.00	4974.81 (4)		
4	4	4962.40	20,146	−2.00	4962.45 (3)		
5	5	4949.19	20,200	−1.00	4949.30 (2)		
6	6	4935.20	20,257	5.00	4935.01 (1)		
7	7	4923.80	20,304	2.00	4923.65 (1)		
8	8	4913.40	20,347	−1.00	4913.37 (½)		
9	9	4903.35	20,388	−3.00	4903.36 (½)		
10	10	4892.82	20,432	2.00			
1	0	4826.12	20,715	0.00		4826.00	
2	1	4818.92	20,746	2.00		4820.00	
3	2	4810.96	20,780	0.00		4811.00	
4	3	4801.93	20,819	−2.00		4802.00	
5	4	4790.95	20,867	2.00		4791.00	
6	5	4780.72	20,911	1.00		4781.00	
7	6	4771.08	20,954	0.00		4771.00	
8	7	4761.78	20,994	0.00			

To start with, the band at λ 5007.13 was taken as the 0–0 band and the rest of the band system was then arranged into the Deslandre's progressions according to the criterion of Heurlinger and Kratzer for the assignment of the vibrational quantum numbers. The vibrational isotopic effect was looked for but no evidence of it was obtained.

The equation in terms of the parameters n' and n'' capable of representing the position of the measured heads is given below.

$$\nu_k = 19,967 + (751n' - 3.06n'^2) - (716n'' - 5.96n''^2).$$

Calculation of the Heat of Dissociation

Having made the assignment of the vibration quantum numbers for the system of bands, the average values of each ΔG_n, i.e., ω^n for the two progressions were calculated and plotted as a function of n. The interval between successive vibrational levels in the lower electronic state is zero when $n' = 125$, i.e. when $751 - 6n' = 0$. The area on the $\omega^n : n$ diagram therefore gives 5.80 volts, which is the heat of dissociation of MgO(gas) into Mg(gas) and O(gas).

Discussion

Mecke,[8] Mulliken,[9] Birge[10] and Hund[11] have shown that the band spectra of diatomic molecules bear a simple systematic relationship with the line spectra of atoms having similar outer electronic configuration. In the case of these it has been definitely proved by Dewar and by Brooks as well that the presence of oxygen is essential to produce these bands. Their emitter, may therefore be legitimately assumed as the oxide of magnesium. The band spectra of MgO will then resemble the line spectra of argon since they have the same outer electronic configuration. The ground state is therefore a singlet ^1S-state in both cases, and in the excited states, one would get singlets and triplets. Hence the MgO bands would be singlets and triplets in character.

There, however, remains the other possibility that the emitter of these bands may be MgO^+. If so, the band spectra would resemble the line spectra of ionized argon atom or of the normal chlorine atom. In either case, they would be doublet in structure.

But in the region in which these bands lie, the quartz spectrograph has a low dispersion and hence the separation of the bands into doublets or triplets could not be detected. We, therefore, reserve our opinion about the nature of the emitter till the line analysis of each individual band is made.

Our best thanks are due to Professor Birge for kindly sending us his monograph for the rapid calculation of the least squares solution of a polynomial, which has been of great use in our investigation.

[8] Mecke, Phys. Zeits. **25,** 597 (1924); Zeits. f. Physik **28,** 261 (1924); **31,** 709, (1925).
[9] Mulliken, Nat. Acad. Proc. **12,** 144 (1926); Phys. Rev. **28,** 19 and 32 (1928).
[10] Birge, Nat. Acad. Proc. **12,** 146 (1926).
[11] Hund, Zeits. f. Physik **40,** 742 (1927); **42,** 93 (1927).

THE ZEEMAN EFFECT IN THE OH BANDS

By Gerald M. Almy
Jefferson Physical Laboratory, Harvard University

(Received April 19, 1930)

Abstract

Apparatus and experimental procedure. The Zeeman effect in the $^2\Sigma \rightarrow {}^2\Pi$ OH bands in the near ultraviolet has been photographed with a 21-foot grating at 7 field strengths, varying from 5000 gauss to 34000 gauss. Up to 22000 gauss a discharge in water vapor was used as the source. Two types of quartz tubes were employed, one viewed laterally, the other end-on and placed between rectangular pole-faces. At high fields the Back-box arc, operating in water vapor, was employed.

Nature of the OH bands. The structure of the bands is briefly reviewed. New data on the satellite lines are presented, from which the ρ-type doubling in the $^2\Sigma$ states for which $v=0$, and 1, is found to be $0.216\,(K+\frac{1}{2})$. Wave-number data on the hitherto unobserved $^{PP}P_{21}$ branch are also given. The agreement between the calculated and observed wave numbers, as well as the Zeeman effect, establishes the identity of this branch.

Theoretical calculation of the Zeeman patterns in OH. Hill's theory of the Zeeman effect in doublet states is applied to OH. In the $^2\Pi$ state the molecule behaves in the field as though quite rigid, symmetrical patterns being produced. The exact treatment of a $^2\Sigma$ molecular state, is given here for the first time. This state gives rise to large magnetic energy patterns which are shown in diagrams, as are also the resulting Zeeman spectrum patterns. The variety of ordering of the magnetic levels in the two states involved is the cause of strange patterns, consisting, for all lines except those near the origin, of a narrow concentrated part and a wide diffuse part.

Results and comparison with the theory. The results of observations on the Zeeman patterns are given in tables and diagrams and quantitatively compared with the theoretical expectations. The lines are treated in three groups, (1) lines near the origin, whose fine structure is resolved, (2) lines of intermediate J'' whose patterns were completely observed, (3) lines of larger J''. The agreement with the theory is satisfactory.

Introduction

THE theory of the effect of a magnetic field on molecular spectra of the doublet type has been discussed in a recent paper by Hill.[1] At the same time the observations of Crawford and the writer[2] on the Zeeman effect in the $^2\Pi \rightarrow {}^2\Sigma$ MgH band at 5211A were correlated quantitatively with the theory with generally satisfactory results. In the present paper the Zeeman effect in the $^2\Sigma \rightarrow {}^2\Pi$ OH bands in the near ultraviolet is similarly treated, particular attention being paid to the (0,0) band at 3064A.

From a spectroscopic point of view the OH molecule differs from the MgH in two essential respects. First, the $^2\Pi$ state in OH is distinctly more rigid, or nearer case (a), as is indicated by the greater doublet separation in

[1] E. L. Hill, Phys. Rev. **34**, 1507 (1929).
[2] G. M. Almy and F. H. Crawford, Phys. Rev. **34**, 1517 (1929).

the bands;[3] second, the $^2\Sigma$ state in OH is obviously a doublet state (ρ-type doubling) for it gives rise to observable satellite branches accompanying the main branches. These satellites permit definite measurements of the magnitude of the doubling.[4] This definite knowledge of the $^2\Sigma$ state enables one to predict quantitatively how it will be affected by the magnetic field. As a result, the appearance of the OH bands in the field can be more definitely calculated than the MgH, especially for the higher rotational lines. Hence the agreement with the theory is more significant than in the case of MgH.

The Zeeman effect in OH has been extensively investigated by Fortrat.[5] His report included a qualitative description of the Zeeman patterns as well as numerical data on displacements from the no-field positions. He made observations at fields of about 5000, 20000, and 40000 gauss on the six branches of each of the bands, (0,0) at 3064Å and (0,1) at 3122Å. He reported that the effect was the same in perpendicular and parallel polarizations. His measurements of displacements (obtained by reference to iron lines) showed odd fluctuations which he thought greater than the experimental error. He did not discuss the resolvable fine structure of the patterns near the origin, except the doublet from the first line in the P_1 and Q_1 branches, nor did he give any data on the unresolved parts of the patterns. Moreover, he did not publish measurements on the weak $^{RR}R_{21}$ branch beyond the head of the band, which furnishes the most certain data on widths of patterns. It is probable that much of this information was to be found on Fortrat's plates but that in the absence of a theory to guide the work it was not recognized as useful. In view of the rather better experimental conditions at hand, it was thought worth while to repeat the investigation of OH. Information was secured on most of the points left in doubt by Fortrat's paper.

The present paper deals, in the first section, with the experimental procedure employed in photographing the Zeeman effect in the OH bands. In the second section, in which the nature of the states giving rise to the bands is discussed, some new data on the satellite branches and a hitherto unobserved non-satellite branch ($^{PP}P_{12}$) are given. The third section contains a discussion of the theoretical behaviour of the two states in the field, according to Hill's results, and the last, a detailed comparison of the observed and theoretical patterns.

[3] The position which a molecular state occupies in the range from case (a) to case (b) is specified by its "coupling constant," λ. For normal case (a) λ is $+\infty$, for inverted case (a), $-\infty$. For case (b) λ is 0 or $+4$. Hence the $^2\Pi$ state in OH ($\lambda = -6.9$) is considerably more removed from the nearer case (b) than in MgH ($\lambda = +5.7$). For the theory of multiplet molecular states, see E. L. Hill and J. H. van Vleck, Phys. Rev. **32**, 250, (1928).

[4] In order to account for the observed doublet widths in MgH at large rotational speeds, it is necessary to assume a considerable ρ-type doubling in the $^2\Sigma$ state. No satellites appear, however, as might be expected, since their theoretical intensity near case (b) is very low. Hence one has no way of determining uniquely the amount of the ρ-type doubling. It was assumed to be zero in the work on the Zeeman effect, which led, of course, to a discrepancy between the observed and theoretical patterns. The discrepancy is discussed in Footnote 13

[5] R. Fortrat, Jour. de Physique et le Rad. **5**, 20 (1924).

Apparatus and Experimental Procedure

The apparatus used in this work, except for the light sources, was that employed in previous work in this laboratory on the Zeeman effect in bands.[2,6] Two types of source were used, an uncondensed discharge in water vapor and the Back-box arc, operating in water vapor at low pressure. The spectrum from the former is freer from impurities but the tubes employed could not be used at very high fields.

Two discharge tubes were used. The first one, made of quartz, had a capillary 4 mm in internal diameter and 5 cm in length. It was mounted vertically between the flat-tipped conical polepieces of the electromagnet. A stream of water vapor from a bulb containing freshly boiled, distilled water was pumped continuously through the tube, the flow being controlled, as suggested by Jack,[7] by means of a 1 mm capillary tube, about 10 cm long, in the inlet of the tube. With a $\frac{1}{2}$-kw transformer, a discharge could not be forced through the tube at fields exceeding about 20000 gauss. It was necessary to cool the tube with an air blast. The OH spectrum produced was very weak. A 20-hour exposure just under 20000 gauss gave a spectrum of excellent definition and purity, though of only fair intensity. A similar exposure was required to get the no-field comparison spectrum.

The difficulty of faintness of source was overcome by using a tube which could be viewed end-on, between polepieces with rather large rectangular faces (3×13.5 cm). The polepieces, which were made in the laboratory shop, were designed in accordance with the theory of polepieces given by Du Bois,[8] in such a way as to give the largest field consistent with the necessary homogeneity. The maximum field attainable with a pole separation of one cm was

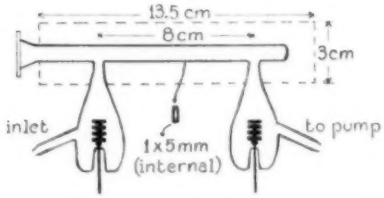

Fig. 1. Construction of the end-on quartz discharge tube. The rectangle shows the size and relative position of the pole-faces. The capillary between the side tubes was flattened, as shown in the section, in order to concentrate the discharge.

about 24000 gauss. That the field was satisfactorily uniform was shown by the sharpness of the Hg atomic line Zeeman patterns, obtained with Hg in the discharge tube. The construction of the discharge tube and its position in the magnetic field is shown in Fig. 1. The tube was made of quartz. The window on the end was fastened with deKhotinsky cement. The whole tube was cooled with a blast of cold air, and water was allowed to drop slowly on a bit of cotton wrapped around the tube just back of the window. The water

[6] E. C. Kemble, R. S. Mulliken, and F. H. Crawford, Phys. Rev. **30,** 448 (1927).
[7] D. Jack, Proc. Roy. Soc. **A115,** 373 (1927).
[8] H. Du Bois, Ann. d. Physik, und Chemie **42,** 934 (1913).

vapor was supplied as before and a more powerful transformer used. With this arrangement the intensity was increased at least ten-fold over that previously obtained.

With the end-on tube, usable photographs were taken at the following fields; 4900 gauss, 1 set of plates; 12900 gauss, 2 sets of plates; 18000–22000 gauss, 4 sets of plates. Two of the exposures near 20000 gauss were extended to 24 hours to bring out the weak $^{RR}R_{21}$ branch lying beyond the head of the band at 3064A. At lower fields this branch was obtained satisfactorily in much less time (7 hours at 12900 gauss).

At high field strengths the Back-box with brass electrodes was used. Water vapor was pumped through the box, the pressure being less than 1 cm Hg. A satisfactory photograph was obtained in about 8 hours, with a field of 33600 gauss. The $^{RR}R_{21}$ branch was not obtained.

The most intense spectra were obtained in the second order of the 21-foot grating, where the dispersion is 0.93A per mm. The third order was usable in some cases. Photographs were taken of the three bands, 3064A, 2811A, 3122A. A no-field comparison spectrum of the bands and the iron arc spectrum were photographed on each set of plates. Eastman Speedway plates were used. The patterns were measured with the aid of a Wolz comparator.

The field strengths were determined, when a discharge tube was the source, from the Zeeman patterns of the Hg atomic lines at 4047A and 4358A. These were obtained by introducing a drop of mercury into the tube and exposing a properly placed plate for a few minutes. When the Back-box was used the field was determined from the Zn triplet, 4680A, 4722A, 4811A, whose Zeeman patterns were photographed in a few minutes with brass electrodes in the box.

Nature of the OH Bands

The OH bands consist of six strong branches forming three branches of doublets, several satellite branches, and two weak branches arising from extraordinary transitions in which K changes by two units instead of one. Mulliken[9] has discussed the structure of the bands and given a diagram showing the arrangement of levels in both states as well as the transitions which produce the first line in each branch.

The $^2\Pi$ state is inverted, having a coupling constant (λ, or Mulliken's $\Delta E/B$) equal to -6.9. The doublet character of the main branches arises from the fact that there are two energy levels associated with each value of K in the $^2\Pi$ state. These states, whose J values are $K \pm \frac{1}{2}$, correspond to the two possible orientations of S and K. The doublet difference decreases from about 125 cm^{-1} at the origin to about 30 cm^{-1} at $K'' = 20$. Each level also shows appreciable Λ-type doubling which, however, does not enter into a consideration of the Zeeman effect.[1]

The $^2\Sigma$ state shows a pronounced ρ-type doubling which increases linearly with K. As in the $^2\Pi$ state there are two levels associated with each value of K, whose J values are $K \pm \frac{1}{2}$. The origin of this doubling, considered

[9] R. S. Mulliken, Phys. Rev. **32**, 388 (1928).

especially by Van Vleck,[10] lies presumably in a combination of (1) a magnetic moment due the rotating nuclei themselves, and (2) a rotational distortion of the electronic motions, also resulting in a magnetic moment along the axis of rotation. Both should produce effects proportional to $K+\frac{1}{2}$. This doubling gives rise to the satellite branches accompanying the main branches. These satellites result from transitions in which ΔJ is not equal to ΔK, as is true for the main branches. The results of several investigations of these satellites have been discussed by Mulliken, who concludes that the width of the ρ-type doublet is 0.22 K, for the lowest vibrational state.

Since the satellites in the (1,0) band at 2811A have not been reported, and because some uncertainty was expressed by Mulliken in his value of the ρ-doubling constant (0.22), it may be worth while to include here measurements on the satellites, made on the comparison spectra. Table I gives

TABLE I. *Displacements in cm^{-1} of satellite lines from main branch lines, arranged according to the value of K in the $^2\Sigma$ state. These displacements are the amounts of the ρ-type doubling in this state. The mean displacements are plotted in Fig. 2 from which the best value of the doublet constant may be obtained.*

K	P_2	Q_1	Q_2	R_1	Mean displacement
		(0,0) band at 3064A			
1			+0.28		0.28
2	+0.50	−0.49		−0.45	.48
3	.77	.73		.73	.74
4	.99	1.00		.98	.99
5		1.24		1.18	1.21
6	1.44	1.45	1.42	1.37	1.42
7	1.58		1.64		1.61
8		1.88	1.86		1.87
9	2.14	2.10	2.00		2.08
10	2.32	2.28			2.30
11			2.45		2.45
12		2.82	2.60		2.71
14		3.12	3.12		3.12
		(1,0) band at 2811A			
2	+0.43		+0.39		0.41
3	.62			−0.67	.64
4	.94	−0.96	.89	.91	.93
5	1.15	1.11			1.13
6	1.40		1.34		1.37
7	1.60	1.56	1.61		1.59
8	1.86	1.78		1.83	1.82
9	2.05			1.99	2.02
10	2.21				2.21

the displacements of the satellites from the main branch lines. The (0,0) band at 3064A furnishes the data on the lowest vibrational state ($^2\Sigma^{(0)}$), the (1,0) band at 2811A on the next higher ($^2\Sigma^{(1)}$). The average values of these displacements are plotted against K in Fig. 2. The data indicate, though none too conclusively, that the ρ-doubling is proportional to $K+\frac{1}{2}$, rather than K, agreeing with Van Vleck's prediction. Within experimental error the doubling in either vibrational state is equal to $0.216\ (K+\frac{1}{2})$.

[10] J. H. Van Vleck, Phys. Rev. **33**, 467 (1929).

A search was also made for the $^{PP}P_{12}$ branch of the (0,0) band which Mulliken predicts should be somewhat stronger than the $^{RR}R_{21}$ branch. It is situated in the midst of the bands at 3064A and 3122A and observation

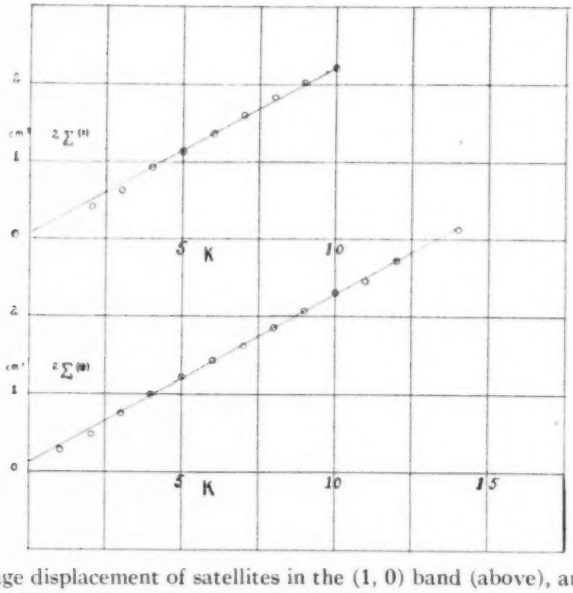

Fig. 2. Average displacement of satellites in the (1, 0) band (above), and the (0,0) band, plotted against K. The ordinate thus gives the amount of ρ-type doubling in the $^2\Sigma$ state involved in each band. From the intercept of the solid, averaging line on the vertical axis it appears that the displacements are proportional to $K+\frac{1}{2}$, rather than K, and that for both states it is about 0.216 $(K+\frac{1}{2})$.

is difficult. As can be seen from Mulliken's energy level diagram the positions can be calculated by the relation:

$$^{PP}P_{12}(J) = Q_2(J) - \Delta_2F_2'(J-1) + 0.216(J-1)$$

where

$$\Delta_2F_2'(J-1) = F_2'(J) - F_2'(J-2)$$

and 0.216 is the ρ-type doubling constant. Δ_2F_2' was obtained from Mulliken's data on the $^{RR}R_{21}$ branch and $Q_2(J)$ from Fortrat's table of wave numbers. The results of these calculations appear in Table II together with the observed wave numbers of what are believed to be the lines of this branch. The agreement is good. This assignment is substantiated by the Zeeman effect of these lines, which will be discussed later. The observed intensities in this branch are about the same as those of the $^{RR}R_{21}$ branch and decrease rapidly with increasing J.

Theoretical Calculation of the Zeeman Patterns in OH

The theory of the Zeeman effect in doublet bands has been discussed in terms of the quantum mechanics by Hill.[1] He has obtained an expression in closed form for the magnetic energy of $^2\Pi$, $^2\Delta$, ... molecular states ranging from case (a) to case (b). Qualitatively, the predicted behavior in

TABLE II. *Wave numbers of* $^{PP}P_{12}(J)$. *When a line coincides with a main branch line the latter is put in parantheses. The intensity scale is arbitrary.*

J	Calculated cm^{-1}	Observed cm^{-1}	Intensity (Obs.)
$1\frac{1}{2}$	32253.29	$(P_2(2\frac{1}{2}))$	
$2\frac{1}{2}$	186.11	$(Q_1(12\frac{1}{2}))$	
$3\frac{1}{2}$	113.50	32113.38	6
$4\frac{1}{2}$	036.02	036.10	6
$5\frac{1}{2}$	31954.89	31954.90	—
$6\frac{1}{2}$	870.04	$(P_1(11\frac{1}{2}))$	
$7\frac{1}{2}$	781.51	$(Q_2(18\frac{1}{2}))$	
$8\frac{1}{2}$	690.31	$(P_2(12\frac{1}{2}))$	
$9\frac{1}{2}$	596.00	31595.85	3
$10\frac{1}{2}$	498.97	498.88	2
$11\frac{1}{2}$	399.07	$(Q_2(23\frac{1}{2}))$	
$12\frac{1}{2}$	296.96	31296.78	1
$13\frac{1}{2}$	192.25	192.26	$\frac{1}{2}$

the field of the $^2\Pi$ state of OH is that of a rigid molecule. Each level (J, K) breaks up into $2J+1$ magnetic sublevels, symmetrically placed about the no-field energy. Their positions are quantitatively given by Hill's Eq. (12):[11]

$$W(\Lambda, K, J, M) = B\{(J+\tfrac{1}{2})^2 - \Lambda^2 + \beta(\Lambda^2+\tfrac{1}{2}) \pm \tfrac{1}{2}[(2J+1)^2(1-\beta)^2 + \Lambda^2(\lambda+\beta)(\lambda-4+5\beta)]^{1/2}\} \quad (1)$$

where the two signs are to be associated with the two states for which $J = K \mp \frac{1}{2}$, $B = h/8\pi^2 cI$, and $\beta = (\Delta\nu_n/B)\ M/J(J+1)$.

In the paper referred to, Hill treated the $^2\Sigma$ state as if it consisted of two coincident levels, neglecting the ρ-type doubling. Such a state should become, in the field, a doublet of twice normal separation, arising from the energy of the spin in the field. This procedure was justifiable in the case of MgH, since its bands have no satellites from which the ρ-type doubling can be estimated.[4] In OH, however, the $^2\Sigma$ state possesses, as has been discussed, a ρ-type doubling equal to $0.216(K+\frac{1}{2})$. At a field of 20000 gauss ($\Delta\nu_n = 0.94$ cm^{-1}) the ρ-type doubling is considerably less at the origin than $\Delta\nu_n$, but it increases linearly with K, becoming considerably greater than $\Delta\nu_n$ rather early in the band. Near the origin, therefore, we may expect a molecular Paschen-Back effect, with the spin parallel or anti-parallel to the field, giving a doublet of twice normal width. But since the interaction energy which gives rise to the ρ-type doubling still remains, each member of this twice normal doublet should be "spread out" to approximately the ρ-type doublet width, the pattern consisting of $2J+1$ closely spaced levels. On the other hand, as K increases, and the ρ-type doublet width becomes much greater than $\Delta\nu_n$, S and K tend to preserve their orientation when in the field. Each member of the no-field doublet splits into $2J+1$ magnetic levels. Their separations from the no-field position run from about $+\Delta\nu_n$

[11] The OH molecule is sufficiently rigid that the δ term in Hill's complete Eq. (22) is negligible. This reduces (22) to (12). In Eq. (12) the terms in the square of the field also turn out to be negligible so that the Zeeman energy level pattern for the $^2\Pi$ state is sensibly symmetrical about the no-field position. In the calculations on MgH Hill's Eq. (22) had to be used.

to $-\Delta\nu_n$, since the magnetic energy is largely that of spin and field, with that of nuclear rotation and field making little contribution.

Precisely this behavior is predicted in the following quantitative treatment of the $^2\Sigma$ state. This treatment is due to Dr. Hill, and I owe him thanks for permission to set it down here. Since the ρ-type doubling is a small effect, compared with other interactions in the molecule, we may treat the motion in the $^2\Sigma$ state as case (b) (i.e., K and S precess regularly about J), perturbed by the magnetic field. Assuming that the perturbation energy is due to the interaction of S and H, it has the form,

$$H_1 = 2\Delta\nu_n(S\cdot H). \tag{2}$$

The matrix elements of this perturbation function may be written:

$$H_1(K_1, M; K_1, M) = \Delta\nu_n\frac{M}{K+\tfrac{1}{2}} = \Delta\nu_n\alpha, \quad \text{where} \quad \alpha = \frac{M}{K+\tfrac{1}{2}}$$

$$H_1(K_1, M; K_2, M) = H_1(K_2, M; K_1, M) = \Delta\nu_n(1-\alpha^2)^{1/2}$$

$$H_1(K_2, M; K_2, M) = -\alpha\Delta\nu_n$$

where K_1 corresponds to $J = K+\tfrac{1}{2}$, K_2 to $J = K-\tfrac{1}{2}$. Let $W(K_1) - W(K_2) = \nu_0$ (energy expressed in cm^{-1}).[12] The energy determinant is,

$$\begin{vmatrix} -\frac{\nu_0}{2} - \alpha\Delta\nu_n - W & \Delta\nu_n(1-\alpha^2)^{1/2} \\ \Delta\nu_n(1-\alpha^2)^{1/2} & \frac{\nu_0}{2} + \alpha\Delta\nu_n - W \end{vmatrix} = 0,$$

where the origin for W is the mid-position of the no-field doublets. The solution of this determinant is,

$$W = \pm\tfrac{1}{2}\{\nu_0^2 + 4\alpha\nu_0\Delta\nu_n + 4\Delta\nu_n^2\}^{1/2} \tag{3}$$

where the upper sign goes with $J = K+\tfrac{1}{2}$, the lower with $J = K-\tfrac{1}{2}$. From (3) the magnetic energy levels may be calculated. The two extreme levels in the K_1 state need separate treatment, since for them, $M = K+\tfrac{1}{2}$, and the non-diagonal terms vanish. Since the upper left term in the determinant is associated with the K_2 state, only the single lower right term remains. Hence the energies for these two extreme magnetic levels of the K_1 state are simply,

$$W = \frac{\nu_0}{2} \pm \Delta\nu_n. \tag{4}$$

Calculations at 12900, 20000, and 33600 gauss of the magnetic energy levels in the two states of OH have been carried through by means of Eqs. (1)

[12] In the $^2\Sigma$ states of some molecules $W(K_1)$ is less than $W(K_2)$, in which case the appropriate change in the sign of ν_0 must be made. The assignment of the two roots of Eq. (3) to the two no-field levels is also changed.

and (3). In the $^2\Pi$ state the values, $\lambda = -6.9$, $B = 18.47$, given by Mulliken, were used. In the $^2\Sigma$ state the ρ-type doubling (ν_0 in Eq. (3)) was supposed to be 0.22 K. As shown above, the subsequent more careful consideration

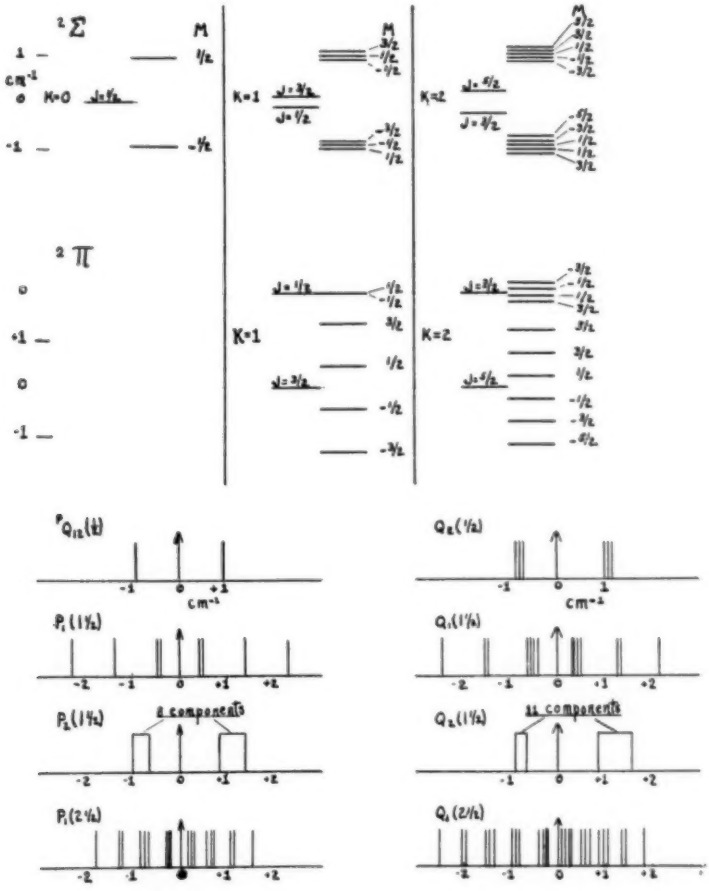

Fig. 3. Magnetic energy levels at 20000 gauss in OH $^2\Sigma$ and $^2\Pi$ states of low values of K, and some of the resulting Zeeman patterns. In each group of energy levels the no-field energies are shown at the left, the energies in the field at the right. In the Zeeman patterns the grouping in clusters is due to the fact that M may change by 0 or ± 1. Hence, since the spacing is quite close in the $^2\Sigma$ state, three lines may fall close together. These groups are not resolvable at attainable fields, but appear as broadened lines on the plates, their intensities roughly proportional to the number in the group. Parts of all of these patterns (except $P_2(1\frac{1}{2})$ and $Q_2(1\frac{1}{2})$) are observed as resolved (Table III). In the $Q_1(2\frac{1}{2})$ pattern, for example, the five low-frequency groups are resolved at 33600 gauss, while the high-frequency part appears as a broad faint band, consistent with the fairly uniform distribution of components in this figure. All intervals are to scale except the $^2\Sigma \rightarrow {}^2\Pi$ interval and the $^2\Pi$ no-field doublet interval.

of the satellites indicates that this doubling is, more precisely, 0.216 $(K+\frac{1}{2})$. However, since the change would make differences of much less than 0.1 cm^{-1} in any of the computed patterns, it was not thought worth while to repeat the calculations.

The magnetic energy levels in both states for a field of 20000 gauss are plotted in Figs. 3 and 4. Fig. 3 shows the fine structure in the two states for low values of K, and, below, the Zeeman patterns of some of the early lines, when all permissible transitions ($\Delta M = \pm 1,0$) are considered. Fig. 4 shows the magnetic energy of the extreme levels ($M = \pm J$) in each state, plotted as a function of K. The fictitious level, $M = 0$, serves merely to locate the center of the number of levels, but, since J is half integral, does not correspond to a real level. In the $^2\Sigma$ state the magnetic energy is calculated with reference to the center of the no-field doublets. The energy separations

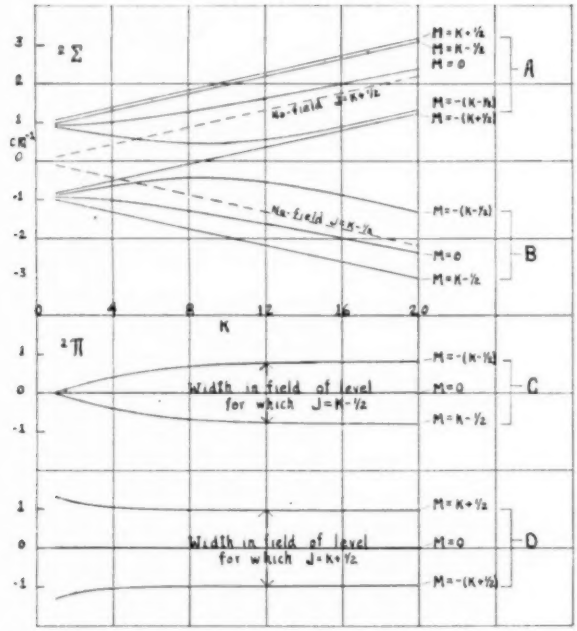

Fig. 4. Magnetic energies at 20000 gauss of the $^2\Sigma$ and $^2\Pi$ states of OH, plotted as a function of K. The levels omitted are quite uniformly spaced between the center "levels" ($M=0$) and the extreme levels ($M=\pm J$). The broken lines show the no-field $^2\Sigma$ levels, the distance between them being the amount of the ρ-type doubling. The Zeeman patterns in Fig. 6 are obtained by considering the transitions between the groups of this figure, taking into account the proper changes in K and M during the transition.

of the latter are given by the distance between the broken lines. Due to the peculiar behavior near the origin of the level for which $M = -(K+\frac{1}{2})$ the levels $M = \pm(K-\frac{1}{2})$ in the upper group are also shown.

In a consideration of the Zeeman spectrum patterns resulting from this arrangement of energy levels, the order of these levels is very significant. Thus, in the group A (Fig. 4) of the $^2\Sigma$ state the level, $M = K+\frac{1}{2}$ is at the top whereas in group B the level $M = -(K-\frac{1}{2})$ is at the top. This is to be expected for large values of K since in A the spin is parallel to the nuclear rotation ($J = K+\frac{1}{2}$), and thus parallel to the field when $M = +J$. In B, on the other hand, the spin is anti-parallel to K, and parallel to the field when

$M=-J$. These states are highest in their respective groups because the magnetic energy is mostly due to the interaction of spin and field. The calculations show that this ordering of energy levels holds continuously to low values of K, where, however, S is to be thought of as quantized independently in the field (molecular Paschen-Back effect).

Similar considerations as to the arrangement of the energy levels apply to the $^2\Pi$ state. The difference in the two groups, for which $J=K\pm\frac{1}{2}$, is shown in Fig. 4, C and D. In C the spin is anti-parallel to K, and the state for which $M=-(K-\frac{1}{2})$ has the greatest energy. In D, spin and K are parallel and the state for which $M=K+\frac{1}{2}$ has the greatest energy.

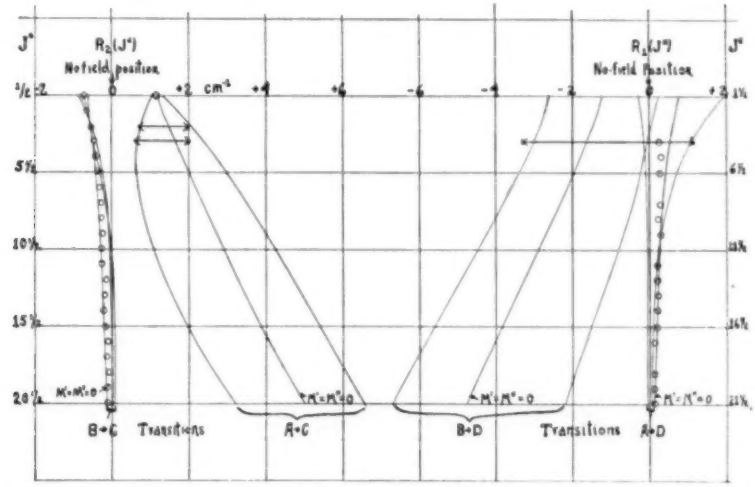

Fig. 5. Zeeman patterns of the R branches in the OH bands at 20000 gauss. The values of J'' are so arranged that the intersection of a horizontal line with the curves gives the outline of a pattern of a no-field R doublet. Two things may be particularly noted: (1) the great difference in width, except near the origin, of the two parts of the pattern of a line, due to the arrangement of magnetic levels in the two states (cf. Fig. 4 and text), (2) the appearance, at intermediate values of J'', of the "center line" ($M'=M''=0$) outside of what would ordinarily be the extreme components. The circles show the observed positions of the narrow intense parts, the two-ended arrows the widths of the observable broad faint parts.

From the energy level diagram of Fig. 4 the outlines of the Zeeman spectrum patterns may be obtained. As an example, the patterns of the R_1 and R_2 branches in a field of 20000 gauss are shown in Fig. 5. Displacement from the no-field position is plotted horizontally and J'', vertically. The extreme components and the center of the *number* of components ($M'=M''=0$) of any line are the intersections of the curves shown with a horizontal line at the corresponding value of J''. The curious effect of one wide and one narrow part of each pattern is due to the arrangement of energy levels in the two states, just discussed. Thus the transitions $B\rightarrow C$ and $A\rightarrow D$ (cf. Fig. 4) result in close clusters of components near the no-field position, because the magnetic effect in one state undoes that in the other, when one considers the transition. But for the transitions $A\rightarrow C$ and $B\rightarrow D$ the displacements in the two states add, giving the extremely wide, and con-

sequently faint, parts of the patterns. In the narrow groups $B \rightarrow C$ and $A \rightarrow D$ it is also to be noted that, except near the origin, the center line, for which $M' = M'' = 0$, falls outside the components which would ordinarily be the extreme edges of the pattern. In other words, each of these groups folds back on itself. The components not shown fall, in all cases, fairly uniformly between the center line and the "extreme" components.[13]

In anticipation of the results to be discussed in the following section, it may be said that the circles in Fig. 5 represent the observed positions of the intense narrow parts of the patterns and the two-ended arrows the observed widths of the more diffuse parts of the patterns.

The theoretical patterns of the Q and P branches are, except for small differences in widths, like those of the R branch. The general appearance of the calculated patterns at 12900 and 33600 gauss is the same as that shown for 20000 gauss. Widths and displacements are different, of course, and roughly proportional to the field.

Results and Comparison with the Theory

A description of the general features of the Zeeman effect in the OH bands will be given and, where feasible, a quantitative account and comparison with the theory. The lines may be considered in three groups, (1) the lines near the origin for which the fine structure is resolved, (2) a number of intermediate lines for which complete patterns are observable, including lines in the ${}^{RR}R_{21}$ and ${}^{PP}P_{12}$ branches, and (3) the lines with larger values of J'', for which only the intense parts of the patterns are observed. Quantitative observations were made extensively only on the (0,0) band at 3064A. Qualitative observations and a few measurements indicated that the (0,1) band at 3122A and the (1,0) band at 2811A behave in very much the same manner.

Fine structure of the lines near the origin. The calculated patterns of several lines near the origin are shown in Fig. 3. It is seen that the fine structure patterns increase rapidly in complexity as one proceeds from the origin. Only branches subscribed "1" have patterns which one might expect to resolve beyond the relatively coarse doubling to be observed in most of the patterns. The numerical description of the patterns observed and comparison with the theory is contained in Table III.

As predicted, $Q_2(\frac{1}{2})$, $R_2(\frac{1}{2})$, ${}^{P}Q(\frac{1}{2})$ become doublets of twice normal separation. The doublets of the first two of these lines are unsymmetrical with

[13] A consideration of the ρ-type doubling would account for the discrepancies appearing in the Zeeman patterns of the high rotational doublets of MgH (Ref. 2). The Zeeman pattern of such a doublet consisted, at 16000 gauss, of an intense part filling the no-field doublet interval and on either side a somewhat fainter, narrow "wing." The central part corresponds to the broad parts of the patterns in OH (Fig. 5), though in MgH they overlapped. The wings correspond to the narrow parts of the OH patterns. (Their faintness was due to the fact that the Paschen-Back effect was setting in.) Thus both the too large width of the central part (according to the previous theory) and the too small width of the wings, as well as the too large no-field doublet width (Cf. Footnote 4), would be accounted for by a consideration like the above for OH of the ρ-type doubling in the ${}^{2}\Sigma$ state.

TABLE III. *Fine structure of lines near the origin. Values given are displacements in cm^{-1} from the no-field position of the line in question. The question mark indicates that the pattern overlaps with another, the identity of the component being uncertain.*

Line	12,900 gauss		20,000 gauss		33,600 gauss	
	Obs.	Calc.	Obs.	Calc.	Obs.	Calc.
$^{P}Q_{12}(\frac{1}{2})$	−0.70 + .52	−0.60 + .60	−0.93	−0.94 + .94		−1.58 +1.58
$P_1(1\frac{1}{2})$	 −0.75 − .20 + .34	−1.45 −0.88 − .28 + .28 + .88 +1.45	 −1.36 −0.51 +.36	−2.28 −1.39 −0.44 + .44 +1.39 +2.28	 −0.84	−3.78 −2.31 −0.74
$P_1(2\frac{1}{2})$					−2.80? −2.17? −1.29 −0.35 + .40	−2.91 −2.09 −1.27 −0.42 + .29
$Q_2(\frac{1}{2})$	−0.59	−0.46 + .75	−0.81	−0.80 +1.08	−1.45	−1.44 +1.73
$Q_1(1\frac{1}{2})$	−1.57 −0.93 − .20 + .37 + .80	−1.53 −0.96 − .22 + .25 + .81 +1.31	−2.36 −1.46 − .43 + .53	−2.41 −1.55 − .55 + .40	−4.20 −2.39 − .57	−3.94 −2.43 − .80 + .66 +2.21 +3.67
$Q_1(2\frac{1}{2})$					−4.03? −3.09 −2.28 −1.30 −0.38 + .28	−3.91 −3.08 −2.24 −1.38 −0.47 + .32
$R_2(\frac{1}{2})$	−0.46 + .74	−0.42 + .86	−0.78 +1.14	−0.75 +1.17	−1.28 +2.00	−1.47 +1.81
$^{RR}R_{21}(1\frac{1}{2})$	 −0.24 + .52 +1.17 +2.03?	−1.16 −0.57 −0.05 + .61 +1.25 +1.82	 +0.00 + .92 +1.74 +2.52	−2.12 −1.13 −0.03 + .87 +1.65 +2.51		

respect to the no-field position. Such asymmetry, which appears throughout the band, is due to the fact that the Zeeman energy levels in the $^2\Sigma$ states are symmetrical with respect to the mid-points of the ρ-type doublet levels, while a no-field line arises from a level displaced from a mid-point by 0.108 $(K+\frac{1}{2})$. The agreement between theory and observation for these lines is not too good. Measurement is difficult in the Q_2 and R_2 doublets because of the prominence of the satellite line in the no-field spectrum of each. It is nearly as intense as the no-field line and barely resolved from it.

No more patterns are resolved in the branches with subscript "2". But the more open patterns of the early lines of the branches with subscript "1" are resolved, where observable. The agreement with theory is generally good.

The intensities fall off rapidly as one proceeds outward from the components nearest the no-field line. This corresponds to the decreasing number of members of the close groups in the theoretical pattern. Data on the first line of the $^{RR}R_{21}$ branch is also given, though the pattern is so faint as to be barely observable on the plates. This pattern is noteworthy because of the unusually large shift of the whole pattern with respect to symmetry about the no-field position. This shift is due to the fact that the ρ-type doubling in the $^2\Sigma$ state for this line is larger than in other lines with the same final J.

Patterns of lines of intermediate J''. Several of the lines of intermediate J'' are so situated that the complete patterns may be observed. The appearance of these patterns is just what would be expected from Fig. 5. Thus the branches with subscript "2" consist of two separated parts, one (the low-frequency) fairly sharp, intense, and less displaced than the other, which is wide and faint. On the other hand, the pattern of a line with subscript "1" consists of two contiguous parts, the high-frequency part being intense, fairly sharply defined, and narrower than the fainter low-frequency part. The fainter part of each type of pattern becomes rapidly too weak to observe as one proceeds out in the band, though on one plate at 20500 gauss the complete patterns of $Q_2(12\frac{1}{2})$ and $Q_1(12\frac{1}{2})$ could be observed. The numerical description of these patterns is contained in Table IV. Some are reproduced in Fig. 6.

In this group should be included the observable lines of the $^{RR}R_{21}$ branch. This branch, being beyond the head of the band, offers excellent opportunity

TABLE IV. *Quantitative description of patterns of lines with intermediate J''. Only patterns which could be fairly completely observed are included. Measurements are given to the nearest* 0.05 cm^{-1}.

a. Lines with subscript "1".

Field	Line	Total width		Intense part			
				Width		Position with respect to no-field	
		Obs.	Calc.	Obs.	Calc.	Obs.	Calc.
20000	$P_1(5\frac{1}{2})$	3.7	4.0	1.6	1.4	+0.45	+0.6
	$P_1(6\frac{1}{2})$	3.2	4.0	1.7	1.2	+ .3	+ .5
33600	$P_1(5\frac{1}{2})$	Indef.		2.4	2.7	+0.9	+1.2
	$P_1(6\frac{1}{2})$	"		2.0	2.5	+ .7	+1.1
20000	$Q_1(4\frac{1}{2})$	4.2	4.0	1.5	1.4	+0.0	+0.6
	$Q_1(5\frac{1}{2})$	4.4	4.1	1.4	1.2	+ .1	+ .5
	$Q_1(6\frac{1}{2})$	4.5	4.1	1.3	1.0	+ .3	+ .4
	$Q_1(9\frac{1}{2})$	4.9	4.2	sharp	.5	+ .25	+ .2
	$Q_1(12\frac{1}{2})$	4.6	4.7	"	.4	+ .25	+ .15
33600	$Q_1(4\frac{1}{2})$	6.45	6.70	2.75	2.75	+1.0	+1.2
	$Q_1(5\frac{1}{2})$	5.8	6.65	2.35	2.45	+0.85	+1.1
	$Q_1(6\frac{1}{2})$	6.25	6.65	2.25	2.25	+ .85	+1.0
	$Q_1(9\frac{1}{2})$	6.3	6.7	1.9	1.7	+ .7	+ .7
20000	$R_1(4\frac{1}{2})$	4.5	4.1	1.3	1.2	+0.5	+0.5
33600	$R_1(4\frac{1}{2})$	6.1	6.8	2.2	2.4	+ .9	+1.2

TABLE IV (*continued*)

b. Lines with subscript "2". (Positions measured with respect to no-field positions.)

Field	Line	High-frequency part of pattern				Low-frequency part of pattern			
		Position		Width		Position		Width	
		Obs.	Calc.	Obs.	Calc.	Obs.	Calc.	Obs.	Calc.
20000	$P_2(3\frac{1}{2})$	+1.45	+1.3	1.7	1.5	−0.65	−0.6	0.9	0.5
	$P_2(4\frac{1}{2})$	+1.5	+1.5	2.2	1.8	− .55	− .5	.95	.45
	$P_2(6\frac{1}{2})$	+2.0	+1.7	3.0	2.1	− .4	− .4	.7	.3
33600	$P_2(3\frac{1}{2})$	+1.9	+2.0	2.1	2.1	−1.1	−1.3	1.05	1.1
	$P_2(4\frac{1}{2})$	+2.1	+2.1	2.8	2.65	−1.0	−1.2	1.2	1.1
	$P_2(6\frac{1}{2})$	Indef.	+2.3	Indef.	3.3	−0.9	−1.0	1.1	1.1
20000	$Q_2(3\frac{1}{2})$	+1.4	+1.45	1.65	1.6	−0.35	−0.6	1.0	0.4
	$Q_2(6\frac{1}{2})$	+1.6	+1.9	3.0	2.5	− .3	− .35	.8	.3
	$Q_2(8\frac{1}{2})$	+2.0	+2.2	2.35	2.9	− .25	− .25	.—	.3
	$Q_2(10\frac{1}{2})$	+2.3	+2.5	2.6	3.2	− .25	− .2	1.0	.3
	$Q_2(11\frac{1}{2})$	+2.6	+2.75	2.9	3.3	− .2	− .2	1.1	.3
	$Q_2(12\frac{1}{2})$	+2.8	+3.0	3.1	3.4	− .2	− .2	1.0	.3
33600	$Q_2(3\frac{1}{2})$					−1.0	−1.2	0.9	0.7
	$Q_2(6\frac{1}{2})$	Too faint				−0.8	−0.9	1.2	0.7
	$Q_2(8\frac{1}{2})$					− .65	− .75	1.0	.6
	$Q_2(10\frac{1}{2})$	to measure				− .6	− .6	1.0	.6
	$Q_2(11\frac{1}{2})$					− .55	− .55	1.2	.6
	$Q_2(12\frac{1}{2})$					− .55	− .5	1.0	.6
20000	$R_2(2\frac{1}{2})$	+1.35	+1.25	1.3	1.3	−0.65	−0.6	sharp	0.1
	$R_2(3\frac{1}{2})$	+1.35	+1.25	1.4	1.45	− .55	− .5	sharp	.1
33600	$R_2(2\frac{1}{2})$	+1.8	+2.05	1.75	1.8	−1.25	−1.15	1.0	0.6
	$R_2(3\frac{1}{2})$	+1.85	+2.20	2.1	2.45	−1.05	−1.05	0.8	.65

Notes to Table IV. 1. The data at 20000 gauss are the average of measurements on 4 sets of plates between 18200 and 20700 gauss, the measurements being adjusted to 20000 gauss, assuming the effects proportional to the field in this range.

2. Since the width of a no-field line, as determined by the blackened portion of the plate, is about 0.5 cm^{-1}, measured widths of less than 1 cm^{-1}, say, have little meaning. In a well-exposed part of a pattern, the observed width might easily be 0.5 cm^{-1} greater than the actual width, or range of wave number, of the part. The negative parts of the Q_2 patterns, however are definitely wider than expected from the theory.

3. In both $P_2(6\frac{1}{2})$ and $Q_2(6\frac{1}{2})$ the observed high-frequency part at 20000 gauss is abnormally wide.

TABLE V. *Quantitative description of the Zeeman patterns of the* $^{RR}R_{21}$ *branch, and comparison with the theory. The values at* 20000 *gauss are figured to the nearest* 0.05 cm^{-1}. *Observations at* 18200 *and* 20500 *were adjusted to* 20000 *gauss, assuming that the effect was proportional to the field, and averaged.*

Field	J''	Total width		Position of negative edge with respect to no-field line		Position of positive sharp comp. with respect to no-field line	
		Obs.	Calc.	Obs.	Calc.	Obs.	Calc
12900	$2\frac{1}{2}$	2.86	2.89	−1.40	−1.31	+1.35	+1.40
	$3\frac{1}{2}$	2.95	2.85	−1.38	−1.25	1.49	1.48
	$4\frac{1}{2}$	2.89	2.96	−1.18	−1.25	1.62	1.63
	$5\frac{1}{2}$	3.06	3.06	−1.22	−1.23	1.81	1.79
20000	$2\frac{1}{2}$	4.4	4.3	−1.9	−2.05	1.4	Indef.
	$3\frac{1}{2}$	4.3	4.2	−2.0	−1.95	1.45	1.4
	$4\frac{1}{2}$	4.35	4.2	−1.85	−1.95	1.4	1.35
	$5\frac{1}{2}$	4.3	4.2	−1.85	−1.9	1.4	1.35
	$6\frac{1}{2}$	4.3	4.25	−2.0	−1.9	1.3	1.35

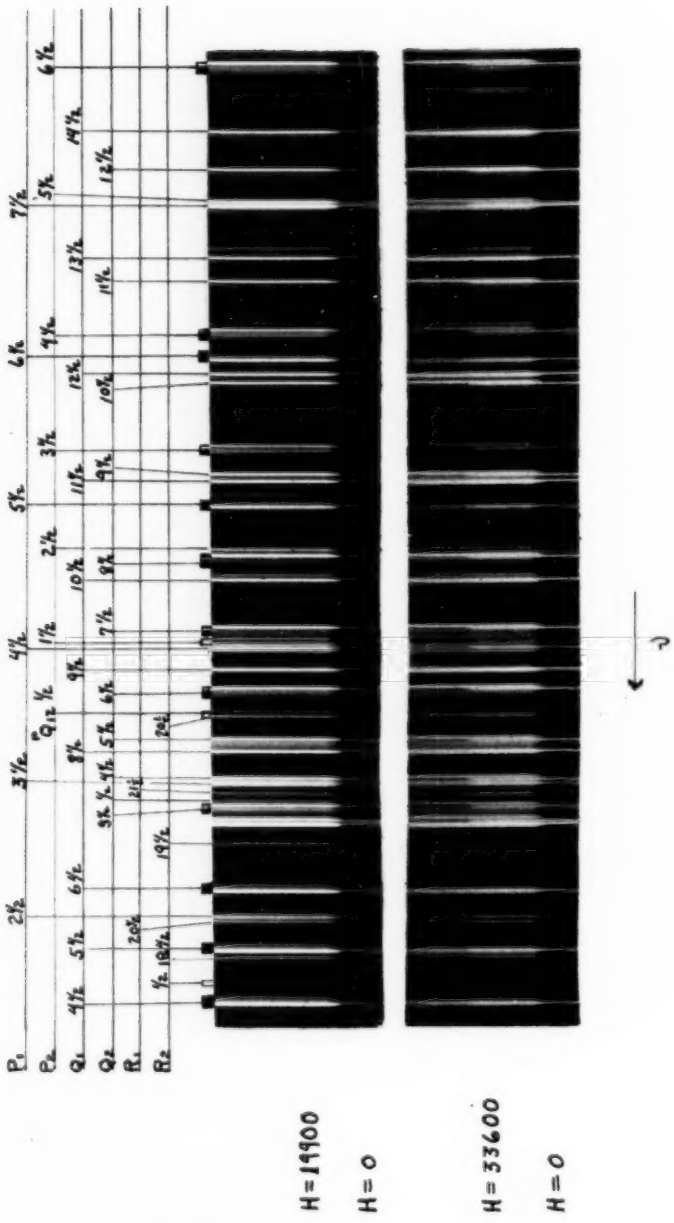

Fig. 6. Reproductions of a part of the 3064A band, at two fields, together with the no-field comparison spectra. The patterns at the lower field are labelled with the usual line notation, and those at the higher field can be identified by comparison. The effects, such as doubling, broadening, and displacement are seen to be roughly proportional to the field. As representative patterns, $P_2(3\frac{1}{2})$, $Q_1(6\frac{1}{2})$, $Q_2(6\frac{1}{2})$, $R_1(20\frac{1}{2})$, $R_2(\frac{1}{2})$ might be suggested. Some satellites can be seen in the no-field spectrum, e.g. in $P_2(3\frac{1}{2})$, $P_2(4\frac{1}{2})$ $P_2(6\frac{1}{2})$, on the high frequency side of the main branch line. There are a great many apparently spurious lines, especially on the high field plate.

for observation, but is very weak. Only 6 or 7 lines were obtained with sufficient intensity to measure accurately. The Zeeman pattern of each of these consists of a broad sharp-edged pattern which is divided into two parts, a broad low-frequency part and a sharper high-frequency part whose sharpness increases with increasing J''. This is exactly the calculated behavior. The two parts have about the same maximum intensity, in contrast to the

TABLE VI. *Zeeman patterns of* $^{PP}P_{12}$ *branch.*

Field	J''	Total width (cm^{-1})		Position of negative edge with respect to no-field position (cm^{-1})	
		Obs.	Calc.	Obs.	Calc.
12900	$3\frac{1}{2}$	2.15	2.4	−1.3	−1.3
	$4\frac{1}{2}$	2.25	2.7	−1.4	−1.45
20000	$3\frac{1}{2}$	3.4	3.75	−1.7	−1.95
	$4\frac{1}{2}$	3.4	4.1	−1.8	−2.15

patterns of the main branch lines. In the latter the intensity of the concentrated part is much greater than that of the wider part, as one would expect. The results of observation and the comparison with theory are contained in Table V.

Of the lines ascribed to the $^{PP}P_{12}$ branch only two have Zeeman patterns sufficiently intense and in the clear to permit definite measurements. These

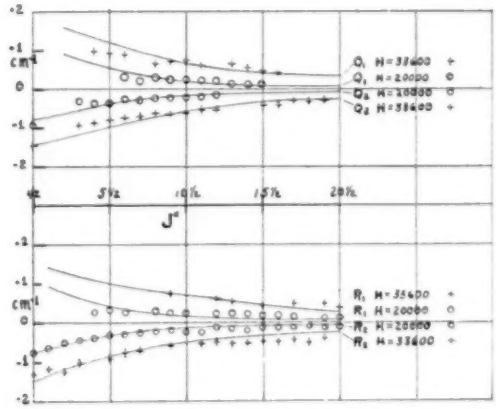

Fig. 7. Displacements of the narrow intense parts of the patterns of Q and R branches. The solid curves give the calculated displacements as estimated from plots like Fig. 5. The crosses and circles are the observed displacements.

two, $J''=3\frac{1}{2}$ and $J''=4\frac{1}{2}$, have been observed at 12900 and 20500 gauss. The total width and position with respect to no-field of these patterns is in fair agreement with the theory (Table VI). The intensity distribution, however, is surprising. For the calculations indicate a fairly uniform distribution of components from edge to edge of the pattern, while the observed pattern consists of two parts, a low-frequency narrow part and a high-fre-

quency wider part, with possibly a faint band between. Other lines assigned to this branch apparently have the characteristic wide patterns, but they are partly obscured by other lines. Since there are no other lines in this spectral region which show such width of pattern, the Zeeman effect substantiates the assignment of these lines to the $^{PP}P_{12}$ branch.

Lines with large values of J''. The Zeeman patterns of lines with large values of J'' theoretically consist of the concentrated slightly displaced part and the wide diffuse part (Fig. 5). The latter is too weak to photograph. The intense sharp part, however, may be followed apparently as far as the band itself. Hence the Zeeman spectrum looks almost like the no-field spectrum, except for a slight broadening and a small displacement of each line, positive for those branches subscribed "1", negative for those subscribed "2". The displacements of these intense parts in the Q and R branches is plotted in Fig. 7. The P branches behave similarly. The solid curves show the calculated displacements. The behavior of the R branches at 20000 gauss is also shown in Fig. 5. Several patterns of large J'' are reproduced in Fig. 6.

I am glad to express my gratitude to Professor E. C. Kemble for suggesting this problem, to Dr. F. H. Crawford for advice and criticism throughout the work, and to Dr. E. L. Hill for many discussions of the application of the theory of the Zeeman effect. I am also very grateful to the laboratory technicians, particularly Mr. H. W. Leighton, for assistance in the manufacture of apparatus. It should also be mentioned that a large part of the apparatus used in this work was acquired through the generosity of the Milton Fund of Harvard University.

THE ZEEMAN EFFECT IN THE RED CaH BANDS

By William W. Watson and William Bender
Sloane Physics Laboratory, Yale University

(Received May 1, 1930)

Abstract

The Zeeman effect in the red $^2\Pi \rightarrow {}^2\Sigma$ and $^2\Sigma \rightarrow {}^2\Sigma$ CaH bands, together with new satellite branches in the $^2\Pi \rightarrow {}^2\Sigma$ system, are reported. Field strengths up to 30,000 gauss were employed, the dispersion of the large concave grating in a parallel light mounting being about 2.1A per mm.

Satellite series in the $^2\Pi \rightarrow {}^2\Sigma$ bands.—The ${}^0P_{12}$ satellite branches are measured for both the A and A' bands. These frequencies together with certain combination relations fix the hitherto uncertain J numbering in the Q branches, and hence the size of the Λ-type doubling. This doubling is very large (70 cm^{-1} at $K=34\frac{1}{2}$) and of opposite sign to that usually found in other bands.

Zeeman effect in the $^2\Pi \rightarrow {}^2\Sigma$ bands.—General agreement with the pattern blocks predicted by Hill's theoretical formulas for the lower K' states is found. Intensity variations with increasing field strength are described. For $K'>19$, where the no-field spin doublet components come together and cross over, uncoupling effects occur. Only the transitions from anti-parallel S and K in the $^2\Pi$ state to parallel S and H in the $^2\Sigma$ state, and from parallel S and K to antiparallel S and H persist. The displacements of these components are proportional to H^2. At 30,000 gauss the high K components in the P_1 branch broaden out and go rapidly to zero intensity, but the P_2 field components remain narrow and strong. With complete uncoupling by this "strong field," these components are probably the transitions from parallel S and H in the $^2\Pi$ state to parallel S and H in the $^2\Sigma$ state. For the highest K levels, these high-field P_2 components are displaced farther from the no-field position and become more diffuse, suggestive of an approach to Hund's case d.

Zeeman effect in the $^2\Sigma \rightarrow {}^2\Sigma$ bands.—Contrary to the usual findings for bands of this type, broad and prominent Zeeman patterns here occur for $K'>8$ which are quite similar to those found in a $^2\Pi$ state. The explanation is probably that an appreciable magnetic moment is created in the upper $4s\sigma^2 3d\sigma\ ^2\Sigma$ state by the increasing component of L along the rotational axis.

Introduction

A THEORETICAL treatment of the Zeeman effect in doublet band spectra has recently been published by E. L. Hill,[1] and the formula for the magnetic field patterns have been nicely verified by Almy and Crawford[2] for the case of the MgH $^2\Pi \rightarrow {}^2\Sigma$ band system. This theory considers molecules which can be classed under Hund's cases (a) and (b) or for cases intermediate between (a) and (b), neglects "rho-type" doubling, and considers the only uncoupling effect to be that on the electron spin. There are examples of diatomic molecules, however, where the rho-type doubling becomes very large, and where the coupling of the electronic orbital angular momentum to the rotational axis would be accompanied by a magnetic

[1] E. L. Hill, Phys. Rev. **34**, 1507 (1929).
[2] G. M. Almy and F. H. Crawford, Phys. Rev. **34**, 1517 (1929).

moment in that direction. In the $\lambda 6389\,^2\Sigma \rightarrow {}^2\Sigma$ and $\lambda 7000\,^2\Pi \rightarrow {}^2\Sigma$ CaH bands, for which these effects become very large, the Zeeman effect predicted by Hill's theory is to be expected, then, for the lower rotational states, but for the highest rotational states new magnetic field patterns should be found. Measurements of this perturbing effect of an external field should increase our knowledge of the dynamics of molecules exhibiting such a very large ρ-type and Λ-type doubling.

The analysis of Hulthén,[3] together with Mulliken's[4] discussion of these data, demonstrate the marked distortion increasing with the rotation in these CaH bands. In the upper electronic state of the $^2\Sigma \rightarrow {}^2\Sigma$ band the orientation energy of the spin S with respect to the nuclear rotation axis, as measured by the separation of the F_1 and F_2 terms, is exceptionally large, the rotational doublets being separated even at the origin of the band by 1.3 cm^{-1}. Also the usual relation for $^2\Sigma$ states, $F_1 > F_2$, is reversed in this case. In the $^2\Pi$ state of the $\lambda 7000$ band the Λ-type doubling is very large (see below), thereby indicating a large L_{perp} (component of orbital angular momentum L perpendicular to the electric axis of the molecule), and the usual $^2\Pi$ state relation, $F_2(J) > F_1(J+1)$, which does hold for low J values is reversed for $J > 19\frac{1}{2}$. The ρ-type doubling in the common lower $^2\Sigma$ state is small, as in most $^2\Sigma$ states.

Experimental Procedure

Our source was an intermittent d.c. arc in a modified Back chamber mounted on the pole faces of a large water-cooled Weiss electromagnet. The moving electrode was a small block of metallic calcium mounted on a tungsten wire, while the fixed electrode was a thin copper strip insulated from the pole face by a piece of mica. The arc was struck in a hydrogen atmosphere at from 5 to 10 cm pressure, and since the arc chamber was not absolutely vacuum tight, a stream of hydrogen gas from a tank was pumped slowly through the apparatus during the exposures. It was necessary to renew the calcium electrode at frequent intervals during each run. The bands were photographed in the second order of a large concave grating mounted in parallel light, the dispersion being approximately 2.1A per mm.

The $\lambda 6389$ band was photographed with Eastman panchromatic plates hypersensitized by an ammonia bath. Plates were taken with field strengths of 14,000, 24,600 and 29,950 gauss with no polarizing prism in the path, and at 29,950 gauss in the perpendicular and parallel polarizations separately, with the exposure times up to 12 hours when the Nicol prism was used. The $\lambda 7000$ band was recorded on Eastman 40 and panchromatic plates dyed with dicyanin. Field strengths of 10,500 and 30,000 gauss were used, the times of actual exposure on the slit running to 18 hours. On every plate in addition to the field exposure a no-field comparison and an iron arc spectrum were photographed. The strength of the magnetic field was determined by measurements of the patterns of the Zn triplet $\lambda\lambda 4680$, 4722, and 4811.

[3] E. Hulthén, Phys. Rev. **29**, 97 (1927).

[4] R. S. Mulliken, Phys. Rev. **30**, 138 (1927), and **32**, 388 (1928).

New Series and Magnitude of Λ-type Doubling in $^2\Pi \rightarrow {}^2\Sigma$ Band

The J values assigned by Hulthén[3] to the lines in the P and R branches of the λ7000 band are correct when reduced by $\frac{1}{2}$ unit in order to agree with the quantum mechanics numbering. But since it is apparent from Hulthén's data that the ordinary PQR combination relation does not even hold approximately, and since no (1, 0) or (0, 1) band seems to be available for combination checking purposes, the J numbering in the Q branches has been heretofore undetermined. Now our spectrograms indicate that all the satellite series to be expected in a $^2\Pi_{ab}$ state[5] are present and with fair intensity in this band. In particular the $^0P_{12}$ satellite branch[6] proceeds to the red from the P branch head in a region clear of other lines. The frequencies of the lines in this branch can be calculated from the relation[7]

$$\begin{aligned} {}^0P_{12}(J) &= Q_1(J-1) + [F_1''(J-1) - F_2''(J-2)] - [F_2''(J) - F_2''(J-2)] \\ &= Q_1(J-1) + 0.045(J - 1\tfrac{1}{2}) - \Delta_2 F_2''(J-1). \end{aligned} \quad (1)$$

The second term on the right side of this equation involves the empirical rule for the separation of the spin components in the lower state of these bands,[5] while the $\Delta_2 F_2''$ values can be taken directly from Hulthén's tables. The proper Q_1 frequencies to so combine with these F'' differences as to give the observed satellite branch lines can be thus uniquely determined, and the important point is that this fixes the J numbering of the Q_1 branch and hence the exact course of the Λ-type doubling in the F_1' levels. Table I

TABLE I. $^0P_{12}$ *Series in* (0,0) *and* (1,1) *CaH* $^2\Pi \rightarrow {}^2\Sigma$ *bands.*

	(0,0) or A band		(1,1) or A' band	
J	ν calc.	ν obs.	ν calc.	ν obs.
$11\frac{1}{2}$	14231.68	14231.58		
$12\frac{1}{2}$	18.66	18.62		
$13\frac{1}{2}$	06.17	05.88		
$14\frac{1}{2}$	193.77	193.48		
$15\frac{1}{2}$	81.55	81.36		
$16\frac{1}{2}$	69.69	69.61	14209.91	14209.78
$17\frac{1}{2}$	58.23	58.08	198.66	198.55
$18\frac{1}{2}$	47.12	46.94	87.81	87.54
$19\frac{1}{2}$	36.21	36.07	77.28	76.92
$20\frac{1}{2}$	25.86	25.61	66.92	66.75
$21\frac{1}{2}$	15.78	15.49	56.97	56.60
$22\frac{1}{2}$	06.02	05.72	47.36	—
$23\frac{1}{2}$	096.53	96.36	38.17	37.84
$24\frac{1}{2}$	87.64	087.35		
$25\frac{1}{2}$	78.97	78.68		
$26\frac{1}{2}$	70.73	70.51		
$27\frac{1}{2}$	62.56	62.70		

[5] Cf. R. S. Mulliken, Phys. Rev. **32,** 388 (1928) for a detailed account of the various possible branches in $^2\Pi \rightarrow {}^2\Sigma$ transitions.

[6] We are using, throughout, the notation recommended by R. S. Mulliken in his forthcoming article in this journal on standardized notation for description of molecular spectra. This branch would be designated formerly as $^{PP}P_{12}$.

[7] Compare level diagram in ref. 5. Note particularly that the $^0P_{12}$ and Q_1 transitions are from the same A sublevels in the upper state.

gives the wave-numbers of the observed ${}^0P_{12}$ lines for both the (0, 0) and (1, 1) bands together with their calculated values from Eq. (1). The agreement of the observed and calculated frequencies can only be produced by increasing Hulthén's J numbering in the Q_1 branch of the (0, 0) band (his A band) by $1\frac{1}{2}$ units, and in the Q_1 branch of the (1, 1) band (his A' band) by $\frac{1}{2}$ unit. Two new Q_1 lines should be added to Hulthén's tabulation for the A band; $Q_1(\frac{1}{2})$ 14393.31 and $Q_1(1\frac{1}{2})$ 14396.71. These are clearly present and of good intensity on our plates. Because of the confusion of stronger lines in the short wave-length side of these bands, the accurate measurement of the corresponding ${}^SR_{21}$ is rendered difficult. Fragments of this branch have been located, however, and seem to indicate similarly that Hulthén's J numbering in the Q_2 branch should also be raised $1\frac{1}{2}$ units. In computing the magnitude of the Λ-type doubling in the F_1' terms we use the relation

$$\begin{aligned}&[R_1(J) - Q_1(J)] - [Q_1(J+1) - P_1(J+1)]\\ &= F_{1B}'(J+1) - F_{1A}'(J) - F_{1A}'(J+1) + F_{1B}'(J)\\ &\cong F_{1B}'(J+\tfrac{1}{2}) - F_{1A}'(J+\tfrac{1}{2}).\end{aligned} \qquad (2)$$

Table II gives in condensed form the course of this doubling, showing that for the lowest J levels the doubling increases in the usual fashion;[8] but that at $J=6\frac{1}{2}$ the separation of these sublevels begins to decrease, becomes

TABLE II. *Λ-type doubling in F_1' levels of* (0,0) ${}^2\Pi\rightarrow{}^2\Sigma$ *band calculated from Eq.* (2).

J	$F_{1B}'(J+\frac{1}{2})-F_{1A}'(J+\frac{1}{2})$	J	$F_{1B}'(J+\frac{1}{2})-F_{1A}'(J+\frac{1}{2})$
$1\frac{1}{2}$	+2.04	$11\frac{1}{2}$	− 0.54
$2\frac{1}{2}$	2.66	$12\frac{1}{2}$	− 1.76
$3\frac{1}{2}$	3.06	$14\frac{1}{2}$	− 4.61
$4\frac{1}{2}$	3.26	$19\frac{1}{2}$	−14.00
$5\frac{1}{2}$	3.27	$24\frac{1}{2}$	−25.89
$6\frac{1}{2}$	3.06	$29\frac{1}{2}$	−53.38
$9\frac{1}{2}$	1.45	$34\frac{1}{2}$	−69.71
$10\frac{1}{2}$	+0.53		

zero at $J=11\frac{1}{2}$, and increases to very large negative values for the highest rotational levels. The F_2' levels proceed apparently in much the same way, although usually[8] F_2 levels show an almost negligible Λ-type doubling.

This large rotational doubling in the Π state is evidence for a very considerable growth in L_{perp}. There is reason therefore for supposing that the effect of an external magnetic field on these high rotational levels would be a variation of that for cases a to b.

THE ZEEMAN EFFECT IN THE ${}^2\Pi\rightarrow{}^2\Sigma$ BAND

We will consider the effect of the magnetic field first for the lines of low and intermediate K values, and then for the high rotation lines. For the lines in the first group the CaH molecule is intermediate between case a and case b, and Hill's theory should give a good description of the observed patterns. Since the ρ-type doubling is small in the lower ${}^2\Sigma$ state, the only effect of the field in this state should be to uncouple the spin S from its weak coupling with K, so that these levels all become sharp doublets of separation

[8] J. H. Van Vleck, Phys. Rev. **33**, 467 (1929). R. S. Mulliken, Phys. Rev. **33**, 507 (1929).

$2\Delta\nu_{norm}$. In general one must make a detailed computation with Hill's equation (22), the constants for our $^2\Pi$ state being $B=4.3\ cm^{-1}$, $\lambda=+19\ cm^{-1}$, $\Lambda=1$. Since for no line have we observed the resolved magnetic fine structure due to all the possible values of M, the magnetic quantum number, it is only necessary to calculate the position and overall widths of the blocks of unresolved components in the patterns by using $M=+J$, 0, and $-J$. These patterns we have calculated for $K'=3$, 10, and 18. For $K'=18$, and even for $K'=10$, Hill's energy equation considerably overestimates the width of the spin doublet interval, since it does not consider ρ-type doubling, and therefore complete quantitative agreement with the observations is not to be expected. The details of the comparison, together with some observations on lines with approximately these K' values are presented in Table III. Figs. 1 and 2 show graphically this comparison for $K'=3$ and 10.

TABLE III. *Comparison of observed and calculated patterns for low and intermediate values of K in $^2\Pi\rightarrow{}^2\Sigma$ band.*

(In this and the other tables + indicates field radiation to the higher frequency side, − to the lower frequency side, of the no-field position.)

Lines	Patterns
$P_1(2\frac{1}{2})$, $(4\frac{1}{2})$ $(5\frac{1}{2})$, $(6\frac{1}{2})$ $Q_1(2\frac{1}{2})$, $(4\frac{1}{2})$, $(5\frac{1}{2})$ $R_1(2\frac{1}{2})$, $(3\frac{1}{2})$	$K'=1$ to 5 $H=10{,}500$ gauss, $\Delta\nu_n=0.49\ cm^{-1}$. Theory predicts at $K'=3$ a symmetrical doublet, with $0.98\ cm^{-1}$ between centers of the two component blocks, separation between "inside" edges 0.61, width of each component 0.38; Obs. doublet width K' P Q R 1 0.78 2 0.84 3 0.71 4 0.83 0.70 0.74 5 0.80 Measurements from center to center showing that since obs. width <theoretical, inside edges are stronger. Components same intensity for $K'1$ and 2, but red component then becomes stronger, and at $K'=5$ is much stronger than violet component. $H=30{,}000$ gauss, $\Delta\nu_n=1.41$. Calculated pattern wide diffuse doublet, approx. symmetrical about no-field position; roughly in agreement with obs. $P_1(4\frac{1}{2})$ pattern. − components inside edge at −0.89; obs. −0.94. Violet block's outermost edge at +1.93; obs. +2.06. Other two edges obscured. Q_1 lines also become diffuse doublets but the intensity distribution is very different: the two blocks are of equal intensity, whereas at the lower field strength the "wings" are more intense; maximum intensity in each block is near the inner edge, nearest the no-field position. Red component's maximum at −0.72, violet's at +0.79, whereas predicted inside edges are −0.89 and $+0.85\ cm^{-1}$.
$P_1(11\frac{1}{2})$, $(12\frac{1}{2})$ $(13\frac{1}{2})$ $Q_1(10\frac{1}{2})$, $(13\frac{1}{2})$ $P_2(9\frac{1}{2})$, $(10\frac{1}{2})$, $(11\frac{1}{2})$ $Q_2(13\frac{1}{2})$	$K'=9$ to 14 $H=10{,}500$. Calculated patterns are doublets. F_1 states: calculated inside edge of red component at −0.08 for $K'=10$; obs. −0.09 −0.08, −0.14 for $P_1(11\frac{1}{2})$, $P_1(12\frac{1}{2})$, and $Q_1(10\frac{1}{2})$ respectively. Width of red components: calc., 0.78; obs., 0.39, 0.35, and 0.30 respectively—i.e., obs. blocks much narrower than calculated width. P_1 and R_1 violet components of negligible intensity, but in $Q_1(10\frac{1}{2})$ the violet component is weaker than the red component but is present starting at the red component and extending to +0.51, against the theoretical max. displacement +0.90. F_2 states: Predicted doublets are approximately symmetrical with respect to no-field line, have components narrower, $0.48\ cm^{-1}$, and separated by $0.98\ cm^{-1}$ between centers for $K'=10$. Observed patterns in good agreement with theory. Violet or "wing" components much stronger than red components and narrower than predicted.

TABLE III (*continued*).

Observed F_2 Patterns

	K'	Doub. width	Component widths	
P_2	9	0.85	−0.37	+0.28
Q_2	14	0.79	−0.46	+0.31

$H=30{,}000$. *F_1 states*: Lines should become broad symmetrical doublets in field according to theory. P_1 and R_1 patterns not present; probably too weak and diffuse. Q_1 lines become strong broad doublets, narrowing with increasing K, and whose inside edges nearest the no-field line are much the stronger parts of the patterns. For $K'=10$ these maxima are at −0.50 and +0.55 as against computed inside edges for the blocks at −0.28 and +0.30 The red "wing" components are just as intense as the violet components.

F_2 states: Calculated field doublets are symmetrical, have inside edges farther from no-field position, and have narrower component blocks. All in agreement with observations, but obs. components much narrower than predicted, hence quite intense; also two components are equally strong.

P_2 component separations from no-field line.

K'	Calc.	Obs.−	Obs.+
9		1.14 to 1.62	1.08 to 1.37
10	0.74 to 2.08	1.15 to 1.45	1.05 to 1.34
11		1.17 to 1.57	0.98 to 1.31

$K'=18$

$P_1(19\frac{1}{2})$
$Q_1(18\frac{1}{2})$
$P_2(18\frac{1}{2})$
$R_2(16\frac{1}{2})$

$H=10{,}500$. According to theory all lines become doublets in the field; the F_1 patterns with very narrow components separated by 0.96. Actually only the red "wing" components can be seen; in $P_1(19\frac{1}{2})$ from −0.08 to −0.43; in $Q_1(18\frac{1}{2})$ from +0.01 to −0.29, although theory has this component at −0.48.

F_2 patterns are calculated to be more diffuse doublets with but 0.21 cm^{-1} between inside edges and center of components at −0.48 and +0.50. For $P_2(18\frac{1}{2})$ only violet component observed from +0.07 to +0.38. $R_2(16\frac{1}{2})$ becomes a doublet with strong violet component from +0.16 to +0.46 and very weak red component at −0.27. Theory predicts no-field spin doublet separation 15.8 cm^{-1}, whereas experimentally it is but 2.5 cm^{-1}.

$H=30{,}000$. Theory predicts widely separated doublets (2.82 cm^{-1}) with components narrow for F_1 patterns. These are not observed. No P_1R_1 field radiation is apparent and the Q_1 pattern is broad and diffused into adjacent patterns. F_2 patterns predicted to be broad diffuse doublets with inside edges at −0.32 and +0.35 and centers at −1.30 and +1.52 for the red and violet components respectively.

Observed F_2 patterns for $K'=18$

$P_2(18\frac{1}{2})$	−0.86 to −1.30	+0.94 to+1.67
$R_2(16\frac{1}{2})$	−0.86 to −1.30	+1.22 to +1.61

Both components intense and considerably narrower than the computed widths.

Some of the more striking features of the observed patterns should be emphasized. In agreement with the theory, all of these lines apparently become doublets in the field, each component of the doublet of course being in reality a block of $2J+1$ unresolved lines, but the observed doublet width is always less than that predicted. This smaller width may be caused by the relative faintness of the outer portions of the patterns. At 10,500 gauss, for all except the very lowest K' values, the intensity is almost entirely in the red components for the P_1, Q_1, R_1 patterns and in the violet components for

the P_2, Q_2, R_2 patterns. These are the transitions from parallel S and K in the $^2\Pi$ state to the $M_s = +\frac{1}{2}$ level in the $^2\Sigma$ state and anti-parallel S and K to $M_s = -\frac{1}{2}$ respectively, and correspond to the "wings" of Almy and Crawford's

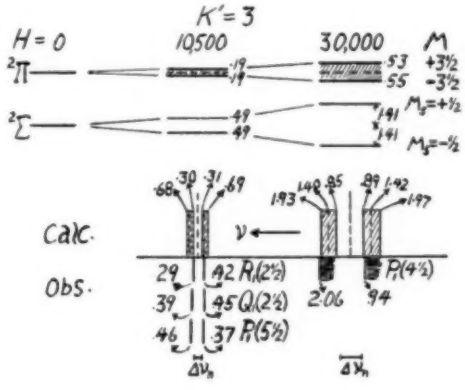

Fig. 1. Calculated splitting of the energy levels and the resulting Zeeman patterns for lines with $K'=3$ from Hill's theoretical equation (ref. 1). Of the observed lines, $P_1(4\frac{1}{2})$ and $R_1(2\frac{1}{2})$ have $K'=3$, while for $Q_1(2\frac{1}{2})$, $K'=2$ and $P_1(5\frac{1}{2})$ has $K'=4$. The corresponding P_2, Q_2, R_2 lines are too weak to observe. Since at 10,500 gauss the field components are narrow, only a measurement of the center of the component in each case was made. At 30,000 gauss due to overlapping patterns only the measurements given on the $P_1(4\frac{1}{2})$ line pattern could be made, but the observations indicate widths for the blocks approximately in agreement with the predictions.

MgH patterns.[2] The components arising from the other two possible transitions[9] we shall refer to as the "inside" components. At 30,000 gauss, however, both components are equally strong for all the patterns measured (P_2, R_2,

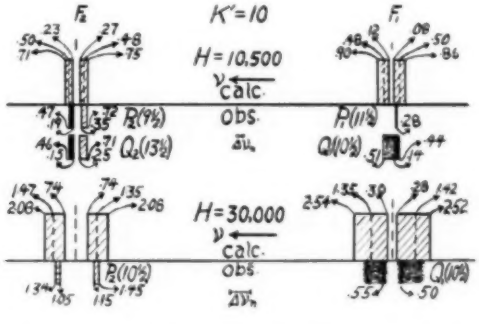

Fig. 2. Comparison of calculated and observed patterns for lines with $K'=10$. The $P_1(11\frac{1}{2})$ $Q_1(10\frac{1}{2})$ and $P_2(10\frac{1}{2})$ lines all have $K'=10$. For $P_2(9\frac{1}{2})$, $K'=9$, while for $Q_2(13\frac{1}{2})$ $K'=14$. At 10,500 gauss the "outside" components are much stronger (indicated by solid black) than the inside (shaded) components. At 30,000 gauss the P_2 components are narrower than predicted, the Q_1 components are strongest at their edges nearest the no-field line position, and both components are in all cases of equal intensity.

Q_1), thus indicating that, because the no-field spin doublet separation is still considerably greater than $\Delta\nu_n$, the coupling of S in the $^2\Pi$ state has not been

[9] Cf. the excellent diagrams illustrating the relation between the possible transitions and the components in ref. 2.

broken down by the field. The intense concentration of the patterns of the Q_1 lines as contrasted with the apparent absence of field radiation for the P_1 and R_1 lines, however, is difficult to explain. The enlargement of a portion of this band in Fig. 3 illustrates some of these pattern changes.

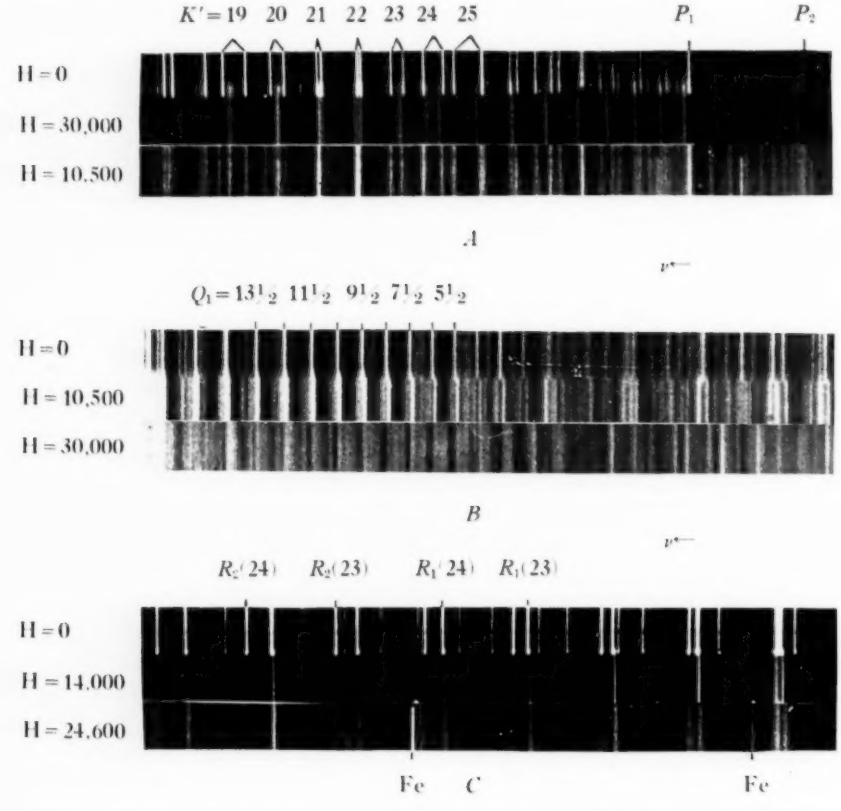

Fig. 3. Enlargements 9 times. A shows the "cross-over" region in the P branches of the $^2\Pi \rightarrow {}^2\Sigma$ band. It is evident that for $K' > 24$ both the P_1 and P_2 lines for $H = 10{,}500$ gauss have "inside" component blocks equally strong, but that for $H = 30{,}000$ gauss the P_1 field radiation has broadened out and become of negligible intensity, although the P_2 components are strong. In the reproduction P_1 and P_2 denote the heads of the two branches in the no-field strip. In B note the greater intensity of the field components on the long wave length side for $H = 10{,}500$ gauss as compared to the equal intensity of the two field components for $H = 30{,}000$ gauss. In the latter case the greater intensity of the field blocks at their inside edges is evident. C gives some of the patterns for high K values in the $^2\Sigma \rightarrow {}^2\Sigma$ band. The R_2 line patterns and the weak components of the R_1 lines on the high frequency side are of insufficient intensity to be brought out well in the reproduction. The breadth of the no-field lines in C is due to over exposure.

For $K' \geqq 19$ where the no-field spin doublet components come close together and then cross over, making $F_1'(J+1) > F_2'(J)$, prominent and interesting "second-order" or Paschen-Back effects appear. These effects are summarized in Table IV and are illustrated in Fig. 3A for the P_1, P_2 lines only. That a "strong field" uncoupling of S is here taking place is evidenced by first, the fact that the wing components decrease to zero intensity

TABLE IV. *Magnetic field patterns at and beyond the cross-over in the P branch spin doublets in the* $^2\Pi \rightarrow {}^2\Sigma$ *band.*

K'	
	10,500 gauss. $\Delta\nu_n = 0.49$ cm^{-1}
19	Practically all the intensity in the "wings". $P_1(20\frac{1}{2})$ wing at -0.28, $P_2(19\frac{1}{2})$ wing at $+0.33$. Very little shading between the lines.
20	Now wings are weaker and the other two "inside" components have appeared. Reckoning from the P_2 line: P_1 wing at -2.07, P_1 no-field, -1.64; inside components fused from -1.36 to -0.44, P_2 wing $+0.51$.
21	Wings have disappeared. P_1 no-field at -0.57, strong field component -0.52 to -0.29, weaker fused field radiation from strong component to $+0.13$.
22	No-field lines have now crossed over. Field pattern one strong broad block approximately width of original spin doublet separation, 0.51. No wings.
23	Fused inside components now separated because spin doublet separation is greater. P_2 no-field at 0.0, P_2 component at $+0.07$, P_1 component $+1.45$, P_1 no-field $+1.54$. These P_1 and P_2 field components are equally strong. No wings. Succeeding P_1 and P_2 lines to the ends of the branches similarly affected.
	30,000 gauss. $\Delta\nu_n = 1.41$ cm^{-1}
	Reckoning all separations from the P_2 no-field line position in each pattern:
19	Weak shading in field starts at P_1 no-field, -2.83, and goes to strong band component starting at -0.91 and ending -0.41, P_2 wing from $+1.74$ to $+2.20$.
20	Weak shading from -1.82 to strong component starting at -1.00 and ending -0.65. P_1 no-field position is -1.64. No evidence now of P_2 wing.
21	Rather strong shading begins sharply at -1.08 and extends to the strong, narrower field component at -0.24. P_1 no-field position is -0.57. No wings.
22	Lines have crossed. Strongest field line and $P_2(22\frac{1}{2})$ position at 0.00, with field radiation extending rather intense to a strong edge at $+0.85$. P_1 position is $+0.51$. No wings.
23	Weaker fused field radiation starts at -0.35 and extends to $+1.94$. Edges of this block are well defined. Strong field component at $+0.45$ superposed. P_1 position is $+1.54$.
24	Strong field component at $+0.54$ with weaker field radiation solid from here to $+2.88$. P_1 position is $+2.50$.
25	Strong field component at $+0.74$. Broad weak field radiation for the P_1 from $+1.75$ to $+4.47$. P_1 position is $+3.53$.
	From here on to the P_1 head, the P_1 field radiation is very diffuse and weak causing the whole background to be slightly blackened. The strong P_2 field component blocks continue out to the P_2 head, the displacements from the no-field positions for the next four lines being $+0.65$, $+0.69$, $+0.75$ and $+0.73$, or about $\frac{1}{2}\Delta\nu_n$. For the last lines near the head, the displacements are a little greater, averaging $+0.80$ cm^{-1} for $K'=36$, 37, 38, and the components are becoming definitely broader and more diffuse.

and the inside components come in strong as the spin doublet separation goes to zero. This is to be interpreted as due to the uncoupling of S from its interaction with the internal field directed along the rotational axis in the molecule, the F_2 state in which S and K are anti-parallel being replaced by the parallel orientation of S and the field H, while the F_1 state or parallel S and K is replaced by the state in which S lies anti-parallel to H.[10] S and K are then separately quantized with respect to the field, giving the quantum numbers M_S and M_K. Since only the inside components representing transitions for which $M_S = 0$ occur for all levels of higher K, we infer that this uncoupling is complete. Second, the displacement of the strong P_2 field components seems to be almost exactly proportional to H^2 rather than to H as in the usual first-order Zeeman effects.

The difference between the patterns of the P_1 and P_2 lines at 30,000 gauss in this uncoupling process is striking. The one inside field component

[10] Reference 1, p. 1513.

of the P_2 lines is rather narrow and intense, whereas the field radiation associated with the P_1 lines in the interval from $K'=20$ to 25 becomes increasingly broader and weaker, and for $K'>25$ is too weak to detect. Apparently the transition from parallel S and H in the $^2\Pi$ state is very much more probable when the field is "strong" than that from the anti-parallel S and H, indicating an instability of this anti-parallel orientation.

Also to be especially noticed are the increasing separation and increasing diffuseness of these high field P_2 components for the highest K levels. This would seem to be related to the exceptionally large Λ-type doubling and consequent relatively large L_{perp}. The electric axis of the molecule at these highest rotational levels is probably becoming less effective in orienting the L, with the result that Λ is no longer a good quantum number. There is a close approach to the case d type of coupling, and the resulting changes in the magnetic moment are reflected in the broadening of these last field patterns.

The Zeeman Effect in the $^2\Sigma \rightarrow {}^2\Sigma$ Band

Neglecting ρ-type doubling, $^2\Sigma \rightarrow {}^2\Sigma$ bands should exhibit no first order Zeeman effect, for the field merely completely uncouples the spin S in both states, and with $\Delta M_S=0$ accurately holding, no displacement of the spectrum lines is to be expected. The very pronounced ρ-type doubling in the λ6389 CaH band, however, indicates a considerable energy of orientation of S with respect to an internal field directed along the rotational axis in the

TABLE V. *Summary of magnetic field measurements in the* λ6389 $^2\Sigma \rightarrow {}^2\Sigma$ *CaH band.*
($H_1=14{,}030$ gauss, $\Delta\nu_n=0.66$. $H_2=24{,}600$ gauss, $\Delta\nu_n=1.16$. $H_3=29{,}950$ gauss, $\Delta\nu_n=1.41$)

K'	Measurements and Remarks
1 to 7	P_1 and R_1 lines (parallel S) unaffected by field $R_2(1\frac{1}{2})$ becomes a doublet in field, components at -0.35 and $+0.55$ for H_2 and -0.36 and $+0.88$ for H_3

Other R_2 lines are affected by field but patterns are confused with other radiation
P_2 lines are doubled in field:

K'	H_1	H_2	H_3
1	-0.42, -0.29, $+0.62$	-0.67 to -0.27, no + comp.	-0.67 to -0.21, no + comp.
2	-0.87 to -0.26, $+0.29$ to $+0.54$	-0.28, no + comp.	—
3	-1.02 to -0.18, $+0.22$ to ?	diffuse + comp.	—
4	-0.74 to -0.12, $+0.35$ to $+0.87$	diffuse + comp. ?	from -0.24 shaded to red, strong and from $+0.53$ shaded to violet, weak

For $K''>8$ all of the R_1 and R_2 lines have the patterns as given below for a few samples:

	R_1			R_2		
	H_1	H_2	H_3	H_1	H_2	H_3
12	-0.60 to -0.25 and shades to $+0.93$	-1.34 to -0.20 and $+0.28$ to $+0.91$	-1.74 to -0.25 and $+0.42$ to ?	0.00 to $+0.76$		
	+ and − components same strength			These single blocks shading to the violet from the no-field position constitute the full R_2 pattern		
15	−comp. at -0.44 no + comp.	-1.15 to -0.19 strong, and $+0.37$ to ? weak				
21	−comp. at -0.35 no + comp.	-1.05 to -0.25 strong, and $+0.49$ to ? very weak	-1.29 to -0.29 strong, and $+0.34$ to ? weak	0.00 to $+0.41$	0.00 to $+1.49$	($K'=23$:) 0.00 to $+0.64$
25	−comp. at -0.34 no + comp.	-0.91 to -0.47 strong, with $+0.36$ to ? very broad and weak	-1.24 to -0.37 strong, with + comp. very weak	0.00 to $+0.36$	($K'=24$:) 0.00 to $+1.50$	0.00 to $+0.58$

upper electronic state. One might anticipate a rather large and unique Zeeman effect in this band, then, and so there is. In Table V we list briefly some of our measurements, and in Fig. 3*C* an enlargement of a portion of one of the spectrograms illustrates the principal pattern types obtained. The measurements are confined mostly to the R branch lines, since the overlapping of the patterns from the rather closely packed lines in the P branches makes their analysis hopeless at this dispersion.

It will be noticed that the P_1 and R_1 lines of low K values are unaffected by the field, but that the P_2 and R_2 lines become rather broad doublets. At about the level $K'=8$ the field patterns change, and take on a form which they retain out to the highest K level observed. The R_1 lines (parallel S and K) become rather diffuse doublets, the red and violet components being at first of about the same intensity, and with the outer edge of each component at about $\Delta\nu_n$ displacement from the no-field position. As K increases, however, the violet component becomes much weaker and the red component becomes narrower and somewhat stronger. The characteristic pattern for all the corresponding R_2 lines (anti-parallel S and K), on the other hand, is just one block of unresolved lines, shading from the no-field position toward higher frequency for an interval of about $\Delta\nu_n$. All patterns appear in both polarizations, although the widths and intensities are perhaps different on the two plates.

These patterns for the higher rotational levels are quite similar to those found in a $^2\Pi$ state for which there is a normal magnetic moment associated with the component of L in the direction of the electric axis. In the upper $^2\Sigma$ electronic state of this $^2\Sigma\rightarrow{}^2\Sigma$ band there is a large magnetic interaction energy between S and an internal field directed along the nuclear rotational axis. This field must be due to a component of L in this direction, the order of magnitude of this component being at least a full unit of angular momentum, for one can interpret these patterns as being the superposition of the pattern due to the symmetrical top on a partial uncoupling of the spin S. The width of the blocks of lines forming the components in the patterns decreases with increasing K, as they should. And the strength of the $-$ components for the R_1 lines and the $+$ components for the R_2 lines is just as found in the $^2\Pi\rightarrow{}^2\Sigma$ band, for these components originate in the "wing" transitions which we have discussed above.

It is not probable that this magnetic moment in this $^2\Sigma$ state could be due to nuclear rotation, for then one would expect similar very large ρ-type doubling in all $^2\Sigma$ states of this and like molecules. Now there is other reason to believe that the outer electron configuration in this $^2\Sigma$ state[11] is $4s\sigma^2 3d\sigma$, this level being derived from the low-lying $3D$ level of the Ca atom. Since $L=2$ (due to the d electron) and the effect of the electric axis is small ($\lambda=\sigma=0$), there is a good chance that the component of L along the perpendicular axis can become large. The accompanying magnetic moment and rather large coupling energy with the S then account for the Zeeman patterns observed.

[11] R. S. Mulliken, Phys. Rev. **33**, 730 (1929).

THE INFRARED ABSORPTION OF SOME ORGANIC LIQUIDS UNDER HIGH RESOLUTION

By R. Bowling Barnes
Johns Hopkins University

(Received April 30, 1930)

Abstract

For the purpose of comparing the Raman effect with infrared absorption spectra, the following organic liquids have been measured from 3.1μ to 3.6μ: benzene, toluene, ortho-, meta- and para-xylene, ethyl-, butyl-, monochlor-, and monobrombenzene. The spectrometer employed an echelette grating, which had 3600 lines per inch, and which concentrated the energy of a Nernst filament into the region which was investigated. The dispersion of the instrument was such that with the slits each 0.25 mm in width, one "slit width" was approximately 25A". The calibration was obtained in terms of the positions of the 5461 line from an auxiliary Hg arc, and the wave-lengths as given are considered accurate to $\pm 0.003\mu$. In every case the bands in this region, due to the C-H vibration, which have hitherto been reported only under low dispersion have been resolved into many component parts. The 3.25μ band of benzene was resolved into three equally strong components lying at 3.231, 3.253 and 3.291μ respectively. The shifts of these bands caused by the various substitutions were studied, and in no case was a shift of over 0.01μ found.

DURING the past two years much has been said concerning a new method of infrared analysis, the Raman effect. Much importance is attached to it, for it offers a very convenient mode of attacking many problems of molecular structure. However, its usefulness depends upon the accuracy of its theoretical interpretation, and the manner in which this latter agrees with experimental evidence. As a direct result of this, all work previously done in the infrared has taken on an added importance, that of furnishing means of investigating and testing the theory of this effect.

The technique of the Raman effect has developed so rapidly that the photographs taken now, are all made under high resolution and hence show considerable detail. These results must be compared with such infrared measurements as may be found in the literature, and since these latter wavelengths are usually known to a rather low degree of accuracy, such comparisons are not fair and in most cases can be only qualitative. So, in order to obtain any quantitative checks between the two phenomena, it seems necessary that many absorption measurements be made with the highest resolution obtainable.

The complete theory of the Raman effect is contained in the theory of dispersion as outlined by Kramers as early as 1925. Further calculations by Dirac,[1] based upon the more recent form of quantum mechanics lead to the same results as those stated in the papers by Kramers and Heisenberg.[2]

[1] Dirac, Proc. Roy. Soc. **A114,** 710 (1927).
[2] Kramers and W. Heisenberg, Zeits. f. Physik **31,** 681 (1925).

Here we learn that the intensity of a Raman line is determined in an entirely different manner from that of an absorption line. Between any two energy levels, say A_1 and A_2, the presence or absence of an absorption line is completely determined by the value of the transition coefficient (a_{12}). However, in the expression for the intensity of the Raman line, this coefficient does not enter, but in its place the transition coefficients to a third level, say B, which can combine with both A_1 and A_2. Thus it is possible to have, between A_1 and A_2, either an absorption line or a Raman line, or both, depending on the values of the transition coefficients (a_{12}), (a_1b) and (a_2b). Further, in case both exist, the intensities are to be entirely independent of each other. That this interpretation is correct, cannot be doubted in view of the beautiful manner in which it agrees (in the case of the simple molecules) with the experimental results obtained by Rasetti, McLennan and McLeod and Wood. In HCl, Wood finds that the so called "missing line" occurs as a rather strong Raman line. It was shown by Kemble and Hill[3] that this was in perfect ac-

TABLE I. STRUCTURAL FORMULAE OF COMPOUNDS STUDIED

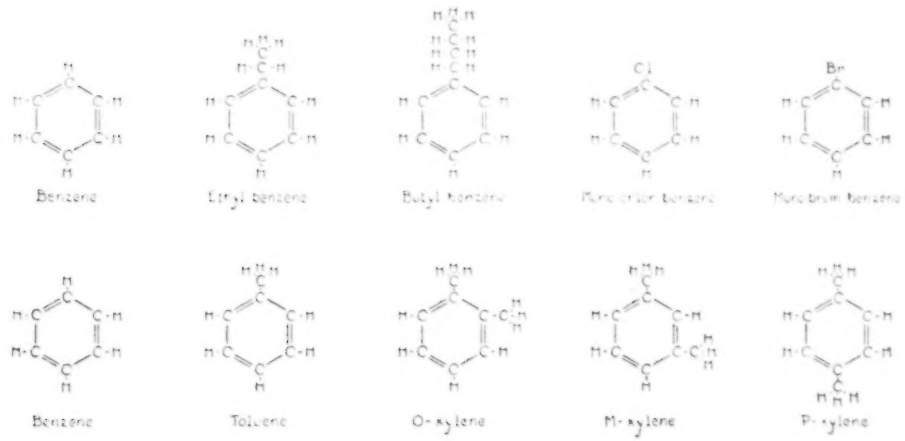

cord with the theory. In the case of more complex molecules further corroboration comes from the work of Coblentz[4] on CCl_4, and of many other experimenters.

It seems well to emphasize here, the fact that one must not expect to find a one-to-one correspondence between absorption and Raman spectra. In spite of the many theoretical papers on the question regarding the difference between the two, experimentalists frequently refer to the fact that absorption lines "predicted" by the Raman effect do not appear in absorption measurements. Only if we know the energy diagram for a given substance, can we really predict from the Raman spectra just what lines shall occur in the absorption spectra. And in the case of the complex molecule usually studied by Raman investigators, these energy schemes are entirely unknown.

[3] Kemble and Hill, Proc. Nat. Acad. Sci. **15,** 387 (1929).
[4] W. W. Coblentz, Bull. Amer. Phys. Soc. **4,** No. 2 (1929).

It is out of the question therefore to expect, as is very frequently done, that strong Raman lines will be found corresponding to each of the intense absorption lines, and vice versa.

It is clear then, that infrared measurements which can state wave-lengths with the same degree of accuracy as those on Raman photographs, will be of great interest. And so, as a step in this direction, we offer here a study of the C-H vibration in the case of the following nine organic liquids whose structural formulae are given in Table I: benzene, toluene, ortho-, meta- and para- xylene, ethyl- butyl-, monochlor-, and monobrom-benzene.[5] It is hoped that these results will be useful in connection with the Raman study of the same compounds made by Wood,[6] for his plates show that this band is in every case quite complex in its structure.

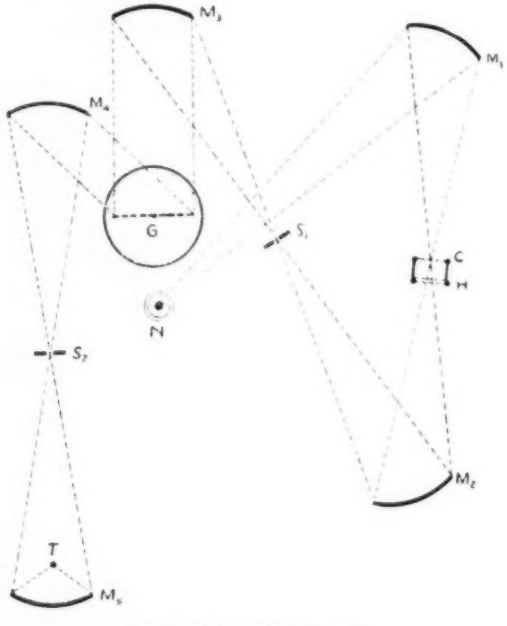

Fig. 1. Plan of apparatus.

Apparatus

A plan of the grating spectrometer, which was used is given in Fig. 1. Radiation from a Nernst glower, operated on a 110-volt storage battery at 0.35 amp., was focussed upon the absorption cell, C. After passing through this, it was focussed upon S_1, the first slit. M_3 then collimated the beam and directed it to G, the eschelette grating. The diffracted beam was then focussed upon S_2, after which it was finally concentrated upon the thermopile T, by the mirror M_5.

Attention is called to several novel features included in this spectrometer. In the major part of these investigations a new type absorption cell was used,

[5] R. B. Barnes, Nature **124,** 300 (1929), Bull. Amer. Phys. Soc. **5,** 10 (1930).
[6] R. W. Wood, Phil. Mag. **7,** 858 (1929).

instead of the customary one of rock-salt. As is shown in Fig. 2(b), this cell consisted of a brass cup so designed that the layer of the liquid to be examined would be contained between the two microscope cover glasses, *b* and *b'*. This thickness could be varied at will, and very easily measured, for a metal "thickness gauge" could be temporarily inserted between the plates, while the horizontal tubes were being sealed in place with sodium silicate. Such a cell has a high uniform transparency in this region, and eliminates the inconveniences caused by evaporation of the solution and fogging of salt plates. The use and design of this new cell was suggested by Dr. Pfund.

The grating was a chromium plated echelette[7] ruled in this laboratory, and concentrated most of the energy in the desired region. Having 3600 lines

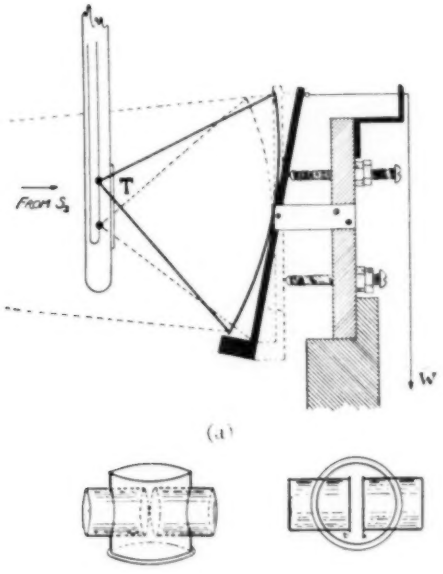

(a)

(b)

Fig. 2. Absorption cell and thermocouple mounting.

per inch, and being 3 inches wide, it had a theoretical resolving power of over 10,000, as compared with about 170 for a 3-inch salt prism, the type usually used in this region. Since a grating, however, superposes orders, the effect of the second order 1.5μ radiation had to be determined. A water cell, which had zero transmission beyond 3μ was used. This had a transparency of about 70 percent at 1.5 to 2.0μ. By making measurements with and without this shutter in place, the second order effect was readily detected and due allowance made for it in the calculations.

The thermocouple was a compensating one made of Hutchings alloys.[8] This was used in series with a high-sensitivity Leeds and Northrup galvanometer of 5 sec. period. The scale distance was about 5 m, and the deflections

[7] R. W. Wood, Phil. Mag. **7,** 742 (1929).
[8] A. H. Pfund, J.O.S.A. **15,** 69 (1927).

were read to 0.5 mm. By means of the arrangement shown in Fig. 2(a) a double deflection method, somewhat analogous to that used by Pfund,[9] was employed. By raising the weight, W, the radiation was focussed upon the lower junction of the thermocouple instead of the upper junction, and a deflection in the opposite direction was obtained. Readings were taken of deflections to the right, left and again to the right, thus eliminating the troublesome zero shift and at the same time realizing a double sensitivity and a greater accuracy.

The calibration was obtained by placing a mercury arc in front of S_1 and observing the positions of the grating as the first eight orders of the 5461 line fell upon S_2. The grating settings were determined by observing the image of a lamp filament, reflected by a small mirror which rotated with the grating. By plotting the grating settings against the respective wave-lengths a perfectly straight calibration curve was obtained. Before and after each set of absorption measurements were made, this was checked at two points. In no case did the image of the filament fail to fall at its appointed place by as much as 0.5 mm, where a distance of 1 mm indicated a change of wave-length of 0.0028μ. The accuracy of the calibration was therefore better than 0.0014μ.

For each setting of the spectrometer we recorded a set of galvanometer deflections, C, for the radiation passing through the absorption cell; a set for transmission through an empty cell, E; and finally a set while the water shutter H, was in place. By dividing (C-H) by (E-H) we obtained directly the percentage transmission for the wave-length indicated by the grating setting.

Results and Discussion

The wave-lengths as stated below are believed to be accurate to less than $\pm 0.003\mu$. Throughout most of the work the two slits were kept at a separation of 0.25 mm. The mercury yellow lines in the 6th order were separated on the face of S_2 by 1.2 mm, which indicated that the "slit-width" must have been very nearly 0.0025μ. Except in regions where a more careful check upon the location of some particular band was desired, readings were taken at intervals of 0.0070μ. Even when these intervals were halved, the author realizes that much of the band structure has been missed.

Fig. 3 shows a comparison of the absorption of benzene and four methyl substitutions. In Fig. 4 we have compared benzene with ethyl-, butyl-, chlor- and brom-benzene. In these curves we have plotted as ordinates the percentage transmission, and while the numerical values are not given, as the curves are each based upon a different zero line, the percentages run in each curve from about 95% to 25 or 30%. The structural formulae of the various compounds, showing the position of the C-H linkages, are given in Table I. Table II gives a list of all the observed bands. The samples used in every case are the same as those used by Dr. Wood in his Raman work, and are of a very high degree of purity.

[9] A. H. Pfund, Pub. of Allegheny Observatory **111**, No. 6 (1913).

TABLE II. *Wave-lengths of observed bands.*

Benzene	Toluene	O Xylene	M Xylene	P Xylene	Ethyl-Benz	Butyl-Benz.	Mono-Chlor Benzene	Mono-Brom Benzene
*3.036μ	*3.163μ	*3.193μ	*3.193μ	*3.186μ	*3.186μ	*3.178μ	*3.156μ	*3.133μ
*3.096	3.238	3.261	3.276	3.231	3.238	3.238	*3.186	*3.163
*3.163	3.261	3.283	3.291	3.291	3.261	3.261	3.253	*3.186
*3.186	3.276	3.313	3.313	3.308	3.298	3.298	3.268	3.261
3.231	3.298	3.366	*3.328	*3.328	*3.328	*3.328	3.298	3.298
3.253	*3.343	3.396	3.381	3.366	3.366	3.381	*3.328	*3.328
3.291	*3.358	3.418	3.396	3.396	3.411	3.411	3.366	3.396
*3.351	3.388	3.456	3.426	3.411	3.456	3.501	3.426	3.426
3.456	3.426	3.473	3.441	3.426	3.478	3.546	3.441	3.478
3.501	3.478	3.501	3.486	3.486	3.568	—	3.456	3.493
—	3.583	3.666	3.658	3.658	—	—	3.478	—

* Bands due to the absorption of water vapor in the atmosphere. More recent investigations, in which better resolution was obtained, have revealed the fact that several of the bands listed in Table II, and which occur in Figs 3 and 4 as very small minima, are due to atmospheric absorption. It is possible also, that in regions where the C-H bands are of about the same intensity as the water-vapor bands, there may be some little uncertainty as to the exact locations of the former due to imperfect resolution. However, in the cases of the stronger C-H bands which I discussed above, this effect plays a negligible role. A complete account of this more recent work is very soon to be published.

In this series of benzene derivatives, we have an excellent opportunity to study and observe the effects of various substitutions and of molecular arrangement and symmetry in causing a shift in the frequency of particular bands. Since benzene is the parent of all of the compounds studied we call especial attention to its characteristic bands.

The C-H band of benzene is always reported at 3.25μ in the literature.[10] In this work we have it clearly resolved into three components of approximately the same intensity lying at 3.231μ, 3.253μ and 3.291μ respectively. We shall follow these bands throughout all of these compounds. Benzene shows other weaker bands as can be seen from Table II. In this discussion however, we shall deal only with the strongest bands in each of the compounds.

In the case of toluene, we find in the literature[10] a single band at 3.34μ, indicating a shift, due to the substitution of the methyl group of 0.09μ. From curve (*b*) of Fig. 3 it can be seen that this is not at all the case. All three of the benzene C-H vibrations persist, each having been shifted by 0.007μ only, and are found at 3.238μ, 3.261μ and 3.298μ respectively. The intensities of the two bands of shorter wave-length have been noticeably decreased, while the band at 3.291μ is still quite strong. The vibrations of the C-H within the methyl group have apparently introduced rather strong bands at 3.276, 3.343, 3.428 and 3.478μ besides other weaker ones. These facts suggest that the presence of the other two H atoms in the CH_3 group makes possible several modes of C-H vibration other than those possible in benzene.

In the xylenes we find many interesting changes. Orthoxylene is very unsymmetrical with respect to benzene, and so we expect the substitution

[10] W. W. Coblentz, Astrophys. J. **20,** 207 (1924); Carnegie Inst. of Wash, No. **35,** 1 (1905).

to have a greater effect on the benzene vibrations than in the case of toluene. In the meta form, the effect should be smaller, and in paraxylene we would expect it to be nearly the same as that in toluene, or possibly less. By examining curves (*c*), (*d*), and (*e*) of Fig. 3 this is seen to be the case. In orthoxylene there is only one band which closely checks the benzene vibrations, the 3.253μ band occurring here at 3.261μ again. In paraxylene on the

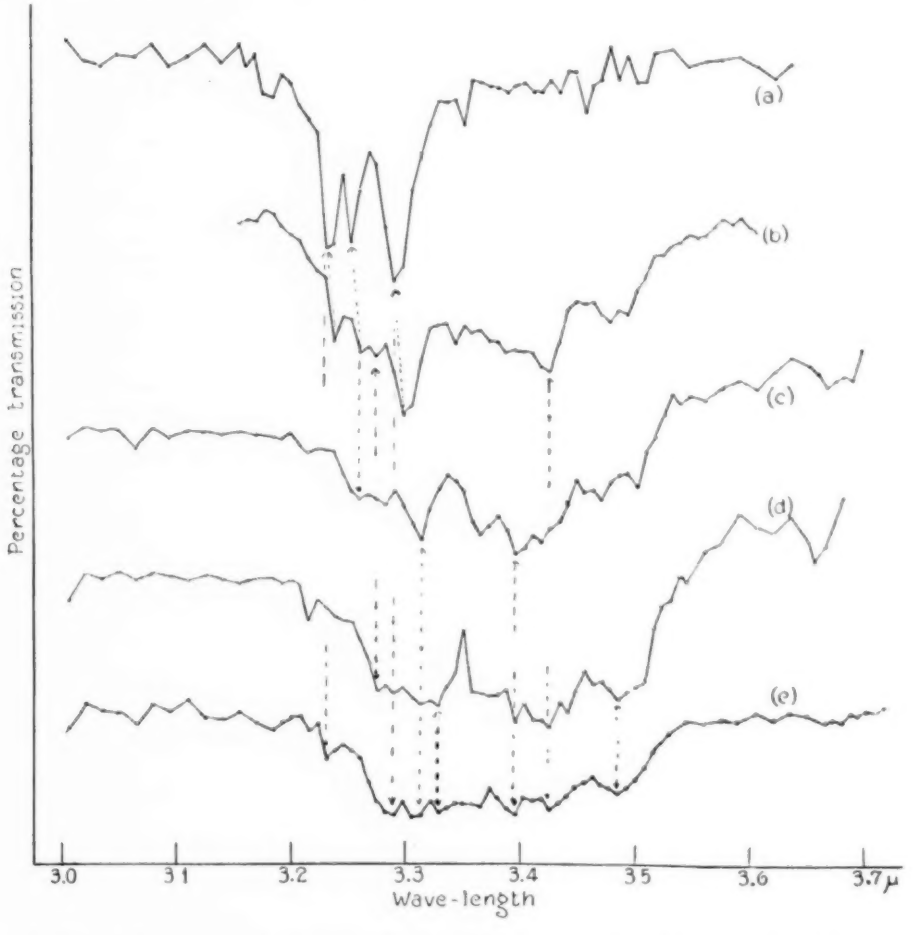

Fig. 3. Absorption curves. (a) benzene (b) toluene (c) orthoxylene (d) metaxylene (e) paraxylene. Thickness, 0.05 mm.

other hand, we find the 3.231μ and the 3.291μ bands recurring with no shift at all.

Since the strong 3.426μ band of toluene, does not appear in orthoxylene, while it does in the meta- and para- forms, we are inclined to look for a mutual effect of the two neighboring CH_3 groups. We find bands at 3.313μ, 3.396μ and 3.486μ occurring almost exactly in all three forms of xylene, while they are entirely absent in toluene, or to say the least, they occur in entirely new locations, again seeming to point to a mutual effect of the two groups.

The cases of ethyl- and butyl- benzene are somewhat similar. In each, we find the three benzene bands each shifted by 0.007μ. Their intensity changes are relatively the same as in the case of toluene. Just as we expected, the other bands, occurring in these two compounds, which are apparently due to the C-H vibrations within the ethyl- and butyl groups, are found at

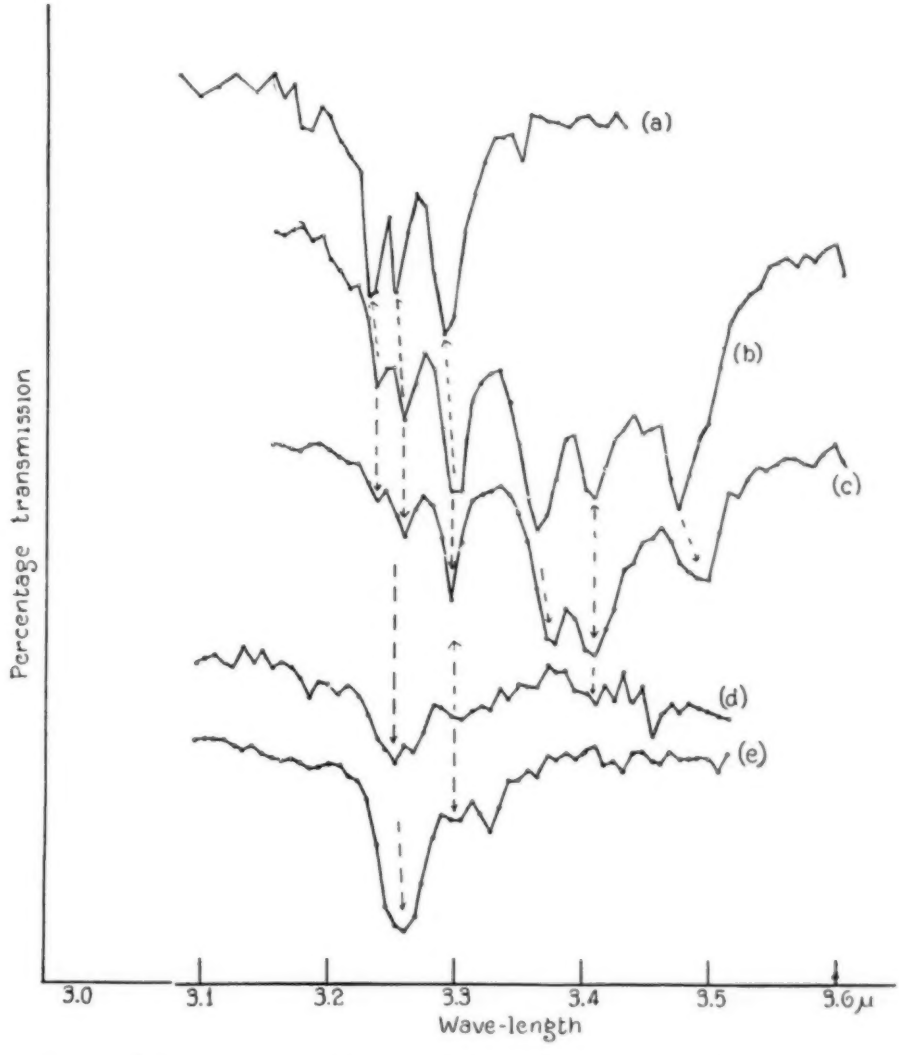

Fig. 4. Absorption curves. Thickness 0.05 mm. (a) benzene (b) ethyl benzene (c) n-butyl benzene (d) monochlor benzene (e) mono-brombenzene.

entirely different wave-lengths in the two cases. This is probably due to a different mutual effect in the two cases.

It is interesting to note that in methyl-, ethyl- and butyl-benzene, whose molecular weights are respectively 92, 106 and 134, the vibrations of the C-H bond in the benzene radical, have been shifted by the same amounts, namely

0.007μ. It must be remembered that 0.007μ is the interval between the spectrometer readings and so the actual shift might even be slightly less than that indicated.

In chlor- and brom- benzene we have a different type of substitution-namely, a single heavy atom instead of a group of C's and H's. Here, the 3.23μ band is absent entirely; the 3.253μ band occurs in each; the 3.291μ vibration appears in each at 3.298μ, and for the first time has its intensity very greatly decreased. Literature[10] gives for each one single band at 3.25μ, with that for brom-benzene being much the stronger of the two, in close agreement with these results.

Conclusions

If we notice in every case the combined effect of the intensity changes and of the new vibrations introduced by the substitutions, we find that the result is just that necessary to cause the center of the absorption region to agree nicely with the wave-lengths given in the lower resolving power work recorded in literature.[10]

Apparently we can follow a particular band through the series of substitutions, noting the shifts and intensity changes which it suffers. We can see the mutual effect of the neighboring atoms upon the C-H radicals, and we can note distinct changes, dependent upon the symmetry of the molecule, as we progress for instance from benzene through toluene, ortha- and metaxylene to paraxylene.

It is thought that from these results, supplemented by further experimental data on temperature effects which we are at present assembling, we shall be able to work out the energy levels of these compounds.

The author wishes to express his sincere appreciation to Dr. Pfund, Dr. Herzfeld, and Professor Wood, who have been very helpful in aiding this work.

QUANTUM KINETICS AND THE PLANCK EQUATION

By Gilbert N. Lewis
Department of Chemistry, University of Calfiornia

(Received May 13, 1930)

Abstract

With the same system that Einstein employed, the Planck equation should issue directly from kinetic principles without the aid of the theory of induced emission. The three fundamental laws of physico-chemical kinetics are (1) the law of entire equilibrium, (2) the law of the duality of elementary processes (or the equality of direct and reverse transition probabilities), (3) the law of equal *a priori* probabilities. It is shown that all three follow from the law of the symmetry of time, and furthermore, that the first and third of these laws are both derivable from the second.

From one of these laws, from the equation of Boltzmann, and from the number of quantum positions in a Hohlruam within a given range of frequency, the equation of Planck is immediately derived. Finally, there is a brief discussion of the more general case of thermal equilibrium in a Hohlraum when the number of photons is permanently or temporarily restricted, resulting in a state of *gray* rather than of *black* radiation.

IN THE justly famous paper in which Einstein[1] derived the Planck equation, he first introduced that coefficient of induced emission which has played so large a part in recent physics. Without in any way minimizing the value of this conception, which indeed seems necessary to an understanding of radiation from the standpoint of field-theory, one may doubt whether it was necessary, or even legitimate, to combine this method of treatment with a totally different method based upon the kinetics of light quanta, or photons; especially as Einstein's treatment seems to be incompatible with the principle of the symmetry of time, which we shall discuss presently.

It should be possible to obtain the laws of radiation by methods of two distinct types. Let us not risk misunderstanding by calling these the method of the wave and the method of the particle. Let us rather say that the first has its analogy in classical electromagnetics, in which a radiating particle is conceived to be immersed in, and in equilibrium with, a field, while the second has its analogy in the classical methods of kinetic theory, such as that of Guldberg and Waage, whereby the radiating atoms may be regarded as reacting with the atoms of light. Einstein borrowed from both types, but we shall see that it is possible by the second type of method alone to obtain, in a remarkably simple way, Planck's law of radiation, without otherwise departing from Einstein's procedure.

The Laws of Quantum Kinetics Derived from the Symmetry of Time

In a paper which is being published in Science, I show what remarkable conclusions may be drawn from the simple law, that in the domain of physical

[1] Einstein, Phys. Zeits. **18**, 121 (1917).

science it is impossible to distinguish between past and future. If this law had been recognized, many of the errors of classical physics would have been avoided, such as the doctrine of Clausius that entropy tends toward a maximum, the theory that energy is radiated in a continuous expanding spherical shell, and the associated use of the retarded potentials. To present problems the law of the symmetry of time finds its most interesting applications in the study of quantum transitions, into which all physico-chemical processes may be resolved.

In discussing thermal equilibrium a special assumption has sometimes been employed which is not derivable from thermodynamics. It has been called the principle of detailed balancing, or of microscopic reversibility, or of entire equilibrium, and has usually been regarded as of useful, but limited, applicability. However, in the paper[2] in which I spoke of it as the principle of entire equilibrium, I proposed that it be regarded as a universal law, valid throughout physics and chemistry. This view was unacceptable to many physicists on the ground that the principle could not apply to cases in which radiation is involved. I think it will be apparent as we proceed that these very cases illustrate in a most satisfactory manner the value and the scope of the principle.

We may regard a physico-chemical system as passing through a succession of well defined quantum states for the whole system, which may be numbered (each degenerate state being separately listed). If the succession of these several quantum states is followed over a period of time long enough to be representative, we say that we are dealing with an equilibrium, and we may inquire how frequently one of these quantum states is reached; how long, on the average, it lasts, and what the chance is of a transition to any other given state.

The law of entire equilibrium demands that on the average the transition from state j to state k will occur just as often as the transition from k to j, or in other words, that the chance of going from j to k is equal to the reverse chance. The chance of going from j to k is equal to the chance p_j that the system is in the state j, multiplied by the intrinsic probability ϕ_{jk} that when it is in state j it will go over in unit time to state k. The law of entire equilibrium then states that,

$$p_j\phi_{jk} = p_k\phi_{kj}. \tag{1}$$

The reason that I felt convinced of the universality of the law of entire equilibrium was that it is directly derivable from the principle of symmetry in time. If it should fail at any point it would be the only known case in the whole of physical science in which time appears as unsymmetrical. The argument is simple: If in any system we should find $p_j\phi_{jk} > p_k\phi_{kj}$, $p_k\phi_{kl} > p_l\phi_{lk}$, $p_l\phi_{lj} > p_j\phi_{jl}$, we might still have equilibrium, but it would be of a cyclic character. We could state as a law for this system that the succession of states is chiefly in the direction $jkljk \cdots$. Now reversing time, we should be obliged to describe the chief sequence as $jlkjl \cdots$, a different law.

[2] G. N. Lewis, Proc. Nat. Acad. Sci. **11**, 179, 422 (1925).

I shall not enter here upon the somewhat more difficult but equally binding, proof, which I give in my other paper, that the law of the symmetry of time also requires the equality of the intrinsic transition probabilities in two directions, namely,

$$\phi_{jk} = \phi_{kj}. \tag{2}$$

This, the most fundamental law of quantum kinetics, has hitherto received no name, except in so far as it has occasionally been confused with the law expressed in Eq. (1). It may be called the law of the duality of elementary processes, in order to indicate that the transition from j to k, and the transition from k to j, are not two separate physical entities, but the same entity regarded from two points of view.

By combining Eqs. (1) and (2), we find

$$p_j = p_k. \tag{3}$$

This is the principle known as the equality of *a priori* probabilities. These three equations, all of which may be derived from the law of the symmetry of time, underlie the whole theory of physico-chemical kinetics.

Both of the other two laws may be obtained from the law of duality, in the following manner. If we say that the probability of finding a system in a given state is determined by the probability of entering that state, and by the probability of leaving it, this means that all the p's are determined when all the ϕ's are given. The equations which suffice for such determination are evidently the ones which express the fact that in the long run the system enters as often as it leaves a given state. Thus,

$$\begin{aligned} p_1\phi_{12} + p_1\phi_{13} + \cdots p_1\phi_{1N} &= p_2\phi_{21} + p_3\phi_{31} + \cdots p_N\phi_{N1} \\ \cdots \quad \cdots \quad \cdots \quad

the complete quantum state of the radiation. The latter may also be simplified by setting up a set of skeleton quantum positions, or cells, and giving the number of photons in each skeleton position, or cell.

The number dn of these cells lying within a given energy range $hd\nu$ has now been obtained by several very different methods, all of which lead to the same result, namely,

$$dn = \frac{8\pi V\nu^2}{c^3}d\nu. \tag{4}$$

By making V indefinitely large, dn can be kept large, however small the range $d\nu$. Indeed, the Planck equation, to which Eq. (4) leads, is strictly valid only for a Hohlraum of infinite volume.

A completely specified individual state of the system is given when we know whether the atom is in state A or B, and when we know the number of photons in each of the skeleton positions or cells. The relative probability that the atom will be in state B or A, we shall assume, with Einstein, to be given by the following equation (although later we shall further consider its validity).

$$\frac{p_B}{p_A} = e^{-h\nu/kT} \tag{5}$$

From Eqs. (4) and (5), and with one of the preceding equations, we may obtain in a variety of ways the equation for black-body radiation. The very simple method which I shall give here I owe in part to a kind communication from Professor L. Brillouin, who has consistently maintained the applicability of the fundamental laws of kinetics to radiative processes.

Let us pick out one particular cell, Q, which corresponds to the energy emitted by state B. Let us then consider a process by which the atom changes from B to A, while the number of photons in cell Q changes from an initial value, m, to $m+1$, all the remaining radiation being unchanged. This may be expressed as

$$B, Q_m \rightarrow A, Q_{m+1}.$$

Calling the two complete states I and II, we have from Equation (3)

$$p_{\mathrm{I}} = p_{\mathrm{II}}.$$

The probability p_I is equal to the probability p_B, that the atom will be in state B, multiplied by the independent probability q_m, that cell Q has m photons; so also for the second state, and we may write

$$p_B q_m = p_A q_{m+1}. \tag{6}$$

Combining this equation with Eq. (5) we now have a result which concerns the radiation alone, and tells the relative probability of having $m+1$ and m photons in a given cell, namely,

$$\frac{q_{m+1}}{q_m} = e^{-h\nu/kT}.$$

If then q_0 represents the chance that cell Q has no photons, q, the chance that it has one, and so on,

$$q_0 + q_1 + q_2 + \cdots = 1 = q_0(1 + e^{-h\nu/kT} + e^{-2h\nu/kT} + \cdots). \quad (7)$$

If the cell Q has no photons, it has zero energy, with one photon it has the energy $h\nu$, with two photons $2h\nu$, so that $\overline{E}$, the probable energy of the cell, is

$$\overline{E} = q_0 h\nu(e^{-h\nu/kT} + 2e^{-2h\nu/kT} + \cdots).$$

Eliminating q_0 by means of the previous equation,

$$\overline{E} = \frac{h\nu(e^{-h\nu/kT} + 2e^{-2h\nu/kT} + \cdots)}{(1 + e^{-h\nu/kT} + e^{-2h\nu k/T} + \cdots)}, \quad (8)$$

and by carrying out the indicated division we find,

$$\overline{E} = h\nu(e^{-h\nu/kT} + e^{-2h\nu/kT} + \cdots) = \frac{h\nu}{e^{h\nu/kT} - 1}. \quad (9)$$

Multiplying $\overline{E}$ by the number of cells lying in the range $d\nu$, from Eq. (4), we find the energy dE lying within this range,

$$dE = \frac{8\pi V h\nu^3 d\nu}{c^3} \frac{1}{e^{h\nu/kT} - 1}. \quad (10)$$

In this straightforward derivation of the Planck equation from simple kinetic principles there is no suggestion of "induced emission," which, I should like to repeat, may appear as a very real phenomenon when the same system is studied from the standpoint of field-theory, but is not a consideration that properly belongs to the kinetic mode of treatment.

Both Eq. (5) and Eq. (10) represent states of thermal equilibrium in the presence of an unlimited supply of photons. It is, however, perfectly possible to find processes by which photons interchange energies, and thus establish thermal distribution with respect to frequencies, without changing the number of photons. In case the concentration of photons of each frequency is less than that of black radiation, we may speak of *gray* radiation. Such a distribution I regard as a true and permanent case of equilibrium. Others who deny this will still admit that such a state may persist for a long time. Such equilibria, whether permanent or temporary, are susceptible to thermodynamic treatment.

In the presence of such a gray equilibrium of radiation, the atom at a given temperature will be less often is state B than when black radiation is present, and we may correct Eq. (5) by writing

$$\frac{p_B}{p_A} = \gamma e^{-h\nu/kT}, \quad (11)$$

where γ may be a function of temperature as well as of the number of photons per unit volume. Using this equation in place of Eq. (5), we obtain the expression for the distribution of energy in gray radiation, which I have previously derived more rigorously,[3] namely,

$$dE = \frac{8\pi V h\nu^3 d\nu}{c^3} \frac{1}{(1/\gamma)e^{h\nu/kT} - 1} \quad (12)$$

[3] G. N. Lewis, Proc. Nat. Acad. Sci. **13**, 471 (1927).

A CONTRIBUTION TO THE QUANTUM MECHANICAL THEORY OF RADIOACTIVITY AND THE DISSOCIATION BY ROTATION OF DIATOMIC MOLECULES

By Oscar Knefler Rice[1]

Institut für Theoretische Physik der Universität, Leipzig

(Received February 26, 1930)

Abstract

In the recent theory of radioactive decay, and also, as is shown, in the theory of dissociation of a diatomic molecule by the acquisition of rotational energy, there occurs a potential energy curve which has the following shape, as we go, say, from left to right. At the left the potential energy is very high, it then comes down to a minimum, increases to a maximum, and again falls off to an asymptotic value. The problems connected with such a curve are of two types. First, we may be given a particle in the region near the minimum, in an energy level which lies below the maximum, and wish to find the chance that it appear by a quantum mechanical process in the region on the other side of the maximum. Second, we wish to find how the "discrete states" in the neighborhood of the minimum are "broadened" by the continuum on the other side of the maximum. To solve these problems we first find the stationary eigenfunctions. By means of them the width and shape of the "broadened discrete levels" are found immediately. We then use these eigenfunctions to set up a wave packet, or, rather, we show how nature may set up a wave packet, which enables us to solve the first of the problems mentioned. The result justifies the use of complex eigenvalues for the solution of the problem.

Introduction

THE theory of radioactive decay, recently proposed by Gurney and Condon,[2] and independently by Gamow[3] makes use of a potential energy curve of the type shown in Fig. 1 (solid curve), the wave equation being of the form

$$d^2\psi/dx^2 + (8\pi^2 M/h^2)(E - U)\psi = 0. \tag{1}$$

The alpha-particle is supposed to be originally in some energy level such as E between x_2 and x_3. There is then a finite probability of its appearing to the right of x_1 which gives the chance of disintegration of the radioactive atom.

Curves of much the same general characteristics also occur in the case of molecules, and can be used to explain the phenomenon of dissociation by rotation; i.e. one can use them to show how rotational energy can cause a diatomic molecule to dissociate. This explanation was given by Oldenberg,[4] but as his work was not put into quantum mechanical form, and as a little more information may be obtained when this is done, it seems worth while to devote a paragraph to indicating how this may be done.

[1] National Research Fellow.

[2] Gurney and Condon, Nature **122,** 439 (1928); Phys. Rev. **33,** 127 (1929).

[3] Gamow, Zeits. f. Physik **51,** 204 (1928).

[4] Oldenberg, Zeits. f. Physik **56,** 563 (1929).

One begins with the wave equation of a rotating and oscillating diatomic molecule, and, in the usual way, separates out the variables which give the orientation of the molecule. One thus obtains a wave equation in r, the dis-

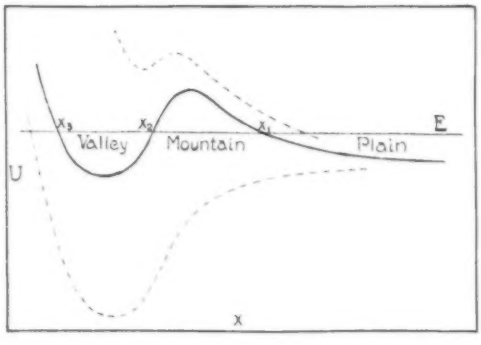

Fig. 1.

tance between the two nuclei. If we let $F=rR$, where R is the part of the eigenfunction which depends on r, this equation is[5]

$$d^2F/dr^2 - j(j+1)F/r^2 + (8\pi^2M/h^2)(E - U_0)F = 0$$

where j is the rotational quantum number, M the reduced mass, E the eigenvalue, and U_0 the potential energy, which is a function of r. The term $j(j+1)/r^2$ when multiplied by $h^2/8\pi^2M$ acts exactly like an addition to the potential energy[6] and we may replace $U_0+(h^2/8\pi^2M)j(j+1)/r^2$ by an effective potential energy U, getting an equation like (1). When $j=0$ the curve has the usual form of the potential energy curve for a molecule (lower dotted curve in Fig. 1). As j increases the curves become like the solid curve of Fig. 1, and finally when j is quite large they are like the upper dotted curve of Fig. 1, the valley becoming shallower and finally disappearing altogether.[7] Now, as we shall see, we can in a certain sense speak of discrete states in the valley, corresponding to an oscillation of the molecule in this region, and we see that the number of discrete states in the valley grows less and less until at last there are no more. Thus if a molecule is in a certain vibrational state, this state will disappear, and the molecule will dissociate, if j exceeds a certain value. This is the phenomenon observed in the case of mercury hydride, and the explanation does not differ greatly from that given by Oldenberg.

For energy levels such as E between the top of the mountain and the level of the plain, the problems which occur in the case of radioactivity will have an analog in the case of molecules. In the case of radioactivity what we observe is that a system starting in the valley goes through the mountain and appears in the plain. In the case of molecular spectra we actually observe another phenomenon. We find that the discrete states in the valley will be broadened

[5] Fues, Ann. d. Physik **80,** 371 (1926).

[6] See Gamow and Houtermans, Zeits. f. Physik **52,** 509 (1928).

[7] The curves of Fig. 1 are quite schematic. For curves drawn to scale see Oldenberg, l.c.

in the same sense as in the case of predissociation,[8] and one in fact observes diffuse rotation lines.

The problem which concerns the rate at which particles appear on the plain, and which, as noted, is of particular interest in the case of radioactivity, has been considered by a number of investigators. In the original papers of Gurney and Condon, and Gamow, no attempt was made to put this calculation on a rigorous basis. Numerous articles have appeared since, attempting to do this.[9] Among the various methods used the introduction of complex eigenvalues offers to my mind the most elegant solution of this problem which has appeared so far. This very ingenious procedure gives very reasonable results. Still the idea of a complex eigenvalue is a rather unusual one. The method also includes the assumption that the decomposition is proceeding in just the same way as if it had been going on for an infinite length of time. This is also not an unreasonable assumption but it can be avoided; at the same time the use of complex eigenfunctions can be justified, and new light thrown on the significance of the whole process by the method we propose to use.

Method of Attack

First of all we shall consider the entire system to be enclosed in a large box, to avoid the necessity of considering a continuum. Then we shall find the stationary eigenfunctions. In general it will be found that the part of the eigenfunction on the plain will be great compared to that in the valley. As we pass through certain energies, however, the relative size of the part inside will increase, reach a maximum and fall off again. To avoid circumlocution we shall refer to these energies as "discrete levels." They will in general occur near an energy where we would expect a discrete level to be if the curve rose continuously to the right of the valley. Since there is a finite energy range over which the part of the eigenfunction in the valley has a relatively large size these discrete levels are "broadened."

We wish now to investigate how our system can appear in a "discrete state," and what it means to say that we start out with our system in the valley, and calculate the probability that it will get out on the plain. To do this we suppose that the system was originally in some real discrete state which might or might not be part of the system of states belonging to the potential energy curve of Fig. 1, but from which no escape from the valley into the plain is possible. We will call the eigenfunction of this state ψ_0 and its energy E_0. Now our system is subjected to a perturbation which causes it to appear in one of the states belonging to the curve of Fig. 1. There is a cer-

[8] Rice, Phys. Rev. **33,** 748 (1929). And see Schrödinger, Sitzungsber. Preuss. Akad. Wiss., (1929) 668.

[9] Kudar, Zeits. f. Physik **53,** 61, 95, 134 (1929); **54,** 297 (1929); Gamow and Houtermans, Zeits. f. Physik **52,** 496 (1928); Gamow, Zeits. f. Physik **53,** 601 (1929); Fowler and Wilson, Proc. Roy. Soc. **A124,** 493 (1929). See also v. Laue, Zeits. f. Physik, **52,** 726 (1928); Sexl, Zeits. f. Physik **54,** 445 (1929); **56,** 62, 72 (1929); Born, Zeits. f. Physik, **58,** 306 (1929); Atkinson and Houtermans, Zeits. f. Physik **58,** 478 (1929); Sexl, Zeits. f. Physik **59,** 579 (1930). Relativity treatment, Møller, Zeits. f. Physik, **55,** 451 (1929).

tain probability that it will land in some one of these states, of energy E, say, which is near some discrete energy, E_d. The eigenfunction of energy E (not including the exponential time factor) will be called $\psi(E)$. The wave packet which is formed by systems jumping from the state to the states $\psi(E)$ will be of the form

$$\psi = \sum a(E)\psi(E) \exp(-2\pi iEt/h)$$

where $a(E)$ is a constant coefficient for any E, and the sum is taken over all allowable values of E, which form a continuous set within the limits allowed by the box.

As a typical example, we shall consider the case where the perturbation which sets up the wave packet ψ for us is due to the action of monochromatic light,[10] of a frequency somewhere near $E_d - E_0$ which difference we will suppose great[11] compared to the "breadth" of the discrete state at E_d. Now we have said that we will have the wave packet produced by monochromatic light. But if light is to be strictly monochromatic we have to shine it in for an infinitely long time. There would be no sense in making any calculation for a process which occurs after such an excitation. In fact there would be no process to calculate. The system after the excitation by light would simply be in one of the stationary states $\psi(E)$. We can, however, shine in light of a given frequency for a short time. It is of particular interest to have it shine in for so short a time that any of the states $\psi(E)$ over a considerable range of energies in the neighborhood of E_d may be excited, and short enough so that no appreciable difference in phase of the exponential factor for the various states $\psi(E)$ in the expression for ψ can arise.[12] The matrix component of the perturbation for the excitation by light from state ψ_0 to a state $\psi(E)$ is proportional to the matrix component,[13] $P_{0E} = \int_0^\infty \psi_0 P \psi(E) dx$, where P is the electrical polarization expressed as a function of x. The $\psi(E)$ must be normalized. $a(E)$ will be proportional to P_{0E} and to find out how P_{0E} depends on E we must make a certain assumption regarding the integral which gives it. We assume that all appreciable contributions to this integral come from the range

[10] Rice, Phys. Rev. **34,** 1454 (1929).

[11] The assumption that $E_d - E_1$ should be great compared to the width of the discrete state at E_d was also made in the previous work, Ref. 9, but it was forgotten to mention it explicitly there. This assumption was necessary to show that a_n in Eq. (5) of that article is proportional to P_{n0}; it makes $E_n' - E_0$ practically independent of E_n' over the important range of E_n'.

[12] As in the case previously considered (Ref. 10, see p. 1458) it seems safe to replace this condition by the statement that the time of illumination must be short compared to the time of decomposition, i.e. in this case the average life of a particle in the valley before it escapes into the plain. If the time of illumination is so short that more than one discrete state is excited the various decompositions from the various states may all be treated separately provided the energy between two discrete states is great compared to the breadth of a discrete state, a condition which must be fulfilled anyhow. This will also presumely be the case, if the perturbation is due to any other cause, provided it lasts for such a short time that no appreciable decomposition takes place in this time. The point is, as we shall see, that the wave packet starts in the neighborhood of the valley, and if the time of the perturbation is short enough, it will not, during that time, get out of the valley.

[13] Dirac, Proc. Roy. Soc. **A112,** 674 (1926).

of x in the valley, because ψ_0 is supposed to have appreciable values only in the valley. In the immediate neighborhood of any given discrete level in the valley, the shape of the part of $\psi(E)$ which is in the valley or the amplitude of the part in the plain will not vary greatly with the energy over a small energy range, but the ratio which we call B, of the magnitude of the valley part of $\psi(E)$ (for some definite value of x, say x^1) to the amplitude of the plain part will vary greatly with the energy. Let us designate the maximum of B as B_1. Then B/B_1 (which does not depend on x^1) is equal to the ratio[14] P_{0E}/P_{0E_1} because the normalization makes all $\psi(E)$ alike in the plain.[14a] The coefficient $a(E)$ is proportional to P_{0E} hence to P_{0E}/P_{0E_1}, hence to B/B_1. Therefore, neglecting a constant factor, ψ becomes

$$\psi = \sum(B/B_1)\psi(E) \exp(-2\pi iEt/h) \tag{2}$$

where the summation is over all allowable values of E. Now it will later be seen that this equation results in the total amount of material in the plain at $t=0$ being zero or almost so, but as time goes on, matter appears in the plain, and the amount of material in the valley suffers an exponential decrease.

If E_0 is greater than E_d so that the wave packet is set up by emission of light the above will also hold.

Calculation of the Stationary Eigenfunction

If ψ now is the stationary eigenfunction for some definite energy E, it has been shown that for regions when $|E-U|$ is not too small, and the slope of the U vs. x curve not too great, that the solutions of the wave equation can be written in the form[15] (disregarding constant factors)

$$\psi = (E-U)^{-1/4} \text{ or } \left\{ \begin{matrix} \sin \\ \cos \end{matrix} \right\} \left\{ \kappa \int (E-U)^{1/2} dx \right\} \tag{3}$$

for $U<E$, and

$$\psi = (U-E)^{-1/4} \exp\left\{ \pm \kappa \int (U-E)^{1/2} dx \right\} \tag{4}$$

for $U>E$, where $\kappa = (8\pi^2 M/h^2)^{1/2}$.

In the immediate neighborhood of such a point as x_1 these solutions do not hold. The question now arises as to what happens if we start with some given solution in the mountain to the left of x_1, and go through x_1 into the plain. On the assumption that the side of the mountain is long and straight, Kramers[16] has shown that, if we start with the solution

$$(U-E)^{-1/4} \exp\left\{ -\kappa \int_x^{x_1} (U-E)^{1/2} dx \right\}$$

far to the left of x_1, after going through x_1 and getting far to the right the solution has become

[14] E_d is not a well defined energy and we could take it as that value of the energy for which B is a maximum. We prefer, however, to designate the latter energy as E_1.

[14a] The matter of normalization is explained in more detail after Eq. (17). See also Ref. 8, p. 749.

[15] See, e.g., Nordheim, Zeits. f. Physik **46,** 842 (1927).

[16] Kramers, Zeits. f. Physik **39,** 828 (1926).

$$2(E-U)^{-1/4}\cos\left\{\kappa\int_{x_1}^{x}(E-U)^{1/2}dx-\pi/4\right\}.$$

This means that the particular solution of the differential equation which has the one form to the left of x_1 has the other form to the right. We express this by using the following notation:

$$(U-E)^{-1/4}\exp\left\{-\kappa\int_{x}^{x_1}(U-E)^{1/2}dx\right\}$$

$$\overset{x_1}{\longleftrightarrow} 2(E-U)^{-1/4}\cos\left\{\kappa\int_{x_1}^{x}(E-U)^{1/2}dx-\frac{\pi}{4}\right\} \quad (5)$$

Putting in the limits is equivalent to evaluating the constant of integration, the integral being a function of x. Kramers and Ittman[17] also point out that

$$(U-E)^{-1/4}\exp\left\{\kappa\int_{x}^{x_1}(U-E)^{1/2}dx\right\}$$

$$\overset{x_1}{\longleftrightarrow} -(E-U)^{-1/4}\sin\left\{\kappa\int_{x_1}^{x}(E-U)^{1/2}dx-\frac{\pi}{4}\right\} \quad (6)$$

Zwaan[18] points out that the relation (5) holds whether the side of mountain is long and straight or not, if we can go from a region where the approximations of the type (4) hold to a region where the approximations of the type (3) hold, *via* a path in the complex plane along which the solutions are of the general type $(E-U)^{-1/4}\exp\left\{i\kappa\int_{x_1}^{x}(E-U)^{1/2}dx\right\}$ and which crosses the curve along which argument of $\int_{x_1}^{x}(E-U)^{1/2}dx$ is $\pi/2$ at a point where the absolute value of $\int_{x_1}^{x}(E-U)^{1/2}dx$ is large.[19]

In similar manner we also have

$$2(E-U)^{-1/4}\cos\left\{\kappa\int_{x}^{x_2}(E-U)^{1/2}dx-\frac{\pi}{4}\right\}$$

$$\overset{x_2}{\longleftrightarrow}(U-E)^{-1/4}\exp\left\{-\kappa\int_{x_2}^{x}(U-E)^{1/2}dx\right\} \quad (7)$$

and

$$-(E-U)^{-1/4}\sin\left\{\kappa\int_{x}^{x_2}(E-U)^{1/2}dx-\frac{\pi}{4}\right\},$$

$$\overset{x_2}{\longleftrightarrow}(U-E)^{-1/4}\exp\left\{\kappa\int_{x_2}^{x}(U-E)^{1/2}dx\right\}. \quad (8)$$

Now if we multiply the left hand side of expression (5) by the factor $\exp\left\{\kappa\int_{x_1}^{x_2}(U-E)^{1/2}dx\right\}$ which we will call $\theta/2$ we see that it coincides exactly with the right hand side of expression (8). Likewise if we multiply the left

[17] Kramers and Ittman, Zeits f. Physik **58** 222 (1929)

[18] Zwaan: Intensitäten im Ca-Funkenspektrum, Thesis, Utrecht (1929), p. 35. I am indebted to Dr. F. Bloch for calling my attention to this work.

[19] Kramers and Ittman state that (6) can be derived in the same way.

hand side of (6) by $2\theta^{-1}$ it coincides with the right hand side of (7). Thus we have established a connection between the solutions to the left of x_2 and to the right of x_1. We see, in fact, that

$$-(E-U)^{-1/4}\sin\left\{\kappa\int_x^{x_2}(E-U)^{1/2}dx-\frac{\pi}{4}\right\}$$

$$\xleftrightarrow{x_2 \text{ and } x_1}\theta(E-U)^{-1/4}\cos\left\{\kappa\int_{x_1}^{x}(E-U)^{1/2}dx-\frac{\pi}{4}\right\} \quad (9)$$

and

$$(E-U)^{-1/4}\cos\left\{\kappa\int_x^{x_2}(E-U)^{1/2}dx-\frac{\pi}{4}\right\}$$

$$\xleftrightarrow{x_2 \text{ and } x_1}-\theta^{-1}(E-U)^{-1/4}\sin\left\{\kappa\int_{x_1}^{x}(E-U)^{1/2}dx-\frac{\pi}{4}\right\}. \quad (10)$$

The actual eigenfunction in the valley must consist of a linear combination of the left hand sides of (9) and (10). If the eigenfunction in the valley is

$$(E-U)^{-1/4}\left[\cos\left\{\kappa\int_x^{x_2}(E-U)^{1/2}dx-\frac{\pi}{4}\right\}\right.$$

$$\left.+\,b\sin\left\{\kappa\int_x^{x_2}(E-U)^{1/2}dx-\frac{\pi}{4}\right\}\right] \quad (11)$$

the same eigenfunction in the plain is

$$-(E-U)^{-1/4}\left[\theta^{-1}\sin\left\{\kappa\int_x^{x}(E-U)^{1/2}dx-\frac{\pi}{4}\right\}\right.$$

$$\left.+\,b\,\theta\cos\left\{\kappa\int_{x_1}^{x}(E-U)^{1/2}dx-\frac{\pi}{4}\right\}\right] \quad (12)$$

The Shape of the Broadened Discrete State

In order that the solution of the wave equation should be an eigenfunction it must satisfy a certain condition to the left of x_3. It is probably good enough to assume that to the left of x_3 the solution must decrease exponentially in absolute value as we go to the left,[16] and the solution to the left of x_3 will therefore be of the form $(U-E)^{-1/4}\exp\left\{-\kappa\int_x^{x_3}(U-E)^{1/2}dx\right\}$. Now

$$(U-E)^{-1/4}\exp\left\{-\kappa\int_x^{x_3}(U-E)^{1/2}dx\right\}$$

$$\xleftrightarrow{x_3}2(E-U)^{-1/4}\cos\left\{\kappa\int_{x_3}^{x}(E-U)^{1/2}dx-\frac{\pi}{4}\right\} \quad (13)$$

(11) must be the same as the right hand side of (13), and it can be made the same as follows. We can easily at any time adjust the amplitude of (11) or (13) so that they will be the same. But we have to adjust the phase of (11)

so that it will coincide with (13). This is done by choosing the value of b. At some energy, say for example at E_1, the value of b will be zero. Then under the mountain we have only the decreasing exponential. The value E_1 will therefore be approximately the same as an eigenvalue of the wave equation if the curve for U increased indefinitely to the right. Kramers[16] has shown that the condition that E_1 should be the energy of such a discrete state is

$$\kappa \int_x^{x_2} (E_1 - U)^{1/2} dx = n\pi \tag{14}$$

when $n = 1/2,\ 3/2,\ 5/2, \cdots$. The phase of the right hand side of (13) (starting from x) is less than that of the first term of (11), at some E not too distant from E_1, by

$$\kappa \int_{x_3}^{x_2} (E - U)^{1/2} dx - \kappa \int_{x_3}^{x_2} (E_1 - U)^{1/2} dx. \tag{15}$$

The amount that the phase of (11) is less than that of its first term is $\tan^{-1} b$. Thus, since (13) and (11) must be alike,

$$b = \tan \left\{ \kappa \int_{x_3}^{x_2} (E - U)^{1/2} dx - \kappa \int_{x_3}^{x_2} (E_1 - U)^{1/2} dx \right\}. \tag{16}$$

Now if the breadth of the "broadened discrete state" is to be narrow compared to the distance between two discrete states, it means that over the "width" of the discrete state (15) must be small compared to π. We assume it so small that we may write

$$\begin{aligned} b &= \kappa \int_{x_3}^{x_2} (E - U)^{1/2} dx - \kappa \int_{x_3}^{x_2} (E_1 - U)^{1/2} dx \\ &= (E - E_1) \frac{\partial}{\partial E} \kappa \int_{x_3}^{x_2} (E - U)^{1/2} dx \end{aligned} \tag{17}$$

which we set $= b'(E - E_1)$. The derivative is taken for $E = E_1$. It is important to note that b' is positive.

We now wish to find how the value of b affects the relative size of the eigenfunction in the valley and on the plain. For large values of x we know that U takes on some asymptotic value, which we can without loss of generality take as 0. Then (12) also has an asymptotic form. In the limiting case when the box is large this part of (12) will determine the normalization, as the integral of ψ^2 over the plain can always, by taking the plain long enough, be made large compared to the integral across the valley. We make $\int_0^\infty \psi^2 dx = 1$. The amplitude of the sinusoidal function represented by (12) is (for large values of x where $U = 0$) equal to $(\theta^{-2} + b^2\theta^2)^{1/2} E^{-1/4}$. To satisfy the normalization conditions the amplitude must be $(2/x_\infty)^{1/2}$ where x_∞ is the largest possible value[20] of x. To normalize we therefore multiply (12) by $(\theta^{-2} + b^2\theta^2)^{-1/2} E^{1/4}$

[20] Giving x a largest value allows in an idealized way for the fact that the system is in a box.

$(2/x_\infty)^{1/2}$. Now (11) must also be multiplied by the same thing, so its amplitude becomes $(1+b^2)^{1/2}(E-U)^{-1/4}(\theta^{-2}+b^2\theta^2)^{-1/2}E^{1/4}(2/x_\infty)^{1/2}$. But if b is small so that (17) holds, then it will also be negligible compared to 1. So the amplitude of (11) becomes

$$(E-U)^{-1/4}(\theta^{-2}+b^2\theta^2)^{-1/2}E^{1/4}(2/x_\infty)^{1/2}.$$

If we divide this expression by its value when $E=E_1$, and hence $b=0$, we get an expression which will no longer depend on the particular value of x between x_2 and x_3, and which will in fact be just equal to the quantity B/B_1 which appeared in Eq. (2). We thus find (assuming that E and θ do not vary appreciably over the range of E included in a broadened discrete state):

$$B/B_1 = (1 + b^2\theta^4)^{-1/2} = [1 + b'^2(E - E_1)^2\theta^4]^{-1/2}. \tag{18}$$

The shape of the broadened discrete state is found by plotting

$$(B/B_1)^2 = [1 + b'^2(E - E_1)^2\theta^4]^{-1} \tag{19}$$

against E. The width w of the state we may define as the energy over which $(B/B_1)^2$ has the value $\frac{1}{2}$ or greater, or twice the absolute value of $E-E_1$ for which $(B/B_1)^2=\frac{1}{2}$. Thus

$$w = 2/b'\theta^2. \tag{20}$$

The Setting-up of the Wave Packet; the Rate of Decay; Proof of Assumption of Complex Eigenvalues

For a very large box the summation in Eq. (2) can be replaced by an integration, which is surely allowable, as it will be seen that the integrand has no singular points. Eq. (2) thus becomes

$$\psi = \int_{-\infty}^{\infty} (B/B_1)\psi(E) \exp(-2\pi iEt/h)dE/\epsilon \tag{21}$$

where ϵ is the distance between energy levels, and is equal to $2\pi E^{1/2}/\kappa x_\infty$ where x_∞ is the largest possible value of x. It is only possible to integrate thus from ∞ to $-\infty$ because only a small range of E's contributes appreciably. To find ψ for $x \gg x_1$ we substitute for $\psi(E)$ in (21) the expression (12) with $U=0$ which must however be multiplied, as noted, by $(\theta^{-2}+b^2\theta^2)^{-1/2}E^{1/4}(2/x_\infty)^{1/2} = \theta(B/B_1)E^{1/4}(2/x_\infty)^{1/2}$. To find $\psi(E)$ for $x_3<x<x_2$ we use (11) multiplied by the same thing. We will, however, find it convenient to multiply (11) and (12) through by $-\theta(B/B_1)E^{1/4}\epsilon$, instead, which is permissible for the following reasons: ψ itself is not normalized, and we can always further multiply or divide (11) and (12) by any factor which does not depend on E. And in the range of values of E which contribute importantly in the integral (21) we may regard ϵ as constant. $E^{1/4}$, $(E-U)^{1/4}$, and θ are also practically constant. So (11) gives, when thus multiplied and substituted in (21) remembering (17) and (19):

$$\psi = -\frac{E_1^{1/4}\theta}{(E_1-U)^{1/4}}\left[\int_{-\infty}^{\infty}\frac{\cos\left\{\kappa\int_x^{x_2}(E-U)^{1/2}dx-\frac{\pi}{4}\right\}\exp(-2\pi iEt/h)}{1+b'^2\theta^4(E-E_1)^2}dE\right.$$

$$\left.+\int_{-\infty}^{\infty}\frac{b'(E-E_1)\sin\left\{\kappa\int_x^{x_2}(E-U)^{1/2}dx-\frac{\pi}{4}\right\}\exp(-2\pi iEt/h)}{1+b'^2\theta^4(E-E_1)^2}dE\right] \quad (22)$$

For great values of x we can substitute $\kappa E^{1/2}x+\zeta$ for $\kappa\int_{x_1}^{x}(E-U)^{1/2}dx-\pi/4$ in (12). We simply let ζ be the difference between these two expressions, this difference being constant for large values of x. Then we multiply (12) by the same expression as we multiplied (11) by, and get

$$\psi = \int_{-\infty}^{\infty}\frac{[\sin\{\kappa E^{1/2}x+\zeta\}+\theta^2b'(E-E_1)\cos\{\kappa E^{1/2}x+\zeta\}]\exp(-2\pi iEt/h)}{1+b'^2\theta^4(E-E_1)^2}dE \quad (23)$$

We assume that the important range of E in this integral is so small that ζ is the same for all the states in this range. We now proceed to evaluate (23).

We substitute $(E-E_1)+E_1$ for E, and $E_1^{1/2}+(E-E_1)/2E_1^{1/2}$ for $E^{1/2}$, as this is allowable for the small values of $E-E_1$ which contribute to the integral. The latter substitution gives the cosine and the sine of the sum of the two angles $\kappa E_1^{1/2}x+\zeta$ and $(\kappa/2E_1^{1/2})(E-E_1)x$. These are reduced by the usual trigonometric formulas. We also write $\exp(-2\pi iEt/h)=\exp(-2\pi iE_1t/h)[\cos\{2\pi(E-E_1)t/h\}-i\sin\{2\pi(E-E_1t/h\}]$. One thus gets a number of parts of the integral which drop out because they are antisymmetrical about the point $E-E_1=0$. The rest of the expression becomes

$$\begin{aligned}\psi = \exp(-2\pi iE_1t/h)&\left[\int_{-\infty}^{\infty}\frac{\sin\{\kappa E_1^{1/2}x+\zeta\}\cos\{(\kappa/2E_1^{1/2})(E-E_1)x\}\cos\{2\pi(E-E_1)t/h\}}{1+b'^2\theta^4(E-E_1)^2}d(E-E_1)\right.\\
&-b'\theta^2\int_{-\infty}^{\infty}\frac{(E-E_1)\sin\{\kappa E_1^{1/2}x+\zeta\}\sin\{(\kappa/2E_1^{1/2})(E-E_1)x\}\cos\{2\pi(E-E_1)t/h\}}{1+b'^2\theta^4(E-E_1)^2}d(E-E_1)\\
&-i\int_{-\infty}^{\infty}\frac{\cos\{\kappa E_1^{1/2}x+\zeta\}\sin\{(\kappa/2E_1^{1/2})(E-E_1)x\}\sin\{2\pi(E-E_1)t/h\}}{1+b'^2\theta^4(E-E_1)^2}d(E-E_1)\\
&\left.-ib'\theta^2\int_{-\infty}^{\infty}\frac{(E-E_1)\cos\{\kappa E_1^{1/2}x+\zeta\}\cos\{(\kappa/2E_1^{1/2})(E-E_1)x\}\sin\{2\pi(E-E_1)t/h\}}{1+b'^2\theta^4(E-E_1)^2}d(E-E_1)\right]\end{aligned}$$

The four integrals we shall designate respectively as I_1, I_2, I_3, I_4. Another trigonometric reduction gives $I_1=\frac{1}{2}[\sin\{\kappa E_1^{1/2}x+\zeta\}](I_1^{+}+I_1^{-})$ and $I_2=\frac{1}{2}[\sin\{\kappa E_1^{1/2}x+\zeta\}](I_2^{+}+I_2^{-})$, where

$$I_1^{\pm}=\int_{-\infty}^{\infty}\frac{\cos\{[(\kappa/2E_1^{1/2})x\pm 2\pi t/h](E-E_1)\}}{1+b'^2\theta^4(E-E_1)^2}d(E-E_1)$$

and

$$I_2^{\pm}=\int_{-\infty}^{\infty}\frac{(E-E_1)\sin\{[(\kappa/2E_1^{1/2})x\pm 2\pi t/h](E-E_1)\}}{1+b'^2\theta^4(E-E_1)^2}d(E-E_1)$$

I_1^+ and I_1^- are to be found from Pierce's Tables[21] and I_2^+ and I_2^- can readily be found by differentiating I_1^+ and I_1^- with respect to the proper parameter $(\kappa/2E_1)^{1/2}x \pm 2\pi t/h$. Now it will be found (as b' is positive) that the contributions from I_1^+ and I_2^+ cancel each other in the expression for ψ, as do also the contributions from I_1^- and I_2^- when $(\kappa/2E_1^{1/2})x > 2\pi h/t$. When, however, $(\kappa/2E_1^{1/2})x < 2\pi h/t$ the latter add. We can treat I_3 and I_4 in a similar way. So ψ is zero for $(\kappa/2E_1^{1/2})x > 2\pi h/t$ and for $(\kappa/2E_1^{1/2})x < 2\pi h/t$ we have

$$\begin{aligned}\psi &= (\pi/b'\theta^2)\left[\sin(\kappa E_1^{1/2}x + \zeta) - i\cos(\kappa E_1^{1/2}x + \zeta)\right] \\ &\quad \exp\left\{\left[(\kappa/2E_1^{1/2})x - 2\pi t/h\right]/b'\theta^2\right\} \exp(-2\pi i E_1 t/h) \qquad (24) \\ &= (\pi/b'\theta^2)\exp\left\{i(\kappa E_1^{1/2}x - 2\pi E_1 t/h - \pi/2 + \zeta)\right\}\exp\left\{\left[(\kappa/2E_1^{1/2})x - 2\pi t/h\right]/b'\theta^2\right\}\end{aligned}$$

We see that this represents a wave going in the positive direction with the particle velocity $(2E_1/M)^{1/2}$, and with an amplitude determined by the second exponential factor for values of x up to the place where $(\kappa/2E_1^{1/2})x = 2\pi t/h$ after which it breaks off. The wave shows an exponential decrease with time and just the proper exponential increase with distance to insure that the amount of matter in the wave is conserved. This is exactly like the outward going wave of Kudar's,[9] which resulted from the use of complex eigenvalues, except that his did not break off, but continued out to infinity in space and negative infinity in time.

We shall now evaluate (22). The sine and cosine of $\kappa\int_x^{x_2}(E-U)^{1/2}dx - \pi/4$ are roughly periodic functions of E, but we know that in the important range of E the functions have gone through a small fraction of a period, as we are considering a discrete state that is narrow compared to the distance between two discrete states We can therefore consider the sine and cosine terms as constant factors in the integration of (22). We write $\exp(-2\pi i E t/h)$ in sine and cosine form, as before, substitute in (22), note that some of the parts of the resulting integral drop out because of antisymmetry of the part of the integrand about $E - E_1 = 0$, integrate the remaining terms, which involve integrals of the type already met with, and get

$$\begin{aligned}\psi = &- \left[\exp(-2\pi i E_1 t/h)\right]\left[(E_1^{1/4}\theta)/(E_1 - U)^{1/4}\right] \\ &\left[(\pi/b'\theta^2)\cos\left\{\kappa\int_x^{x_2}(E_1 - U)^{1/2}dx - \pi/4\right\}\exp(-2\pi t/hb'\theta^2)\right. \\ &\left. - i(\pi/b'\theta^4)\sin\left\{\kappa\int_x^{x_2}(E_1 - U)^{1/2}dx - \pi/4\right\}\exp(-2\pi t/hb'\theta^2)\right]. \qquad (25)\end{aligned}$$

Since the distance between two discrete states is by (17) and (14) of the order of $1/b'$ and since, if w is to be small compared with this, θ^2 must, by (20), be large compared to 1, the last term in the expression (25) is negligible, and we are left with

$$\begin{aligned}\psi = &- \left[\exp(-2\pi i E_1 t/h)\right]E_1^{1/4}\theta(E_1 - U)^{-1/4}(\pi/b'\theta^2) \\ &\cos\left\{\kappa\int_x^{x_2}(E_1 - U)^{1/2}dx - \pi/4\right\}\exp(-2\pi t/hb'\theta^2), \qquad (26)\end{aligned}$$

[21] Pierce, "A short Table of Integrals," Ginn and Co., Formula 490.

a standing wave, except for the exponential decrement with time. Actually, if we consider terms of higher order, the wave function in the valley will not be expected to be merely a standing wave with exponential decrement with time.

Now if the mountain is not too thick through (i.e. if x_1-x_2 is not too great)[22] we may find the expression for ψ in the mountain the same way as we found it for ψ in the valley. We simply assume that $\exp\{\kappa\int_{x_2}^{x}(U-E)^{1/2}dx\}$ does not vary over the effective range of $E-E_1$, and this is, in fact included in the assumption we have already made that θ does not vary appreciably over this range. The integrations are then readily performed. We get an expression which again contains the factor $\exp(-2\pi iE_1t/h-2\pi t/hb'\theta^2)$. Also just to the right of x_1, (23) does not give an exact expression for ψ. The difference between the true value of ψ and that given by (23) will, however, not be appreciably different from 0 for any great distance to the right of x_1, and for this range we may also assume that $\kappa\int_{x_1}^{x}(E-U)^{1/2}dx$ does not vary appreciably with E over the range w, or at least that it is a linear function of $E-E_1$. In either case it is easily seen that the expression for ψ will contain the factor $\exp(-2\pi iE_1t/h-2\pi t/hb'\theta^2)$. Thus we see that the assumption of a complex eigenvalue is at least approximately correct, and that the smaller w is the better the approximation is. It also depends on the relations (9) and (10). It is also, of course, necessary that t should not be too small.

The rate of decay, γ, of ψ^2 is of course given by twice the real factor of t in this exponential time factor. We have[23]

$$\begin{aligned}\gamma &= 4\pi/hb'\theta^2 \\ &= \frac{\pi}{h}\left(\frac{\partial}{\partial E}\kappa\int_{x_2}^{x_1}(E-U)^{1/2}dx\right)^{-1}\exp\left\{-2\kappa\int_{x_2}^{x_1}(U-E)^{1/2}dx\right\}.\end{aligned} \tag{27}$$

It is seen from (20) that

$$w/\gamma = h/2\pi \tag{28}$$

the same relation that held in the case of predissociation, where we have a different type of interaction between discrete and continuous states.[24]

Generalization of the Results

Our results so far are somewhat unsatisfactory inasmuch as the general validity of the relations (5), (6), (7) and (8) depends upon the properties of $E-U$ considered a function of x when x is a complex variable, which are a little hard to investigate in a general way, or upon the assumption that the

[22] In order for the discrete state not to be too broad, θ must be great. The condition just cited states that a sufficient portion of this greatness must be caused by the height rather than the breadth of the mountain. If the mountain and the valley are of somewhat the same width the required condition will be sufficiently well fulfilled.

[23] This expression agrees with that of Kudar, Zeits. f. Physik **53,** 99 (1929) also that of Fowler and Wilson, l.c., in the exponential part, but not in the factor. The difference is probably due to the fact that Kudar and Fowler and Wilson considered a type of potential energy curve to which Kramer's approximation method could hardly apply.

[24] Ref. 10, p. 1457.

mountain-sides are long and straight. We may, however, show that the general character of the results depends only on the broadening of the discrete state being sufficiently small so that any given solution of the wave equation does not change its general character in that range. For then we may assume that a particular solution in the plain (far to the right of x_1) is connected with a particular type of solution in the mountain and in the valley. Thus the two solutions $E^{-1/4}\frac{\cos}{\sin}(\kappa E^{1/2}x+\zeta)$ are connected with solutions in the mountain and valley which do not change much over the range of energies in the width of the discrete state. This will be true no matter what value we choose for ζ. Let us choose ζ so that if $E=E_1$ the eigenfunction in the plain becomes $E^{-1/4}\sin(\kappa E^{1/2}x+\zeta)$. For any other value of E the eigenfunction in the plain is

$$[E^{-1/4}\sin(\kappa E^{1/2}x+\zeta)+gE^{-1/4}\cos(\kappa E^{1/2}x+\zeta)]/(1+g^2)^{1/2}. \tag{29}$$

If $E-E_1$ is small enough g can be written as a linear function of $E-E_1$ say $g'(E-E_1)$ and in general it may be expected to be of the order of $b'\theta^2(E-E_1)$ as before, but the general character of the results, and the possibility of the use of complex eigenvalues do not depend on this. (The sign of g' is important but is surely the same as that of $b'\theta^2$.) Since we assume that the range of $E-E_1$ is so small that the shape of the eigenfunction in the valley is not affected we see that $(B/B_1)^2$ is given by $1/[1+g'^2(E-E_1)^2]$, hence all our previous results follow with g' substituted for $b'\theta^2$. Except, therefore, for this substitution we see that our results depend only on general properties of the solutions of the wave function, and not on their specific form.

I wish to thank Professor W. Heisenberg and Dr. F. Bloch for discussing this problem with me. I am informed by Dr. Bloch that much the same thing has been worked out independently by Professor Kramers, though without indicating, as is done here, how the wave packet is probably formed in nature.

PERTURBATIONS IN MOLECULES AND THE THEORY OF PREDISSOCIATION AND DIFFUSE SPECTRA. II

By Oscar Knefler Rice[1]
Institut für Theoretische Physik der Universität, Leipzig

(Received March 8, 1930)

Abstract

Further consideration is given to the problems which arise when the continuum of one electronic state of a diatomic molecule occurs in the same range as the discrete states of another electronic state. In the finding of electronic states and the potential curves which go with them certain approximations must be made; a better approximation can then be obtained by quantum mechanical perturbation theory. The discrete states are broadened, and this will appear, inasmuch as spectral lines involving these states are broadened. In this paper the shape of the broadened spectral lines is found, certain properties of the perturbation matrix are considered, and a wave packet is set up or rather one such as would be set up by nature is used to give all the details of a radiationless transition from a discrete state to the overlying continuum.

Shape of a Spectral line in Cases of Predissociation

THE simple result obtained in the preceding paper[2] for the shape of the absorption line in the case of radioactive decay and other similar processes, suggests that it would be well to try to obtain an explicit result for the shape of the line in the case of predissociation, for purposes of comparison. The shape of line could of course be calculated from the expressions in the first paper with the above title[3] (hereafter referred to as (I)), but it turns out that these can be somewhat simplified.

In this paper it was shown that the absorption coefficient over a broadened spectral line (see Abstract above) as a function of $E-E_1$ (called $-E$ in (I)) where E is the energy of the light absorbed and E_1 the energy of the center of the line, is proportional to K^2, where

$$K^2 = \left(\frac{1}{(\epsilon/2+\beta)^2} + \frac{1}{(3\epsilon/2+\beta)^2} + \cdots + \frac{1}{(\epsilon/2-\beta)^2} + \frac{1}{(3\epsilon/2-\beta)^2} + \cdots \right)^{-1} \quad (1)$$

where ϵ is the distance between unperturbed continuous levels[4] (the system being in a box) and where β is a parameter given by the equation[5]

[1] National Research Fellow.

[2] Rice, Phys. Rev. preceding paper in this issue.

[3] Rice, Phys. Rev. **33**, 748 (1929).

[4] ϵ can of course be varied arbitrarily by varying the size of the box, but in any given problem can be regarded as a constant. None of the results depend on it in any essential particular, and it will always cancel out of expressions for things which are experimentally determinable. Nevertheless it has been found very convenient to treat the system as if contained in a box, so the continuous levels really become a very close-spaced set of discrete ones, and we shall continue to do so.

[5] (I), Eq. (26), since $v_{cd}=v_{dc}$ (see Rice, Phys. Rev., **34**, 1459 (1929), especially footnote 19).

$$E - E_1 = -2\beta A v_{cd}^2 \tag{2}$$

where $A = (\pi/2\epsilon\beta)\,[2\cot(2\pi\beta/\epsilon) - \cot(\pi\beta/\epsilon)]$ and v_{cd} is the component of the perturbation matrix giving the interaction between the discrete level and the continuous levels. Now A is easily reduced to the form $-(\pi/2\epsilon\beta)\tan(\pi\beta/\epsilon)$, hence (2) becomes

$$E - E_1 = (v_{cd}^2\pi/\epsilon)\tan(\pi\beta/\epsilon) \tag{3}$$

Eq. (1) can also be further reduced as follows. A was originally expressed as an infinite series,[6]

$$\left(\frac{1}{\beta^2 - (\epsilon/2)^2} + \frac{1}{\beta^2 - (3\epsilon/2)^2} + \cdots\right)$$

which is equal to

$$\frac{1}{2\beta}\left(\frac{1}{\epsilon/2 + \beta} + \frac{1}{3\epsilon/2 + \beta} + \cdots - \frac{1}{\epsilon/2 - \beta} - \frac{1}{3\epsilon/2 - \beta} - \cdots\right).$$

From this and (1) we see that K^{-2} is equal to $-2d(\beta A)/d\beta = (\pi/\epsilon)^2\sec^2(\pi\beta/\epsilon)$. Disregarding the constant factor, the absorption coefficient is given as a function of β/ϵ by $(K\pi/\epsilon)^2 = [\sec^2(\pi\beta/\epsilon)]^{-1} = [1+\tan^2(\pi\beta/\epsilon)]^{-1}$. By (3) this becomes

$$(K\pi/\epsilon)^2 = 1/[1 + 4(E - E_1)^2 w^{-2}] \tag{4}$$

where $w = 2\pi v_{cd}^2/\epsilon$ is the width of the line. Hence the shape of the broadened discrete line is the same in the case of predissociation as in the case of radioactive decay or dissociation by rotation.

Some Properties of the Eigenfunctions and Perturbations

In previous work on the rate of predissociation[7] it has never as yet been possible to follow the wave of dissociating molecules in the same way as in the preceding paper we have followed the wave of departing alpha particles in the case of radioactivity or the dissociating molecules in the case of dissociation by rotation. We are now in a position to do this in the case of predissociation. First we must consider certain properties of the eigenfunctions and perturbations involved.

To get the unperturbed eigenfunctions we first hold the distance, r, between the nuclei fixed, and solve the wave equation for the electrons and the rotation of the nuclei. We can write this equation in the following form

$$(H_\Theta - U_m)\Theta_m = 0 \tag{5}$$

H_Θ is the Hamiltonian[8] with respect to the electrons and the rotation, Θ_m

[6] See (I), Eq. (23), and text just after (23).

[7] Wentzel, Phys. Zeits. **29,** 333 (1928); Kronig, Zeits. f. Physik **50,** 360 (1928); Rice, Phys. Rev. **34,** 1451 (1929).

[8] We use the following system of coordinates. We refer everything to a set of axes which pass through the center of gravity of the *system as a whole*. But in the case of the nuclei we use

is an eigenfunction, U_m an eigenvalue with quantum numbers designated collectively as m. We then set up arbitrarily the following wave equation for a function $F_{m,k}$ of r:

$$d^2F_{m,k}/dr^2 + \kappa^2(E_{m,k} - U_m)F_{m,k} = 0$$
$$\kappa^2 = 8\pi^2M/h^2 \tag{6}$$

where M is the reduced mass, h Planck's constant $E_{m,k}$ an eigenvalue of (6), U_m being the eigenvalue (a function of r) previously found from (5).

---

instead of the six rectangular coordinates, the three coordinates of the center of gravity of the *nuclei*, the two coordinates ϕ and θ giving the direction of the line joining the nuclei, and r. The coordinates of the center of gravity of the two nuclei are counted among the electronic and rotational coordinates. Now if r is so large that interaction between the two atoms forming the molecule is negligible (a case which will later be of importance) then the potential energy function for any given ϕ and θ will depend on $x_1-\alpha rl$, $y_1-\alpha rm$, $z_1-\alpha rn$, $x_2-\alpha rl$, $\cdots$, where l, m, and n are the direction cosines of the line joining the nuclei, α is a constant depending on the relative masses of the two nuclei and on which nucleus the electron in question is (αr being the distance to the given nucleus from the center of gravity of the nuclei), and $x_1y_1z_1x_2, \cdots$, are the coordinates of the electrons, and also on the coordinates of the center of gravity of the *nuclei*, but not otherwise on r than as noted above, provided the coordinates of the system have values at all probable. Therefore the eigen-function Θ_m will depend upon r only in like manner. From this we see that any function of Θ_m and its derivatives when integrated over all coordinates except r, ϕ, θ will very approximately be independent of r. For we can always substitute the variables $x_1-\alpha rl$ for the original variables, and $d(x_1-\alpha rl)$ for dx_1 for constant r. Further integration over ϕ and θ of course leaves the expression independent of r.

Note added in proof: Since Footnote 8 may not be clear it may be well to explain it in more detail. The reason that Θ_m involves r only in the form $x_1-\alpha rl$ when r is large is as follows. A partial differentiation with respect to x_1 is the same as a partial differentiation with respect to $x_1-\alpha rl$. So if in finding our eigenfunction we first hold ϕ and θ fixed as well as r we get an eigenfunction depending only on $x_1-\alpha rl$, etc., and the coordinates of the center of gravity of the nuclei. We call this eigenfunction N and will omit subscripts. For the dependence on ϕ and θ we multiply by a spherical harmonic, Y. The NY form a complete orthogonal set in terms of which the Θ_m can be expanded. The perturbation matrix components are found in much the same way as the others (v_{ss} and v_{st}) in this paper, and are due to the fact that the terms

$$\frac{1}{r^2\sin^2\theta}\frac{\partial}{\partial\theta}\left(\sin\theta\frac{\partial}{\partial\theta}\right)+\frac{1}{r^2\sin^2\theta}\frac{\partial^2}{\partial\phi^2}$$

in the Hamiltonian must operate on the whole expression NY instead of just on Y, since l m, and n which are involved in N depend on ϕ and θ. We have

$$\partial N/\partial\theta = -\alpha r\,(\partial l/\partial\theta)\,\partial N/\partial\,(x_1-\alpha rl),$$

and correspondingly for the second derivative, etc. Wherever the second partial derivatives of N with respect to $x_1-\alpha rl$, etc., occur a factor r^2 cancels the r^{-2} in the perturbation operator, and subsequent integration over x_1, etc., removes the dependence on r in the way discussed near the end of footnote 8. The terms in a perturbation matrix component involving only a first derivative of N will contain r to the minus first power, hence will be small for large r. Therefore, for large r, the coefficients of the of NY's in the expression for Θ_m will not involve r and Θ_m will depend on r only as stated.

Another remark we should like to make is this. The coordinates of the actual distance of an electron to its nucleus (if X_0, etc., are the coordinates of the center of gravity of the nuclei) are $x_1-\alpha rl-X_0$ and the potential energy depends more directly on this quantity than on $x_1-\alpha rl$, but this does not matter for our purposes.

As the unperturbed eigenfunction we use $\Theta_m F_{m,k}/r$. This is the usual procedure for molecules, it being generally conceded that it gives the energy levels of molecules to a good approximation.[9]

The unperturbed eigenfunction obviously obeys the equation:

$$(F_{m,k}/r)(H_\Theta - U_m)\Theta_m - \kappa^{-2}(\Theta_m/r)d^2F_{m,k}/dr^2 - (\Theta_m/r)(E_{m,k} - U_m)F_{m,k} = 0 \quad (7)$$

Since H_Θ and $E_{m,k}$ and U_m contain no derivatives with respect to r we may write

$$H_\Theta(\Theta_m F_{m,k}/r) - \kappa^{-2}(\Theta_m/r)d^2F_{m,k}/d^2r - E_{m,k}(\Theta_m F_{m,k}/r) = 0 \quad (8)$$

The actual Hamiltonian for the system, however, is

$$H = H_\Theta - \kappa^{-2}\left(\frac{\partial^2}{\partial r^2} + \frac{2}{r}\frac{\partial}{\partial r}\right). \quad (9)$$

The actual wave equation, therefore, if it operates on $\Theta_m F_{m,k}/r$ contains the extra terms[10]

$$-\kappa^{-2}\left[(F_{m,k}/r)(\partial^2\Theta_m/\partial r^2) + (2/r)(\partial\Theta_m/\partial r)(dF_{m,k}/dr)\right]. \quad (10)$$

Now to get the real solution of the wave equation we can expand in terms of the $\Theta_m F_{m,k}/r$ which form an orthogonal set.[10] We can treat the $\Theta_m F_{m,k}/r$ as solutions of equations like (8) and use the extra terms in setting up a perturbation matrix, (10) being considered as the result of an operator acting in a special way on $\Theta_m F_{m,k}/r$.

Now in the case of predissociation we expand the perturbed eigenfunction in terms of a $\Theta_m F_{m,k}/r$ belonging to a discrete state,[11] which we will call simply ψ_d, and a set of continuous ones, which belong to another electronic level, and which we designate as $\Theta_c F_{c,i}/r$ where i runs over the set of continuous states. It is to be noted that the continuous property arises from the $F_{c,i}$'s, as Θ_c for all r's is a discrete eigenfunction of (5).

The perturbed eigenfunction, ψ'_n may thus be written as a linear function of the unperturbed, thus:[12]

$$\psi_n' = S_{dn}\psi_d + \Theta_c \textstyle\sum_i S_{in}F_{c,i}/r. \quad (11)$$

For large values of r the first term of (11) gives no appreciable contribution, hence for this case

$$\psi_n' = \Theta_c \textstyle\sum_i S_{in}F_{c,i}/r = \Theta_c F_n'/r \quad (12)$$

[9] Born and Oppenheimer, Ann. d. Physik **84,** 457 (1927).

[10] Perturbations of this nature were first set up in practically this form by Slater, Proc. Nat. Acad. Sci. **13,** 423 (1927), which should be seen for details. Our formulation differs only in that we have put the r part of the eigenfunction in the form $F_{m,k}/r$.

[11] Only one discrete state is to be considered, for we assume as throughout that any other discrete states which interact with the set of continuous states we are interested in are so far away in the term spectrum that their effect may be neglected. Also, of course we consider that the given discrete state interacts with only one set of continuous ones. See (I) pp. 751–2.

[12] (I), Eq. (29) It has been, unfortunately, necessary to change the notation somewhat.

where $F_n' = \sum_i S_{in} F_{c,i}$. The perturbed wave equation may be written

$$(H - E_n')\psi_n' = 0 \tag{13}$$

where E_n' is the corresponding eigenvalue.

This gives, for large r, using (9) and (12)

$$H_\Theta(\Theta_c F_n'/r) - \kappa^{-2}(\Theta_c/r)d^2F_n'/dr^2 - E_n'(\Theta_c F_n'/r) - \kappa^{-2}(F_n'/r)\partial^2\Theta_c/\partial r^2 - \kappa^{-2}(2/r)(\partial\Theta_c/\partial r)(dF_n'/dr) = 0. \tag{14}$$

We now proceed to reduce (14) to an equation in F_n'. To do this we first multiply through by r, then by Θ_c and integrate over all values of the electronic and rotational coordinates. (We call the volume element $d\tau'$.) We remember that $\int\Theta_c H_\Theta \Theta_c d\tau' = U_c$ and note that[13] $2\int\Theta_c(\partial\Theta_c/\partial r)d\tau' = \int(\partial\Theta_c^2/\partial r)d\tau' = (d/dr)\int\Theta_c^2 d\tau' = d1/dr = 0$, since the Θ_m are an orthogonal set. Further we set $\kappa^{-2}\int\Theta_c(\partial^2\Theta_c/\partial r^2)d\tau' = I_c$. Eq. (14) thus becomes

$$d^2F_n'/dr^2 + \kappa^2(E_n' + I_c - U_c)F_n' = 0 \tag{15}$$

For large distances, r, the integral I_c must be independent of r, because for large distances r the molecule is separated into atoms which do not interact appreciably. Θ_c will always be affected the same way by a displacement, dr, regardless of what r is, provided it is large enough (see footnote 8). Eq. (15) shows us that F_n' satisfies a wave equation of the usual type for a problem of one degree of freedom, and hence is a sinusoidal function of the usual type.

Concerning the Perturbation Matrix and the Perturbation Problem

Before we proceed further we must introduce some considerations about the perturbation matrix. The diagonal matrix component for a given continuous state is by (10) remembering that the r part of the volume element is r^2dr (we substitute c for m in (10)—also we write s for k to correspond to the notation used in previous papers—unfortunately we cannot make the correspondence complete, as in this paper it has been necessary to use two subscripts):

$$v_{ss} = -\kappa^{-2}\int_0^\infty F_{c,s}^2 dr \int \Theta_c(\partial^2\Theta_c/\partial r^2)d\tau' - 2\kappa^{-2}\int_0^\infty F_{c,s} r(dF_{c,s}/dr)\,dr \int \Theta_c(\partial\Theta_c/\partial r)d\tau'$$

For the method of setting up this expression Slater's article[10] can be consulted. The last term vanishes since $\int\Theta_c(\partial\Theta_c/\partial r)d\tau' = 0$ as noted above. Remembering the definition of I_c we find

$$v_{ss} = -\int_0^\infty F_{c,s}^2 I_c dr.$$

[13] Kronig, l. c., p. 355.

Now I_c approaches a constant value for large r. Let us call this value I_{c1}. Then $I_c = I_c' + I_{c1}$ where I_c' differs from zero only for small r, and there will be of the order of I_{c1}. From the orthogonal properties of the $F_{c,s}$ we see that

$$v_{ss} = -\int_0^\infty F_{c,s}^2 I_c' dr - I_{c1}. \tag{16}$$

In similar manner, for two different continuous states s and t belonging to the same electronic-rotational state c, we get, remembering the orthogonal properties of the $F_{c,s}$

$$v_{st} = -\int_0^\infty F_{c,s} F_{c,t} I_c' dr.$$

Therefore the contributions to v_{st} come from a range in which r is small, and our previous deductions that v_{st} is small enough to be neglected are valid.[14] The same deductions hold for the first term of the right of (16). Hence, very approximately

$$v_{ss} = -I_{c1} \tag{17}$$

The method of handling cases where v_{ss} is not small has already been indicated.[14] In fact, it consists simply in adding v_{ss} (which is practically independent of s) to the corresponding energy $E_{c,s}$ and proceeding exactly as before. Now suppose instead of (6) we write (for the case $m=c$ and $k=s$)

$$d^2F_{c,s}/dr^2 + \kappa^2(E_{c,s} - U_c - v_{ss})F_{c,s} = 0 \tag{18}$$

Then $E_{c,s}+v_{ss}$ takes the place of $E_{c,s}$ ($m=c$, $k=s$) as eigenvalue in Eq. (6). We could therefore take (18) as the unperturbed equation for the electronic-rotational state c, and otherwise disregard v_{ss}. This is the most convenient way of handling the problem, for the relations between the eigenvalues of (18) and the perturbed eigenvalues E_n' will be just the same as the relation between the eigenvalues of (6) and the E_n' *would have been* were v_{ss} actually 0, and this relationship has been deduced in the previous work.

The relationship is as follows. Between every two eigenvalues of (18) lies a value E_n'. Let us denote as $E_{c,n}$ the eigenvalue of (18) which is just above the particular value E_n'. Then from the original definition[15] of the quantity β which appeared earlier in the paper

$$E_{c,n} - E_n' = \beta + \epsilon/2. \tag{19}$$

The Wave Packet for the Dissociating Molecules

Now it has been shown[16] that the wave packet for the dissociation from the discrete state into the overlying continuum is given by

[14] (I), Appendix I. Correction, Phys. Rev. **34,** 1462.
[15] (I), p. 755.
[16] Rice, Phys. Rev. **34,** 1451 (1929).

$$\psi = \sum_n S_{dn}\psi_n' \exp(-2\pi i E_n' t/h) \tag{20}$$

where $S_{dn}=K/v_{cd}$. For values of r large compared to atomic sizes, we have from (12), (4), and (20)

$$\psi = \frac{\epsilon\Theta_c}{\pi v_{cd} r}\sum_n \frac{F_n' \exp(-2\pi i E_n' t/h)}{[1+4(E_n'-E_1)^2/\omega^2]^{1/2}}. \tag{21}$$

We shall now find the relation between the F_n' and the eigenfunctions $F_{c,s}$ of Eq. (18). The latter may be written in the following form for large r

$$F_{c,s} = \sin\{\kappa(E_{c,s}-U_c-v_{ss})^{1/2}r+\zeta_s\} \tag{22}$$

where ζ_s is a phase constant. The condition that $F_{c,s}=0$ at $r=r_1$ where r_1 is the largest value r can take (the system being in a box) requires

$$\sin\{\kappa(E_{c,s}-U_c-v_{ss})^{1/2}r_1+\zeta_s\} = 0. \tag{23}$$

But the quantum condition in the neighborhood of $r=0$ requires that ζ_s should be the same[17] for all s. At any rate this will be practically true over a range of energies greater than the small breadth, w, of the broadened discrete state It would always be exactly true if U_c were constant for small r, as well as large, (i.e. if (22) actually held for small r), and the smallest value r could take were 0. Now since F_n' obeys the equation (15) we have for large r

$$F_n' = \sin\{\kappa(E_n'-U_c-v_{ss})^{1/2}r+\zeta_n'\} \tag{24}$$

F_n' must be 0 at $r=r_1$ so

$$\sin\{\kappa(E_n'-U_c-v_{ss})^{1/2}r_1+\zeta_n'\} = 0 \tag{25}$$

Eq. (25) will obviously be satisfied if

$$\zeta_n' = \zeta_s+\kappa(E_{c,n}-U_c-v_{ss})^{1/2}r_1-\kappa(E_n'-U_c-v_{ss})^{1/2}r_1 \tag{26}$$

(see Eq. (23) and see also just before Eq. (19) for definition of $E_{c,n}$). Now as the difference between the quantities $(E_{c,n}-U_c-v_{ss})^{1/2}$ and $(E_n'-U_c-v_{ss})^{1/2}$ is very small[18] we may write it as $\frac{1}{2}(E_{c,n}-E_n')\ (E_{c,n}-U_c-v_{ss})^{-1/2}$ or, by (19) as $\frac{1}{2}(\beta+\epsilon/2)\ (E_{c,n}-U_c-v_{ss})^{-1/2}$. Now $\epsilon=2\pi\kappa^{-1}(E_{c,n}-U_c-v_{ss})^{1/2}r_1^{-1}$. So we see that

$$\zeta_n' = \zeta_s+\pi\beta/\epsilon+\pi/2 = \zeta_s+\pi/2+\tan^{-1}\{(E_n'-E_1)\epsilon/\pi v_{cd}^2\}$$
$$= \zeta_s+\pi/2+\tan^{-1}\{2(E_n'-E_1)/w\} \tag{27}$$

by (3) and remembering that $w=2\pi v_{cd}^2/\epsilon$. We thus get an expression for ζ_n' which can be used in evaluating F_n'. Now

$$\sin\{x+\tan^{-1}y\} = (\sin x+y\cos x)\ (1+y^2)^{-1/2}.$$

[17] Or differ only by multiples of π. We can choose that they should be all the same.

[18] It may be made as small as we please by making r_1 large.

Using this formula we get from (24), (27), and (21)

$$\psi = \frac{e(\Theta)}{\pi v_{cd} r} \sum_n \frac{\{\sin\frac{1}{\hbar}\kappa(E_n' - U_c - v_{ss})^{1/2} r + \zeta_s + \pi/2\} + \{2(E_n' - E_1)/w\}\cos\frac{1}{\hbar}\kappa(E_n' - U_c - v_{ss})^{1/2} r + \zeta_s + \pi/2\}\exp(-2\pi i E_n t/\hbar)}{1 + 4(E_n' - E_1)^2/w^2}.$$

The sum over n can be converted to an integral with respect to E_n', and then, except for the factor $1/r$, which merely means that here we have taken all three dimensions of space into account, and so have a spherical wave, the part which involves r has exactly the same form as Eq. (23) of the preceding paper. We thus have a wave of dissociating particles of exactly the same type as before, with exponential decrement with time bearing the same relation to the width of the discrete state, in fact the same in all details. There is thus a complete analogy in results between these two different types of decompositions. Also the part of the wave for small r can be handled as in the preceding paper, since for small r the eigenfunctions will not vary appreciably over a small range of energies.

I wish to express my thanks to Professor Heisenberg for his interest in this work, and helpful discussion.

CONCERNING THE ABSORPTION METHOD OF INVESTIGATING β-PARTICLES OF HIGH ENERGY: THE MAXIMUM ENERGY OF THE PRIMARY β-PARTICLES OF MESOTHORIUM 2.

By N. Feather*

Physical Laboratory, Johns Hopkins University, Baltimore

(Received April 30, 1930)

Abstract

For the primary β-particles of radium C, radium E and mesothorium 2 the maximum effective mass range, R, has been determined in paper and aluminum by the method of Chalmers. In the two former cases the maximum energy of the particles, E, is known, and these results and earlier data lead to the relation

$$R=0.511E-0.091$$

for $E>0.7$. Here R is measured in grams/cm² and E in millions of electron volts. For mesothorium 2, $R=0.955\pm0.015$ gm/cm², so that the maximum energy of the particles is $2.05\pm0.03\times10^6$ electron volts. Reasons are advanced for employing the empirical relation above quoted rather than results obtained with particles of a single velocity, as in the experiments of Varder and Madgwick, in the interpretation of absorption measurements made upon primary β-particles.

Introduction

THE earliest recognition of the emission of two distinct types of corpuscular radiation from radioactive material followed immediately upon the adoption of absorption methods of investigation; continuously throughout the development of the subject these methods have been applied afresh in the study of the radiations from the β-ray bodies. Beyond a general qualitative analysis, however, they provide little information which admits of easy interpretation. We now know, for example, that exponential absorption reflects no fundamental property of the different natural radiations—and, in consequence, exponential absorption coefficients have lost much of their significance. Moreover most of the early work was directed toward their determination.

And yet, despite this indefiniteness, absorption measurements do provide, simply and without ambiguity, the maximum effective range, in the medium employed, of the particles submitted to analysis. Now it is of considerable interest to determine the maximum energy appearing as kinetic energy in each of the cases of β-particle disintegration and it is evident that absorption measurements make this determination possible when the necessary data relating effective range with the energy of the particle are available. Such data in fact exist, and already the method has been applied to the β-ray bodies of the active deposit of thorium by Chalmers[1] and to those of the active

* Fellow of Trinity College, Cambridge; Associate in Physics, Johns Hopkins University.

[1] Chalmers, Proc. Camb. Phil. Soc. **25,** 331 (1929).

deposit of actinium by Sargent.[2] But the data in question, upon which the interpretation of these experiments depends, in themselves are ambiguous: the ranges in aluminum given by Madgwick[3] are more than 10 percent greater than the corresponding ranges as determined by Varder.[4]

Eddy[5] has recently made a more detailed study of the absorption of β-particles of somewhat less energy than those with which we are here chiefly concerned and has concluded that the discrepancies between the results of Varder and Madgwick are to a large extent due to the different arrangements of ionization chamber which these authors employed. This conclusion, coupled with the fact that the conditions obtaining in absorption measurements on the complete natural radiations are quite different from those effective in the two investigations under discussion, makes a review of the precise relevance of the data of Varder and Madgwick to the present problem of considerable interest. The results of each investigator show that the effective range is a linear function of the energy of the particle for values of the energy greater than 0.65 million electron volts, or formally

$$R = aE + b \tag{1}$$

for $E > 0.65$ (million electron volts). Varder's data for aluminum are best represented by $a = 0.469$, $b = -0.071$, R being expressed in grams/cm^2; Madgwick's figures by $a = 0.552$, $b = -0.097$. It is to be expected that a similar relation must apply to the conditions of experiment in the primary β-particle case also, but it should be pointed out that the relation in question no longer connects the effective range with the energy for particles initially homogeneous in velocity, but rather it relates the maximum effective range with the maximum energy when particles of continuously varying energy are present. It is very probable that this circumstance makes the determination of the effective range more independent of the conditions than it appears to be in the case of particles of a single velocity,[6] but obviously it cannot result otherwise than that the maximum effective range which is measured should be determined by the highest energy particles present in the beam. Nevertheless there is no simple reason for believing this range to be precisely the same as the effective range determined by extrapolation from the absorption curve taken under any arbitrary conditions with β-particles of that unique limiting velocity. For the purposes of interpretation of experiments performed upon the full natural β-radiation from different substances we ought in preference to employ a calibration curve determined under closely comparable conditions. Such a curve may be obtained by applying the absorption method to the determination of the maximum effective range of the β-particles from bodies which have already been studied in greater detail by the method of magnetic spectroscopy.

[2] Sargent, Proc. Camb. Phil. Soc. **25,** 514 (1929).

[3] Madgwick, Proc. Camb. Phil. Soc. **23,** 970 (1927).

[4] Varder, Phil. Mag. **29,** 725 (1915).

[5] Eddy, Proc. Camb. Phil. Soc. **25,** 50 (1929).

[6] A necessary condition for the truth of this statement is that the continuous spectrum of velocities should have a sharply defined upper limit. This seems to be the case: cf. Chalmers, reference 1, p. 337, Gurney, reference 9, p. 549.

The experiments of Chalmers[1] and Gurney[7] provide the first point on such a curve. Chalmers fixed the maximum effective range of the β-particles of thorium C at 0.98 gm/cm^2 of aluminum whilst Gurney showed that the maximum energy of the particles was 2.18×10^6 electron volts. The first portion of the present work is devoted to the determination of the maximum effective range of the radium E β-particles and of those of radium C. The limiting energies to which these ranges correspond are known from the measurements of Madgwick,[8] and Gurney,[9] respectively. Then two more points are added to the curve and the most probable values of the constants a and b of Eq. (1) may be determined.

The second part of the work consists in a similar absorption experiment upon the primary β-particles of mesothorium 2 and the newly determined range-energy relation makes possible its interpretation.

General Experimental Arrangement

The β-ray electroscope used in all the measurements consisted of a gold leaf system suspended in the usual manner at the center of a cubical aluminum case of 11 cm edge and 3 mm thickness of wall. In the base of the electroscope a hole 7.5 cm square was closed with aluminum foil weighing 6.5 mg/cm^2. The electroscope was supported on a wooden stand with a space of 24 cm between its base and the surface of the bench. A wooden slide could be inserted in various positions below the base of the instrument. This slide carried both the active material and the absorbing foils. The former was placed at the bottom of a shallow cylindrical hole (depth 1.1 cm, diameter 3.2 cm) cut in the slide and the latter, in the form of sheets 5 cm square, were placed upon the slide so as to cover the hole symmetrically. In most cases the slide was inserted in the highest position, and in these circumstances the source was about 3.5 cm below the base of the electroscope. In all the experiments the decay of the source and the varying density of the air in the electroscope were corrected for by making frequent measurements under standard conditions of absorption. In general the mean of ten independent observations was obtained for each point plotted on an absorption curve. Adopting this routine it was not found necessary to employ a magnetic field to separate β- and γ- ray effects, even in the case of radium C where the latter effect is very pronounced, and indeed it is the writer's opinion that the avoidance of such a method is much to be preferred whenever that is possible, for it is difficult to estimate the effect of the stray magnetic field on the γ-ray ionization in the electroscope in any of the simpler experimental arrangements that have been used.

Experimental Results. Part I

Radium E. Madgwick[8] has determined the upper limit of the continuous spectrum of the β-particles of radium E as 1.07×10^6 electron volts energy. This is the datum with which our range measurements are to be combined.

[7] Gurney, Proc. Roy. Soc. **112A,** 380 (1926).
[8] Madgwick, Proc. Camb. Phil. Soc. **23,** 982 (1927).
[9] Gurney, Proc. Roy. Soc. **109A,** 540 (1925).

Absorption methods have, in fact, already been applied to the determination of the range in this case. In 1912 Gray [10] first pointed out[11] the phenomenon of an end point to the β-particle absorption with a source of radium E. His measurements lead to an effective mass range between 0.45 and 0.49 gm/cm^2 of paper. Douglas[12] extended the measurements to other absorbing media and gave 0.474 and 0.460 gm/cm^2 for the effective ranges in paper and aluminum respectively. But the sources employed were weak and the logarithmic method of extrapolation was used to fix the range. It was thought worthwhile to repeat the determinations[13] with a stronger source employing the method of simple extrapolation of Chalmers. This method has been adopted as standard throughout.

The results are shown in Fig. 1. They refer to a source of radium D, E and F in equilibrium[14] deposited by evaporation on a small platinum dish. The

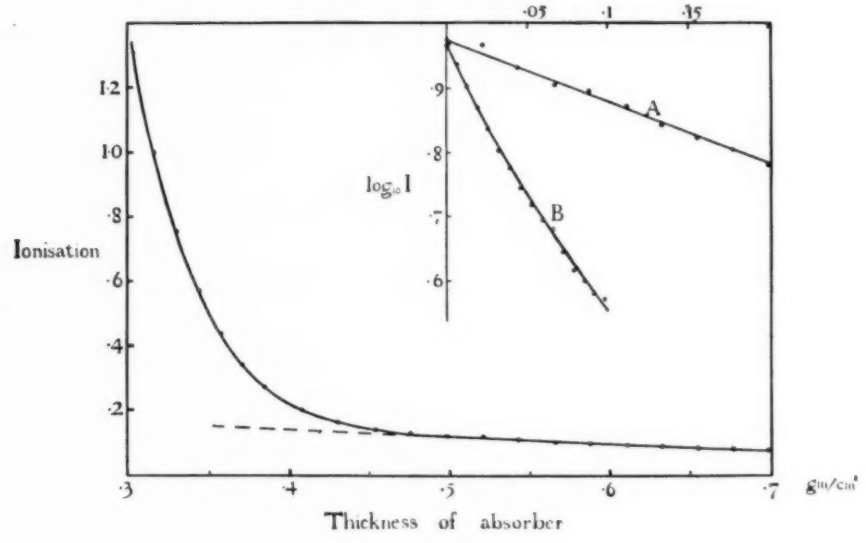

Fig. 1. Radium E.

weight of deposit, more than 1 cm^2 in extent, was a few milligrams only. Unwhitened paper was used as absorber and the maximum effective mass range in this medium may be taken as 0.475 ± 0.005 gm/cm^2.

A simple experiment was also made upon the radiation unabsorbed by this thickness of material. The source was covered with sheets of paper repre-

[10] Gray, Proc. Roy. Soc. **87A,** 487 (1912); Trans. Roy. Soc. Canada **16 III,** 125 (1922).

[11] The end point is clearly shown in absorption curves published by Schmidt in 1907 (Phys. Zeits. **8,** 362 (1907)).

[12] Douglas, Trans. Roy. Soc. Canada, **16 III,** 113 (1922).

[13] Absorption measurements by Aston (Proc. Camb. Phil. Soc. **23,** 935, (1927)) and by Fournier and Guillot (Comptes rendus **189,** 1079 (1929)) also have reference to a region including the β-particle end point but, being concerned chiefly with the weak γ-radiation, permit of no accurate range values being drawn from them.

[14] The writer wishes to thank Dr. C. F. Burnam of the Kelly Hospital, Baltimore, for a supply of old radon tubes from which this material was extracted.

senting (together with the air gap and the base of the electroscope) 0.499 gm/cm^2 of absorber. Aluminum foils were then added and the further progress of the absorption followed. The curve *B*, Fig. 1, exhibits these results, the logarithm of the corrected ionization being plotted against the foil thickness. Curve *A* represents the parallel case where the absorption was in paper throughout. A mass absorption coefficient of 2.3 cm^2/gm is a sufficiently good approximation here; the initial absorption in aluminum, however, is roughly five times as great, for equal mass of absorber. This is what we should expect if the absorption were chiefly photoelectric, and the numerical values also suggest that the effective radiation is for the most part the very soft component, probably the *LX*-radiation of radium D, for which a mass absorption coefficient of 16.5 cm^2/gm in aluminum is accepted as correct.[15] The smaller value (11.3 cm^2/gm) found with the present arrangement is to be attributed largely to the fact that the first 0.5 gm/cm^2 of paper has already reduced this soft component to about a quarter of its original intensity, so that the influence of the less intense though harder components is no longer negligible. It is of interest to record that the last point on the curve *B*, representing the smallest ionization current involved in this series of measurements, yet represents a current about forty times as great as the natural leak of the electroscope effective at the time.

Radium C. The primary β-particles of this body comprise a continuous spectrum of energies having a sharp upper limit at 3.15×10^6 electron volts (Gurney[9]). On the other hand no data have hitherto been available concerning the maximum effective range of these particles as determined in the present type of experiment. The problem here presented is considerably more difficult than in the case of radium E, on account of the very great intensity of the γ-radiation from radium C and of the rapid decay of this body. The latter difficulty may be overcome by using a radon tube as a β-particle source, although this procedure increases the γ-ray effect, by adding the γ-rays of radium B to those of its subsequent product. Moreover the radiation thus added is in general much less penetrating than the latter, and it is the softer components of the radiation which constitute the greater source of error. An attempt was made to minimise this effect in the arrangement finally adopted.

A small glass bulb, about 3 mm in diameter, originally containing about 800 equivalent milligrams of radon was employed as the source of β-particles at the stage when its activity had fallen to a few thousandths of its initial value.[16] In this way the points of Fig. 2 were obtained. The absorbing material consisted of aluminum to the extent of 1.012 gm/cm^2 placed directly over the source, with sheets of paper for the remainder. By using the aluminum it was hoped to cut down the softer components of the γ-rays to reasonable proportions whilst the use of paper for the rest of the absorption was governed by considerations of ease of manipulation and of the sharper type of absorption

[15] Rutherford and Richardson, Phil. Mag. **26,** 324 (1913). Curie and Fournier, Comptes rendus **176,** 1301 (1923).

[16] For this material also the writer is indebted to Dr. Burnam.

limit thereby obtained. Moreover Chalmers failed to find any appreciable difference between the mass ranges of the thorium C β-particles in paper and aluminum. The equivalence of these materials in this respect has been assumed in the present experiments. The walls of the radon tube were not negligibly thin and an estimate of their thickness was made in two ways, by direct weighing, and by a subsequent absorption experiment after the lapse of a few weeks, when the radium E β-particles were responsible for the greater proportion of the ionization as measured through small thicknesses.[17] The difference

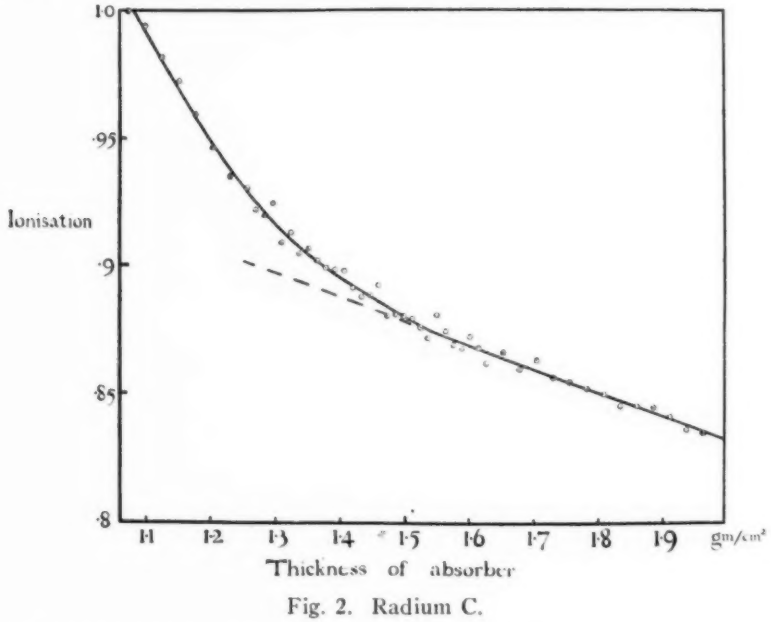

Fig. 2. Radium C.

between the apparent maximum effective range of these particles as determined with this source and in the direct experiments on radium E described above was attributed to absorption in the glass walls of the bulb. Both methods suggested an equivalent thickness of glass of 0.03 gm/cm^2. So corrected the maximum effective mass range of the primary β-particles of radium C in aluminum or paper may be given as 1.54 ± 0.02 gm/cm^2, as indicated in the figure.

The range-energy relation. The data which are to be employed in constructing our calibration curve are given in Table I.

TABLE I. *Data used in constructing calibration curve.*

Source of β particles	Maximum energy electron volts $\times 10^{-6}$	Maximum effective mass range gm/cm^2
RaE	1.07	0.475
ThC	2.18	0.98
RaC	3.15	1.54

[17] The final decay of the emanation originally contained in the bulb is responsible for the production of about 0.3 equivalent milligrams of radium D, E, and F.

Within experimental error this material is consistent with a linear relation such as that given by Eq. (1) and is best represented by the straight line

$$R = 0.511E - 0.091 \qquad (2)$$

which, by analogy with the relations of Varder and Madgwick, may probably be regarded as valid for values of E greater than 0.7 (million electron volts). It may be remarked that the present straight line occupies a position intermediate between those of Varder and Madgwick—and it may be pointed out that the results of Eddy occupy a similar position in the region of smaller energies where the curve is no longer linear. But the intention of any very close comparison between the present results and results having reference to particles of a single velocity has already been disclaimed, so that no primary importance is attached to this apparent agreement. Moreover, not only was the work of Eddy concerned with particles of a single velocity, but it was carried out by the method of electrical counting, providing a further reason for caution in its comparison with the results of ionization measurements.

Experimental Results. Part II

Mesothorium 2. The β-particles of mesothorium 2 have been studied by Yovanovitch and d'Espine[18] by the direct deviation method of magnetic spectroscopy. These authors suggest that the high energy limit of the continuous spectrum occurs in the region of 1.6 million electron volts energy. It is not unreasonable to suppose, from a knowledge of the general characteristics of the method, however, that this represents merely a lower limit to the maximum energy of the particles.[19]

The difficulties in the way of absortion measurements with mesothorium 2 are similar to those obtaining with radium C: there are γ-rays of considerable intensity and the pure substance is of fairly rapid decay. The broad scheme of the experiments, therefore, was first to determine an absorption curve in full detail with a source of mesothorium 1 and 2 in equilibrium and then to make confirmatory tests with a small number of selected thicknesses of absorber and a source of pure mesothorium 2, in order to be certain that the main features of the former curve, in the region of the β-particle end point at least, were due to the latter body alone.

A solution of mesothorium 1, freed from radiothorium by repeated precipitation with iron, and from a large fraction of the ammonium chloride which accumulates as a result of such operations, was allowed to stand so that the thorium X should decay. Being neutralized the solution was electrolysed with platinum anode and silver cathode at a temperature of about 90°C.[20]

[18] Yovanovitch and d'Espine, J. de Physique. **8,** 276 (1927).

[19] For a constant value of the field the dispersion decreases rapidly as the energy of the particles increases, and this, together with the peculiarities of photographic registration, must necessarily introduce considerable distortion. Both in the case of the primary β-particles of radium C and for those of radium E this method has given too low a value for the maximum energy (2.74×10^6 electron volts in the former case and 0.94×10^6 in the latter).

[20] Meitner, Phys. Zeits. **12,** 1097 (1911).

Mesothorium 1 and 2 were obtained together, the latter in about 90 percent of its equilibrium amount. The silver plate (about 2 cm² in area), carrying the deposit on one surface only, was enclosed in an airtight container to prevent the diffusion of emanation. A thin sheet of mica was employed for the upper face of the vessel which fitted neatly in the whole cut in the electroscope slide already described. Since originally the mesothorium was extracted directly from monazite, radium was known to be present as "impurity." But the duration of the previous heat treatment of the solution, and of the electrolysis, was such that immediately after its preparation the β-particle source could be regarded as free from all contamination except by radium element itself. Provided, therefore, that measurements were carried out within the

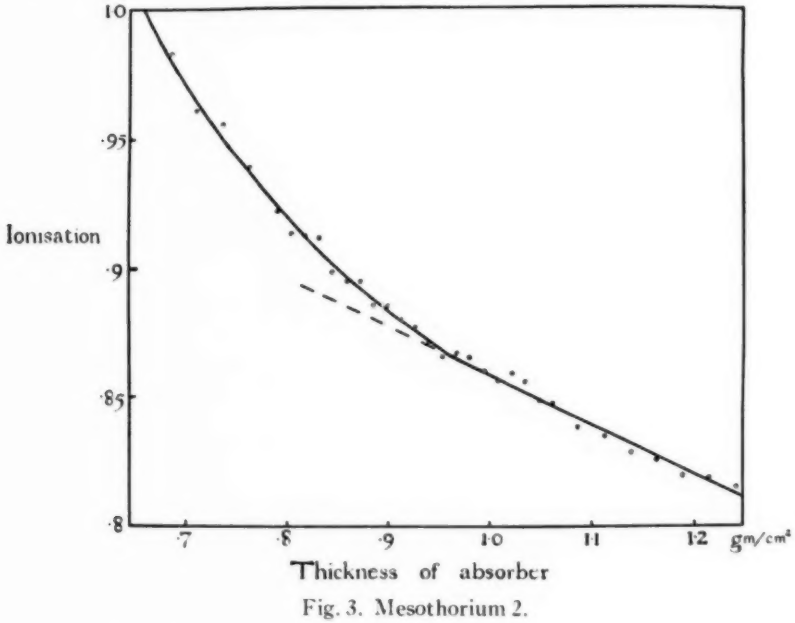

Fig. 3. Mesothorium 2.

first 24 hours after the source was prepared they were unlikely to be seriously affected by the growing β-particle activity arising from the active deposit of radium.

The results of measurements with this source are shown in Fig. 3, the last measurement being completed 22 1/2 hours after the source was obtained on the plate. As in the experiment on radium C roughly the first two-thirds of the absorption was in aluminum—a thickness of 0.646 gm/cm² of this metal being succeeded by sheets of paper. In an attempt to detect any possible effect of the gradual building up of radium C in the source during the period of observation measurements were made in the following order, namely through

44, 40, ... ,0,
11, 15, ... ,27,
2, 6, ... ,42,
29, 25, ... ,13

sheets of paper, in turn. This sequence was, of course, interrupted periodically to permit of measurements with a standard absorber in place. It will be seen from the figure that no such effect as was sought was observed.[21] In this way the β-particle end point was fixed at 0.955 ± 0.015 gm/cm^2 and it only remained to confirm its identification with the maximum effective mass range of the primary β-particles of mesothorium 2 by an independent experiment.

A source of mesothorium 2 was prepared in the usual manner by precipitation with a trace of iron from a solution containing mesothorium 1 and 2 in equilibrium. Three thicknesses of absorber, corresponding respectively to the first and last points in Fig. 3 and to the point nearest the absorption discontinuity, were chosen and two sets of measurements made, separated in time by about 3 1/2 hours. Table II contains the results.

TABLE II. Results

Thickness of absorber	Relative ionizations	
gm/cm^2	(1)	(2)
0.660	1.000	1.000
0.952	0.867	0.870
1.241	0.825	0.824

The decay of activity, corresponding to a half period of 6.4 hours, showed that the source was sufficiently pure for the test to be conclusive, and the figures given, when compared with the values 1.000, 0.868, 0.812 read directly from the curve, establish the identity which was in question. The exact agreement in the second instance is probably fortuitous but it is obvious first of all that no appreciable amount of unrecognized radioactive impurity was present in the orginal source, and secondly that any γ-rays emitted by mesothorium 1 were of little or no consequence in the measurements made with that source.

Inserting the value 0.955 gm/cm^2 for R in Eq. (2) we have $E = 2.05$ million electron volts and consequently, as the result of these experiments, may adopt this as the most probable value for the maximum energy of the primary β-particles of mesothorium 2. As was pointed out earlier in the discussion, a value considerably in excess of that given by Yovanovitch and d'Espine was almost to be expected.

Finally, in addition to acknowledgements already made, the writer wishes to record his appreciation of help received from the Rumford Fund of the American Academy of Arts and Sciences, a grant from which made possible the purchase of the mesothorium employed in these researches.

[21] Further measurements were made on the source at three different absorptions within the range of the figure after 4 and 10 days, respectively. Also a rough absorption curve extending over this range was determined for a source of radium B+C in equilibrium. All the measurements could be explained simply by assuming that 8.7 percent of the ionization through 0.66 gm/cm^2 of aluminum at the end of 4 days, and 17.0 percent at the end of 10 days, was due to the β and γ-rays of radium B+C which had grown in the interim.

THE MOTION OF ELECTRONS IN CARBON MONOXIDE

By H. B. Wahlin
Department of Physics, University of Wisconsin

(Received May 5, 1930)

Abstract

With the same data as were presented in an earlier paper it is shown that K. T. Compton's theory of electron mobilities holds within the limits of experimental error for high pressures and low fields, provided it is assumed that the energy loss of the electrons on impact with the molecules is greater than that due to momentum transfer.

The electron mean free path in CO has been calculated and, when the electrons are in thermal equilibrium with the gas, is 0.069 cm at a pressure of 1 mm.

I

IN AN earlier paper[1] it was shown that the mobility of electrons in CO can be represented as a function of the field strength and the pressure by an equation of the form

$$u = \frac{a}{P(B + x/p)^{1/2}}$$

with a high degree of accuracy. It is only for low fields that a systematic deviation from this equation appears.

Later, K. T. Compton[2] showed that from theoretical considerations, the mobility should be given by

$$u = \frac{0.815e\lambda}{m^{1/2}[\alpha T + (\alpha^2 T^2 + 1.76\lambda^2 e^2 x^2/f)^{1/2}]^{1/2}}. \qquad (1)$$

That this equation is applicable to the mobility of electrons in H_2 and He (at least for low fields and high pressures) has been shown by the writer.[3]

It was in order to test the validity of the Compton equation when applied to CO that the calculations submitted herewith were undertaken. The data are the same as were used in the earlier paper.

The method used in obtaining the data was the Rutherford alternating potential one for determining mobilities and has been described in detail earlier.

The Compton equation may be written in the form

$$u = \frac{a}{[1 + (1 + Bx^2)^{1/2}]^{1/2}}.$$

[1] H. B. Wahlin, Phys. Rev. **21**, 517 (1923).
[2] K. T. Compton, Phys. Rev. **22**, 333 (1923).
[3] H. B. Wahlin, Phys. Rev. **27**, 558 (1926).

If the electron is moving under the action of a sine wave alternating field the velocity in the direction of the field at any instant is, according to this equation,

$$\frac{dy}{dt} = \frac{aX \sin 2\pi nt}{[1 + (1 + BX^2 \sin^2 2\pi nt)^{1/2}]^{1/2}}$$

Imposing the condition that during one half cycle of the alternating field the electrons shall travel a distance d (the distance between the plates in the Rutherford method) we get on reducing the elliptic integral obtained and solving for n

$$n = \frac{a(2r)^{1/2}}{\pi d(B)^{1/2}} 2[E(k,\phi) - F(k,\phi)] \tag{2}$$

where $r = (BX^2 + 1)^{1/2}$, $k = \left(\frac{r+1}{2r}\right)^{1/2}$, $\phi = \sin^{-1}\left(\frac{r-1}{r+1}\right)^{1/2}$

and X is the peak value of the field corresponding to the voltage intercept of the mobility curves.

This equation may be verified directly with the data at hand.

Placing $A = 16{,}800$ and $B = 0.005$ it is seen that at a pressure of 722 mm good agreement between the experimental results and the theoretical curve

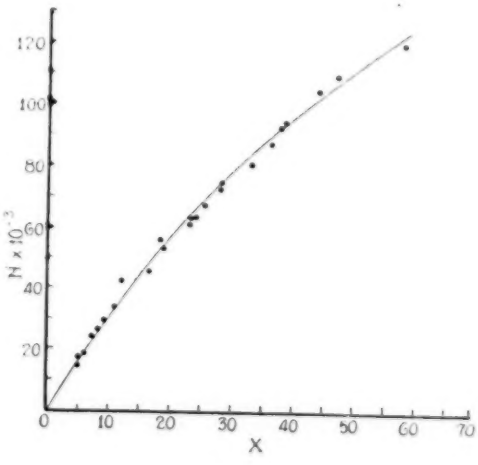

Fig. 1.

calculated from Eq. (2) is obtained. (Fig. 1). Here the points are experimental and show the relation between the frequency and the effective value of the field.

Fig. 2 shows the comparison between theory and experiment for a pressure of 500 mm. Here A and B have been corrected for the change in λ with pressure, assuming that λ varies inversely as the pressure.

At a pressure of 250 mm the agreement is good for low fields (Fig. 3). In fields above 35 volts/cm a systematic deviation appears—*viz.* the mobility

decreases more rapidly with field strength than is to be expected on the basis of the theory. This deviation is best ascribed to the beginning of the Ramsauer effect.

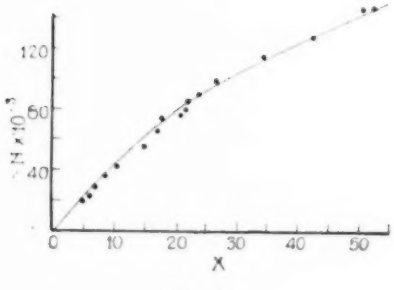

Fig. 2.

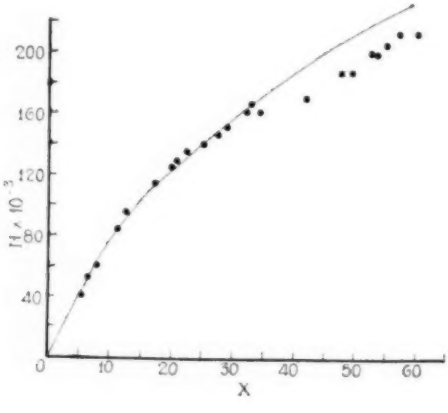

Fig. 3.

A comparison of theory and experiment may also be made as follows. If it is assumed that the mobility is independent of the field strength, it is possible to calculate the mobility from the relation

$$k = \pi n d^2 / 2^{1/2} V$$

where n is the frequency, d the distance between the plates, and V the r.m.s. value of the alternating voltage of the intercept of the mobility curves.

The value calculated from this equation for the case of electrons will be an average mobility defined so that the average velocity with a mobility k shall be the same as the average velocity determined from Compton's equation. This may be written

$$\int_0^d dy = \int_0^{1/2n} kX \sin 2\pi ntdt = \int_0^{1/2n} \frac{aX \sin 2\pi ntdt}{[1 + (1 + BX^2 \sin^2 2nt)^{1/2}]^{1/2}}.$$

Integrating and solving for k we get

$$k = \frac{a(2r)^{1/2}}{X(B)^{1/2}} [2E(k,\phi) - F(k,\phi)].$$

Here r, k, ϕ and X have the same significance as in Eq. 2 above.

Fig. 4 shows the relation between the theoretical and experimental values of k at a pressure of 722 mm. In plotting the curve the same values of A and B were used as in the calculation of n.

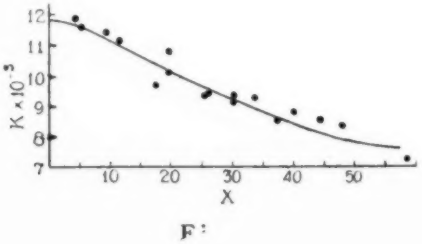

F:

II

The limiting mobility for zero field will be given by $u = A/2^{152}$. Substituting the known value of A in this equation, the limiting mobility found is 11,900 cm/sec/volt/cm, at a pressure of 722 mm.

From this value of u the electron free path may be calculated using the theoretical relation $u = 0.75e\lambda/m\bar{c}$. The value thus calculated, placing $\bar{c} = 1.065 \times 10^7$ cm/sec (the thermal electron velocity at room temperature), is 0.069 cm at a pressure of 1 mm.

This value is 1.75 times the value calculated from the kinetic theory molecular free path, assuming the electron free path to be $4(2)^{\frac{1}{2}}$ the molecular one. It is also 1.68 times the electron free path in H_2, whereas the kinetic theory prediction is that it should be less. It seems impossible therefore to apply molecular free path data to the calculation of electron free paths. This is also borne out by the results on N_2[4] in which it was found that the electron free path is 2.55 times the predicted value.

III

The value of B used in the calculations above is much smaller than the value calculated on the assumption that the impacts of the electrons with the molecules are elastic. For this case the expression for B becomes

$$B = \frac{1.76\lambda^2 e^2 M}{2\alpha^2 T^2 m}$$

assuming $f = 2m/M$ where m is the electronic and M the molecular mass. This expression gives

$$B = 0.278$$

whereas the value found above is 0.005.

On the basis of Compton's theory one must conclude one of two things: Either the electrons do not reach their terminal thermal energy under the action of a sine wave field, or the fraction of its energy that an electron loses on impact with a CO molecule is greater than it would be if the loss were due to momentum transfer only. In the case of N_2 and H_2 referred to above, it was shown that any error due to a non-terminal state is negligible, and it seems reasonable to conclude that this will also be the case for CO. The second alternative is therefore the more probable.

[4] H. B. Wahlin, Phys. Rev. **23,** 169 (1924).

THE MAGNETIC SUSCEPTIBILITY OF GASES I. PRESSURE DEPENDENCE

By Francis Bitter*
Norman Bridge Laboratory of Physics, Pasadena, California

(Received April 28, 1930)

Abstract

A method is described for measuring the magnetic susceptibility of gases which has certain advantages over those used by previous observers. With such an apparatus, it is found that the volume susceptibility of CO_2, N_2 and H_2 is proportional to the pressure. Deviations from proportionality of the type observed by Glaser are found in the above gases upon introducing water vapor as an impurity in amounts probably less than a few hundredths of a percent.

IN ATTEMPTING to interpret the results of magnetic observations on matter, it is difficult to determine what effects are due to the molecules themselves, and what due to their interaction with each other. Because of this, results obtained with gases may be interpreted with most confidence, since in this case, isolated molecules without interaction are most nearly approximated. The fundamental quantity to be observed is K, the volume susceptibility, which measures the average induced moment per cc. Classical mechanics and quantum theory agree in predicting

$$K = \left(\frac{a}{T} + b\right)\frac{p}{T} \tag{1}$$

or

$$K = cp. \tag{2}$$

a is a positive constant which is zero if there is no permanent magnetic moment in the molecule, and b is a negative[1] constant which measures the distribution of electric charge in the molecule. The experiments described below were undertaken to check Eq. (2). In a future communication I hope to take up the absolute values of the constants a and b, and their interpretation for various gases.

The proportionality between the volume susceptibility and the pressure must be established before any interpretation of the constants a and b can be undertaken as it is equivalent to the statement that the molecules in a gas do behave as isolated units with only thermal interactions to establish thermodynamic equilibrium. The first attempt to verify Eq. (2) experimentally was made by Glaser[2,3,4] who found that it held only for O_2 and atomic

* National Research Fellow.

[1] b may, for polyatomic molecules, be positive, though no such case has actually been observed or even suggested. See, for instance, J. H. Van Vleck, Phys. Rev. **31,** 597 (1928).

[2] A. Glaser, Ann. d. Physik **75,** 459 (1924).

[3] A. Glaser, Ann. d. Physik **78,** 641 (1925–6).

[4] A. Glaser, Ann. d. Physik **1,** 814 (1929).

diamagnetic gases, but that for CO_2, CO, N_2 and H_2 certain characteristic deviations occurred. Subsequently, Lehrer,[5] Hammar,[6] and Vaidyanathan[7,8] repeated this work, and found no anomalies of the type reported by Glaser. Hammar in a further paper[9] suggested that the effect observed by Glaser might be due to the absorption of water vapor on the test body by means of which measurements are carried out, as he once found the effect, but made it disappear again by renewing the P_2O_5 in his cleaning train. Further Buchner[10] showed that small temperature differences, if present, in the various parts of Glaser's measuring apparatus, might account for the observed phenomenon. Thereupon, Glaser in a brilliant series of papers[11,12,13] succeeded in showing that by introducing small amounts (1%) of O_2 in CO_2, he could produce a mixture which satisfied Eq. (2), but that with greater concentrations of O_2 anomalies reappeared; that in all probability adsorbed water vapor on his test body could not produce the effects observed; and that thermal disturbances were not present in his apparatus in a sufficient degree to influence his observations. From these results he deduces, and this is the weak point in his arguments, that other observers *had* O_2 as an impurity in their gases in just sufficient amounts (1% for CO_2) to hide the anomaly.

According to these papers, the relevant factors are small impurities of O_2 and H_2O. For the sake of completeness, let us add molecular orientation, which was first considered by Glaser himself, and two further ones whose influence has been tacitly neglected: excited states and ions. Molecular orientation in fields of the order of magnitude of those at present in use is not understandable[14] on the basis of our present conception of the laws governing the behavior of molecules in a magnetic field, and may therefore be dismissed until the other possibilities are definitely disposed of. The presence of any radiation in the apparatus other than black-body radiation corresponding to the temperature of the gas under observation would destroy thermodynamic equilibrium and invalidate Eq. (2). As a matter of fact, excess of incoming radiation would produce an effect of the type observed by Glaser, though as nearly as one can calculate, it should be much smaller. Exact computations are impossible, as the electrical constitution of excited states is unknown. Actual observation on N_2 under various conditions of illumination ranging from almost complete darkness to very intense illumination of the gas between the pole pieces of the magnet gave no effect of the order of magnitude of that observed by Glaser. Further, the presence of 2 mg of radium within a few cm of the test body (see diagram of the apparatus in Fig. 1) gave no

[5] E. Lehrer, Ann. d. Physik **81,** 229 (1926).
[6] G. W. Hammar, Proc. Nat. Acad. Sci. **12,** 594 (1926).
[7] V. I. Vaidyanathan, Ind. Journal Phys. **1,** 183 (1926).
[8] V. I. Vaidyanathan, Phil. Mag. **5,** 380 (1928).
[9] G. W. Hammar, Proc. Nat. Acad. Sci. **12,** 597 (1926).
[10] H. Buchner, Ann. d. Physik **1,** 40 (1929).
[11] A. Glaser, Ann. d. Physik **2,** 233 (1929).
[12] A. Glaser, Ann. d. Physik **3,** 1119 (1929).
[13] A. Glaser, Ann. d. Physik **4,** 82 (1930).
[14] F. Bitter, Phys. Zeits. **30,** 501 (1929).

change in the deflections of the order of magnitude of those to be expected if the Glaser effect is to be explained on the basis of the anomalous [illegible] of ions which are, of course, always present unless very elaborate precautions are taken.

Experimentally, then, the problem reduces itself to the determination of the effect of small amounts of impurities. To settle this question definitely for all possible impurities in varying amounts in all the gases on which observations have been made would require a very long investigation. In the following, I have gone only part way. The results obtained experimentally are that,

(1) CO_2, N_2 and H_2 in which certainly not more than traces of H_2O and O_2 are present obey Eq. (2).

(2) A mixture of CO_2 and about 11% O_2 when dried as efficiently as possible, obeys Eq. (2).

(3) Co_2, N_2 and H_2, when contaminated by small amounts of H_2O (probably less than a few hundredths of a percent) do not obey Eq. (2), but give deviations of the type observed by Glaser.

The proof of these statements is contained in the rest of this report. Assuming their correctness, the present state of our knowledge concerning the applicability of Eq. (2) is summed up on the following statements.

Both linearity and departure from linearity have been observed in pressure susceptibility curves on samples CO_2, N_2 and H_2 considered pure by the observers. The one observer, Glaser, who consistently obtains departure from linearity finds that linearity can be produced in CO_2 by critical amounts of O_2 impurity. He assumes that a similar effect exists for N_2 and H_2 and assumes that the samples used by other observers are contaminated with just this critical amount of impurity. Presumably, this critical amount of impurity would vary from gas to gas. The above assumption is possibly applicable to some observations, but it is certainly very improbable that it applies to all. It is certainly not applicable to the observations reported in this paper, since spectroscopic evidence is given that the purifying train removed all observable traces of O_2 from N_2. Further, since the purifying train removed O_2 from N_2 satisfactorily, it probably did so equally well for H_2 and CO_2. Further, since a mixture consisting of CO_2 and 11% of O_2 showed linearity, it is impossible to contend that this linearity was due to a 1% O_2 contamination. This much of the evidence seems straightforward, and disposes of the assumption that linearity in all observations is due to a critical O_2 impurity. The interpretation of the remainder of the evidence, that the addition of water vapor to the above gases gives anomalous effects, is not so clear. It shows merely that Glaser's results may be due to water vapor. But it is also conceivable that other substances might have a similar effect, and it is quite possible though highly improbable, that Glaser's results are due to some still undetermined and unsuspected cause. Taking the evidence all in all, however the following conclusions seem most plausible: that dry gases and gas mixtures obey Eq. (2); and that Glaser's anomalies are due to the presence of water vapor in his measuring apparatus.

should be noticed that the mechanism by which H_2O influences the magnetic behavior of gases is by no means specified; it need not be adsorption in the test body, and in the light of Glaser's[12] work probably is not. It is, however, known that small amounts of H_2O do produce anomalous effects in gases. (For instance, ion mobilities[15]). This might suggest a clustering of gas molecules around H_2O molecules. Further the absence of any anomaly in argon and neon in Glaser's apparatus might be explained by assuming that these gases because of their chemical inertness do not cluster around H_2O molecules. However, such assumptions need experimental verification, and further discussion at present is useless. One more fact should, however, be observed, and that is that Glaser's arrangements for drying his gases are, as nearly as one can tell from his publications, extremely good, expecially in his purifying train for H_2, where the last unit is a liquid air trap containing charcoal! The only way in which any vapor could possibly contaminate this H_2 is if it were introduced in transferring the gas from the cleaning train to the apparatus (a step which is not described in his papers) or from the walls and ground joints of the apparatus itself.[16] The latter is probably the only possibility, as in order to explain the fact that Glaser can repeat his results over and over again, a constant source of impurities would have to be assumed.

Description of the Experiments

The method used in the measurements described below is essentially that employed by Glaser,[2] Hammar[4] and Vaidyanathan.[7] It consists in measuring the torque exerted by a gas on a solid body suspended in an inhomogeneous magnetic field. This solid body, called the test body, was constructed as shown in Fig. 1*a* and *b*. It is entirely of Pyrex glass with fused joints. At the bottom of a glass rod is a cylindrical vessel divided radially into four equal chambers. Two of these, *A*, had small holes in them to permit the surrounding gas to enter. The other two, *B*, could be sealed off. In this particular set of experiments, they were first exhausted, and sealed at *C'*. Then *C'* was dipped into liquid air, and they were sealed off at *C*. Above this test body was a small glass rod *D* so mounted that it could be either moved vertically or rotated horizontally around the stem of the test body. A small spring of tungsten wire was attached to hold it in place in any given position. If the test body with a vacuum in all four quadrants, is suspended between the pole-pieces of a magnet, it will be in equilibrium in some position which is adjustable by moving *D*. Actually *D* was moved and the suspension twisted until the test body would hang as nearly as possible with the dividing walls parallel and perpendicular to the line joining the pole pieces, both when the

[15] H. Erikson, Phys. Rev. **34,** 635 (1929).

[16] In one of his papers,[12] Glaser performed two experiments to show that water vapor does not enter his apparatus at this point. One consisted in showing that P_2O_5 was not attacked in a tube sealed to his system near the measuring apparatus; the other consisted in showing that a glass rod which changed its resistance when water vapor was adsorbed on its surface, did not do so in the course of a series of measurements. One can only say that these measurements are not quantitative and until one knows how little water vapor can be detected, no inference can be drawn.

magnet was on and off. If now, with the field on, a gas is admitted to the chambers A, the test body will evidently be deflected in such a way that A will approach the pole-pieces if the gas is paramagnetic, or recede from them if it is diamagnetic. The advantage of this test body over that used by Glaser is that it is made entirely of diamagnetic glass, and consequently, the

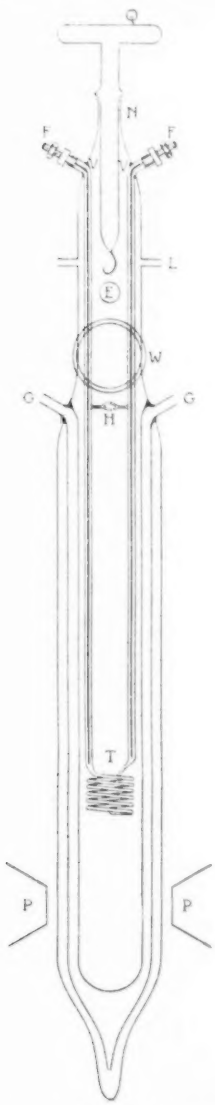

Fig. 2. Diagram of apparatus.

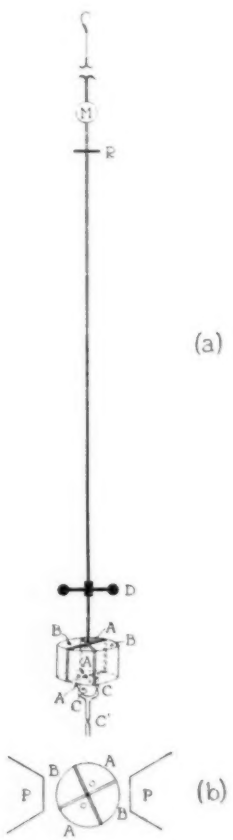

Fig. 1a. and 1b. Diagram of test body.

magnetic forces acting on it are practically independent of the temperature. The advantage over Hammer's test body lies in its symmetry, so that the magnetic forces acting on it do not have to be compensated by a large twist of the supporting fiber. In this way, the zero position (position of rest in a vacuum) is made practically independent of the field strength and of

the temperature. *M* is a mirror by means of which changes in position are read off on a scale 3 meters away. The suspension consisted of two small quartz hooks with a fiber drawn out between them. The test body hangs in the chamber shown in Fig. 2. The lower part is a Dewar flask. Liquid air or other condensed gases may be admitted at *G* into a chamber surrounded by a vacuum. In the present investigation, the chamber *G* contained air at room temperature. The inner chamber in which the test body was suspended had four openings; *E*, for admitting gases was fused to the purifying train; *W*, where a large plane window was sealed on with picein; and the lid, sealed at *L* and *N* with picein. *N* was introduced to lower and raise the test body, as the method of drawing the fiber made it impossible to predetermine its length to more than approximately 1 cm. To the lid were fused the glass tubes *V* terminating in a spiral of small thin tubing containing a platinum wire used as a resistance thermometer with terminals at *F*. *H* is a glass collar drawn in perspective which, when the test

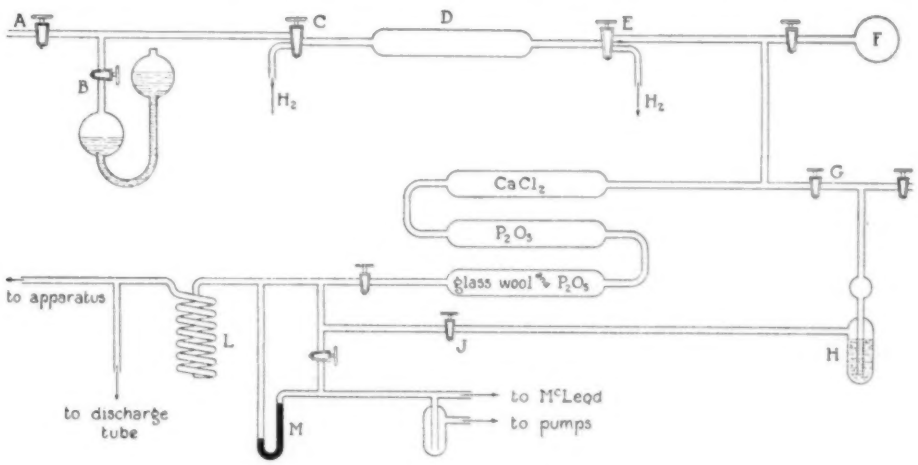

Fig. 3. Diagram of cleaning train.

body was in place, came just below *R*, Fig. 1*a*, so that if in lowering the system into its container the fiber should break, the test body would be caught by *H* instead of dropping to the bottom of the container.

For the preliminary experiments the purifying train was very simple, consisting of a small quartz furnace, containing copper wire, a tube containing $CaCl_2$ and finally a liquid air trap. With this apparatus, the effect of light and γ-rays was investigated, and found to have no influence on the shape of the pressure susceptibility curves, as mentioned above. The gases used were taken from steel cylinders under pressure. The first measurements were made on CO_2 and the curves in Fig. 4 obtained. The liquid air trap was, of course, not in operation. The system was so slow in coming to rest that before proceeding with the measurements, a small damping coil of copper wire was attached to the rod *D*, Fig. 1*a*. This greatly improved the accuracy with which readings could be made. The next measurements were made with N_2, and the curves in Fig. 5 repeated several times, alternately

with and without liquid air. These experiments indicated that the critical factor was purification and that probably the water vapor given off by the $CaCl_2$[17] (which has a partial pressure of about 0.3 mm) was responsible for the departures of the observations from linearity, since the introduction

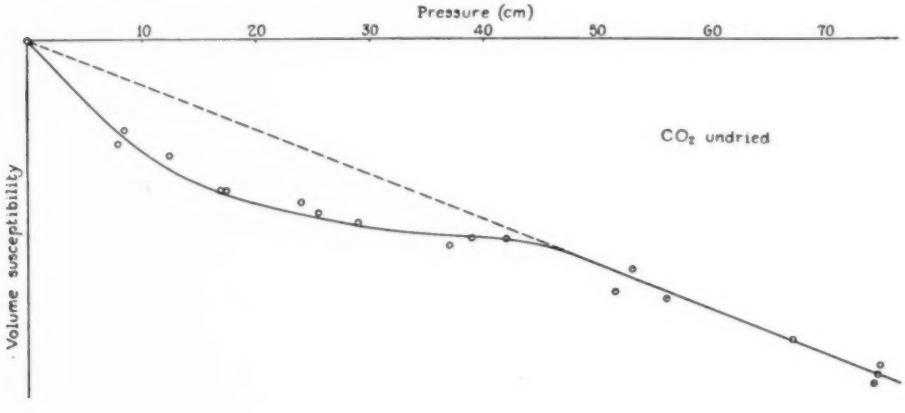

Fig. 4. Pressure susceptibility curve of undried CO_2.

of a liquid air trap gave readings along a straight line. Consequently, the cleaning train was rebuilt with a view to carefully checking the effect of impurities. The system built is shown in Fig. 3. The tank containing the gas to be measured is connected to the system at *A*. *B* is a gasometer containing

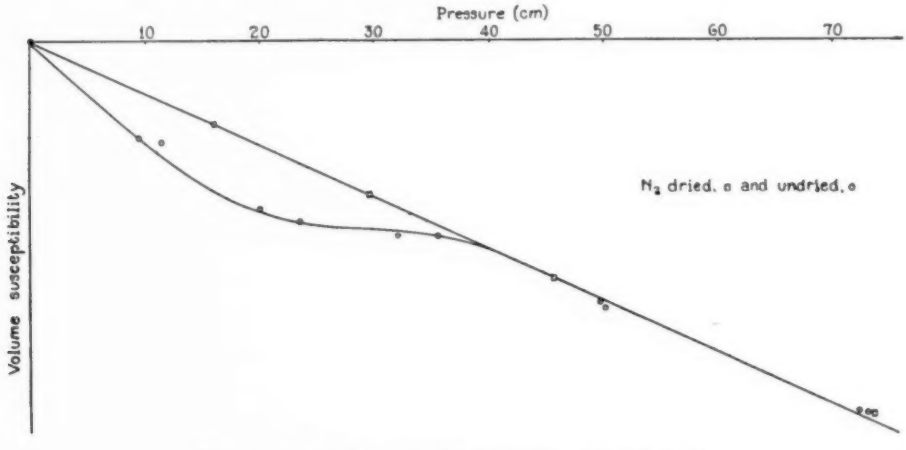

Fig. 5. Pressure susceptibility curves. □ and ○ N_2.

pump oil, and was a great convenience in admitting the gases. *D* is a quartz tube 60 cm long and 2.5 cm in diameter filled with copper wire. At either end the tube was fused to short pieces of smaller tubing and these sealed with

[17] This $CaCl_2$ was in the system while adjustments were being made, and had already taken up a good deal of water. The partial pressure of 0.3 mm is given in A. Goetz, Physik und Technik des Hochvakuums, p. 114, Second Edition.

sealing wax to the two way stopcocks *C* and *E*. The tube *D* was first covered with asbestos, then wound with chromel resistance wire in such a way that the near end from the point of view of gas entering the system could be kept red hot, while the far end did not glow at all. *F* is a bulb containing O_2 for measurements on gases mixed with O_2. From this point, there were two approaches to the measuring apparatus. One went through a wash bottle *H* containing an 85% mixture of H_2SO_4 and H_2O whose specific gravity was 1.775. Such a mixture has according to the Landolt Bernstein Tables a vapor pressure of 0.15 mm. This path could be isolated from the system by means of the stopcocks *G* and *J*, and these were not opened until the first measurements with dry gases were finished. The other path went through three drying tubes, each about 1 meter long and 2–3 cm in diameter. The first contained $CaCl_2$, the second P_2O_5, and the third P_2O_5 spread on glass wool. At this point the two paths joined again and were connected through a large stopcock to the pumps, a McLeod gauge, a mercury manometer, and to the apparatus through a glass spiral containing approximately 2 meters of glass tubing which could be immersed in liquid air. Immediately before the measuring apparatus a small discharge tube with a quartz window was fused to the system, so that a photograph of the spectrum of every gas could be taken immediately after a measurement. The procedure in filling in a gas was to pump out the whole apparatus from *E* on, except for the measurements with dry gases, in which the wash-bottle *H* was not evacuated. In about 10 minutes the pressure could be reduced to 10^{-3} mm. The oil in the gasometer was sucked up to the stopcock *B*, which was then closed. The gas to be measured was then blown through the apparatus from *A* and out at *E*. Then the furnace *D* was heated and H_2 flushed over the copper to activate it. Then more gas was flushed through from *A* to remove the H_2. Then *E* was closed and *B* opened until the gasometer was full, when the stopcock *A* was closed. Then by opening *E*, gas could be let into the measuring apparatus from the gasometer. In this way the system could be filled without applying a vacuum to the reducing valve on the gas tank. Before beginning measurements the apparatus was filled and evacuated two or three times. The magnet was operated by a bank of storage batteries, giving 21 amperes and the current kept constant to about 0.01%. The coils were immersed in transformer oil which was cooled with water circulation, so that with the above current, the magnet was at a temperature only a few degrees above room temperature.

With this equipment the experiments were resumed. The first gas examined was CO_2. The results of three runs are shown in Fig. 6. The gas went through the drying tubes at the rate of about 2 liters an hour. The spiral *L* was at room temperature. Although the points are somewhat scattered about the line drawn in the figure, there can be little doubt that they lie along a straight line. All measurements on CO_2 were complicated by the fact that in spite of the damping, the test body would continue to swing over a range of a few tenths of a millimeter for some time, usually about 1/2 hour, sometimes longer, and these swings were not perfectly regular. The

effect was especially large at atmospheric pressure. Apparently the swinging would die down and then suddenly start up again. This effect was observed only with CO_2, not with a vacuum, or air, or O_2 or N_2 or H_2 in the apparatus. The observed points on Fig. 6 at atmospheric pressure are indicated by a line, as no single definite deflection could be obtained. Further, the zero

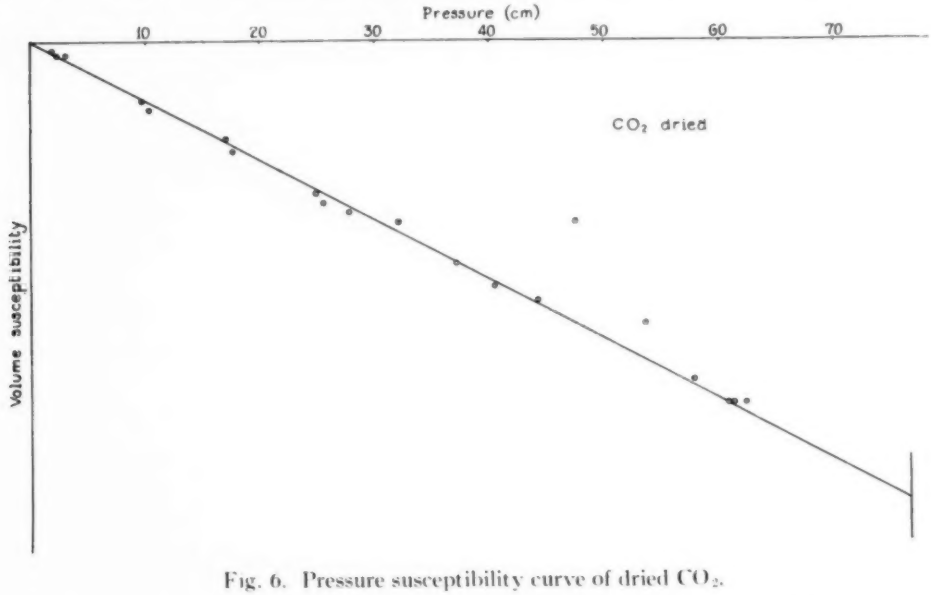

Fig. 6. Pressure susceptibility curve of dried CO_2.

position of the apparatus did change between runs, as observed by Glaser in his papers. The cause of this zero-shift has not been determined. I am of the opinion that it is due to the changes in adsorbed layers on the test body, and hope eventually to build an apparatus that can be baked out to

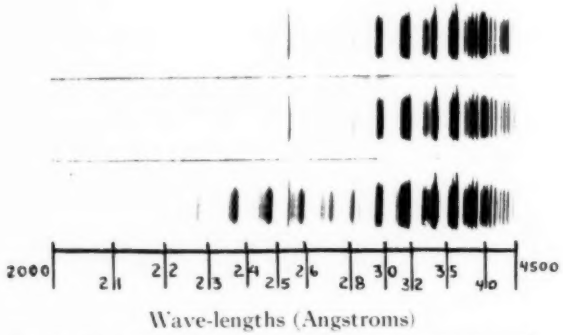

Wave-lengths (Angstroms)

Fig. 7. N_2 band spectrum in varying degrees of purity.

test this point. The next measurements were made on N_2 with and without a liquid air trap, and three runs gave points lying on a straight line at least as closely as the points in Fig. 5. The spectroscopic photographs for N_2 proved to be the only useful ones. With CO_2 and H_2, small impurities of O_2 and H_2O did not show. The spectrograph used was a small one made by Hilger with a quartz prism for use in the ultraviolet. In Fig. 7, are repro-

ductions of sample photographs. All three photographs were given the same exposure, 30 secs, with the same current and were taken with a gas pressure of about 3 cm in the discharge tube.

The first photograph was taken with N_2 passed over the hot copper, $CaCl_2$, P_2O_5 and the liquid air trap. In the second, the liquid air trap was removed. In the third, the liquid air trap was replaced but the furnace which heated the copper turned off. In the first picture, the NO bands are entirely absent. In the second, they begin to appear. This means that the water vapor which has passed all three drying tubes is sufficient, on dissociation, to produce a detectable amount of NO. The NO bands in the third photograph are due entirely to the O_2 present in the gas, as it comes from the tank, all water having been absorbed[18] in the liquid air trap. A gas analysis showed that the N_2 in the tank contained only 0.6% of O_2.

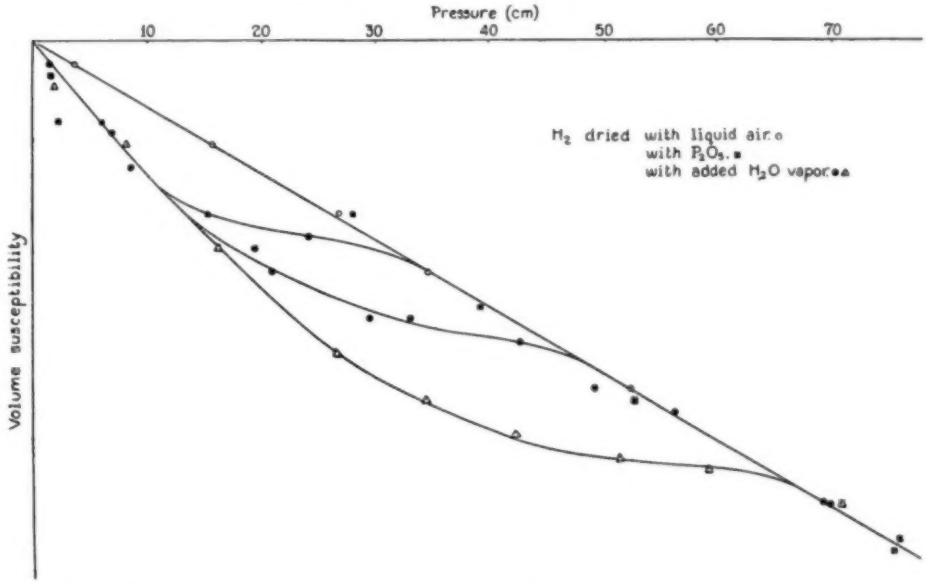

Fig. 8. Pressure susceptibility curves of H_2 with varying amounts of water vapor.

The next measurements were made on H_2 dried over P_2O_5, but not with liquid air. This gave a very small Glaser effect. Upon the introduction of liquid air, however, a further run gave a perfectly straight line. The interpretation of this seems very straightforward; namely, that in spite of preliminary flushings over the copper in the furnace, this was not completely reduced, and that therefore, the H_2 entering the drying tubes contained more water vapor than any of the gases previously used; if this is so, it follows that a drying train, in all 3 meters in length, left sufficient amounts of water vapor in the gas to be detectable. It is also interesting to note that the one gas in

[18] With longer exposure times the NO bands would appear even on photographs of N_2 as pure as I could make it. That this was due to the heating of the electrodes could be shown by taking two photographs of 30 secs duration each immediately after each other. The second showed NO bands, while the first did not. This sets a lower limit to the amount of water vapor detectable, but this is surely very small, as P_2O_5 has a vapor pressure of 10^{-4}mm and ice at liquid air temperatures 10^{-7}mm. See Goetz.[17]

which Hammar observed a Glaser effect was H_2, which, for the reasons given above, probably contained more water vapor than either N_2 or CO_2. The view that the H_2 leaving the furnace was very wet is further substantiated by the next measurements. The liquid air was removed and the gas admitted to the apparatus via the wash bottle *H*. The first runs gave very large Glaser effects, as in the lower curve in Fig. 8, but after considerable flushing, it was possible to repeat several times the curve in Fig. 8, which showed an intermediate Glaser effect. If the gases were saturated in the wash bottle, this corresponds to a water vapor pressure of .15 mm.

The results obtained so far seemed fairly conclusive, except for CO_2, where it might conceivably be contended that the straight line in Fig. 6 is due to just that amount of O_2 (1%) impurity which according to Glaser destroys the anomaly. The first argument against such a view is that the furnace certainly purified N_2 so that nothing like 1% of O_2 was left as an impurity, and that consequently, there is every reason to believe that it

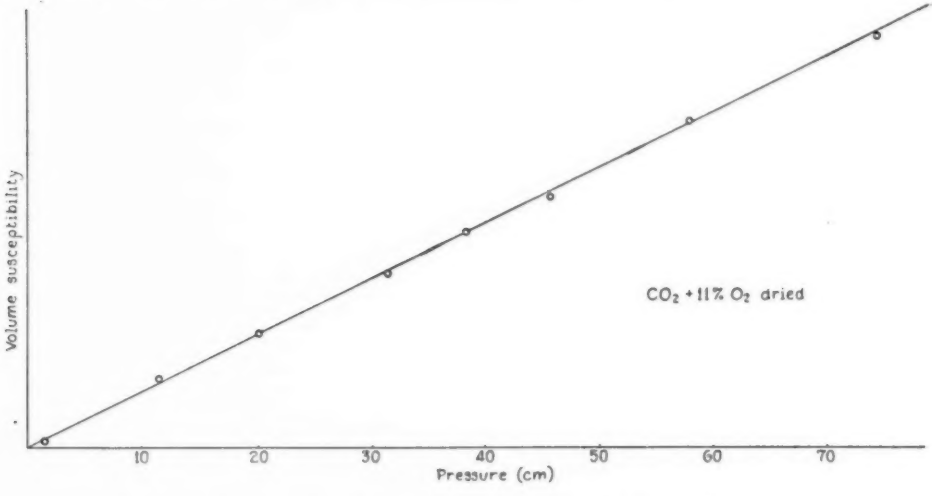

Fig. 9. Pressure susceptibility curve of the mixture 89% CO_2+11% O_2.

did the same for CO_2. The problem can, however, be attacked from another angle. According to Glaser,[11] the paramagnetic mixture of CO_2 plus about 11% O_2 should definitely show an anomaly at low pressures. This was tried with the gas dried in the train described above, and the observations indicated no such effect. The results are plotted in Fig. 9. The concentration of O_2 in this experiment was calculated on the basis of the relative deflections for the mixture and pure CO_2. Deflection for CO_2 plus O_2/Deflection for pure $CO_2 = +7.5/-9.0 = -.83$. According to Glaser, an anomaly should certainly be observed for O_2 concentrations corresponding to values of the above ratio between $-.9$ and 0. This effectively disposes of the argument that normal behavior of CO_2 is due to a 1% O_2 impurity, since such normal behavior is found in a mixture which certainly contains much more than 1% of O_2.

In conclusion, I wish to take this opportunity of expressing my appreciation of the very beautiful work done by Mr. William Clancy in blowing the glass parts of the apparatus previously described.

LETTERS TO THE EDITOR

Prompt publication of brief reports of important discoveries in physics may be secured by addressing them to this department. Closing dates for this department are, for the first issue of the month, the twenty-eighth of the preceding month; for the second issue, the thirteenth of the month. The Board of Editors does not hold itself responsible for the opinions expressed by the correspondents.

Scattering of Alpha-Rays and High Speed Electrons in Radial Fields

Wentzel,[1] Sommerfeld,[2] and Mitchell,[3] among others, have derived by the wave mechanics first approximation formulae for elastic scattering of alpha-rays and high speed electrons in spherically symmetrical fields. They all use Born's perturbation method and differ from each other only in their assumptions as to the potential fields that represent the scattering system. The fundamental expression, however, from which their particular scattering formulae may be derived, by the special assumptions as to the potential functions, may be written as:

$$\left|\frac{\psi_1}{\psi_0}\right| = \frac{K^2}{rE v}\int_0^\infty \rho V(\rho)\sin \rho u d\rho \qquad (1)$$

where $|(\psi_1/\psi_0)|$ is the absolute value of the ratio of the amplitude of the scattered alpha-ray or electron wave at a large distance r from the scattering atom, to that of the incident wave, and is a function of the argument u. E is the energy of the particle, M its mass, and $K^2=8\pi^2ME/h^2$; $u=2K\sin\theta/2$ where θ is the angle of scattering. $V(\rho)$ is the potential energy of the particle when it is at a distance ρ from the center of the scattering system.

A Coulomb potential $V(\rho)$ should theoretically lead to the Rutherford scattering formula, but as it gives a divergent integral, Wentzel assumed that $V(\rho)=(A/\rho)^{-\alpha\rho}$. Sommerfeld made essentially the same assumption, though he justified it physically by deriving it from the wave mechanical model of a nucelus screened by its electrons concentrated in the K shell. Mitchell, supposed the electrons to be distributed as in the Thomas-Fermi statistical theory of the heavier atoms. These various assumptions do lead to scattering formula which differ from the Rutherford formula only to the extent that the $V(\rho)$ assumed differ from the Coulomb value.

As experimentally it is definitely established that deviations from Rutherford's formula do occur, Sommerfeld,[2] Kirchner,[4] and Mott[5] have attributed these deviations to the electron distributions about the nuclei of the scattering atoms, and consequent deviations from the Coulomb potential. These authors have computed by Eq. (1) the scattering to be expected from certain types of potential function and have compared them with the observed scattering. But since we are after all more interested in a direct determination of the potential field and electron distribution within an atom than in merely checking observed with predicted scattering formulae according to assumed types of potential field, we propose to reverse the problem heretofore considered. Thus we propose to determine directly the potential field $V(\rho)$ and the electron distribution *from the observed scattering*.

This problem can be solved, in principle, by applying Fourier's reciprocal theorem to Eq. (1); we then obtain:

$$V(\rho)=\frac{2rE}{\pi K^2\rho}\int_0^\infty v\left|\frac{\psi_1}{\psi_0}\right|\sin \rho u dv \qquad (2)$$

The classical charge density σ is then given by:

[1] G. Wentzel, Zeits. f. Physik **40**, 590 (1927).

[2] A. Sommerfeld, Erganzungsband, p. 226.

[3] A. C. G. Mitchell, J. of Franklin Institute.

[4] F. Kirchner, Naturwiss. Jan. 24, 1930.

[5] N. F. Mott, Nature, Dec. 28, 1929.

$$\sigma = \frac{-1}{4\pi\epsilon}\Delta^2 V = \frac{-rE}{2\pi^2 K^2 \epsilon\rho\partial}\,\frac{\partial^2}{\partial\rho^2}\int_0^\infty v\left|\frac{\psi_1}{\psi_0}\right|\sin\rho u dv \quad (3)$$

where ϵ is the charge of the alpha-particle or electron.

Although physically u and hence $|\psi_1/\psi_0|$ is only defined for $0 \leqq v \leqq 2K$, the integration in (2) and (3) implies that the *functional form* of $|\psi_1/\psi_0|$ is to be used, as derived from the experimental curves. And even when the integration can only be carried out graphically, the region for $u > 2K$ may be safely neglected anyway except for very small y values of ρ, since K will always be at least of the order of 10^9 for any case to which the present approximation applies. In fact, the major difficulty in carrying out the integrations is for small values of u, for these give the largest contribution to the integrals, while at the same time the values of $|\psi_1/\psi_0|$ for small values of u will be the most uncertain since accurate scattering measurements at small angles are very difficult. Computations are now being made to test the possibility of making reasonable extrapolations and deriving reasonable distributions by equations (2) and (3).

We may point out, too, that Eq. (3) gives the net charge distribution, of both the nuclear positive charge and the enveloping electronic charge. Thus to the extent that the data can be obtained with accuracy and the integration carried out accurately, it will afford a means of studying the charge distribution of the nucleus as well as of the electrons. Heretofore, the nucleus has been considered as a point charge so that σ would have meaning only for $\rho > 0$ and then give the electron density only. From our present point of view we need make no such assumption, but rather determine simultaneously the positive and negative charge distribution which gives the resultant scattering $|\psi_1/\psi_0|$. Of course, if σ turns out to be negative for all $\rho > 0$ it would be proof that the nucleus is essentially a point charge, but we do not have to assume this to begin with.

It is of interest to note that if we assume the Rutherford scattering formula: $|\psi_1/\psi_0| = A/v^2$, we immediately get from Eq. (2) the Coulomb potential, and avoid Wentzel's convergence difficulty. It is easily verified also that using Sommerfeld's formula: $|\psi_1/\psi_0| = A/v^2 + d^2$ we get his expression for $V(\rho)$.

Finally, it may be observed that our point of view of reversing the problem of scattering as heretofore considered, may also be applied to the interpretation of x-ray scattering intensities. In this problem, the structure factor, F, which determines the interference of the scattered rays and depends on the charge distribution of the scattering atom, may be expressed as:

$$F = \frac{\lambda}{4\pi\sin\epsilon}\int_0^\infty \frac{U(r)}{r}\sin\left|\frac{4\pi r\sin\theta}{\lambda}\right| dr \quad (4)$$

where $U(r)/4\pi r^2$ is the charge density, assumed to have spherical symmetry, at a distance r from the center of the scattering system, θ is the angle of reflection, and λ is the wave-length. An inversion of this integral will again give directly the charge distribution as an integral of the same type as (2) with the observable function, F, in the integrand.

MORRIS MUSKAT

Gulf Research Laboratory,
Pittsburgh, Pa.,
May 31, 1930

Nuclear Electrons

It has been suggested by Heitler and Herzberg (Naturwissenschaften **17,** 673, 1929) to explain the observations of Rasetti (Proc. Nat. Acad. Sci. **15,** 515, 1929) on the Raman effect in N_2 that the electron in the nucleus loses its spin and its contribution to the statistics of the nucleus. If all the nuclear particles (electrons as well as protons) are effective in determining whether the nuclear spin factor makes the total Ψ function symmetrical or antisymmetrical in the nuclei, there is great difficulty (cf. R. S. Mulliken, Trans. Faraday Soc. **25,** 644, 1929) in explaining the fact that in the Raman spectrum of N_2 the transitions between the even rotational levels are the stronger, whereas for H_2 the Raman lines representing transitions between odd rotational levels are more intense. For both H_2 and N_2 have a $^1\Sigma$ normal state, built up out of two equal atoms in S states, each with an odd number of nuclear particles (1 for the H atom, 21 for the N atom). And therefore, since for both molecules $\Lambda = 0$, and since the electron configurations are in both cases composed of closed shells, making Σl_r for the external electrons an even number, one would

expect the odd K levels to be the stronger levels, symmetrical in the nuclei.

If, however, only the nuclear protons have a spin, then the interchange of electrons in the two nuclei does not affect the symmetry of the Ψ function. Consequently the nuclear spin factor will make the total Ψ function either symmetrical or antisymmetrical in the nuclei, according as the number of protons is even or odd. But the stronger K levels should always be symmetrical in the nuclei with respect to the nuclear spin factor, and so a rule that Ψ must be symmetrical in the nuclei if the number of protons is even, antisymmetrical in the nuclei if the number of protons is odd, would require that the even K levels be stronger in N_2 (14 protons) and the odd K levels be stronger in H_2 (1 proton). There is then no contradiction with previous conclusions as to the electronic configuration of the normal state for N_2 and H_2. Furthermore, there is now also agreement with the 2:1 alternating intensity ratio found in the N_2^+ bands, for this ratio requires a nuclear spin $= 1 \cdot h/2\pi$ for the N atom, which is to be interpreted as a parallel orientation of the spins of the two protons in excess of α-particle configurations. The nuclear spin $= 3/2 \cdot h/2\pi$ recently reported by Harvey and Jenkins (Phys. Rev. **35,** 789, 1930) is, as they suggest, additional evidence in support of the view that the spin of the electron is not effective in the nucleus.

In this connection it is interesting to recall that the radius of a non-rotating Lorentz electron of mass $8.994(10)^{-28}$ gm calculated on classical electromagnetic theory is $1.88(10)^{-13}$ cm, whereas that of a Lorentz electron with a spin of a half quantum which has a mean mass equal to the figure above is $3.98(10)^{-9}$ cm. On the other hand, a Lorentz proton of mass $1.661(10)^{-24}$ gm has a radius of $1.02(10)^{-16}$ cm if it has no rotation and a radius of $2.15(10)^{-12}$ cm if it is assumed to have a half quantum of spin. If the radius of the nucleus is of the order of magnitude of 10^{-12} cm as suggested by experiments on the scattering of α-rays, these figures indicate that the size of a spinning electron is too great to permit its inclusion in the nucleus. It may be for this reason that nuclear electrons have no spin. The dimensions of a spinning proton, on the other hand, are of the same order of magnitude as those of the nucleus.

LEIGH PAGE
WILLIAM W. WATSON

Sloane Physics Laboratory,
Yale University,
May 21, 1930.

Concerning the Existance of a New Term in Hg I

T. Takamine[1] and T. Suga have recently made an excellent photographic investigation of the near infrared spectrum of Hg. On their spectrograms they find two new series of lines given by $X - m^3S_1$ and $X - m^3D_3$ having a common final term of value 15299 cm^{-1}. They state that this new term is of the nature of a P term but that other evidences would certainly be necessary before its reality is established. It is the purpose of this note to present other evidence which supports their assumption.

All of the lines of longer wave-length—except two (outside of the region covered)—necessary to complete the two series appear on the writer's[2] records of this spectrum and were reported as unclassified lines. These two series with the writer's additions are tabulated below. The value of X is taken as

[1] T. Takamine and T. Suga, Sc. Pap. I. P. C. R., No. 232, **13,** (1930).

[2] E. D. McAlister, Phys. Rev. **34,** No. 8, Oct. 15 (1929).

Sharp Series				Diffuse Series			
λ_{vac}	ν	ν_{calc}	Int.[2]	λ_{vac}	ν	ν_{calc}	Int.[2]
15300A	6536	−6534	30.	—	—	2547	—
19705	5075	5077	4.2	12131A	8243	8245	3.3
10711	9336	9332	1.1	9245T	10817	10818	—
8786T	11381	11384		8198T	12198	12201	
7979T	12532	12532		7678T	13024	13027	
7552T	13241	13239		7370T	13568	13562	
7294T	13710	13707		7175T	13937		
7126T	14033			7045T	14195		
				6948T	14393		

15297 cm^{-1} since this gives a closer agreement between observed and calculated frequencies when the writer's additions are included. Fowler's term values are used. Takamines' lines are marked with a T.

Of particular interest is the first line (negative ν_{calc}) of this "sharp" series $\lambda = 15300$A (λ_{vac} Paschen[3]) which is one of the strong lines in the infrared spectrum of Hg. Paschen[4] attempted to use it as the first line of another series but this attempt failed to gain recognition. It does not fit into the once-ionized Hg scheme and appears much too strong in the arc spectrum to be a spark line. Hence this assignment of it to Takamine's series seems quite reasonable.

The deviations from the calculated values are somewhat larger than is desirable but the discrepancies are probably due to the difficulty of accurate wave-length measurements in this region. The intensity[2] (mm deflection) of the first three lines in the "sharp" series and of the second line in the "diffuse" series are particularly convincing as to the correctness of the present assignment. The writer has inserted in the "diffuse" series a line $\lambda_{air} = 9243$A appearing on Takamine's pictures which he did not include. This line appears as a sharp line on all of Takamine's pictures while most of the others in this series are diffuse or "washy." This must be why Takamine does not include it. However the photographic method undergoes an enormous change in sensitivity between this line and the others in this series, and also the other lines appear much sharper on his one hour exposure than they do on the 10 hour one. It thus seems likely that this line really belongs to the series.

E. D. McAlister

Physics Department, University of Oregon,
Eugene, Oregon,
May 31, 1930.

[3] Paschen, Ann. d. Physik **27,** 558 (1907).
[4] Paschen, Ann. d. Physik **29,** 663 (1909).

Boundary Conditions in Wave Mechanics Reply to Criticism

Mr. Eckart's letter in the May 15th issue of the Physical Review about my paper of April 15th on the above subject seems to call for some reply. If the potential varies sufficiently gradually from the constant value zero to a constant value V' then there is no reflexion and if there is no reflexion for a particular wave-length there will be none for any shorter wave-length. My calculation showed that there may be no reflexion at the layers on the surfaces of metals because the thickness of these layers may be sufficient to allow the potential variation to be sufficiently gradual for this when $E > V'$. According to this the usual boundary conditions at a discontinuity may not be applicable to these layers. I therefore suggested new boundary conditions giving no reflexion when $E > V'$ which can therefore be used with these layers when they give no reflexion with $E > V'$. I also suggested that these new boundary conditions may be correct for an actual discontinuity if such a thing can exist.

Mr. Eckart suggests that the absence of reflexion is due to the potential variation acting like an étalon with a spacing of one quarter-wave length. The distance in which the potential changes may be made any multiple or fraction of a wave-length, without reflexion, by suitably changing the constant β so that I do not think the action is really at all analogous to that of an étalon.

I quite agree with what Mr. Eckart says about the very limited generality of the solution of the wave equation which I obtained.

H. A. Wilson

Rice Institute,
Houston, Texas,
June 6, 1930.

Ionization Potential of Carbon

The ionization potential of carbon was estimated as 11.2 volts by Fowler and Selwyn (Proc. Roy. Soc. **A118,** 34, 1928). The basis for this estimation was the C I spectrum which they arranged into series for the first time and a comparison of this spectrum, which was not extensive enough for accuracy, with that of the related spectra of N II and O III.

In my work on the helium continuous spectrum (Phys. Rev. **35,** 1113, 1930) I had noticed that a series of lines shone brightly in the ultraviolet when the stopcock grease contaminated the helium. I followed up this observation by purposely introducing carbon monoxide into the helium with the result that the spectrum of C I has been greatly

extended in the vacuum region and some new features of this spectrum observed. In this note I shall deal only with a small phase of the data now on hand, namely that concerned with the ionization potential of carbon. The fuller treatment is reserved for the complete paper that will be published when the examination of these data is finished.

The most obvious feature of the new ultraviolet spectrum is that it contains three series of multiplets that converge to the same threefold limit, the $^3P_{0,1,2}$ of the atom. These have been measured to eight members and form the basis of the present determination of the ionization potential of normal carbon. The series multiplets are not resolved after the first three members so one has to deal with diffuse lines for the higher terms. Fortunately, however, the middle series is much stronger than the other two. It stands out like a ridge in the mist and is easily measured. It is the middle series that has been used for the calculation of the terms and the ionization potential.

The following is a list of the "ridge" groups: λ1649.93 (2), (uncertain if C I), 1277.53 (5) seen as triplet in second order; 1193.17 (5), 1158.02 (4); 1139.80 (3); 1129.12 (2); 1122.32 (1); and 1117.68 (0). The series limit is $A=90834$ cm^{-1} and the effective quantum numbers for the above lines are 1.905; 2.955; 3.952; 4.948; 5.949; 6.952; 7.955; and 8.970. It is seen that this is very nearly a Rydberg series. The values are not too smoothly arranged but are as good as the nature of these unresolved multiplets when superimposed on two other converging groups might be expected to yield.

Using the known values of the separations of the lowest ^3P term of C I, and assuming that the above limit refers to its center of gravity, the term values have been calculated to be $^3P_2=90817.7$, $^3P_1=90845.2$ and $^3P_0=90860$. The metastable levels ^1D and ^1S listed by Fowler and Selwyn lie 1.179 volts and 2.593 volts respectively above the $^3P_0$ state, and the ionization potential of the carbon atom from the $^3P_0$, lowest normal state, is 11.217 volts.

JOHN J. HOPFIELD
University of California,
May 23, 1930.

The Ultraviolet Light Theory of Aurorae and Magnetic Storms

The ultraviolet light theory of aurorae and magnetic storms[1] contained some unsettled points and some conclusions in disagreement with observation. The further development of the theory of the outer atmosphere[2] and the recognition of an effect hitherto unseen have now automatically removed the discrepancies. So that the theory, with no change in the original assumptions, begins to assume a more finished appearance. The new effect has emerged directly from the results of Page.[3] Page showed, on the assumption of an earth with no excess charge, that the long free path ions in the upper atmosphere would drift westward. We now point out that the westward drift is hindered by collisions of the ions with the neutral molecules of the atmosphere which move approximately with the earth's rotation. As a result of the hindrance there is a displacement of positive ions to polar regions and negative ions to equatorial regions. This sets up an electric field which, together with the earth's magnetic field, causes the high flying ions to move partially with the angular velocity of the earth. They descend into the 50° to 70° latitudes during the evening hours to cause aurorae and the diurnal variation phase of the world wide magnetic storms. With the new values of the electrical conductivity[2] of the upper atmosphere the diurnal variation phase is seen to be due to the gravitational magnetic drift currents set up by the polar ionic concentrations. Agreement is secured throughout with the observations. The second phase of the world wide magnetic storm is found to arise mainly from reactions in the atmosphere rather than to induced currents in the earth.

E. O. HULBURT
Naval Research Laboratory,
Washington, D. C.,
May 28, 1930.

[1] Phys. Rev. **33,** 412 (1929), **34,** 344 (1929).
[2] Phys. Rev. **34,** 1167 (1929), **35,** 240 (1930).
[3] Page, Phys. Rev. **33,** 823 (1929).

BOOK REVIEWS

Elementare Quantenmechanik. M. Born and P. Jordan. Pp. 434. J. Springer, Berlin, 1930. Price bound RM 29.80.

This book appears in the "Struktur der Materie" series edited by Born and Franck as the second volume of the former's well-known "Vorlesungen uber Atommechanik." Written by the founders of the matrix mechanics, it is the first book on the subject to give a systematic and thorough account of the formulation of quantum mechanics by matrix methods.

The guiding view-point is expressed in the preface: "We are convinced that the true connection of the classical and the new mechanics lies not so much in the formal similarity of the wave-mechanical differential equations and boundary value problems with the methods of classical mechanics of continua, as in the correspondence principle of Niels Bohr; we see in the new mechanics the rigorous working out of Bohr's program."

The authors have succeeded in giving an admirably clear account of the subject from this standpoint. After chapters devoted to mathematical methods and the basic ideas of quantum mechanics there is a valuable chapter devoted to theorems on angular momentum from the standpoint of invariance under the rotation group. The chapter on perturbation theory gives a full account of dispersion theory including natural optical activity and the Kerr and Faraday effects The two remaining chapters are devoted to the statistical interpretation of quantum mechanics and the quantized electromagnetic wave approach to radiation theory.

The notation is unwieldy and shows perhaps the richest efflorescence of subscripts, superscripts and diacritical marks that has yet blossomed in any physical treatise. Can we hope to understand nature in terms of equations like

$$2\overset{(k)}{U}_{\rho\sigma}{}^{(rr)} = -\sum_{l=1}^{k-1}\sum_{j,r}\overset{(l)}{U}_{\rho r}{}^{+(r\,j)}\overset{(k-l)}{U}_{r\sigma}{}^{(j\,r)}\,.$$

The notation devised by Dirac for his forthcoming book is much simpler and it is to be hoped that it rather than that of this book, will be the one to find general acceptance.

The book is to be recommended as the most important that has thus far appeared on the subject. The word elementary in the title has to be taken more in the sense of fundamental and first principles, rather than simple, easily understood and suitable for a first introduction to the subject.

E. U. Condon

AUTHOR INDEX TO VOLUME 35

References with (A) are to abstracts of papers presented at meetings of the Physical Society and references with (L) are to Letters to the Editor.

Adams, John Mead. Origin of snowflakes—113(L)
——— Photographs of single crystals of ice, grown from the vapor—136(A)
Allison, Fred and Edgar J. Murphy. A magneto-optic method of chemical analysis—124(A)
——— **and Edgar J. Murphy.** Evidence of the presence of element 87 in samples of pollucite and lepidolite ores—285(L)
Allison, Samuel K. and John H. Williams. Experiments on the reported fine structure and the wave-length separation of the $K\beta$ doublet in the molybdenum x-ray spectrum—135(A), 149
——— **and John H. Williams.** Resolving power of calcite for x-rays and the natural widths of the molybdenum K_α doublet—1476
Almasy, F. and C. V. Shapiro. Fluorescence spectrum of benzene—1422(A)
Almy, Gerald M. Zeeman effect in the OH bands—1495
——— **F. H. Crawford, and E. L. Hill.** Zeeman effect in λ5211 MgH band—124(A)
Anderson, Carl D. Space-distribution of x-ray photoelectrons ejected from the K and L atomic energy-levels—1139
Andrews, Donald H. Relation between Raman spectra and the molecular structure of organic compounds—662(A)
——— **and John C. Southard.** Calculation of the specific heats of solid organic compounds from Raman spectra—670(A)
——— (See Kettering, C. F.)—1422(A)
Arnott, E. G. F. (See Smyth, H. D.)—126(A)
Austin, Allen. Dielectric constants of aqueous KCl solutions—1428(A)
Austin, J. B. and Ian Armstrong Black. Emission spectrum of benzene in the region 2500–3000A—452
Babcock, Harold D. New absorption band of atmospheric oxygen and the vibrational frequency of the normal molecule—125(A)
Babcock, R. W. Thermal convection—1008
Bacher, R. F. (see Goudsmit, S.)—127(A), 129(A)
Badger, Richard M. Absorption of acetylene and ethylene in the near infrared—1433(A)
——— Absorption bands of ammonia gas in the visible—1038
Balinkin, Isay A. On the mechanism of very absorbable radiation emitted by compressed crystalline substances under high potentials—1443(A)
Band, William. A new relativity theory of the unified physical field—115(L)
——— A new unified field theory and wave mechanics—1015(L)
——— Capture of electrons by alpha-particles—1128(L)
——— X-ray emission independent of temporary excitation—1129(L)
Barnes, Arthur H. Capture of electrons by alpha-particles—217
——— **Bergen Davis and H. L. Hull.** Capture of electrons by alpha-particles—1433(A)
Barnes, R. Bowling. High dispersion in the infrared—662(A)
——— Infrared absorption of some organic liquids under high resolution—1524
——— **and A. H. Pfund.** Effect of aberrations in limiting the resolving power of infrared spectrometers—1434(A)
Barnes, S. W. and F. K. Richtmyer. Excitation potential of the $L\alpha$ satellites of Ag(47)—661(A)
——— (see Richtmyer)—1428(A)
Barrett, Charles S. X-ray fiber structure of alloys containing precipitated crystals—1425(A)
Bartlett, James H., Jr. Relative intensities of supermultiplet lines—229
Bartlett, Russell S. A space charge interpretation of thermionic work function—669(A)
Barton, Henry A. A new regularity in the list of existing nuclei—408
Bateman, H. Variable flow in pipes—177
——— Book review—654
Beams, J. W. Spectral phenomena in spark discharges—24
——— **and E. C. Stevenson.** Electric double refraction in gases—1440(A)
——— **and J. C. Street.** Initial stages of electrical breakdown—658(A)
Bearden, J. A. Independence of x-ray absorption on temperature—1443(A)
——— Spectroscopic analysis of scattered x-rays—1427(A)

Beattie, James A. Simple equation for the Joule-Thomson effect in real gases—643
——— A rational basis for the thermodynamic treatment of mixtures of real gases—1435(A)
Becker, J. A. Ion-grid theory of the decrease in work function for composite surfaces—1431(A)
Bedell, Frederick and Jackson G. Kuhn. Stabilized oscilloscope with amplified stabilization—657(A)
Bender, William (see Watson, William W.)—1440 (A), 1513
Bergstein, Milton, J. F. Rinke and C. M. Gutheil. Studies in contact rectification. II. Cupric sulfide-magnesium junction—1425(A)
Bichowsky, F. R. (see Lunn, E. G.)—563(L), 671(A)
Birge, Raymond T. Vibrational isotope effect—133(A)
——— Atomic weights of hydrogen and helium—1015(L)
——— Book review—872
——— (see King, A. S.)—133(A)
Bitter, Francis. Magnetic susceptibility of gases. I. Pressure dependence—1572
Black, Ian Armstrong (see Austin, J. B.)—452
Blake, F. C. An interesting case of a unit lattice made up of interpenetrating lattices—660(A)
——— **and James O. Lord.** Sorting the variables in the crystal structures of certain chromium-nickel alloys—660(A)
Bleakney, Walker. A study of the ions produced in mercury vapor by electron impact—123(A)
——— Probability and critical potentials for the formation of multiply charged ions in Hg vapor by electron impact—139
——— Ionization of hydrogen by single electron impact—1180
——— **and John T. Tate.** Primary ions formed by electron impact in hydrogen—658(A)
Bless, A. A. Composition of the interior of the earth—1436(A)
——— Polarization and the electric moment of tung oil—1442(A)
Blodgett, Katharine B. (see Langmuir, Irving)—478
Bloomenthal, Sidney. Vibrational quantum analysis and isotope effect for the lead oxide band spectra—34
——— (see Christy, Andrew)—46
Boeckner, C. Resonance and quenching of the third principal series line of caesium—664(A)
——— (see Mohler, F. L.)—664(A)
Bowie, R. M. (see Woodrow, Jay W.)—1423(A)
Boyd, James H., Jr. Viscosity of compressed gases—1284
Bozorth, Richard M. and Joy F. Dillinger. Barkhausen effect. II. Determination of the average size of the discontinuities in magnetization—733
Bramley, Arthur. X-rays generated by three element tube—869(L)
——— **and Allen C. G. Mitchell.** Possibility of bringing mean life directly into Schroedinger equation for the hydrogen atom—1419(A)
Brasefield, Charles J. Electron velocities in a high frequency discharge in hydrogen—92, 122(A)
——— Conductivity of a high frequency discharge in hydrogen—1073
Brattain, Walter H. Effect of absorbed thorium on the thermionic emission from tungsten—1431(A)
Braun, M. L. (see Stuhlman, Otto, Jr.)—1436
Breit, G. Separation of angles in the two-electron problem—569
——— Possible effects of nuclear spin on x-ray terms—1447
——— **M. A. Tuve and O. Dahl.** A laboratory method of producing high potentials—51
——— (see Tuve, M. A.)—66
——— Book review—1411
Brennen, Herbert J. Nernst heat theorem—121(A)
——— A new equation of state—129(A)
——— Use of homogeneous coordinates in physics and chemistry—294(A)
Brewer, A. Keith. Photoelectric and thermionic properties of platinum coated glass filaments—1360
Brice, Brooks A. Band spectrum of silver chloride—960
Brickwedde, F. G. and R. B. Scott. Photoelectric cell thermoregulator—670(A)
——— (see Scott, R. B.)—670(A)
Bridgman, P. W. Book reviews—873, 1301
Briggs, H. B. (see Ives, Herbert E.)—669(A)
Briggs, L. J. and H. L. Dryden. Airfoils of circular-arc section for use at high speeds—1416(A)
Brode, Robert B. Effective collision cross-section of cadmium and zinc atoms for slow electrons—134(A), 504
——— (see Normand, C. E.)—1438(A)
Brown, Joseph G. Electric space charge in the lower atmosphere—135(A)
——— Variation of the electric potential gradient in the lower atmosphere—135(A)
Browne, T. E. Jr. and F. C. Todd. Extinction of short a.c. arcs between brass electrodes—1441(A)
——— (see Todd, F. C.)—1441(A)
de Bruyne, Norman A. Temperature dependence of field currents—172
Bryan, A. B. and C. W. Heaps. Magnetostriction measurements using a heterodyne beat method—298(A)
Burdine, Theodore (see Plyler, E. K.)—605
Busang, P. F. (see Smith, W. O.)—1416(A)
Canfield, R. H. Inhomogeneities in crystals—114(L)
——— Stability of metallic crystal lattices—530

Canfield, R. H. Classes of symmetry possible in crystals of elements—660(A)
——— Mosaic crystals of elements—671(A)
Cartwright, C. Hawley. Black bodies in the extreme infrared—415
Castlemen, R. A., Jr. On the mechanism of "atomization"—1014(L), 1416(A)
Chaffee, E. L. (see Perry, Charlotte T.)—1437(A)
Chamberlain, C. W. A recording interferometer—663(A)
Chamberlain, Stuart H. An interference method of measuring distance—663(A)
Child, C. D. Absorption of light by flames containing sodium—294(A)
Christy, Andrew and Sidney Bloomenthal. Fine structure analysis of the bands in the *A* and *D* systems of lead oxide—46
Claus, W. D. Temperature effect in diffuse scattering of x-rays from rocksalt—1427(A)
Collins, J. R. Effect of high pressure on the near infrared absorption spectra of certain liquids—1433(A)
Collins, T. R. D. (see Fagan, H. D.)—421
Colson, DeVer. Voltage-intensity relations of the cadmium spectra—294(A)
Colwell, R. C. Effect of cyclones and anti-cyclones upon the intensity of radio signals—1425(A)
Compton, A. H. Efficiency of x-ray fluorescence—127(A)
——— Determination of electron distributions from measurements of scattered x-rays—925, 1427(A)
K. T. Compton (see Van Voorhis, C. C.)—1438(A)
Condon, E. U. Complete dissociation of H_2—658(A)
——— **and J. E. Mack.** An interpretation of Pauli's exclusion principle—579
——— **and G. H. Shortley.** Singlet-triplet interval ratios for *sp*, *sd*, *sf*, p^5s, and d^9s configurations—1342, 1419(A)
——— Book reviews—567, 654, 872, 1588
——— (see Villars, D. S.)—1028
Constant, F. W. Microstructure of some magnetic alloys of high platinum concentration—116(L)
Cooksey, Charlton Dows and Donald Cooksey. Glancing angle of reflection from calcite for silver ($K\alpha_1$) x-rays—564(L)
Cooksey, Donald. (see Cooksey, Charlton Dows)—564(L)
Copeland, L. C. On the heat of formation of molecular oxygen—1443(A)
Copeland, Paul L. Secondary electrons from contaminated surfaces—293(A), 982
Cork, J. M. Absolute measurement of certain x-ray wave-lengths—128(A)
Cork, J. M. Molybdenum *L* series wave-lengths by ruled gratings—1456
Cox, I. W. Absorption of lithium ions in mercury vapor—123(A)
Cravath, A. M. A search for critical potentials for electron recombination with Hg^+—659(A)
Crawford, F. H. (see Almy, G. M.)—124(A)
Cunningham, H. L. (see Woodrow, Jay W.)—125(A)
Curtiss, L. F. Nature of cosmic radiation—1433(A)
Dahl, O. (see Breit, G.)—51
——— (see Tuve, M. A.)—1406(L)
Dasannacharya, Balebail. Polarization of x-rays from thin aluminum anticathodes—129(A)
Davey, W. P. and D. C. Duncan. Absorption of ultraviolet light by lacquer films—1423(A)
Davis, Bergen. Limiting resolving power of a crystal grating—209(L)
——— (see Barnes, A. H.)—1433(A)
Davis, G. E. and Gilbert Greenwood. Changes in the specific resistance of aluminum—1429(A)
Deming, W. Edwards. Application of least squares—665(A)
Dempster, A. J. Deflection of hydrogen positive rays by calcite—298(A)
——— Reflection of positive ions by crystals—1405(L)
Dennison, David M. Book review—874
Dershem, Elmer. Index of refraction and absorption coefficient of gold for the $K\alpha$ line of carbon—128(A)
——— **and Marcel Schein.** Intensity of reflection of the $K\alpha$ line of carbon from a quartz surface—292(A)
Dewey, Jane M. Intensity maxima in the continuous helium spectrum—155
——— Stark effect near the series limit—1439(A)
Dickinson, Roscoe G. and S. Stewart West. Raman spectra from sulfur dioxide—1126(L)
Dieke, G. H. (see Wood, R. W.)—1355
Dillinger, Joy F. (see Bozorth, Richard M.)—733
Donal, John S., Jr. Studies of abnormal shot effect in gaseous discharges—1430(A)
Dow, M. T. (see Drake, F. H.)—613
Drake, F. H., G. W. Pierce and M. T. Dow. Measurement of the dielectric constant and index of refraction of water and aqueous solutionsof KCl at high frequencies—613
Dryden, H. L. and G. C. Hill. Wind pressure on cylindrical stacks—1416(A)
——— (see Briggs, L. J.)—1416(A)
Duffendack, O. S. and L. B. Headrick. Collisions of the second kind and their effect on the field in the positive column of a glow discharge in mixtures of the rare gases and mercury vapor—1421(A)
——— (see Thomas, C. H.)—72

DuMond, Jesse and Harry Kirkpatrick. Multiple crystal x-ray spectrograph—136(A)
——— (see Kirkpatrick)—136(A)
Duncan, D. C. (see Davey, W. P.)—1423(A)
Dunham, J. L. Intensities of vibration-rotation bands with special reference to those of HCl—1347
Dunnington, Frank G. (see Lawrence, Ernest O.)—134(A), 396
Eckart, Carl. Boundary conditions in wave mechanics—1298(L)
——— Penetration of a potential barrier by electrons—1303
Edwards, R. L. and G. W. Stewart. Dependence of viscosity in liquids upon the molecular space arrangement as shown by x-ray diffraction—291(A)
Ellett, A. Specular reflection of atoms from crystals—293(A)
——— Effect of hyperfine structure due to nuclear spin on polarization of resonance radiation—588
Ellis, Joseph W. Doublets in the vibration spectrum of cyclohexane—437(L)
——— Spectroscopic evidence of two types of ammonia molecule—595
Ellwood, W. B. Spontaneous temperature changes accompanying magnetization in steel—1440(A)
Estey, Roger S. New measurements in the fourth positive CO bands—309
Fagan, H. D. and T. R. D. Collins. Peltier and Thomson effects for bismuth crystals—421
Farnsworth, H. E. Certain effects accompanying electron diffraction—1131(L)
——— Satellites of electron diffraction beams—1432(A)
Feather, N. On the distribution in time of the scintillations produced by the alpha-particles from a weak source—705
——— Concerning the absorption method of investigating β-particles of high energy: the maximum energy of the primary β-particles of mesothorium 2—1559
Findlay, J. H. Spark spectrum of cobalt (Co II)—1420(A)
Foard, Castle W. Electron energy losses in mercury vapor—293(A), 1187
Foote, Paul D. (see Smith, W. O.)—1416(A)
Fox, Gerald W. Oscillations in the glow discharge in neon—1066
Fox, G. W. (see Headrick, L. B.)—1033
Freed, Simon and Frank H. Spedding. A comparison of the reflection spectra of $SmCl_3 \cdot 6H_2O$ at room temperature and at that of liquid air with its absorption spectra at low temperatures 212(L)
Freed, Simon and Frank H. Spedding. Paschen-Back effect on the line spectra of solids—1408(L)
Froman, Darol K. Young's modulus determined with small stresses—120(A), 264
Galli-Shohat, N. On the question of aberration of the light from terrestrial sources and its application to the experiment of Esclangon—664(A)
——— Suggested explanation of Michelson-Morley-Miller experiment—1418(A)
Gartlein, C. W. Book review—871
Gaviola, E. On the concentration of metastable mercury atoms—1226
Ghosh, P. N., P. C. Mahanti and B. C. Mukkerjee. Vibrational quantum analysis of the blue-green bands of magnesium oxide—1491
Gibbs, R. C. (see Shapiro, C. V.)—1422(A)
Gillespie, Louis J. A test of the Dalton-Gibbs law of partial pressures—1435(A)
Gingrich, Newell S. Double crystal spectra of scattered x-rays—1444(A)
Glasser, Otto and V. B. Seitz. Measurement of the intensity of gamma-rays of radium in r-units—1432(A)
Goetz, Alexander. On mechanical and magnetic factors influencing the orientation and perfection of bismuth single-crystals—193
Goucher, F. S. Contact resistance and microphonic action—1429(A)
Goudsmit, S. A remark, on hyperfine structure—436(L)
——— Predictions of manganese hyperfine structure—440(L)
——— An extension of Houston's and Slater's multiplet relations—1325
——— **and R. F. Bacher.** Relations between hyperfine structure separations—127(A)
——— **and R. F. Bacher.** Paschen-Back effect of hyperfine structure—129(A)
——— **and L. A. Young.** Magnetic moment of the lithium nucleus—1418(A)
Greenwood, Gilbert. (see Davis, G. E.)—1429(A)
Gunn, Ross. Electrodynamic damping in pulsating stars—107, 295(A)
——— On the anomalous rotation of the sun—635
Gutheil, C. M. (see Bergstein, Milton)—1425(A)
Hafstad, L. R. (see Tuve, M. A.)—66, 1406(L)
Hall, Harvey and J. R. Oppenheimer. Why does molecular hydrogen reach equilibrium so slowly?—132(A)
Hamer, Richard. Transient earth currents accompanying the recent Newfoundland earthquake of 1929—656(A)
Hamburger, F., Jr. Polar molecules—their contribution to energy loss—657(A), 1119

Hammond, H. E. E.m.f., resistance and capacitance phenomena in photovoltaic cells containing Grignard reagents—998

Hardy, J. D. A theoretical and experimental study of the resonance radiometer—662(A)

Harkins, William D. Atomic stability as related to nuclear spin—434(L)

——— **and A. E. Schuh.** Frequency of occurrence of the disintegrative-synthesis of oxygen 17 from nitrogen 14 and helium—130(A), 809

Harnwell, Gaylord P. Note on electron scattering in atomic and molecular hydrogen—285(L)

Harrington, M. C. (see Uyterhoeven, W.)—124(A), 438(L), 1421(A)

Harrison, George R. Equivalent temperatures in the electric arc as measured by multiplet intensities—133(A)

——— A 21 ft. vacuum spectrograph for intensity measurements in the Schumann region—1443(A)

——— (see Leighton, Philip A.)—134(A)

Harrison, J. R. Excitation of overtones of shear vibrations in Y-cut quartz plates—1417(A)

Hart, O. P. and O. Stuhlman, Jr. Relative intensities of arc and spark lines of the electrodeless discharge in mercury vapor—1437(A)

Harvey, A. and F. A. Jenkins. Blue-green absorption bands of Li_2—132(A), 789

Harvey, G. G. and G. E. M. Jauncey. Electron distribution in the chlorine ion—1427(A)

Headrick, L. B. and G. W. Fox. New measurements on the fourth positive bands of carbon monoxide—1033

——— (see Duffendack, O. S.)—1421(A)

Heaps, C. W. (see Bryan, A. B.)—298(A)

Herzfeld, Karl F. Surface heat of charging—248

——— Book reviews—1137, 1411, 1412

Hesthal, Cedric E. Intensity relations in some of the stronger multiplets of chromium I and chromium II—126(A)

Hidnert, Peter. Thermal expansion of Carboloy—120(A)

——— **and W. T. Sweeney.** Thermal expansion of lead—296(A)

——— **and W. T. Sweeney.** Thermal expansion of copper-nickel-tin alloy—667(A)

Hill, E. L. (see Almy, G. M.)—124(A)

Hill, G. C. (see Dryden, H. L.)—1416(A)

Hodgman, Charles D. Transmission of ultraviolet radiation by lake water—1423(A)

Hoffacker, J. V. Construction of a master clock with light controlled contacts—121(A)

Hollabaugh, Cleveland B. An x-ray determination of crystal orientation in silver sheet, produced by cold rolling—1426(A)

Holmes, F. T. Temperature shift of spectral lines and pole effect in vacuum arc—652(L)

Hootman, James A. and W. S. Nelms. Radioactivity of Stone Mountain—1431(L)

Hopfield, John J. Absorption and emission spectra in the region λ600–1100—1133(L)

——— Ionization potential of carbon—1586(L)

Houston, William V. Method of calculating complex spectra—136(A)

——— Quantum theory of the photoelectric and thermionic effects in metals, (title)—1414

Howe, Carl E. The *L* series spectra of the elements from calcium to zinc—717

——— A vacuum spectrograph for the precision measurement of x-rays of long wave-lengths—1428(A)

Howell, Lynn G. (see Johnston, Morris)—274

Hubbard, J. C. Methods of acoustic interferometry for the measurement of velocity and absorption of sound in gases—1442(A)

Huggins, M. L. and Ruth Parrish. Valence electrons in the diamond—136(A)

Hughes, A. L. and J. H. McMillen. Angle and energy distribution of electrons rebounding from gaseous molecules—1438(A)

——— (see Jauncey, G. E. M.)—1439(A)

Hulburt, E. O. Ionization in the upper atmosphere variation with longitude—240

——— Zodiacal light and the gegenschein as phenomena of the earth's atmosphere—295(A), 663(A), 1098

——— On the theory of the solar corona—297(A), 1379

——— Spectra of gases lighted with strong discharges—1420(A)

——— Ultraviolet light theory of auroras and magnetic storms—1587(L)

——— Book reviews—1410

Hull, H. L. (see Barnes, A. H.)—1433(A)

Hummel, A. (see Kunz, J.)—123(A)

Hyman, Hugh H. Resonance of $(B-A)$ bands of the hydrogen molecule—1419(A)

Inglis, D. R. (see Laporte, O.)—1337

Ives, Herbert E. Pictures in relief made with a large diameter lens—1424(A)

——— **and H. B. Briggs.** Photoelectric properties of extremely thin films of alkali metals—669(A)

Jauncey, G. E. M. and A. L. Hughes. An attempt to detect collisions between photons—1439(A)

——— (see Harvey, G. G.)—1427(A)

Jenkins, F. A. Fine structure of the beryllium fluoride bands—315

——— (see Harvey, A.)—132(A), 789

Johnson, J. R. (see Shapiro, C. V.)—1422(A)

Johnson, Thomas H. Reflection of hydrogen atoms from crystals of lithium fluoride—650(L), 658(A)

Johnson, Thomas H. Photographic record of first order diffraction of H atoms by a lithium fluoride crystal—1299(L), 1444(A)
——— An attempt to detect de Broglie waves of hydrogen atoms—1432(A)
Johnston, Helen (see Urey, Harold C.)—869(L)
Johnston, Norris and Lynn G. Howell. Sedimentation equilibria of colloidal particles—274
Kaplan, C. and F. D. Murnaghan. On the fundamental constitutive equations in electromagnetic theory—763
Kaplan, Joseph. Heat of dissociation of oxygen—436(L)
——— Afterglow in air—600
——— Heat of dissociation of carbon monoxide—957
——— A new system of bands in CO—1298(L)
Karapetoff, Vladimir. Relativity transformation of an oscillation into a traveling wave, and de Broglie's postulate in terms of velocity angle—127(A)
Kassel, Louis S. Persistence of velocity and the theory of second order gas reactions—261
——— Equilibrium between matter and radiation—778
Kemble, E. C. Book reviews—566, 1018
Kennard, E. H. Shatter oscillations, their nature and theory—428
—— On the reason for Pauli's exclusion principle—1127(L)
Kennard, Ralph B. Motion of positive ions through gases—1129(L)
Kettering, C. F., L. W. Shutts and D. H. Andrews. A representation of the dynamic properties of molecules by mechanical models—1422(A)
Kievit, Ben Jr. and Geo. A. Lindsay. Fine structure in *K* x-ray absorption spectra—292(A)
Killian, Thomas J. Uniform positive column of an electric discharge in mercury vapor—1238
King, A. S. and R. T. Birge. Carbon isotope, mass 13—133(A)
Kinsey, E. L. Effect of dilution upon the Raman spectra of nitric acid—284(L)
Kirkpatrick, Harry (see DuMond, Jesse)—136(A)
——— **and Jesse DuMond.** Adjustments and tests of the multiple crystal x-ray spectrograph—136(A)
Knipp, Charles T. (see Sparks, F. M.)—259, 297(A)
Knowles, D. D. and S. P. Sashoff. Grid glow tube relays—1431(A)
Korff, S. A. Scattering of light in sodium vapor—435(L)
——— **and J. L. Nickerson.** Absorption of sodium vapor in the extreme ultraviolet—1433(A)
Kovarik, Alois F. Disintegration constant of actinouranium and ratio of actinium to uranium—1432(A)
Kozanowski, H. N. Shot effect of the emission from oxide cathodes—1430(A)
Kuhn, Jackson G. (see Bedell, Frederick)—657(A)
Kunz, Jakob. A relation between the Compton effect and the diffraction by electrons—129(A)
——— Torsion of rhombic prisms and of cylinders in the elastic and plastic state—1417(A)
——— **and A. Hummel.** Ionization efficiency of electrons in potassium vapor—123(A)
——— (see Tykocinski-Tykociner, J.)—1436(A)
Lane, C. T. Magnetic susceptibility of rubidium—977
Lang, R. J. and R. A. Sawyer. Spectrum of singly ionized indium—126(A)
——— Second spark spectrum of antimony and a note on the first spark spectrum of tin—445
——— Spectrum of doubly-ionized antimony—664(A)
Langer, R. M. Generalization of the Rydberg formula—649(L)
Langmuir, Irving, Sauders MacLane and Katharine B. Blodgett. Effect of end losses on the characteristics of filaments of tungsten and other materials—478
Laporte, Otto. On the origin of the line absorption spectra of the rare earths—130(A)
——— **and D. R. Inglis.** Resonance separations in configurations of type p^5s and d^9s—1337
Lawrence, Ernest O. and Frank G. Dunnington. On the early stages of electric sparks—134(A), 396
——— **and Leon B. Linford.** Effect of intense electric fields on the photoelectric behavior of thin potassium films—1421(A)
Leighton, Philip A. and George R. Harrison. Photographic photometry in the extreme ultraviolet—134(A)
Lewis, Gilbert N. Quantum kinetics and the Planck equation—1533
Lind, S. C. Book review—1301
——— The origin of O^{17}—1408(L)
Lindsay, Geo. A. (see Kievit, Ben Jr.)—292(A)
Lindsay, R. B. An acoustical analogy of the Schrodinger wave equation—666(A)
Linford, Leon B. (see Lawrence, Ernest O.)—1421(A)
Loeb, Leonard B. Ionic mobilities in Cl_2 and in Cl_2-air mixtures—137(A), 184
Loomis, F. W. Iodine fluorescence in the infrared—662(A)
Lord, James O. (see Blake, F. C.)—660(A)
Lowry, E. F. Function of the base metal in oxide-coated filaments—121(A)

Lowry, E. F. Phenomena in oxide-coated filaments—668(A)
——— Role of the core metal in oxide-coated filaments—1367
Lowry, W. Norwood. Location of the electromotive force in the photovoltaic cell—1270
Luhr, Overton. Recombination of ions in air and oxygen in relation to the nature of gaseous ions—1394
Lunn, E. G. and F. R. Bichowsky. Collision diameter of the hydrogen atom—563(L)
——— **and F. R. Bichowsky.** Scattering of atomic hydrogen by gases: mercury, argon, oxygen and iodine—671(A)
McAlister, E. D. Concerning the existence of a new term in Hg I—1585(L)
McCracken, E. C. An electrical method of determining the gelation temperature of starch—1423(A)
McFarlan, Ronald L. An x-ray study of molecular orientation in the Kerr effect—211(L)
——— Effect of an electric field on the x-ray diffraction pattern of a liquid—1426(A), 1469
McKeehan, L. W. Magnetoresistance and elastoresistance in permalloy—657(A)
——— Book reviews—654, 1017
McMillen, J. H. (see Hughes, A. L.)—1438(A)
Mack, J. E. and R. A. Sawyer. Sodium and magnesium spark lines in the far ultraviolet, and the quantitative application of the irregular doublet law to isoelectronic sequences—299, 661(A)
——— Book review—118
——— (see Condon, E. U.)—579
MacLane, Saunders (see Langmuir, Irving)—478
Mahanti, P. C. (see Ghosh, P. N.)—1491
Maris, H. B. Carbon dioxide theory of the ice ages—1016(L)
Martin, John R. (see Miller, Dayton C.)—1417(A)
Marx, Erich. On a new photoelectric effect in alkali cells—1059
Maxwell, Louis R. Comet tail bands of carbon monoxide—665(A)
Meggers, William F. and Bourdon F. Scribner. Regularities in the spectra of lutecium—1420(A)
——— **and A. G. Shenstone.** Spark spectrum of ruthenium—868(L)
Mendenhall, C. E. Influence of surface conditions on the photoelectric effect, (title)—1414
Meyer, A. Wesley. X-ray scattering by mixtures of organic liquids—291(A)
Miller, Dayton C. and John R. Martin. Influence of the walls enclosing a sounding air column upon the tone quality—1417(A)
Miller, W. Lash. Book review—566
Milikan, R. A. Most probable 1930 values of the electron and related constants—1231, 1433(A)
Milne, W. E. Numerical determination of characteristic numbers—863
Mitchell, Allan C. G. Polarization of sensitized fluorescence—1422(A)
——— (see Bramley, A.)—1419(A)
Mohler, F. L. Photoelectric ionization of gases, (title)—1414
Mohler, F. L. and C. Boeckner. Effect of gases on ionization of caesium by line absorption—664(A)
Morse, Philip M. Quantum mechanics of electrons in crystals—1310
——— (see Stueckelberg, E. C. G.)—116(L), 659(A)
Mortimore, Roy H. Measurement of the intensity of high frequency magnetic fields—753
Mott-Smith, L. M. Possibility of determining the energy of the cosmic beta-particles by magnetic deflection—1125(L)
Mouzon, J. Carlisle (see Sutton, Richard M.)—694
Mukkerjee, B. C. (see Ghosh, P. N.)—1491
Mulder, Peter J. and Joseph Razek. Further experiments with an automatic photoelectric spectrophotometer—1424(A)
——— **and Joseph Razek.** Measurement of the variation in intensity of the helium lines with voltage by means of selected filters and a photoelectric cell—1442(A)
——— (see Razek, Joseph)—1423(A)
Murdock, Carleton C. Form of the x-ray diffraction bands for regular crystals of colloidal size—8
Murnaghan, F. D. (see Kaplan, C.)—763
Murphy, Edgar J. (see Allison, Fred)—124(A), 285(L)
Muskat, Morris. Dispersion formula and Raman effect for the symmetrical top—1442(A), 1262
——— Distribution of nonreacting fluids in the gravitational field—1384, 1415(A)
——— Scattering of alpha-rays and high speed electrons in radial fields—1583(L)
Nadai, A. Some applications of the theory of plastic deformations of ductile metals—1418(A)
Naudé, S. M. An isotope of nitrogen, atomic weight 15—130(A)
Nelms, W. S. (see Hootman, James A.)—1431(A)
Nicholas, Warren W. Efficiency of production of continuous spectrum x-rays—128(A)
Nichols, W. A. Jr. (see Rodebush, W. H.)—649(L).
Nickerson, J. L. (see Korff, S. A.)—1433(A)
Nordheim, L. W. A theory of the resistance of alloys—1430(A)
Normand, C. E. Absorption coefficient for slow electrons in gases—1217
——— **and R. B. Brode.** Absorption coefficient for slow electrons in gases—1438(A)
Nottingham, W. B. Effective photoelectric work function reduced by weak accelerating fields—669(A)

Nottingham, W. B. Influence of accelerating fields on the photoelectric and thermionic work function of composite surfaces—1128(L)

Nusbaum, C. Radial-asterism in multi-crystalline materials—1426(A)

Nutting, F. L. Position and width of the modified line of the spectrum of scattered x-rays—661(A)

Olpin, A. R. Effect of red light on stopping potentials of photoelectrons liberated by blue light—112(L)

——— Validity of Einstein's photoelectric equation for red sensitive sodium compounds—670(A)

——— Selective maxima in the spectral response curves of light-sensitive compounds as a function of valence—671(A)

Olshevsky, D. E. Molecular beams in electromagnetic fields—659(A)

——— Alloys for vacuum-light glass-metal joints—1424(A)

Olson, Howard. An observed periodicity in the packing fraction—213(L)

Onsager, L. Simultaneous irreversible processes—666(A)

Oppenheimer, J. R. Note on the theory of the interaction of field and matter—461

——— On the theory of electrons and protons—562(L)

——— Two notes on the probability of radiative transitions—939

——— (see Hall, Harvey)—132(A)

Ornstein L. S. and G. E. Uhlenbeck. On the theory of the Brownian motion—1434(A)

Osgood, Thomas H. Photoelectric effect and the J phenomenon—1407(L)

Ostensen, Floyd C. Voltage intensity of $\lambda 2537$ in mercury—286(L)

Page, Leigh—Book reviews—287, 1135

——— **and William W. Watson.** Nuclear electrons—1584(L)

Parrish, Ruth (see Huggins, M. L.)—136(A)

Peek, R. L. Jr. On the solution of certain cases of the general equation of diffusion—554

Perry, Charlotte, T. and E. L. Chaffee. A direct measurement of the velocity of cathode rays—1437(A)

Pfund, A. H. Bismuth-black and its applications—1434(A)

——— (see Barnes, R. Bowling)—1434(A)

Phipps, T. E. (see Shaw, E. J.)—1126(L)

Pielemeier, W. H. Absorption and velocity of high frequency sound in oxygen—1417(A)

Pierce, G. W. (see Drake, F. H.)—613

Pietenpol, W. B. and **H. H. Scott.** Surface tension of molten glass at temperatures near the melting point—296(A)

Plyler, E. K. and Theodore Burdine. Infrared absorption of some organic liquids—605

Pool, M. L. Life and radius of the metastable mercury atom—1419(A)

Pooler, Louis Gordon. Velocity of propagation of longitudinal waves in liquids at audio-frequencies—832

Poulter, Thos. C. A glass window mounting for withstanding pressures of 30,000 atmospheres—297(A)

Ramberg, E. (see Richtmyer, F. K.)—661(A), 1428(A)

Randall, Robert H. Mean lives of lines of mercury triplet 2^3P_{012}—2^3S_1—1161

——— **and Harold W. Webb.** Average lives of lines of mercury triplet 2^3P—2^3S—665(A)

Rashevsky, N. Thermodynamics of systems with several equilibria—666(A)

——— A thermodynamic theory of excitation of nerves—1435(A)

Razek, Joseph and Peter J. Mulder. Measurement of intensity of helium lines with voltage using a photoelectric device—1423(A)

——— (see Mulder, Peter J.)—1424(A), 1442(A)

Reid, Charles D. Some investigations into the velocity of sound at ultrasonic frequencies using quartz oscillators—814

Reyerson, L. H. Book review—1138

Reynolds, Neil B. Schottky effect and contact potential measurements on thoriated tungsten filaments—158

Rice, O. K. A contribution to the quantum mechanical theory of radioactivity and the dissociation by rotation of diatomic molecules—1538

——— Perturbations in molecules and the theory of predissociation and diffuse spectra. II.—1551

Richardson, D. E. Resistance of an electrolytic conductor at various frequencies—297(A)

Richtmyer, F. K. and E. Ramberg. Satellites of $K\alpha$ for the elements Ni(28) to As(33)—661(A)

——— **S. W. Barnes and E. Ramberg.** A direct-reading two-crystal spectrometer for x-rays—1428(A)

——— (see Barnes, S. W.)—661(A)

——— Photoelectric multiple ionization by x-rays, (title)—1414

Rinke, J. F. (see Bergstein, Milton)—1425(A)

Ritschl, R. (see White, H. E.) 208 (L), 1146.

Roberts, O. L. An x-ray study of very pure iron—1426 A

Robertson, H. P. A general formulation of the uncertainty principle and its classical interpretation—667(A)

Rodebush, W. H. Third law of thermodynamics—210(L)
——— **and W. A. Nichols Jr.** Atomic oxygen as a reducing agent—649(L)
——— **(see Shaw, E. J.)**—1126(L)
Roebuck, J. R. Porous plug measurements with air—121(A)
——— Book review—871
Rojansky, Vladimir. On the interaction of Stark effect and electron spin in alkali atoms—782
Rollefson, R. A possible origin of the band at 2540 in the spectrum of mercury vapor—1177
——— (see Winans, J. G.)—1436(A)
Roller, Duane. Photoelectric behavior of solid and liquid mercury—122(A)
Ruedy, Richard. On the active nitrogen glow—125(A)
——— Rectifier characteristics and detection diagrams—129(A)
——— Changes in the ozone concentration of the atmosphere—295(A)
Sabine, Paul E. Book review—1017
Salant, E. O. and A. Sandow. On the vibration frequencies of HCl and HBr in the liquid state—214(L)
Salkover, Meyer. Unified field-theory and Schwarzschild's solution—I 209(L), II 214(L)
Sandow, A. (see Salant, E. O.)—214(L)
Sashoff, S. P. (see Knowles, D. D.)—1431(A)
Sawyer, C. B. and C. H. Tower. Rochelle salt as a dielectric—269
Sawyer, R. A. Excitation processes in the hollow cathode discharge—1421(A)
——— (see Mack, J. E.)—299, 661(A)
——— (see Lang, R. J.)—126(A)
Sawyer, R. B. Reflection of lithium ions from metal surfaces—124(A), 1090
Schein, Marcel (see Dershem, Elmer)—292(A)
Schuh, A. E. (see Harkins, William D.)—130(A), 809
Schwingel, Christion H. and John Warren Williams. Variation dielectric constant with temperature. I. Electric moments of the carbon bisulphide and nitrous oxide molecules-855
Scott, Arnold H. Time lag in changes of electrical properties of rubber with temperature and pressure 1429 (A)
Scott, H. H. (see Pietenpol, W. B.)—296(A)
Scott, R. B. and F. G. Brickwedde. Apparatus for maintaining constant low temperatures—670(A)
——— (see Brickwedde, F. G.)—670(A)
Scribner, Bourdon F. (see Meggers, William F.)—1420(A)
Seitz, V. B. (see Glasser, Otto)—1432(A)
Shapiro, C. V., R. C. Gibbs and J. R. Johnson. Electronic transitions in the spectra of benzene—1422(A)
Shapiro, C. V. (see Almasy, F.)—1422(A)
Shaw E. J., T. E. Phipps, and W. H. Rodebush. Magnetic moment of the sulfur molecule—1126(L)
Shearin, P. E. Relation between the intensity and position of the overtones of some organic liquids—973
Shenstone, A. G. A surplus level in the arc spectrum of palladium—1420(A)
——— (see Meggers, W. F.)—868(L)
Shortley, G. H. (see Condon, E. U.)—1342, 1419(A)
Shutts, L. W. (see Kettering, C. F.)—1422(A)
Sillers, Frederick Jr. An instrument for high-voltage x-ray spectrography and radiography—1428(A)
Sixtus, K. J. and L. Tonks. Propagation of large Barkhausen discontinuities along wires—1441(A)
Skinner, E. W. Diffraction of x-rays in liquids and the effect of temperature—128(A)
Slack, Francis G. Hydrogen atom in the Stark effect—1170
Slater, J. C. Note on Hartree's method—210(L)
——— Cohesion in monovalent metals—509
Smith, Lloyd P. Emission of positive ions from tungsten and molybdenum—381
——— Effect of positive ion shot effect on space charge limited electron currents—1430(A)
Smith, Philip T. and John T. Tate. Ionization of helium and neon by electron impact—1438(A)
Smith, Stanley. An extention of the spectrum of Tl II—235
Smith, W. O., Paul D. Foote and P. F. Busang. Capillary retention of liquids in assemblages of homogeneous spheres—1416(A)
Smyth, H. D. and E. G. F. Arnott. Excitation of certain nitrogen bands by positive ion impact—126(A)
Snow, C. P. Excited radicals in chemical compounds—563(L)
Southard, John C. (see Andrews, Donald H.)—670(A)
Sparks, F. M. and Charles T. Knipp. Change of spacing of positive column striations with temperature—259, 297(A)
Spedding, Frank H. (see Freed, Simon)—212(L), 1408(L)
Stauffer, L. H. Electro-optical modifications of light waves—1440(A)
Stearns, J. C. An x-ray search for the origin of ferromagnetism—1,292(A)
Stern, Otto. Diffraction of molecules—298(A)
Stevenson, E. C. (see Beams, J. W.)—1440(A)
Stewart, G. W. Extent of noticeable cybotactic condition in a liquid as exhibited by triphenolmethane—291(A)
——— Two different types of association of alcohol molecules in the liquid state—296(A)

Stewart, G. W. The cybotactic (molecular group) condition in liquids; the nature of the association of octyl alcohol molecules—726
——— Problems suggested by an uncertainty principle in acoustics—1441(A)
——— X-ray diffraction in water 2 to 98°C: Nature of molecular association—1426(A)
——— (see Edwards, R. L.)—291(A)
Stewart, O. M. Book review—287
Street, J. C. Time lags in spark discharges at high overvoltages—1437(A)
——— (see Beams, J. W.)—658(A)
Stueckelberg, E. C. G. and Philip M. Morse. Recombination of electron and alpha-particle—116(L)
——— **and Philip M. Morse.** Recombination of hydrogen-like atoms—659(A)
Stuhlman, O. Jr. (see Hart, O. P.)—1437(A)
——— **M. D. Whitaker and M. L. Braun.** High-frequency electrodeless discharge characteristics—1436(A)
Sutton, Richard M. and J. Carlisle Mouzon. Ionization of helium by potassium positive ions—694
Swann, W. F. G. Relativity and aether drift—127 (A), 336
Sweeney, W. T. (see Hidnert, Peter)—296(A), 667(A)
Swenson, H. N. Intensity measurements in neon spectrum—126(A)
Szczeniowski, S. Spatial distribution of photoelectrons—122(A), 347
Tanberg, R. On the cathode of an arc drawn in vacuum—294(A), 1080
Tate, John T. (see Bleakney, Walker)—658(A)
——— (see Smith, Philip T.)—1438(A)
Taylor, A. M. Molecular agregation—668(A)
Taylor, John B. Reflection of beams of the alkali metals from crystals—375
Thomas, Ancil R. Absorption of resonance radiation in mercury vapor—1253
Thomas, C. H. and O. S. Duffendack. Anode spots and their relations to the absorption and emission of gases by the electrodes of a Geissler discharge—72
Thompson, James S. Slow caesium ions in hydrogen and helium—123(A)
——— Motion of slow positive ions in gases—1196
Thibaud, Jean. On the reflection of the $K\alpha$ line of carbon from a glass mirror—1452
Tolman, Richard C. On the use of the energy-momentum principle in general relativity—875
——— On the use of the entropy principle in general relativity—896
Tolman, Richard C. On the weight of heat and thermal equilibrium in general relativity—904
——— Book reviews—568, 1302
Todd, F. C. and T. E. Browne, Jr. Restriking of short a. c. arcs—1441(A)
——— (see Browne, T. E. Jr.)—1441(A)
Tonks, L. (see Sixtus, K. J.)—1441(A)
Tower, C. H. (see Sawyer, C. B.)—269
Trivelli, A. P. H. Quantum theory of x-ray exposures on photographic emulsions—662(A)
Tuve, M. A., G. Breit and L. R. Hafstad. Application of high potentials to vacuum-tubes—66
——— Multiple coincidences of Geiger-Muller tube-counters—651(L)
——— (see Breit, G.)—51
——— L. R. Hafstad, and O. Dahl. High-voltage tubes—1406(L)
Tykocinski-Tykociner, J. and Jakob Kunz. Striations and magnetic effect in electrodeless discharges—1436(A)
Tyndall, E. P. T. Growth of zinc crystals—868(L)
——— **and W. W. Wertzbaugher.** Magnetic properties of thin films of cobalt—292(A)
Uhlenbeck G. E. On the principle of Huyghens—1439(A)
——— (see Ornstein, L. S.)—1434(A)
Urey, Harold C. and Helen Johnston. Regularities in radioactive nuclei—869(L)
Uyterhoeven, W. and M. C. Harrington. Secondary emission from metals by impact of metastable atoms and positive ions—124(A), 438(L)
——— **and M. C. Harrington.** Secondary emission from nickel in neon discharge—1421(A)
Valasek, J. Structure of certain K series emission lines—291(A)
——— Book reviews—567, 1410
Vallarta, M. S. Unified field theory and Schwarzschild's solution: a reply—435(L)
Van Voorhis, C. C. and K. T. Compton. Heating of a cathode by positive gas ions, and their "accommodation coefficient"—1438(A)
Verman, Lal C. Reflection of radio waves from the surface of the earth—1425(A)
Villars, D. S. and E. U. Condon. Predissociation of diatomic molecules from high rotational states—1028
——— Book review—1136
Vonwiller, O. U. Intensity measurements in the arc spectrum of thallium—802
Wagner, Paul Berthold. Secondary electrons of high velocity from metals bombarded with cathode rays—98
Wahlin, H. B. Motion of electrons in carbon monoxide—122(A), 1568

Wahlin, H. B. Emission of positive ions from thoriated tungsten—653(L)

Warburton, F. W. Will the magnetic pole vanish? —292(A)

Ware, L. A. Thomson effect in zinc crystals—667 (A), 989

Waterman, A. T. Density distribution of electron gas in equilibrium with a hot body—668(A)

Watson, William W. (see Page, Leigh)—1584(L)

——— **and William Bender.** Zeeman effect in the calcium hydride band spectra—1440(A), 1513

Webb, Harold W. (see Randall, R. H.)—665(A)

Weeks, Isabel C. Effect of hydrogen ion concentration on the measurement of the mean particle size of emulsions—668(A)

Wegel, R. L. Book review—874

Weld, LeRoy D. Analysis of cosmic-ray observations—295(A)

Wells, P. V. Flarimeter: a clinical instrument for testing circulatory fitness—1418(A)

Wentzel, G. Velocity distribution of x-ray photoelectrons, (title)—1414

Wertzbaugher, W. W. (see Tyndall, E. P. T.)—292(A)

West, S. Stewart (see Dickinson, Roscoe G.)—1126(L)

Whitaker, M. D. (see Stuhlman, Otto Jr.)—1436(A)

White, H. E. Nuclear spin and hyperfine structure—441, 664(A)

——— **and R. Ritschl.** Hyperfine structure in the spectra of neutral manganese—208(L)

——— **and R. Ritschl.** Hyperfine structure in neutral manganese, Mn I—1146

Wilkins, T. R. and J. A. Wood. A modification of Wiechert's experiment—657(A)

Williams, John H. (see Allison, Samuel K.)—135 (A), 149, 1476

Williams, John Warren (see Schwingel, Christian H.)—855

Wilson, H. A. Boundary conditions and the meaning of wave groups in wave mechanics—948; reply to criticism—1586(L)

Winans, J. G. and R. Rollefson. Energy of dissociation of normal Cd_2—1436(A)

Wold, P. I. Mass-weight ratio of metals under strain—296(A)

Wollan, Ernest O. Electron distribution in magnesium oxide—127(A), 1019

Wood, J. A. (see Wilkins, T. R.)—657(A)

Wood, R. W. Raman spectra excited by the helium hot-cathode arc and a new type of tube for small volumes of liquid—670(A)

———Plasmoidal high-frequency oscillatory discharges in "non-conducting" vacua—658(A), 673

——— **and G. H. Dieke.** Raman effect in HCl gas—1355

Woodrow, Jay W. and R. M. Bowie. Chemiluminescence of metallic sodium—1423(A)

——— **and H. L. Cunningham.** Absorption spectrum characteristic of vitamin A—125(A)

Workman, E. J. A new method for measuring the variation of specific heats of gases with pressure —667(A)

Wyckoff, Ralph W. G. Reflecting powers of atoms for x-rays of different wave-lengths—215(L)

——— X-ray scattering powers of nickel and oxygen in nickel oxide—583

Wyman, Jeffries Jr. Measurements of the dielectric constants of conducting media—623

Young, L. A. (see Goudsmit, S.)—1418(A)

Zahl, Harold A. Reflection of zinc atoms from NaCl crystals—293(A)

Zahn, C. T. Dielectric constant and the molecular structure of CS_2—848

——— Evidence for quantization from the electric polarization of acetic acid vapor—1047

——— An extension of Van Vleck's theory of dielectric polarization—1056

Zartman, I. F. A direct measurement of molecular velocities—134(A)

Zeleny, John. On the potential relations in the striated positive column of electrical discharges through hydrogen—699

——— Mobilities of ions in moist and dry air—1441(A)

Zimmerman, E. E. Influence of temperature on polarization capacity and resistance—543

Zwicky, F. Inhomogeneities in crystals (a reply)—283(L)

ANALYTIC SUBJECT INDEX TO VOLUME 35

References marked (A) are to abstracts of papers presented at meetings of the American Physical Society, those marked with (L) refer to letters to the Editor.

Aberration of light
From terrestrial sources, N. Galli-Shohat—664(A)

Absorption of light
Hg vapor, resonance radiation, A. R. Thomas—1253
Lacquer films, ultraviolet, W. P. Dewey, D. C. Duncan—1423(A)
Lake water, ultraviolet, C. D. Hodgman—1423(A)
Liquids, near infrared, effect of pressure, J. R. Collins—1433(A)
Na vapor, 300–1300A, S. A. Korff, J. L. Nickerson—1433(A)
Na vapor in flames, C. D. Child—294(A)
Organic liquids, infrared, E. K. Plyler, T. Burdine—605; R. B. Barnes—662(A), 1524
Organic liquids, intensity and position of overtones, P. E. Shearin—973
$SmCl_3 \cdot 6H_2O$, comparison with reflection at high and low temperatures, S. Freed, F. H. Spedding—212(L)
Various bodies, $\lambda > 50\mu$, C. H. Cartwright—415
Vitamin A, characteristic, J. W. Woodrow, H. L. Cunningham—125(A)

Acoustics
Absorption and velocity of high frequency sound in oxygen, W. H. Pielemeier—1417(A)
Absorption and velocity of sound in gases, interferometer method, J. C. Hubbard—1442(A)
Analogue of Schroedinger wave equation, R. B. Lindsay—666(A)
Tone quality, influence of walls—D. C. Miller, J. R. Martin—1417(A)
Uncertainty principle, problems, G. W. Stewart—1441(A)
Velocity in liquids at audio-frequencies, L. G. Pooler—832
Velocity of ultrasonic waves, C. D. Reid—814

Aerodynamics (see also **Hydrodynamics**)
Airfoils of circular cross-section, L. J. Briggs, H. L. Dryden—1416(A)
Wind pressure on cylindrical stacks, H. L. Dryden, G. C. Hill—1416(A)

Afterglow
Air, production and characteristics, J. Kaplan—600
Nitrogen, R. Ruedy—125(A)

Alpha-particles
Recombination with electrons; measurements, A. H. Barnes—217; A. H. Barnes, B. Davis, H. L. Hull—1433(A); explanation, W. Band—1128(L); theory, E. C. G. Stueckelberg, P. M. Morse—116(L), 659(A)
Scattering in radial fields, M. Muskat—1583(L)
Scintillations, time distribution, from weak source, N. Feather—705

Anode spots
In Geissler tube, relation to absorption and emission of gases, C. H. Thomas, O. S. Duffendack—72

Arcs (see also **Discharge of electricity in gases, Spark discharge**)
A.c., between brass electrodes, extinction, T. E. Browne, Jr., F. C. Todd—1441(A)
A.c. restriking, F. C. Todd, T. E. Browne, Jr.—1441(A)
Temperature, from multiplet intensities, G. R. Harrison—133(A)
Vacuum, cathode characteristics, R. Tanberg—294(A), 1080
Vacuum, pole effect, temperature shift of spectra, F. T. Holmes—652(L)

Astrophysics
Anomalous rotation of sun, R. Gunn—635
Pulsating stars, electrodynamic damping, R. Gunn—107, 295(A)
Solar corona, theory, E. O. Hulburt—297(A), 1379

Atomic beams
Alkali metals, reflection from crystals, J. B. Taylor—375
Hydrogen, attempt to detect de Broglie waves, T. H. Johnson—1432(A)
Hydrogen, collisions in Hg vapor, radius of atom, E. G. Lunn, F. R. Bichowsky—563(L)
Hydrogen, diffraction by LiF crystal, T. H. Johnson—1444(A); 1299(L)
Hydrogen, reflection from calcite, A. J. Dempster—298(A), 1405(L)
Hydrogen, reflection from LiF crystals, T. H. Johnson—650(L), 658(A)
Hydrogen, scattering by Hg, A, O_2, I_2, E. G. Lunn, F. R. Bichowsky—671(A)

Oxygen, as reducing agent, W. H. Rodebush, W. A. Nichols, Jr.—649(L)
Reflection, specular, from crystals, A. Ellett—293(A)
S, magnetic moment, E. J. Shaw, T. E. Phipps, W. H. Rodebush—1126(L)
Zn, reflection from NaCl, H. A. Zahl—293(A)

Atomic weights
H and He, R. T. Birge—1015(L)
Packing fraction, periodicity, H. Olson—213(L)

Atomization
Mechanism, R. A. Castlemen, Jr.—1014(L), 1416(A)

Atmospheric electricity
Auroras and magnetic storms, theory, E. O. Hulburt—1587(L)
Ionization in upper atmosphere, variation with longitude, E. O. Hulburt—240
Potential gradient in lower atmosphere, variation, J. G. Brown—135(A)
Space charge in lower atmosphere, J. G. Brown—135(A)

Barkhausen effect
Propagation along wires, K. J. Sixtus, L. Tonks—1440(A)
Size of discontinuities, R. M. Bozorth, J. F. Dillinger—733

Beta-particles
From mesothorium 2, maximum energy, N. Feather—1559

Biophysics
Excitation of nerves, theory, N. Rashevsky—1435(A)
Flarimeter, for testing circulatory fitness, P. V. Wells—1418(A)
Vitamin A, absorption of light, characteristic, J. W. Woodrow, H. L. Cunningham—125(A)

Black body
Bismuth-black, properties, A. H. Pfund—1434(A)
For $\lambda > 50\mu$, C. Cartwright—415

Book reviews
Adam, Neil Kensingtion, The Physics and Chemistry of Surface—1411
Belling, John, The Use of the Microscope—1410
Benedicts, C. B., Jetziger Stand der grundlegenden Kentnisse der Thermoelectrizität—1301
Birtwistle, George, La Nouvelle Mecanique des Quanta—654
Born, M., and P. Jordan, Elementare Quantenmechanik—1588
Bruhat, Georges, Traite de Polarimetrie—1410
Chazy, Jean, La Theorie de la Relativite et la Mecanique Celeste—1302
Condon, E. U. and P. M. Morse, Quantum Mechanics—566
Debye, P., Dipolmoment und Chemische Struktur—1412
Einführung in die Geophysik, II, Erdmagnetismus und Polarlicht, Wärme—und Temperaturverhältnisse der Obersten Bodenschichten, Luftelektrizität, von A. Nippoldt, J. Keränen, E. Schweidler—1410
Einführung in die Geophysik, III, Dynamische Ozeanographie, von A. Defant—1410
Einstein, A., Die Grundlage der allgemeinen Relativitätstheorie—568
Ergebnisse der Exakten Naturwissenschaften, Jetziger Stand der grundlegenden Kenntnisse der Thermoelektrizität—1301
Estermann, I., Elektrische Dipolmomente von Molekulen—1412
Eucken, A., Lehrbuch der Chemischen Physik—1137
Flint, H. T., Wave Mechanics, Being One Aspect of the New Quantum Theory—872
Föppl, L., Technische Mechanik—1135
Foster, William, Inorganic Chemistry for Colleges—1138
Fry, Thornton C., Elementary Differential Equations—567
Gortner, R. A., Outlines of Biochemistry—566
Griffith, R. O. and A. McKeown, Photo Processes in Gaseous and Liquid Systems—1301
Handbuch der Experimental Physik, Band VIII, 2 Teil, Warmeausdehnung, Zustandsgrossen und Theorien der Warme—873
Handbuch der Experimental Physik, Band IX, 1 Teil, High and Low Temperature by H. von Wartenberg, Liquefaction of Gases by H. Lenz, Heat Conduction by Oscar Knoblauch and H. Reiher, Heat Radiation by W. Wien and C. Muller—871
Houstoun, R. A., Intermediate Dynamics and Properties of Matter—1135
Hund, F., Molekelbau—1018
Kellogg, O. D., Foundations of Potential Theory—1135
Mason, Max and Warren Weaver, The Electromagnetic Field—287
Molecular Spectra and Molecular Structure. A General Discussion Held by the Faraday Society, September, 1929—874
Müller-Pouillets, Lehrbuch der Physik, 11 aufl., 2 band, Lehre von der Strahlenden Energie (Optik) 2 hälfte, 1 and 2 teil, Karl Wilhelm Meissner, editor—118
Pollard, A. F. C., The Kinematical Design of Couplings in Instrument Mechanisms—871
Robertson, John Kellock, Introduction to Physical Optics—567

Roller, Duane, The Terminology of Physical Science—654
Ruark, Arthur E. and Harold C. Urey, Atoms, Molecules, and Quanta—1136
Ruedy, Richard, Bandenspektren auf experimenteller Grundlage—872
Sack, H., Dipolmoment und Molekularstruktur—1412
Stanley, Douglas, The Science of Voice—874
Stoner, Edmund C., Magnetism—1017
Terry, Earle M., Advanced Laboratory Practice in Electricity and Magnetism—287
Tietjens, O., Hydro-und Aeromechanik, Vol. I—654
Wien-Harms, Handbuch der Experimental Physik Vol. X, G. Hoffman, Das Elektrostatische Feld; W. O. Schumann, Hochspannungstechnik—1411
Watson, F. R., Acoustics of Buildings—1017

Brownian motion
Theory, L. S. Ornstein, G. E. Uhlenbeck—1434(A)

Capillary action (see **Surface tension**)

Cathode rays (see **Electrons**)

Chemical analysis
Magneto-optical method, F. Allison, E. J. Murphy—124(A); application to search for element 87—285(L)

Chemical reactions
Reducing action of atomic oxygen, W. H. Rodebush, W. A. Nichols, Jr.—649(L)
Second order, effect of persistence of velocities. L. S. Kassel—261

Chemiluminescence
Na, effect of moisture, J. W. Woodrow, R. M. Bowie—1423(A)

Clock
Master, with light-controlled contacts, J. V. Hoffacker—121(A)

Cohesion
In monovalent metals, theory, J. C. Slater—509

Collision diameter (see also **Electrons in gases, Ions**)
Of hydrogen atom, E. G. Lunn, F. R. Bichowsky—563(L)

Colloids
Emulsions, particle size, influence of p_H, I. C. Weeks—668(A)
Sedimentation equilibria of particles, N. Johnston, L. G. Howell—274
Gelation temperature of starch, E.C.McCracken—1423(A)

Compton effect (see also **X-rays, diffraction**)
Position and width of modified line, F. L. Nutting—661(A)
Relation to electron diffraction, J. Kunz—129(A)

Conductivity, thermal (see **Thermal conductivity**)

Contact potentials
Thoriated tungsten, N. B. Reynolds—158

Cosmic rays
Analysis of observations, L. D. Weld—295(A)
Method of measuring energy by magnetic deflection, L. M. Mott-Smith—1125(L)
Method of study, M. A. Tuve.—651(L)
Nature, L. F. Curtiss—1433(A)

Crystals and crystal structure
Ag sheet, cold rolled crystal orientation, C. B. Hollabaugh—1426(A)
Alloys containing precipitated crystals, C. S. Barrett—1425(A)
Alloys, magnetic, of high Pt content, microstructure, F. W. Constant—116(L)
Alum, radiation emitted under pressure in electric field, I. A. Balinkin—1443(A)
Bi, methods of forming, factors influencing orientation and perfection effect of magnetic field, A. Goetz—193
Calcite, grating space, C. D. Cooksey, D. Cooksey—564(L)
Colloidal crystals, x-ray diffraction bands, theory, C. C. Murdock—8
Cr-Ni alloys, variables, F. C. Blake, J. O. Lord—660(A)
Electron distribution, theory, P. M. Morse—1310
Fe, radial asterism, C. Nusbaum—1426(A)
Fe, very pure, x-ray study, O. L. Roberts—1426(A)
$GdCl_3 \cdot 6H_2O$, line spectra, Paschen-Back effect, S. Freed, F. H. Spedding—1408(L)
Ice, grown from vapor, J. M. Adams—136(A)
Inhomogeneities, theory, R. H. Canfield—114(L); reply, F. Zwicky—283(L)
Mosaic crystals of elements, R. H. Canfield—671(A)
Possible symmetries, R. H. Canfield—660(A)
Stability of lattices, theory, R. H. Canfield—530
Unit lattice of interpenetrating lattices, example, F. C. Blake—660(A)
Zn, method of growth, E. P. T. Tyndall—868(L)

Cybotactic State
Alcohols, G. W. Stewart—296(A), 726
Liquids, organic, mixtures, A. W. Meyer—291(A)
Liquids, organic, temperature effect, E. W. Skinner—128(A)
Resumé of evidence, A. M. Taylor—668(A)
Triphenolmethane, G. W. Stewart—291(A)
Viscosity relations, R. L. Edwards, G. W. Stewart—291(A)

Water, molecular association, G. W. Stewart—1426(A)
Dielectric constant and properties
Acetic acid vapor, C. T. Zahn—1047
Conducting media, J. Wyman, Jr.—623
CS_2 and NO, temperature variation, electric moments, C. H. Schwingel, J. W. Williams—855
CS_2 vapor, C. T. Zahn—848
Energy losses, effect of polar molecules, F. Hamburger, Jr.—657(A), 1119
H_2O and KCl solutions, high frequencies, F. H. Drake, G. W. Pierce, M. T. Dow—613
KCl solutions, A. Austin—1428(A)
Polarization, extension of Van Vleck's theory, C. T. Zahn—1056
Rochelle salt, temperature effect, C. B. Sawyer, C. H. Tower—269
Rubber, temperature and pressure variation, time lag, A. H. Scott—1429(A)
Tung oil, polarization and electric moment, A. A. Bless—1442(A)
Diffraction of atoms (see **Atomic beams**)
Diffraction of electrons (see **Electrons, diffraction**)
Diffraction of molecules (see **Molecular beams**)
Diffraction of radiation (see **X-rays, diffraction**)
Discharge of electricity in gases (see also Arc, Spark)
Anode spots, relation to absorption and emission of gases, C. H. Thomas, O. S. Duffendack—72
Cathode characteristics, R. Tanberg—294(A), 1080
Cathode heating by He^+, Ne^+, A^+, C. C. Van Voorhis, K. T. Compton—1438(A)
Excitation processes in hollow cathode, R. A. Sawyer—1421(A)
H_2, high frequency, conductivity, C. J. Brasefield—1073; electron velocities—92, 122(A)
High frequency, characteristics, O. Stuhlman, Jr., M. D. Whitaker, M. L. Braun—1436(A)
H_2, striations, potential relations, J. Zeleny—699
Hg, positive column, T. J. Killian—1238
Ne, oscillations, G. W. Fox—1066
Ne, secondary electrons from Ni, W. Uyterhoeven, M. C. Harrington—1421(A)
Plasmoidal, high frequency oscillatory discharges, R. W. Wood—658(A), 673
Rare gases and Hg vapor, positive column, collisions of second kind, O. S. Duffendack, L. B. Headrick—1421(A)
Shot effect, abnormal, J. S. Donal, Jr.—1430(A)
Striations, temperature variation of striations, F. M. Sparks, C. T. Knipp—259, 297(A)
Striations and magnetic effect in electrodeless discharges, J. Tykocinski-Tykociner, J. Kunz—1436(A)
Dispersion of light
By symmetrical top-like molecules, theory, M. Muskat—1442(A), 1262
Dissociation
Diatomic molecules, by rotation, O. K. Rice—1538
H_2, by electron impact measurement, W. Bleakney, J. T. Tate—658(A), 1180; theory, E. U. Condon—658(A)
Predissociation of diatomic molecules, D. S. Villars, E. U. Condon—1028
Dissociation, heat of (see also **Molecular structure and constants**)
AgCl, from spectra, B. A. Brice—960
AlH, from spectra, D. S. Villars, E. U. Condon—1028
Cd_2, J. G. Winans, R. Rollefson—1436(A)
CO, from spectra, J. Kaplan—957
O_2, from spectra, J. Kaplan—436(L)
O_2, heat of formation, L. C. Copeland—1443(A)
Double refraction
Electrical, in gases, J. W. Beams, E. C. Stevenson—1440(A)
Earth (see **Geophysics**)
Elasticity
Metals, mass-weight ratio under strain, P. I. Wold—296(A)
Plastic deformation of ductile metals, A. Nadai—1418(A)
Shear vibrations in quartz, overtones, J. R. Harrison—1417(A)
Tensile stress and conductivity, in permalloy, L. W. McKeehan—657(A)
Torsion of rhombic prisms and cylinders, J. Kunz—1417(A)
Young's modulus for small stresses, D. K. Froman—120(A), 264
Electrical conductivity and resistance
Al, changes with working, G. E. Davis, G. Greenwood—1429(A)
Alloys, theory, L. W. Nordheim—1430(A)
Contact resistance, microphonic action, F. S. Goucher—1429(A)
Electrolytes, variation with frequencies, D. E. Richardson—297(A)
Permalloy, effect of stress and magnetic field, L. W. McKeehan—657(A)
Electrical discharge in gases (see **Discharge of electricity in gases**)
Electric moment (see **Dielectric constant**)
Electrolytic phenomena
E.m.f. location in photovoltaic cells W. N. Lowry—1270

E.m.f. resistance, capacitance in photovoltaic cells, H. E. Hammond—998
Polarization capacity and resistance temperature effect E. E. Zimmerman—543
Resistance at various frequencies D. E. Richardson—297(A)

Electromagnetic theory
Constitutive equations C. Kaplan F. D. Murnaghan—763
Interaction of field and matter J. R. Oppenheimer—461
Magnetic poles F. W. Warburton—292(A)

Electrons
Density distribution in equilibrium with hot body, A. T. Waterman—668(A)
Distribution in atoms and molecules, from x-ray scattering: He, A. H. Compton—925, 1427(A); Cl, G. G. Harvey, G. E. M. Jauncey—1427(A); MgO, E. O. Wollan—127(A), 1019
Equilibrium concentration in universe, L. S. Kassel—778
Motion in crystals, theory, P. M. Morse—1310
Nuclear, spin, L. Page, W. W. Watson—1584(L)
Relation to protons, theory, J. R. Oppenheimer—562(L)
Photoelectric (see **Photoelectric effect**)
Recombination with alpha-particles: measurements, A. H. Barnes—217; A. H. Barnes, B. Davis, H. L. Hull—1433(A); explanation, W. Band—1128(L); theory, E. C. G. Stueckelberg, P. M. Morse—116(L), 659(A)
Recombination with Hg^+, search for critical potentials, A. M. Cravath—659(A)
Scattering in radial fields, M. Muskat—1583(L)
Valence, in diamond, M. L. Huggins, R. Parrish—136(A)
Velocity, direct determination, T. R. Wilkins, J. A. Wood—657(A); C. T. Perry, E. L. Chaffee—1437(A)

Electron, charge
Most probable value, R. A. Millikan—1433(A), 1231

Electrons, diffraction
Crystals, quantum theory, P. M. Morse—1310
Cu crystal, H. E. Farnsworth—1131(L); satellites—1432(A)
Relation to Compton effect, J. Kunz—129(A)

Electrons in gases
Absorption coefficients, collision diameters: Cd and Zn vapors, R. B. Brode—134(A), 504; H_2, He, A, Ne, N_2, CO, C. E. Normand, R. B. Brode—1438(A), 1217
Energy losses: H_2, analysis of ions, W. Bleakney, J. T. Tate—658(A), 1180; He, Ne, ionization efficiencies, P. T. Smith, J. T. Tate—1438(A); Hg vapor, C. W. Foard—293(A), 1187; Hg vapor, analysis of ions, W. Bleakney—123(A), 139; K vapor, ionization efficiencies, J. Kuns, A. Hummel—123(A)
Mobility and velocity: in CO, H. B. Wahlin—122(A), 1568; in H_2, high frequency discharges, C. J. Brasefield—92, 122(A)
Scattering, angular distribution: H and H_2, G. P. Harnwell—285(L); He, A, H_2, A. L. Hughes, J. H. McMillen—1438(A)

Electrons in metals
Alloys, resistance, theory, L. W. Nordheim—1430(A)
Field currents, temperature dependence, N. A. de Bruyne—172

Electrons, photoelectric (see **Photoelectric effect**)

Electrons, scattered (see **Electrons in gases**)

Electrons, secondary
From Au, Ag, Al when bombarded by 16–40 Kv cathode rays, P. B. Wagner—98
From contaminated surfaces, P. L. Copeland—293(A), 982
From Ni, by impact of metastable atoms and positive ions, W. Uyterhoeven, M. C. Harrington—124(A), 438(L), 1421(A)

Electrons, thermionic (see **Thermionic emission of electrons**)

Electro-optical effects
Modification of light waves by electrical oscillations on Kerr cell, L. H. Stauffer—1440(A)

Element 87
Presence in pollucite and lepidolite, F. Allison, E. J. Murphy—285(L)

Emulsions
Particle size, effect of p_H, I. C. Weeks—668(A)

End losses
Effect on characteristics of filaments, I. Langmuir, S. MacLane, K. Blodgett—478

Faraday effect
Lag, method of chemical analysis, F. Allison, E. J. Murphy—124(A); search for element 87, F. Allison, E. J. Murphy—285(L)

Ferromagnetism
Origin, magnetic and silicon steel, J. C. Stearns—1, 292(A)

Field currents
Temperature dependence, N. A. de Bruyne—172

Fine structure (see also **Hyperfine structure**)
BeF bands, F. A. Jenkins—315
PbO bands, A. Christy, S. Bloomenthal—46
Mo $K\beta$ doublet, S. K. Allison, J. H. Williams—135(A), 149

Flarimeter
For testing circulatory fitness, P. V. Wells—1418(A)

Fluorescence
C_6H_6, spectrum, F. Almasy, C. V. Shapiro—1422(A)
Cs, third principal series line, C. Boeckner—664(A)
Iodine, infrared, by Hg arc, F. W. Loomis—662(A)
Sensitized, polarization, A. C. G. Mitchell—1422(A)
X-rays, efficiency, A. H. Compton—127(A)
Gases
Equation of state, H. J. Brennen—129(A)
Persistence of molecular velocities, second order reactions, L. S. Kassel—261
Geiger-counters
Multiple coincidences, M. A. Tuve—651(L)
Gelation temperature
Starch, method of determination, E. C. McCracken—1423(A)
Geophysics (see also **Atmospheric electricity**)
Composition of earth interior, A. A. Bless—1436(A)
Earth currents, transient, and earthquake, R. Hamer—656(A)
Ice ages, CO_2 theory, H. B. Maris—1016(L)
Ozone concentration in atmosphere, R. Ruedy—295(A)
Zodiacal light, theory, relation to magnetic storms, E. O. Hulburt—295(A), 663(A), 1098
Gravitation
Mass-weight ratio of metals under strain, P. I. Wold—296(A)
Heat conductivity (see **Thermal conductivity**)
Heat of Dissociation (see **Dissociation, heat of**)
Huyghens principle
Applicability, G. E. Uhlenbeck—1439(A)
Hydrodynamics
Distribution of non-reacting fluids in gravitational field, M. Muskat—1415(A), 1384
Shatter oscillations in liquids, nature and theory, E. H. Kennard—428
Thermal convection, R. W. Babcock—1008
Variable flow in pipes, theory, H. Bateman—177
Hyperfine structure
Effect on polarization of resonance radiation, A. Ellett—588
Error in literature, S. Goudsmit—436(L)
Mn I, observations and theory, H. E. White, R. Ritschl—208(L), 1146
Mn, predictions, S. Goudsmit—440(L)
Paschen-Back effect, S. Goudsmit, R. F. Bacher 129(A)
Relations between separations, theory, S. Goudsmit, R. F. Bacher—126(A)
Relation to nuclear spin, theory, H. E. White—441, 664(A)
Intensities in spectra
Cd, voltage relations, D. Colson—294(A)
Cr I, Cr II, multiplets, C. E. Hesthal—126(A)
HCl, vibration-rotation bands, J. L. Dunham—1347
He, continuous, maxima, J. M. Dewey—155
He, variation with voltage, J. Razek, P. J. Mulder—1423(A), 1442(A)
Hg, electrodeless discharge, O. P. Hart, O. Stuhlman, Jr.—1437(A)
Hg λ2537, variation with potential, F. C. Ostensen—286(L)
In Schumann region, vacuum spectrograph, G. R. Harrison—1443(A)
Li_2, isotope effect, A. Harvey, F. A. Jenkins—789
Multiplets, temperatures of arc, G. R. Harrison—133(A)
Ne, multiplets, measurements, H. N. Swenson—126(A)
Super-multiplet lines, theory, J. H. Bartlett, Jr.—229
Tl I, measurements, O U. Vonwiller—802
Interference
Method of measuring distance, S. H. Chamberlain—663(A)
Interferometer
Recording, C. W. Chamberlain—663(A)
Ionization by Impact
H_2, by electrons, analysis of ions, W. Bleakney, J. T. Tate—658(A), 1180
H_2, by electrons, theory, E. U. Condon—658(A)
He, by K^+ ions, Richard M. Sutton, J. C. Mouzon—694
He, Ne by electrons, efficiency 0–5000 volts, P. T. Smith, J. T. Tate—1438(A)
Hg, by electrons, efficiency of production of Hg^+, Hg^{2+}, Hg^{3+}, Hg^{4+}, Hg^{5+}, W. Bleakney—123(A); 139
K vapor, by electrons, efficiency, J. Kunz, A. Hummel—123(A)
Ionization by radiation (see **Photoionization**)
Ions
Accomodation coefficient, He^+, N^+, A^+, on Mo surface, C. C. Van Voorhis, K. T. Compton—1438(A)
Diffraction, H^+ by crystals, A. J. Dempster—298(A), 1405(L)
Motion in gases, excitation of spectra, Hg^+ in N_2, H. D. Smyth, E. G. F. Arnott—126(A)
Motion in gases, ionization, K^+ in He, R. M. Sutton, J. C. Mouzon—694
Motion in gases, neutralization, retardation, scattering, R. B. Kennard—1129(L); Cs^+, Li^+ in H_2 and He, J. S. Thompson—123(A), 1196; Li^+ in Hg vapor, I. W. Cox—123(A)

Recombination coefficient, air and oxygen, O. Luhr—1394
Recombination with electrons, Hg^+, A. M. Cravath—659(A)
Reflection; H^+ from crystals, A. J. Dempster—298(A), 1405(L); Li^+ from metals, R. B. Sawyer 124(A), 1090
Thermionic emission (see **Thermionic emission of positives**)
Velocity, direct determination, T. R. Wilkins, J. A. Wood—657(A)

Ions, mobility
In Cl_2 and Cl_2-air mixtures, L. B. Loeb—137(A), 184
In moist and dry air—J. Zeleny—1441(A)

Isotopes
Ag and Cl, from AgCl band spectra, B. A. Brice—960
C_{13}, from band spectra, A. S. King, R. T. Birge—133(A)
Li, from band spectra, A. Harvey, F. A. Jenkins—789
Metals, magneto-optical effect, F. Allison, E. J. Murphy—124(A)
N_{15}, from band spectra, S. M. Naude—130(A)
O_{17}, disintegrative synthesis, W. D. Harkins, A. E. Schuh—130(A); origin, S. C. Lind—1408
Pb, effect in PbO bands, S. Bloomenthal—34
Regularities in nuclei, H. A. Barton—408; in radioactive nuclei, H. C. Urey, H. Johnston—869(L)
Vibrational shift in band spectra, R. T. Birge—133(A)

Joule-Thomson coefficient
Air, J. R. Roebuck—121(A)
Real gases, simple equation, J. A. Beattie—643

Kerr effect
Alternating fields, modulation of light wave L. H. Stauffer—1440(A)
In gases, pressure variation, J. W. Beams, E. C. Stevenson—1440(A)
X-ray study of molecular orientation, R. L. McFarlan—211(L), 1426(A), 1469

Kinetic theory of gases
Equation of state, H. J. Brennan—129(A)
Molecular velocities, direct measure, I. F. Zartman—134(A)
Persistence of velocities, second order gas reactions, L. S. Kassel—261

Light waves
Modification by electrical oscillation on Kerr cell, L. H. Stauffer—1440(A)
Huyghen's principle, applicability, G. E. Uhlenbeck—1439(A)

Luminescence
Chemiluminescence of Na, J. W. Woodrow, R. M. Bowie—1423(A)

Magnetic fields
High frequency, intensity measurements, R. H. Mortimore—753

Magnetic storms (see **Geophysics**)

Magnetic properties
Barkhausen effect, propagation along wires, K. J. Sixtus, L. Tonks—1440(A); size of discontinuities, R. M. Bozorth, J. F. Dillinger—733
Bi, influence of magnetic field on crystal formation, A. Goetz—193
Co, thin films, E. P. T. Tyndall, W. W. Wertzbaugher—292(A)
Ferromagnetism, search for origin, J. C. Stearns—1, 292(A)
Moment of Li nucleus, S. Goudsmit, L. A. Young 1418(A)
Moment of sulphur molecule, E. J. Shaw, T. E. Phipps, W. H. Rodebush—1126(L)
Permalloy, effect of stress on resistance in magnetic field, L. W. McKeehan—657(A)
Rb, susceptibility, C. T. Lane—977
Steel, temperature changes accompanying magnetization, W. B. Ellwood—1440(A)
Susceptibility of gases, pressure dependence, Francis Bitter—1572

Magneto-optical effects
Faraday effect, lag, search for element 87, F. Allison, E. J. Murphy—285(L)
Method of chemical analysis, F. Allison, E. J. Murphy—124(A)

Magnetostriction
Measurements by heterodyne method, A. B. Bryan, C. W. Heaps—298(A)

Mathematics
Least squares, application, W. E. Deming—665(A)

Matter
Electrons and protons, theory; J. R. Oppenheimer—562(L)
Equilibrium with radiation in universe, L. S. Kassel—778
Interaction with field, J. R. Oppenheimer—461

Mechanics, quantum
Boundary conditions, meaning of wave groups, H. A. Wilson—948; criticism, C. Eckart—1298(L); reply, H. A. Wilson—1586(L)
Characteristic energy levels, method of calculation, W. E. Milne—863
Cohesion in metals, J. C. Slater—509
Complex spectra, calculation, W. V. Houston—136(A)

Dielectric polarization, extention of Van Vleck's theory, C. T. Zahn—1056
Dispersion and Raman effect for symmetrical top, M. Muskat—1442(A), 1262
Electrons and protons, J. R. Oppenheimer—562(L)
Electrons in crystals, P. M. Morse—1310
Field theory, W. Band—1015(L)
Hartree's method, J. C. Slater—210(L)
Intensities of super-multiplet lines, J. H. Bartlett, Jr.—229
Interaction of field and matter, J. R. Oppenheimer—461
Mean life of excited states, A. Bramley, A. C. G. Mitchell—1419(A)
Nuclear spin and hyperfine structure, H. E. White—441, 664(A)
Nuclear spin, effect on x-ray terms, G. Breit—1447
Ortho and para-hydrogen, equilibrium rate, H. Hall, J. R. Oppenheimer—132(A)
Recombination of alpha-particles and electrons, E. C. G. Stueckelberg, P. M. Morse—116(L)
Recombination of electrons with H-like atoms, E. C. G. Stueckelberg, P. M. Morse—659(A)
Pauli's exclusion principle, interpretation, E. U. Condon, J. E. Mack—579; origin, E. H. Kennard—1127(L)
Penetration of potential barrier by electrons, C. Eckart—1303
Predissociation and diffuse spectra, O. K. Rice—1551
Predissociation of diatomic molecules, D. S. Villars, E. U. Condon—1028
Quantum kinetics and the Planck equation, G. N. Lewis—1533
Radiative transitions, probability, J. R. Oppenheimer—939
Radioactivity and dissociation by rotation, O. K. Rice—1538
Relativity, W. Band—1016(L)
Rydberg formula, generalization, R. M. Langer—649(L)
Schrödinger equation, acoustical analogy, R. B. Lindsay—666(A)
Separation of angles in two-electron problem, G. Breit—569
Spatial distribution of photoelectrons, S. E. Szczeniowski—122(A), 347
Stark effect and electron spin in alkali atoms, V. Rojansky—782
Stark effect near series limit, J. Dewey—1439(A)
Stark effect of H atom, F. G. Slack—1170
Uncertainty principle, general formulation, H. P. Robertson—667(A)

Mechanics, statistical
Brownian motion, theory, L. S. Ornstein, G. E. Uhlenbeck—1434(A)
Electron density distribution in equilibrium with hot body, A. T. Waterman—668(A)

Metastable atoms
Excitation of spectra, R. A. Sawyer—1421(A)
Fluorescence, sensitized, A. C. G. Mitchell,—1422(A)
Hg, concentration, E. Gaviola—1226
Hg, life and radius, M. L. Pool—1419(A)
Hg mixed with rare gases, effect on field in positive column, O. S. Duffendack, L. B. Headrick—1421(A)
Ne, impacts on Ni, secondary electrons, W. Uyterhoeven, M. C. Harrington—124(A), 438(L), 1421(A)

Meterology
Cyclones and anticyclones, effect on radio, R. C. Colwell—1425(A)
Ice ages, CO_2 theory, H. B. Maris—1016(L)
Origin of snow flakes, J. M. Adams—113(L)
Ozone concentration in atmosphere, R. Ruedy—295(A)

Methods and instruments
Acoustics interferometry, J. C. Hubbard—1442(A)
Alloys for vacuum-tight glass-metal joints, D. E. Olshevsky—1424(A)
Bismuth-black as absorber of radiation in bolometers and thermopiles, A. H. Pfund—1434(A)
Chemical analysis, magneto-optic method, F. Allison, E. J. Murphy—124(A)
Clock, master, with light-controlled contacts, J. V. Hoffacker—121(A)
Flarimeter for testing circulatory fitness, P. V. Wells—1418(A)
For determing gelation temperature of starch, E. C. McCracken—1423(A)
For directly measuring corpuscular velocities, T. R. Wilkins, J. A. Wood—657(A); I. F. Zartman—134(A)
For making pictures in relief, Herbert E. Ives—1424(A)
For maintaining low temperatures, R. B. Scott, F. G. Brickwedde—670(A)
For measuring intensity of high frequency magnetic fields, R. H. Mortimore—753
For producing high potentials, G. Breit, M. A. Tuve, O. Dahl—51
Glass window mounting for pressures of 30,000 atmospheres, T. C. Poulter—297(A)
High voltage x-ray spectrography and radiography, F. Sillers, Jr.—1428(A)
Infrared spectrometer, resolving power, R. B. Barnes, A. H. Pfund—1434(A)

Interferometer, recording, C. W. Chamberlain—663(A)
Measuring distance, interference method, S. H. Chamberlain—663(A)
Oscilloscope, stabilized, F. Bedell, J. G. Kuhn—657(A)
Photometer, photoelectric, P. J. Mulder, J. Razek—1424(A)
Photometry, photographic, in extreme ultraviolet, P. A. Leighton, G. R. Harrison—134(A)
Radiometer, resonance, J. D. Hardy—662(A)
Rectifier characteristics, R. Ruedy—129(A)
Relays, grid-glow tubes, D. D. Knowles, S. P. Sashoff—1431(A)
Specific heats of gases, variation with pressure, E. J. Workman—667(A)
Spectrograph, vacuum, for intensity measurements in Schumann region, G. R. Harrison—1443(A)
Spectrograph, vacuum, x-ray, C. E. Howe—1428(A)
Spectrometer, x-ray, two-crystal, F. K. Richtmyer, S. W. Barnes, E. Ramberg—1428(A)
Thermoregulator, photoelectric, F. G. Brickwedde, R. B. Scott—670(A)
Vacuum tubes, high-voltage, M. A. Tuve, L. R. Hafstad, O. Dahl—1406(L)
X-ray spectrograph, multiple crystal, J. DuMond, H. Kirkpatrick—136(A), adjustments and tests, H. Kirkpatrick, J. DuMond—136(A)

Michelson-Morley experiment
Relation to relativity, W. F. G. Swann—127(A), 336
Suggested explanation, N. Galli-Shohat—1418(A)

Microphone
Microphone action and contact resistance, F. S. Goucher—1429(A)

Mobility of ions (see **Ions, mobility**)

Molecular beams
Diffraction by crystals, O. Stern—298(A)
In electromagnetic fields, D. E. Olshevsky—659(A)
Velocities, direct measure, I. F. Zartman—134(A)

Molecular structure and constants (see also **Spectra, molecular**)
AgCl, heat of dissociation, B. A. Brice—960
Aggregation in solid state, from solubility, A. M. Taylor—668(A)
Be F, from bands, F. A. Jenkins—315
Cd_2, heat of dissociation, J. G. Winans, R. Rollefson—1436(A)
CO, heat of dissociation, J. Kaplan—957
CO, heat of dissociation, moment of inertia, R. S. Estey—309
CS_2, dielectric constant and structure, C. T. Zahn—848
CS_2, NO, electric moments, C. H. Schwingel, J. W. Williams—855
H_2, para and ortho, equilibrium time, H. Hall, J. R. Oppenheimer—132(A)
Mechanical model to represent dynamic properties, C. F. Kettering, L. W. Shutts, D. H. Andrews—1422(A)
NH_3, two types, spectroscopic evidence, J. W. Ellis—595
O_2, heat of dissociation, J. Kaplan—436(L)
O_2, heat of formation, L. C. Copeland—1443(A)
Organic compounds, relation to Raman effect, D. H. Andrews—662(A)
PbO, rotational constants, nuclear separation, A. Christy, S. Bloomenthal—46
Sulphur, magnetic moment, E. J. Shaw, T. E. Phipps, W. H. Rodebush—1126(L)

Multiplets (see also **Spectra, atomic**)
Extension of Houston's and Slater's relations, S. Goudsmit—1325

Nuclear structure
Disintegrative synthesis of oxygen, W. D. Harkins, A. E. Schuh—130(A), 809
Electron spin, L. Page, W. W. Watson—1584(L)
Li, magnetic moment, S. Goudsmit, L. A. Young—1418(A)
Nuclear spin and hyperfine structure, H. E. White—441, 664(A)
Packing fraction, periodicity, H. Olson—213(L)
Regularities in list of nuclei, H. A. Barton—408
Regularities in radioactive nuclei, H. C. Urey, H. Johnston—869(L)
Stability and nuclear spin, W. D. Harkins—434(L)

Oscilloscope
Stabilized, with amplified stabilization, F. Bedell, J. G. Kuhn—657(A)

Packing effect
Periodicity in packing fraction, H. Olson—213(L)

Pashen-Back effect
In hyperfine structure, S. Goudsmit, R. F. Bacher—129(A)

Pauli's exclusion principle
Interpretation, E. U. Condon, J. E. Mack—579; origin, E. H. Kennard—1127(L)

Peltier effect
Bi crystals, Thomson effect, H. D. Fagan, T. R. D. Collins—421

Photoelectric effect
Alkali metals, properties, H. E. Ives, H. B. Briggs—669(A)

And J phenomenon, T. H. Osgood—1407(L)
Hg, solid and liquid, characteristics, D. Roller—122(A)
K, thin films, effect of intense electric fields, E. O. Lawrence, L. B. Linford—1421(A)
Na compounds, red sensitive, validity of Einstein's law, A. R. Olpin—670(A)
Pt coated glass filaments, characteristics, A. K. Brewer—1360
Selective maxima as function of valence, A. R. Olpin—671(A)
Spatial distribution of electrons, theory, S. E. Szczeniowski—122(A), 347
Spectrophotometer, P. J. Mulder, J. Razek—1424(A)
Stopping potentials, effect of red light, A. R. Olpin—112(L); E. Marx—1059
Thermoregulator, F. G. Brickwedde, R. B. Scott—670(A)
Threshold, temperature variation, K. F. Herzfeld—248
Work function, reduction by weak fields, W. B. Nottingham—669(A), 1128(L)
X-ray, fluorescence yield, A. H. Compton—127(A)
X-ray, space distribution of K and L electrons, C. D. Anderson—1139

Photography
Photometry in extreme ultraviolet, P. A. Leighton, G. R. Harrison—134(A)
Stereoscopic, H. E. Ives—1424(A)
X-ray, quantum theory of exposures, A. P. H. Trivelli—662(A)

Photoionization
Cs, by line absorption, effect of gases, F. L. Mohler, C. Boeckner—664(A)

Photometry
Photoelectric, P. J. Mulder, J. Razek—1442(A)
Photographic, in extreme ultraviolet, P. A. Leighton, G. R. Harrison—134(A)

Photons
Collisions between, attempt to detect, G. E. M. Jauncey, A. L. Hughes—1439(A)

Photovoltaic cells
E.m.f., resistance capacitance, H. E. Hammond—998
Location of e.m.f., W. N. Lowry—1270

Plasmoidal discharges (see **Discharge of electricity in Gases**)

Piezoelectric effect
Rochelle salt, characteristics, C. B. Sawyer, C. H. Tower—269

Polarization of radiation
Fluorescence, sensitized, A. C. G. Mitchell—1422(A)
Resonance radiation, effect of hyperfine structure, A. Ellett—588
X-rays from thin Al, B. Dasannacharya—129(A)

Pole effect
In vacuum arc, F. T. Holmes—652(L)

Porous plug experiment
Air, measurements, J. R. Roebuck—121(A)
Real gases, theory, J. A. Beattie—643

Potentials, critical (see also **Spectra**)
Ag Lα satellites, S. W. Barnes, F. K. Richtmyer—661(A)
Carbon, ionization, from spectra, J. J. Hopfield—1586(L)
H_2, ionization, analysis of ions, W. Bleakney, J. T. Tate—658(A), 1180
Hg^+, recombination with electrons, A. M. Cravath—659(A)
Hg vapor, electron energy losses, C. W. Foard—293(A), 1187
Hg vapor, formation of multiply charged ions, W. Bleakney—123(A), 139
In II, ionization, spectra, R. J. Lang—126(A)
Sb III, term values, R. J. Lang—445, 664(A)
Tl II, ionization, S. Smith—235

Potentials, high
Application to vacuum tubes, M. A. Tuve, G. Breit, L. R. Hafstad—66, 1406(L)
Method for producing, G. Breit, M. A. Tuve, O. Dahl—51

Pressures, high
Glass window for withstanding, T. C. Poulter—297(A)

Power factor (see **Dielectric constant and properties**)

Proceedings of the American Physical Society
Chicago Meeting, November 29 and 30, 1929—119
Stanford Meeting, December 7, 1929—132
Des Moines Meeting, December 30 and 31, 1929—289
New York Meeting, February 21 and 22, 1930—656; erratum—1414
Washington Meeting, April 24 to 26, 1930—1415

Protons
And electrons, theory, J. R. Oppenheimer—562(L)
Equilibrium concentration in universe, L. S. Kassel—778

Radiation
Emitted by compressed alum in electric field, I. A. Balinkin—1443(A)
Equilibrium with matter in universe, L. S. Kassel—778
From heated glass, extreme infrared, C. H. Cartwright—415

Radio
Intensity, effect of cyclones and anti-cyclones, R. C. Colwell—1425(A)
Reflection from earth's surface, L. C. Verman—1425(A)
Radioactivity
Disintegration constant of actino-uranium, ratio Ac to U, A. F. Kovarik—1432(A)
Gamma-ray intensity of radium, O. Glasser, V. B. Seitz—1432(A)
Mesothorium 2, maximum energy of beta-particles, **N**. Feather—1559
Of Stone Mountain, J. A. Hootman, W. S. Nelms—1431(A)
Origin of O_{17}, S. C. Lind—1408(L)
Quantum mechanical theory, O. K. Rice—1538
Synthesis of O_{17} from N, W. D. Harkins, A. E. Schuh—130(A), 809
Rate of transformation, N. Feather—705
Regularities in radioactive nuclei, H. C. Urey, H. Johnston—869(L)
Radiometer
Resonance, theory and practice, J. D. Hardy—662(A)
Raman effect
Excited by He arc, new methods, R. W. Wood—670(A)
For symmetrical top-like molecules, theory, M. Muskat—1442(A), 1262
HCl, R. W. Wood, G. H. Dieke—1355
HCl and HBr (liquid) vibration frequencies, E. O. Salant, A. Sandow—214(L)
HNO_3, effect of dilution, E. L. Kinsey—284(L)
Organic compounds, relation to molecular structure, D. H. Andrews—662(A)
Organic liquids, R. B. Barnes—662(A), 1524
Solid organic compounds, specific heats, D. H. Andrews, J. C. Southard—670(A)
SO_2 spectra, R. G. Dickinson, S. S. West—1126(L)
Recombination
Alpha-particles and electrons, measurements, A. H. Barnes—217; A. H. Barnes, B. Davis, H. L. Hull—1433(A); explanation, W. Band—1128(L); theory, E. C. G. Stueckelberg, P. M. Morse—116(L), 659(A)
Ions and electrons, Hg^+, A. M. Cravath—659(A)
Ions and ions, air and oxygen, O. Luhr—1394
Rectifiers
Characteristics, R. Ruedy—129(A)
Contact, cupric sulphide-magnesium junctions, M. Bergstein, J. F. Rinke, C. M. Gutheil—1425(A)
Reflection of corpuscles
Alkali metal atoms, from crystals, J. B. Taylor—375
Atoms, from crystals, A. Ellett—293(A)
H atoms, attempt to detect de Broglie waves, T. H. Johnson—1432(A)
H atoms from LiF crystal, T. H. Johnson—1299(L), 1444(A)
H^+, by crystals, A. J. Dempster—298(A), 1405(L)
Li^+ from metal surfaces, R. B. Sawyer—124(A), 1090
Molecules, diffraction by crystals, O. Stern—298(A)
Zn atoms from NaCl, H. A. Zahl—293(A)
Reflection of light
$SmCl_3 \cdot 6H_2O$ comparison with absorption at high and low temperatures, S. Freed, F. H. Spedding—212(L)
Refractive index
H_2O and KCl solution at high frequencies, F. H. Drake, G. W. Pierce, M. T. Dow—613
Au, for C $K\alpha$ x-rays, E. Dershem—128(A)
Relativity
Aberration of light from terrestrial sources, N. Galli-Shohat—664(A)
Field and matter, interaction, J. R. Oppenheimer—461
General, energy-momentum principle, R. C. Tolman—875; entropy principle—896; weight of thermal equilibrium—904
Michelson-Morley experiment, suggested explanation, N. Galli-Shohat—1418(A)
Relation to aether drift, W. F. G. Swann—127(A), 336
Transformation of oscillation to travelling wave, de Broglie's postulate, V. Karapetoff—127(A)
Unified field theory and wave mechanics, W. Band—1015(L)
Unified field theory, Schwarzschild's solution, M. Salkover—I 209(L), II 214(L), reply, M. S. Vallarta—435(L)
Unified physical field, W. Band—115(L)
Resolving power
Calcite, for x-rays, S. K. Allison, J. H. Williams—1476
Crystal grating, limits, B. Davis—209(A)
Resonance radiation
Cs, third principal series line, quenching, C. Boeckner—664(A)
Hg, absorption in Hg vapor, A. R. Thomas—1253
Polarization, effect of hyperfine structure, A. Ellett—588
Scattering of light (see also **Raman effect**)
In Na vapor, S. A. Korff—435(L)
Schottky effect (see also **Photoelectric effect, Thermionic emission**)
Thoriated tungsten, N. B. Reynolds—158

Sedimentation
Equilibria of colloidal particles, N. Johnston, L. G. Howell—274
Shatter oscillations
Nature and theory, E. H. Kennard—428
Shot effect
Abnormal, in gas discharge, J. S. Donal, Jr.—1430(A)
Of positive ions, effect on space charge limited electron current, L. P. Smith—1430(A)
Oxide-coated filaments, H. N. Kozanowski—1430(A)
Snow flakes
Origin, J. M. Adams—113(L)
Solar physics
Anomalous rotation of sun, R. Gunn—635
Spark discharge
Early stages, time of appearance of spectra, temperature, ion concentration, E. O. Lawrence, F. G. Dunnington—134(A), 396
Initial stages, time lag in characteristics, J. W. Beams, J. C. Street—658(A)
Time differences in appearance of spectrum lines, J. W. Beams—24
Time lags at overvoltages, J. C. Street—1437(A)
Specific heats
Gases, variation with pressure, E. J. Workman—667(A)
Solid organic compounds from Raman spectra, D. H. Andrews, J. C. Southard—670(A)
Spectra, atomic
Alkali atoms, Stark effect and electron spin, theory, V. Rojansky—782
C I, ionization potential, J. J. Hopfield—1586(L)
Cd, voltage-intensity relations, D. Colson—294(A)
Co II, analysis, J. H. Findlay—1420(A)
Complex spectra, method of calculating, W. V. Houston—136(A)
Cr I, Cr II, intensities in multiplets, C. E. Hesthal—126(A)
Cs, resonance and quenching of third principal series line, C. Boeckner—664(A)
Excitation, in hollow cathode, R. A. Sawyer—1421(A)
$GdCl_3 \cdot 6H_2O$, line spectra from solid, S. Freed, F. H. Spedding—1408(L)
H, variation with pressure and capacitance, E. O. Hulburt—1420(A)
He, H, N, O, 600–1100A, J. J. Hopfield—1133(L)
He, continuous, intensity maxima, J. M. Dewey—155
He, intensities, J. Razek, P. J. Mulder—1423(A)
He, intensity-voltage relations, P. J. Mulder, J. Razek—1442(A)
Hg, average lives of 2^3P-2^3S triplet, R. H. Randall, H. W. Webb—665(A)
Hg, intensity potential relations for λ2537, F. C. Ostensen—286(L)
Hg $2^3P_{012}-2^3S_1$, mean lives, R. H. Randall, H. W. Webb—665(A), 1161
Hg, relative intensities in electrodeless discharge, O. P. Hart, O. Stuhlman, Jr.—1437(A)
Hg I, new term, E. D. McAlister—1585(L)
Hyperfine structure and nuclear spin, H. E. White—441, 664(A)
Hyperfine structure, error in literature, S. Goudsmit—436(L)
Hyperfine structure, Paschen-Back effect, S. Goudsmit, R. F. Bacher—129(A)
Hyperfine structure, relations between separations, S. Goudsmit, R. F. Bacher—126(A)
In II, measurements and classification, R. J. Lang—126(A)
In spark discharge, time of appearance of lines, J. W. Beams—24
Interval ratios, rule for *sp*, *sd*, *sf*, configurations, E. U. Condon, G. H. Shortley—1419(A), 1342
Li, magnetic moment of nucleus, S. Goudsmit, L. A. Young—1418(A)
Lu, regularities, W. F. Meggers, B. F. Scribner—1420(A)
Mn, hyperfine structure, H. E. White, R. Ritschl—208(L)
Mn I, hyperfine structure, H. E. White, R. Ritschl—1146
Mn, prediction of hyperfine structure, S. Goudsmit—440(L)
Multiplets, extension of Houston's and Slater's relations, S. Goudsmit—1325
Multiplets, intensities, temperature of arcs, G. R. Harrison—133(A)
Na III, Mg IV, Mg V, for ultraviolet, new levels, irregular doublet law, J. E. Mack, R. A. Sawyer—229, 661(A)
Ne, intensities, H. N. Swenson—126(A)
Pd, surplus level, A. G. Shenstone—1420(A)
Rare earths, origin of line absorption spectra, O. Laporte—130(A)
Resonance separations in p^5s and d^5s configurations, O. Laporte, D. R. Inglis—1337
Ru I, analysis, W. F. Meggers, A. G. Shenstone—868(L)
Rydberg formula, generalization, R. M. Langer—649(L)
Sb III, Sn II, classification, R. J. Lang—445, 664(A)
$SmCl_3 \cdot 6H_2O$, reflection and absorption, S. Freed, F. H. Spedding—212(L)
Spark discharge, time of appearance of lines, E. O. Lawrence, F. G. Dunnington—134(A), 396

Stark effect near series limit, J. Dewey—1439(A)
Super-multiplet lines, intensities, J. H. Bartlett, Jr.—229
Temperature shift and pole effect in vacuum arc, F. T. Holmes—652(L)
Tl I, intensity measurements, O. U. Vonwiller—802
Tl II, extention and analysis, S. Smith—235

Spectra, molecular (see also **Raman effect**)
Acetylene, ethylene, 6800–9200A, R. M. Badger—1433(A)
AgCl, analysis, B. A. Brice—960
Air, afterglow, J. Kaplan—600
BeF, wave-lengths, analysis, molecular constants, F. A. Jenkins—315
CaH, red bands, Zeeman effect, W. W. Watson, W. Bender—1440(A), 1513
Cd_2, heat of dissociation, J. G. Winans, R. Rollefson—1436(A)
C_6H_6 fluorescence, F. Almasy, C. V. Shapiro—1422(A)
C_6H_6, electronic transitions, C. V. Shapiro, R. C Gibbs, J. R. Johnson—1422(A)
C_6H_6, emission 2500–3000A, J. B. Austin, I. A. Black—452
CO, comet tail bands, emitter, L. R. Maxwell—665(A)
CO, fourth positive bands, new measurements and classification, R. S. Estey—309
CO, fourth positive bands, wave-lengths, L. B. Headrick, G. W. Fox—1033
CO, new band system, J. Kaplan—1298(L)
Cyclohexane, vibration doublets, J. W. Ellis—437(L)
Excited radicals in compounds, constancy of vibration frequencies, C. P. Snow—563(L)
H_2 absorption 600–1100A, J. J. Hopfield—1133(L)
H_2, $(B-A)$ bands, resonance, H. H. Hyman—1419(A)
HCl, vibration-rotation bands, intensities, J. L. Dunham—1347
Hg band at 2540, origin, R. Rollefson—1177
Iodine, fluorescence, infrared, by Hg arc, F. W. Loomis—662(A)
Isotope shift, R. T. Birge—133(A)
Li_2, blue-green absorption, A. Harvey, F. A. Jenkins—132(A), 789
MgH, λ2511 band, Zeeman effect, G. M. Almy, F. H. Crawford, E. L. Hill—124(A)
MgO, blue-green, analysis, P. N. Ghosh, P. C. Mahanti, B. C. Mukkerjee—1491
N_2, afterglow, R. Ruedy—125(A)
N_2, excited by positive ion impact, H. D. Smyth, E. G. F. Arnott—126(A)
NH_3, absorption in visible, R. M. Badger—1038
NH_3, evidence of two molecular types, J. W. Ellis—595
OH bands, Zeeman effect, G. M. Almy—1495
O_2, atmospheric new absorption band, H. D. Babcock—125(A)
Organic liquids, absorption, infrared, E. K. Plyler, T. Burdine—605
Organic liquids, C-H vibration, Raman effect, R. B. Barnes—662(A)
Organic liquids, intensity and position of overtones, P. E. Shearin—973
PbO, fine structure analysis, A. Christy, S. Bloomenthal—46
PbO, quantum analysis and isotope effect, S. Bloomenthal—34
Predissociation from high rotational states, D. S. Villars, E. U. Condon—1028
$SmCl_3 \cdot 6H_2O$, reflection and absorption, S. Freed, F. H. Spedding—212(L)

Spectra, reflection
$SmCl_3 \cdot 6H_2O$, comparison with absorption, S. Freed, F. H. Spedding—212(L)

Spectrograph, Spectrometer
Infrared, resolving power, R. B. Barnes, A. H. Pfund—1434(A)
Vacuum, for intensity measurements in Schumann region, G. R. Harrison—1443(A)
X-ray, two-crystal, F. K. Richtmyer, S. W. Barnes, E. Ramberg—1428(A)
X-ray, multiple crystals, J. DuMond, H. Kirkpatrick—136(A); adjustments and tests, H. Kirkpatrick, J. DuMond—136(A)
X-ray, vacuum, C. E. Howe—1428(A)

Stark effect
Alkali atoms, electron spin, theory, V. Rojansky—782
Hydrogen atom, theory, F. G. Slack 1170
Near series limit, J. Dewey—1439(A)

Stars (see **Astrophysics**)

Sun (see **Astrophysics**)

Surface tension
Glass, molten, W. B. Pietenpol, H. H. Scott—296(A)
Retention of liquids in assemblages of homogeneous spheres, W. O. Smith, P. D. Foote, P. F. Busang—1416(A)

Susceptibility, magnetic (see **Magnetic properties**)

Thermal conductivity
Solution of general equation for certain cases, R. L. Peek, Jr.—554

Thermal convection
In fluids, R. W. Babcock—1008

Thermal expansion
Carboloy, measurements, P. Hidnert—120(A)

Cu-Ni-Sn alloy, P. Hidnert, W. T. Sweeney—667(A)
Pb, measurement, P. Hidnert, W. T. Sweeney—296(A)
Thermal radiation
Of glass for $\lambda > 50\mu$, C. H. Cartwright—415
Thermionic emission of electrons
Composite surfaces, work function, effect of fields, W. B. Nottingham—1128(L); ion-grid theory, J. A. Becker, 1431(A)
Electron density distribution in equilibrium with hot body, A. T. Waterman—668(A)
From various filaments, effect of end losses, I. Langmuir, S. MacLane, K. B. Blodgett—478
Oxide-coated filaments, characteristics, E. F. Lowry—668(A), role of base metal, E. F. Lowry—121(A), 1367; shot effect, H. N. Kozanski—1430(A)
Pt-coated glass filaments, characteristics, A. K. Brewer—1360
Relation to surface heat of charging, K. F. Herzfeld—248
Shot effect, abnormal, in Ne gas, J. S. Donal, Jr.—1430(A)
Thoriated tungsten, variation with extent of thoriation, W. H. Brattain—1431(A); contact e.m.f., Schottky effect, N. B. Reynolds,—158
Work function, space charge interpretation, R. S. Bartlett—669(A)
Thermionic emission of positives
From thoriated tungsten, H. B. Wahlin—653(L)
From W and Mo, characteristics, L. P. Smith—381
Shot effect, effect on space charge limited electron currents, L. P. Smith—1430(A)
Thermodynamics
Dalton-Gibbs law, test, L. J. Gillespie—1435(A)
Entropy in general relativity, R. C Tolman—896
Equation of state for gases, H. J. Brennen—129(A)
Excitation of nerves, theory, N. Rashevsky—1435(A)
Homogeneous coordinates, uses, H. J. Brennan—294(A)
Joule-Thomson effect, theory, J. A. Beattie—643; measurements with air, J. R. Roebuck—121(A)
Mixtures of real gases, theory, J. A. Beattie—1435(A)
Nernst heat theorem, H. J. Brennen—121(A)
Simultaneous irreversible processes, L. Onsager—666(A)
Systems with several equilibria, N. Rashevsky—666(A)
Third law, W. H. Rodebush—210(L)
Thermoelectric properties
Bi crystals, Peltier and Thomson effects, H. D. Fagan, T. R. D. Collins—421
Thermoregulator
For low temperatures, R. B. Scott, F. G. Brickwedde—670(A)
Photoelectric, F. G. Brickwedde, R. B. Scott—670(A)
Thomson effect in Zn crystals, L. A. Ware—667(A), 989
Thomson effect (see **Thermoelectric properties**)
Transitions, radiative
Probability, theory, J. R. Oppenheimer—939
Ultrasonic waves
Velocity measurements, C. D. Reid—814
Uncertainty principle
In acoustics, G. W. Stewart—1441(A)
Formulation and classical interpretation, H. P. Robertson—667(A)
Vacuum tubes
For high-voltages, M. A. Tuve, G. Breit, L. R. Hafstad—66; M. A. Tuve, L. R. Hafstad, O. Dahl—1406(L)
Grid-glow tube relays, D. D. Knowles, S. P. Sashoff—1431(A)
Valence
Valence electrons in diamond, location, M. L. Huggins, R. Parrish—136(A)
Viscosity
Dependence on molecular space arragement, R. L. Edwards, G. W. Stewart—291(A)
Of compressed gases, J. H. Boyd, Jr.—1284
Voltmeter
Vacuum tube, improvements, R. H. Mortimore—753
Wave equation
Huyghens principle, G. E. Uhlenbeck—1439(A)
Work function (see **Thermionic emission**)
X-rays, absorption
Au, for $K\alpha$, E. Dershem—128(A)
Temperature independence, J. A. Bearden—1443(A), 1463
X-rays, diffraction, reflection and scattering (see also **Compton effect**)
Alcohols, molecular association, G. W. Stewart—296(A), 726
Alcohols, relation to viscosity, R. L. Edwards, G. W. Stewart—291(A)
Calcite, glancing angle for Ag$K\alpha$, C D. Cooksey, D. Cooksey—564(L)
Compton effect, position and width of modified line, F. L. Nutting—661(A)
Crystals of colloidal size, form of bands, theory, C. C. Murdock—8
Diamond, Valence electrons, M. L. Huggins, R. Parrish—136(A)
Fe crystal, magnetized and unmagnetized, J. C Stearns—1, 292(A)

Fe, Ni, Cu atoms, R. W. G. Wyckoff—215(L)
Glass, C. $K\alpha$ line, J. Thibaud—1452
He, distribution of electrons, A. H. Compton—1427(A)
Liquids, effect of electric field, R. L. McFarlan—211(L), 1426(A), 1469
Liquids, organic mixtures, A. W. Meyer—291(A)
Liquids, organic, temperature effect, E. W. Skinner—128(A)
Magnetite and silicon steel, magnetized and unmagnetized, J. C. Stearns—1
MgO, electron distribution, E. O. Wollan—1019
NaCl, electron distribution in Cl, G. G. Harvey, G. E. M. Jauncey—1427(A)
NaCl, temperature effect, W. D. Claus—1427(A)
Ni, O, in NiO, R. W. G. Wyckoff—583
Quartz, C $K\alpha$, E. Dershem, M. Schein—292(A)
Spectra, N. S. Gingrich—1444(A)
Spectroscopic analysis, J. A. Bearden—1427(A)
Theory, relation to electron distribution in atoms, A. H. Compton—925, 1427(A)
Triphenolmethane, G. W. Stewart—291(A)
Water, molecular association, G. W. Stewart—1426(A)

X-rays, emission
Efficiency, W. W. Nicholas—128(A)
From three-element tube, A. Bramley—869 (L)
Mechanism, W. Band—1129(L)

X-rays, fluorescence
Efficiency, A. H. Compton—127(A)

X-rays, photoelectric effect
Relation to J phenomenon, T. H. Osgood—1407(L)
Space distribution of K and L electrons, C. D. Anderson—1139

X-rays, photographic effect
Theory, A. P. H. Trivelli—662(A)

X-rays, polarization
From thin Al anticathode, B. Dasannacharya—129(A)

X-rays, refraction
Au, for $K\alpha$, E. Dershem—128(A)

X-rays, spectra and Spectroscopy
Absolute measure of wave-lengths, J. M. Cork—128(A)
Ag $L\alpha$ satellites, excitation potential, S. W. Barnes, F. K. Richtmyer—661(A)
By double crystal, N. S. Gingrich—1444(A)
Ca, Cr, Mn, Co, Ni, Cu, Zn, K absorption, fine structure, B. Kievit, Jr., G. A. Lindsay—292(A)
Cu, Mo, Ag K lines, structure, J. Valasek—291(A)
Effect of nuclear spin on term values, theory, G. Breit—1447
Instrument for high-voltage, F. Sillers, Jr.—1428(A)
$K\alpha$ satellites of Ni I As, F. K. Richtmyer, E. Ramberg—661(A)
Limiting resolving power of crystal grating, B. Davis—209(L)
L series, Ca to Zn, measurements, C. E. Howe—717
Mo $K\alpha$, natural width, S. K. Allison, J. H. Williams—1476
Mo K_β doublet, separation and fine structure, S. K. Allison, J. H. Williams—135(A), 149
Mo L series, wave-lengths by ruled grating, J. M. Cork—1456
Scattered x-rays, N. S. Ginrich—1444(A)
Spectrograph and radiograph, F. Sillers, Jr.—1428(A)
Spectrograph, multiple crystal, J. DuMond, H. Kirkpatrick 136(A); adjustments and tests, H. Kirkpatrick, J. DuMond—136(A)
Spectrograph, vacuum, C. E. Howe—1428(A)
Spectrometer, two-crystal, F. K. Richtmyer, S. W. Barnes, E. Ramberg—1428(A)

Young's modulus
Under small stresses, D. K. Frohman—120(A), 264

Zeeman effect
CaH bands, W. W. Watson, W. Bender—1440(A), 1513
Hyperfine structure, Paschen-Back effect, S. Goudsmit, R. F. Bacher—129(A)
$GdCl_3 \cdot 6H_2O$, line spectra of solid, Paschen-Back effect, S. Freed, F. H. Spedding—1408 (L)
MgH λ5211 band, G. M. Almy, F. H. Crawford, E. L. Hill—124(A)
OH bands, G. M. Almy—1495

Zodiacal light
Theory, E. O. Hulburt—295(A), 663(A), 1098

STANDARD-SIGNAL GENERATOR

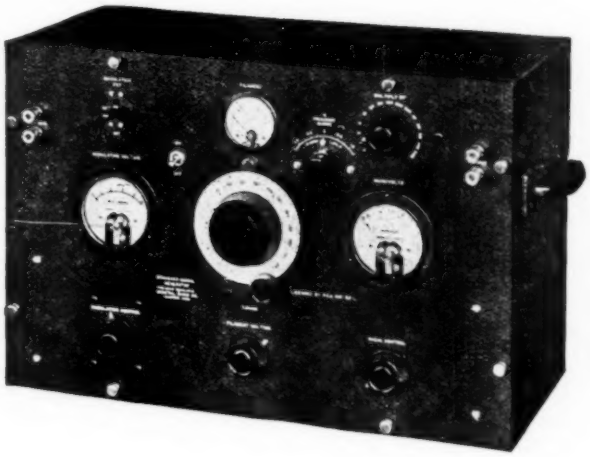

THE Type 403-B Standard-Signal Generator is a calibrated oscillator for delivering known radio-frequency voltages which are localized between two terminals. Its principal use is in measuring radio field intensity (field strength) and in taking sensitivity, selectivity, and fidelity characteristics on radio receivers. It may be used either with or without modulation, a 400-cycle modulating oscillator is contained in the instrument and there is provision for supplying modulating voltages from an external oscillator.

Its range is from 500 to 1500 kilocycles, but others can be built to cover other bands on special order.

GENERAL RADIO COMPANY
30 STATE STREET
CAMBRIDGE A, MASSACHUSETTS

GENERAL RADIO INSTRUMENTS

FOR MEASURING ELECTRICAL QUANTITIES AT ALL FREQUENCIES

GR

STANDARD AND SPECIAL ITEMS FOR LABORATORY AND INDUSTRIAL USE

INFORMATION FOR CONTRIBUTORS TO THE PHYSICAL REVIEW

Purpose of the Review is to publish articles that add to our knowledge of experimental or theoretical physics.

Articles which have not previously been published may be submitted by any physicist whether American or not. Each manuscript will be acknowledged by the Managing Editor as soon as received. An article to be considered must be in English and in a form ready for publication; it must be provided with a preliminary abstract prepared in accordance with the directions given on a following page. Carelessly written articles and figures not carefully drawn will be returned for revision. All manuscripts should be typed double space and symbols written in with great care so as to be quite clear to the printer.

Suggestions as to Contents. On account of the high cost of printing, brevity is of great practical importance. Historical summaries of previous results and also discussions which consider various possible explanations without leading to definite conclusions should be made very brief, except in special cases. The greater part of the paper should be devoted to the actual new results and to a concise presentation of the conclusions to which they lead. Attention should be directed to the more accurate and more conclusive experiments, omitting any which add nothing. The amount of detail included should be governed somewhat by the importance of the results and their interest to physicists.

Suggestions as to form. Clearness is of great importance. Pains should be taken to insure that the order and form of presentation are such as to enable the reader to grasp the new information as easily and quickly as possible. In general the order should be: Statement of the problem and of the purpose, scope and general method of the investigation, followed by a description of the apparatus, experiments and results in such order as to bring out clearly the evidence for the main conclusions, the paper ending with perhaps a brief discussion of the significance and bearing of the results on other problems. Avoid the historical or laboratory note-book style; use rather the text-book or lecture style. Footnotes should be numbered consecutively and each reference should contain author's name.

Abbreviations. Omit periods after such symbols for units as the following: cm, mm, kv, lb, A, °C; also after I, II, . . . and percent, and after headings in columns in Tables. Write a.c., e.m.f., abscissas, disk, in vacuum, wave-length, x-rays, percent. Refer to figures as Fig. 1, Figs. 3 and 4; and to equations as: Eq. (5); Eqs. (7) and (8). Number equations on the right.

Mathematics. Indicate division by a slant line where possible. Avoid unusual symbols, symbols with rules over them, cumbersome fractions.

Figures or illustrations. Use only jet black ink, on white or on blue-lined cloth or paper. Tracing cloth is especially suitable. Curves plotted or traced on such cloth or paper may have co-ordinates ruled in black at desired intervals, say every centimeter or inch, as blue lines are not reproduced photographically. *Colors other than blue and black should be avoided.* Indicate observed points on all plots. Arrange material in each figure compactly. It is well when possible, to make the longer dimension horizontal, as larger reproduction can then be permitted; if vertical figures are necessary space may be saved by making two of the same height, and putting them side by side. *All lettering should be at least* $\frac{3}{16}$″ *high* for an 8″×10″ figure, so as to be legible after reduction. Lettering left in pencil will be inked in by a draftsman in this office. In general each figure and table should have a caption, describing it briefly. Reduce the number of tables and figures to the necessary minimum.

Proofs. Galley proof of each article is sent directly from the publishers to the author and should be corrected with great care so as to eliminate all errors, as page proof cannot always be submitted. Only necessary changes should be made; extensive additions will mean the delay of a month in publication. All corrected proof should be sent promptly with the manuscript to THE PHYSICAL REVIEW, University of Minnesota, Minneapolis.

Permission to republish any article is given, if proper acknowledgment is made.

Reprints ordered on the proper form with the return of the galley proof, will be furnished by the printer according to the prices given on the form.

PHYSICAL REVIEW

PREPARATION OF PRELIMINARY ABSTRACTS

An article will not be accepted for publication in THE PHYSICAL REVIEW unless the manuscript is accompanied by an adequate abstract for publication at the beginning of the article. This abstract is intended to aid the reader by furnishing an index and a brief summary of the contents of the article. Besides serving these purposes it should also be suitable for reproduction in abstract journals so as to make it unnecessary for the editors of these journals to have another abstract prepared.

As *an index* it should be complete; all the subjects, major and minor, concerning which new information is presented, should each be given, with sufficient precision so that any reader can tell from the abstract whether the article contains anything of interest to him. The subject indexes of abstract journals are fundamental in reference work. These indexes are prepared exclusively from the abstracts and whatever is omitted from the abstracts cannot be included in the index and may thus be lost. The writer of an abstract should therefore feel himself under an important obligation to his scientific colleagues to make sure that the abstract is accurate and complete, at least as an index.

As a summary the abstract should give briefly the conclusions of the article important advances in experimental technique and theory, and all numerical results of general interest that may be conveniently given including all that might belong in a hand book and table of contents. It should give all the information that readers who are not specialists in the particular field involved might desire to know about the article thus saving them the time and trouble in referring to the article itself. Experience has shown that in general the length of the abstract should be from four to eight percent of the length of the article.

THE PHYSICAL REVIEW 1923-1925 contains many examples of adequate abstracts. Most of these contain paragraph titles and subtitles which indicate the subjects concerning which new information is given and it is required that authors include such subtitles when all the information contained in the article does not refer to the subject indicated by the title of the article Such subtitles may be frequently avoided by rewording the title so as to make it more precise.

ACCELERATION APPARATUS

Fletcher Design

First American made design available for Colleges and Universities

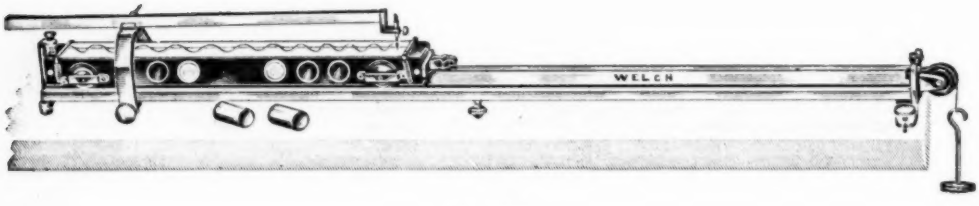

No. 848

This new American made design embodies all standard features with the following improvements of distinct merit:

1. **All-metal car**
2. **Simple release mechanism**
3. **Positive arrest mechanism**
4. **Movable holder for vibrator**
5. **Removable paper record**
6. **Cone-bearing pulleys**

The machined steel base 140 cm long is provided with a V-groove in which two of the three car wheels run. All pulleys have cone bearings and the pulley over which the cord runs is molded Bakelite.

Six removable cylindrical weights are provided so as to double, triple, and quadruple the effective weight of the car.

No. 848 Acceleration Apparatus, After Fletcher. Complete as illustrated with six weights, vibrator, stylus, and weight hanger.....**$60.00**

PACIFIC COAST DISTRIBUTORS

Braun-Knecht-Heimann Company
576-584 Mission Street
San Francisco, California

The Braun Corporation
363-371 New High Street
Los Angeles, California

A Sign of Quality QUALITY WELCH SERVICE *A Mark of Service*

W. M. Welch Scientific Company

1516 Orleans Street Manufacturers, Importers and Exporters of Scientific Apparatus and School Supplies **Chicago, Ill., U. S. A.**

Professor Werner Heisenberg's first book—

THE PHYSICAL PRINCIPLES OF THE QUANTUM THEORY

"Professor Heisenberg's leading position in the development of the new quantum mechanics is well recognized. In this book he discusses primarily the physical significance of the new theory, emphasizing the equal applicability of the corpuscular and wave concepts and the need for his uncertainty principle to reconcile the two points of view."—Arthur H. Compton

To be published in July. $2.00

THE UNIVERSITY OF CHICAGO PRESS
CHICAGO, ILLINOIS

PHYSICIST: preferably with doctor's degree in Physics; wanted for research department of metallurgical plant; located in New Jersey; in reply please give information on training, experience (if any), age, and salary desired.

Address Box 15

PHYSICAL REVIEW
UNIVERSITY OF MINNESOTA
MINNEAPOLIS, MINNESOTA

CLARK-HAYES
Cylindrical Camera

THIS camera will permit crystal analysis by the following methods:

1. **Laue Method, which now is the most important of all types for crystal analysis.**
2. **Debye-Scherrer Powder Method.**
3. **Bragg or Oscillation Method for single crystal.**
4. **Monochromatic Pinhole Method for fibrous structure.**

This Camera and our Oscillating Spectrograph constitute the most versatile and economical universal spectrograph obtainable.

Our camera may be used on any type of power unit including the General Electric Multiple Diffraction Apparatus.

This camera is but one single item of our complete line of equipment for X-Ray laboratories. All of our apparatus can be supplied from stock.

We will gladly quote prices on any special apparatus.

J. B. Hayes Machine Co.
ENGINEERS—INSTRUMENT MAKERS
URBANA, ILLINOIS

Announcement . . .

We wish to announce to our customers recent changes in the executive and administrative personnel of our company.

J. M. Roberts, for many years a valued Director and our Secretary, has retired from all his activities with the company.

A. H. McConnell and H. C. Arms have resigned their respective offices of President-Treasurer and Vice President, but continue to maintain their active association with the company and serve as an Executive and Finance Committee.

It is with special pleasure that we announce that Paul E. Klopsteg, Director in charge of our Development and Manufacturing Division, Sterling L. Redman, Director in charge of our Sales and Purchasing Division, and C. P. McConnell, Director in charge of our Operating and Service Division, are elected officers of the company as follows:

President.....P. E. KLOPSTEG
Vice President.....S. L. REDMAN
Secretary and Treasurer.....C. P. MCCONNELL

We appreciate the favor of your business in the past years and assure you of our earnest desire to increase the usefulness and value of our service for the future.

CENTRAL SCIENTIFIC COMPANY
A. H. MCCONNELL,
H. A. ARMS,
Executive Committee

June 1st, 1930

CENTRAL SCIENTIFIC COMPANY
LABORATORY Apparatus CENCO Supplies Chemicals
460 E. Ohio St. Chicago U.S.A.

GEORGE BANTA PUBLISHING COMPANY, MENASHA, WISCONSIN